

(NASA-CR-142983) STEADY AND OSCILLATORY,
SUBSONIC AND SUPERSONIC, AERODYNAMIC
PRESSURE AND GENERALIZED FORCES FOR COMPLEX
AIRCRAFT CONFIGURATIONS AND APPLICATIONS TO
FLUTTER M.S. Thesis (Boston Univ.) 201 p

N75-25871

Unclas
26621

G3/02

BOSTON UNIVERSITY



DEPARTMENT OF AEROSPACE ENGINEERING
COLLEGE OF ENGINEERING
BOSTON, MASSACHUSETTS

BOSTON UNIVERSITY
COLLEGE OF ENGINEERING

STEADY AND OSCILLATORY,
SUBSONIC AND SUPERSONIC, AERODYNAMIC
PRESSURE AND GENERALIZED FORCES FOR
COMPLEX AIRCRAFT CONFIGURATIONS
AND APPLICATION TO FLUTTER

by

Lee-Tzong Chen
B.S.M.E., National Taiwan University
(1970)

Submitted in partial fulfillment
of the requirements for the
degree of Master of Science
in Aerospace Engineering

1975

APPROVED BY

Chairman

Luigi Morino
Associate Professor of Aerospace Engineering

First
Reader

Daniel Z. Gleditsch
Professor of Aerospace Engineering

Second
Reader

Pao-Tan Hsu
Associate Professor of Systems Engineering

ABSTRACT

A general method for steady and oscillatory, subsonic and supersonic, potential linearized aerodynamic flow around complex configurations is introduced. By applying the Green function method, a linear integral equation relating the unknown, small perturbation potential on the surface of the body, to the known downwash is obtained. The surfaces of the aircraft, wake and diaphragm (if necessary) are divided into small quadrilateral elements which are approximated with hyperboloidal surfaces. The potential and its normal derivative are assumed to be constant within each element. This yields a set of linear algebraic equations. The coefficients are evaluated analytically. By using Gaussian elimination method, equations are solved for the potentials at the centroids of elements. The pressure coefficient is evaluated by the finite difference method. The lift and moment coefficients are evaluated by numerical integration. Numerical results are presented. Applications to flutter are also included.

ACKNOWLEDGEMENTS

The author would like to express his sincere appreciation to Prof. Luigi Morino for his invaluable guidance and many helpful suggestions during this research, and also for his generous assistance during the final preparation of this thesis. The author is also indebted to Profs. Daniel G. Udelson and Pao Tan Hsu for acting as readers of this thesis, as well as to Miss Ming-mei Yu for her kindness and patience in editing this thesis.

This work was supported by NASA Langley Research Center under NASA Grant NGR 22-004-030. Dr. E. Carson Yates, Jr. is the monitor of this program.

TABLE OF CONTENTS

<u>SECTION</u>		<u>PAGE</u>
1	INTRODUCTION	
1.1	Genesis of Problem	1-1
1.2	Outline of the Method	1-2
1.3	Outline of Work	1-3
2	THEORETICAL FORMULATION	
2.1	Introduction	2-1
2.2	Basic Flow Equation	2-1
2.3	Boundary Condition	2-2
2.4	Green Function Method	2-4
2.4.1	Green Theorem for Steady Subsonic Flow	2-6
2.4.2	Green Theorem for Oscillatory Subsonic Flow	2-7
2.4.3	Green Theorem for Steady Supersonic Flow	2-8
2.4.4	Green Theorem for Oscillatory Supersonic Flow	2-8
2.5	Numerical Formulation	2-9
2.6	Pressure and Pressure Coefficient	2-10
2.7	Generalized Forces	2-11
3	STEADY SUBSONIC FLOW	
3.1	Introduction	3-1
3.2	Numerical Formulation	3-1
3.3	Analytical Expressions of C_{hk} , b_{hk} and W_{hk}	3-3
3.4	Numerical Result	3-6
3.4.1	Comparison With Lifting Surface Theories	3-6
3.4.2	Comparison With Experimental Results	3-6
3.4.3	Analysis of Convergence	3-8
3.4.4	Total Lift Coefficient	3-8
3.4.5	Wing-Body Configurations	3-9
4	OSCILLATORY SUBSONIC FLOW	
4.1	Introduction	4-1
4.2	Numerical Formulation	4-1
4.3	Numerical Results	4-3
4.3.1	Comparison With Experimental Results	4-4
4.3.2	Analysis of Convergence	4-4
4.3.3	Analysis of Wake Effect	4-5
4.3.4	Results of Generalized Forces	4-6

TABLE OF CONTENTS (Continued)

<u>SECTION</u>		<u>PAGE</u>
5	STEADY SUPERSONIC FLOW	
5.1	Introduction	5-1
5.2	Numerical Formulation	5-1
5.3	Diaphragm	5-4
5.4	Numerical Results	5-5
5.4.1	Comparison With Experimental Results	5-5
5.4.2	Analysis of Convergence	5-6
5.4.3	Delta Wings	5-7
5.4.4	Circular Cone (Analysis of Diaphragm Existence)	5-8
5.4.5	Wing-Body Configuration	5-8
6	OSCILLATORY SUPERSONIC FLOW	
6.1	Introduction	6-1
6.2	Numerical Formulations	6-1
6.3	Numerical Results	6-3
6.3.1	Comparison With Experimental Results	6-3
6.3.2	Analysis of Convergence	6-4
6.3.3	Results of Generalized Forces	6-4
7	FLUTTER ANALYSIS	
7.1	Introduction	7-1
7.2	Mathematical Model	7-1
7.3	Lagrange's Equation of Motion	7-3
7.4	Generalized Forces	7-4
7.5	Aerodynamic Forces	7-5
7.6	Flutter Analysis	7-7
7.7	Numerical Results	7-8
8	CONCLUSIONS	
8.1	Introduction	8-1
8.2	General Comments	8-1
8.3	Computer Program	8-2
8.4	Computer Time and Memory Space	8-2
Appendix A — Formulations for Steady Subsonic Flow		
A.1	Introduction	A-1
A.2	Basic Equations	A-1
A.3	Doublet Integral	A-2
A.4	Source Integral	A-5
A.5	Wake Coefficient	A-7

TABLE OF CONTENTS (Continued)

<u>SECTION</u>	<u>PAGE</u>
Appendix B — Formulation for Steady Supersonic Flow	
B.1 Introduction	B-1
B.2 Doublet Integral	B-2
B.3 Source Integral	B-4
B.4 Finite Parts of Integrals	B-6
B.5 Integral Equation for Diaphragm-Attached Configuration . . .	B-10
Appendix C — Formulation for Oscillatory Flow	
C.1 Boundary Condition	C-1
C.1.1 Subsonic Flow	C-1
C.1.2 Supersonic Flow	C-4
C.2 Pressure Coefficient	C-4
C.2.1 Subsonic Flow	C-5
C.2.2 Supersonic Flow	C-5
Appendix D — Useful Equations	
D.1 Introduction	D-1
D.2 Proof of Equation (D.1)	D-1
D.3 Proof of Equation (D.2)	D-2
D.4 Proof of Equation (D.3)	D-3
D.5 Proof of Equation (D.4)	D-4
D.6 Proof of Equations (D.5) and (D.6)	D-4
D.7 Proof of Equation (D.7)	D-6
Appendix E — List of Computer Program	E-1

LIST OF ILLUSTRATIONS

Figure No.

- 1 Hyperboloidal Element.
- 2a Wing Planform.
- 2b Wake Element.
- 2c Two Types of Element-Grids for Delta Wings.
- 3 Airfoil Model for Flutter Analysis.
- 4 The distribution of $c_{l\alpha}$ along $2y/b = .7$ for a rectangular wing with $AR = 1.0$, $M = .2$, and $NX = NY = 7$ for comparison with results of Ref. 11.
- 5 The distribution of c_l along $2y/b = .707$ for a tapered swept wing with $AR = 3$, $TR = .5$, $\Lambda_{1/4} = 45^\circ$, $M = .8$, $\alpha = 5^\circ$, and $NX = NY = 7$ for comparison with results of Ref. 13.
- 6 The distribution of the section lift coefficient per unit angle of attack for a rectangular wing with $AR = 4$, $M = .507$ and $NX = NY = 7$ and 10 for comparison with results of Ref. 14.
- 7 The distribution of c_p on the upper and lower surfaces of a symmetric rectangular wing with $AR = 3$, $\tau = 5\%$, $\alpha = 0^\circ$, $M = .24$, and $NX = NY = 10$ for comparison with results of Ref. 15.
- 8a The distribution of the lift coefficient, c_l , on a symmetric rectangular wing with $AR = 3$, $\tau = 0.05$, $\alpha = 5^\circ$, $M = .24$ and $NX = NY = 7$ for comparison with results of Ref. 15.
- 8b The distribution of c_p on the upper and lower surfaces of a symmetric rectangular wing with $AR = 3$, $\tau = 0.05$, $\alpha = 5^\circ$, $M = .24$ and $NX = NY = 6$ for comparison with results of Ref. 15.
- 9 Analysis of Convergence: Potential Distribution, Φ , Versus x/c , at $y = 0$, for Rectangular Wing With Biconvex Section, in Steady Subsonic Flow, for $AR = 3$, $\tau = 0.05$, $M = 0.24$, $\alpha = 0^\circ$, $NX = NY = 5, 6, 7$.
- 10 Lift Distribution Coefficient, $c_{l\alpha}$, Versus Aspect Ratio AR , for Delta Wing in Steady Subsonic Flow, With $\tau = 0.001$, $M = 0$, $N_x = N_y = 7$. Comparison With Lifting Surface Theory of Reference 16.
- 11a The distribution of section lift coefficient, c_l , for a wing-body configuration with $\alpha_w = 6^\circ$, $\alpha_B = 0^\circ$, $\tau = 9\%$, $M = 0$, $b = 6c$, $r = 0.5c$ and 200 elements on the whole wing for the comparison with results of Ref. 17.

LIST OF ILLUSTRATIONS (Continued)

Figure No.

- 11b The distribution of $\phi_U - \phi_\ell$ along three circumferential stations for a wing-body configuration with $\alpha_w = 6^\circ$, $\alpha_B = 0^\circ$, $\tau = 9\%$, $M = 0$, $b = 6c$, $r = 0.5c$.
- 12 The distribution of lift coefficient, \tilde{c}_ℓ , for a rectangular wing oscillating in bending mode with $k = \omega c / 2U_\infty = .47$, $M = .24$, $AR = 3$, $\tau = 0.05$, $N_W = 20$, $L_W = 2.5c$ and $N_X = N_Y = 7$ for comparison with results of Ref. 15.
- 13a Analysis of Convergence: The distribution of \tilde{c}_ℓ versus x/c at $2y/b = 0.5$ for a rectangular wing oscillating in bending mode with $k = \omega c / 2V_\infty = .47$, $M = .24$, $AR = 3$, $\tau = 0.01$, $\alpha = 0^\circ$, $N_W = 30$, $L_W = 3.5c$, $N_X = N_Y = 5, 6, 7$.
- 13b Analysis of Convergence: Lift Distribution Coefficient, \tilde{c}_ℓ , Versus x/c , at $2y/b = 0.1328$, for Rectangular Wing With Biconvex Section, Oscillating in Bending Mode in Subsonic Flow, for $AR = 3$, $\tau = 0.01$, $M = 0.24$, $\alpha = 0^\circ$, $K = 0.47$, $N_W = 30$, $L_W = 3.5c$, $N_X = N_Y = 5, 6, 7$.
- 14 Analysis of Convergence: Lift Distribution Coefficient, \tilde{c}_ℓ , Versus x/c , at $2y/b = 0.1328$ for Rectangular Wing With Biconvex Section, Oscillating in Bending Mode in Subsonic Flow, for $AR = 3$, $\tau = 0.01$, $M = 0.24$, $\alpha = 0^\circ$, $K = 0.47$, $L_W = 4c$, $N_X = N_Y = 7$.
- 15 Analysis of Convergence: Lift Distribution Coefficient, \tilde{c}_ℓ , Versus x/c , at $2y/b = 0.1328$, for Rectangular Wing With Biconvex Section, Oscillating in Bending Mode in Subsonic Flow, for $AR = 3$, $\tau = 0.01$, $M = 0.24$, $\alpha = 0^\circ$, $K = 0.47$, $\Delta x_W = 0.01$, $N_X = N_Y = 7$.
- 16a Lift Coefficient, \tilde{C}_L , Versus k , for Delta Wing Oscillating in Pitch, With $AR = 4$, $\tau = 0.005$, $M = 0$, $N_X = 10$, $N_Y = 6$, $N_W = 20$, $L_W/c = 2$. Comparison With Results of Reference 18.
- 16b Moment Coefficient, \tilde{C}_M , Versus k , for Delta Wing Oscillating in Pitch With $AR = 4$, $\tau = 0.005$, $M = 0$, $N_X = 10$, $N_Y = 6$, $N_W = 20$, $L_W = 2c$. Comparison With Results of Reference 18.
- 17a Lift Coefficient, \tilde{C}_L , Versus M , for Rectangular Wing Oscillating in Pitch, With $AR = 2$, $\tau = 0.001$, $k = 1$, $N_X = 10$, $N_Y = 6$, $N_W = 20$, $L_W/c = 2$, $N_D = 30$. Comparison With Results of Reference 18.
- 17b Moment Coefficient, \tilde{C}_M , Versus M , for Rectangular Wing Oscillating in Pitch, for $AR = 2$, $\tau = 0.001$, $k = 1$, $N_X = 10$, $N_Y = 6$, $N_W = 20$, $L_W/c = 2$, $N_D = 30$. Comparison With Results of Reference 18.

LIST OF ILLUSTRATIONS (Continued)

Figure No.

- 18a Thickness effects in oscillatory subsonic and supersonic flows. Results are total lift coefficient, \tilde{C}_L , versus M , for a rectangular wing with $AR = 2$ and $K = \omega_c/2U_\infty = 1.0$ oscillating in pitch about axis $X = X_m$.
- 18b Thickness Effect in Oscillatory Subsonic and Supersonic Flows. Results are total moment coefficient, \tilde{C}_M , versus M , for a rectangular wing with $AR = 2$ and $k = \omega_c/2U_\infty = 1.0$ oscillating in pitch about axis $X = X_m$.
- 19a Lift Coefficient, \tilde{C}_L , Versus k , for Rectangular Wing Oscillating in Plunge, With $AR = 2$, $\tau = 0.001$, $M = 0$, $N_x = 10$, $N_y = 6$, $N_W = 20$, $L_W = 2c$. Comparison With Results of Reference 18.
- 19b Moment Coefficient, \tilde{C}_M , Versus k for a Rectangular Wing Oscillating in Plunge, With $AR = 2$, $\tau = 0.001$, $M = 0$, $N_x = 10$, $N_y = 6$, $N_W = 20$, $L_W = 2c$. Comparison With Results of Reference 18.
- 20a Total lift coefficient, C_L , versus M , for a rectangular wing with $AR = 2$, $\tau = 0.19$ and $k = \omega_c/2U_\infty = 1.0$ oscillating in plunge. Results are related to both subsonic and supersonic flows.
- 20b Total moment coefficient, C_M , versus M , for a rectangular wing with $AR = 2$, $\tau = 0.1\%$, and $k = \omega_c/2U_\infty$ oscillating in plunge. Results are related to both subsonic and supersonic flows (same problem as Figure 20a).
- 21 The pressure distribution on a symmetric rectangular wing with $AR = 3$, $\tau = 5\%$, $\alpha = 0^\circ$, $M = 1.3$ and $NX = NY = 7$ for the comparison with results of Ref. 15
- 22a The lift distribution on symmetric rectangular wing with $AR = 3$, $\tau = 5\%$, $\alpha = 5^\circ$, $M = 1.3$ and $NX = NY = 7$ for the comparison with results of Ref. 15.
- 22b The distribution of C_p on the upper and lower surfaces of a symmetric rectangular wing with $AR = 3$, $\tau = 5\%$, $\alpha = 5^\circ$, $M = 1.3$ and $NX = NY = 6$ for comparison with results of Ref. 15.
- 23 Analysis of Convergence: Potential Distribution, Φ , Versus x/c , at $y = 0$, for Rectangular Wing With Biconvex Section, in Steady Supersonic Flow, for $AR = 3$, $\tau = 0.05$, $M = 1.3$, $\alpha = 0^\circ$, $N_D = 3N_x$, $NX = NY = 5, 6, 7$.
- 24 Lift Distribution Coefficient, $C_{l\alpha}$, for Delta Wing With Supersonic Leading Edge, in Steady Supersonic Flow, With $B/\tan \Lambda = 1.2$, $\tau = 0$, $N_x = 8$, $N_y = 12$. Comparison With Exact, Conical-Flow Solution, Reference 20.

LIST OF ILLUSTRATIONS (Continued)

Figure No.

- 25 Lift Distribution Coefficient, $C_{l\alpha}$, for Delta Wing With Subsonic Leading Edge, in Steady Supersonic Flow, With $B/\tan \Lambda = 0.833$, $\tau = 0$, $N_x = N_y = 7$. Comparison With Exact Conical-Flow Solution, Reference 20.
- 26 Study of existence of diaphragm; the distribution of velocity potential, ϕ , for a circular cone with subsonic leading edge, $r = 1$, $\ell = 5$, $M = 2.0$ and $NX = 12$, $NY = 5$. Results obtained with and without diaphragm are compared.
- 27a The distribution of $\beta C_{l\alpha}/\alpha_w$ on the wing section for a wing-body configuration (shown in Figure 27c) with $M = 1.48$, $\alpha_w = 1.92^\circ$ and $\alpha_B = 0^\circ$, for the comparison with results of Ref. 21.
- 27b The distribution of $\beta C_{l\alpha}/\alpha_w$ on the fuselage at three circumferential stations for the same problem of Figure 27a.
- 27c Wing-body Configuration in Supersonic Flow.
- 28 Lift coefficient, \tilde{C}_l , for a rectangular wing oscillating in bending mode with $k = \omega c/2U_\infty = 0.1$, $M = 1.3$, $AR = 3$ and $NX = NY = 10$.
- 29 Analysis of Convergence: Distribution of $\hat{\xi} = \tilde{\xi} e^{i\Omega MX}$ Versus x/c , at $2y/b = 0.5$, for Rectangular Wing With Biconvex Section, Oscillating in Bending Mode in Supersonic Flow, for $AR = 3$, $\tau = 0.01$, $M = 1.3$, $K = 0.1$, $\alpha = 0^\circ$, $N_D = 3N_x$, $NX = NY = 5, 6, 7$.
- 30a C_{Lh} as a function of aspect ratio for a rectangular wing with $\tau = 0.1\%$, $M = 0$ and $NX = 8$, $NY = 10$ ($X_{EA} = -.2c$).
- 30b $C_{L\alpha}$ as a function of aspect ratio for a rectangular wing with $\tau = .1\%$, $M = 0$ and $NX = 8$, $NY = 10$ ($X_{EA} = -.2c$).
- 30c \tilde{C}_{Mh} as a function of aspect ratio for a rectangular wing with $\tau = 0.1\%$, $M = 0$ and $NX = 8$, $NY = 10$ ($X_{EA} = -.2c$).
- 30d $\tilde{C}_{M\alpha}$ as a function of aspect ratio for a rectangular wing with $\tau = 0.1\%$, $M = 0$ and $NX = 8$, $NY = 10$ ($X_{EA} = -.2c$).
- 31 Parameter $A = \omega_\alpha^2/\omega^2$ as a function of reduced frequency, $K = \omega c/2U_\infty$, for a rectangular airfoil with $AR = 16$, $M = 0$, $\omega_h/\omega_\alpha = 0.5$, $X_\alpha = 0.2$, $r_\alpha = 0.5$, $M = 5$ and $NX = 8$, $NY = 10$ ($X_{EA} = -.2c$).
- 32a Flutter speed as a function of ω_h/ω_α for a rectangular wing with $AR = 16$, $M = 0$, $\tau = 0.1\%$, $\mu = 5$, $X_\alpha = 0.2$, $r_\alpha = 0.5$, and $NX = 8$, $NY = 10$. Results are compared with exact solution given by two dimensional airfoil theory (Ref. 24) ($X_{EA} = -.2c$).

LIST OF ILLUSTRATIONS (Continued)

Figure No.

- 32b Flutter speed as a function of ω_h/ω_α for a rectangular wing with $AR = 16$, $M = 0$, $\tau = 0.1\%$, $\mu = 10$, $X_\alpha = 0.2$, $r_\alpha = 0.5$ and $NX = 8$, $NY = 10$. Results are compared with exact solution given by two dimensional airfoil theory (Ref. 24) ($X_{EA} = -.2c$).
- 33a \tilde{C}_{Lh} as a function of the reduced frequency, $k = \omega c/2U_\infty$, for a rectangular wing with $AR = 16$, $\tau = 0.1\%$, $M = 0$ and $NX = 8$, $NY = 10$. Comparison with the exact solution given by 2-D airfoil theory (Ref. 24) ($X_{EA} = -.2c$).
- 33b $\tilde{C}_{L\alpha}$ as a function of the reduced frequency, $k = \omega c/2U_\infty$ for a rectangular wing with $AR = 16$, $\tau = 0.1\%$, $M = 0$ and $NX = 8$, $NY = 10$. Comparison with the exact solution given by 2-D airfoil theory (Ref. 24) ($X_{EA} = -.2c$).
- 33c \tilde{C}_{Mh} as a function of reduced frequency, $k = \omega c/2U_\infty$ for a rectangular wing with $AR = 16$, $\tau = 0.1\%$, $M = 0$ and $NX = 8$, $NY = 10$. Comparison with the exact solution given by 2-C airfoil theory (Ref. 24) ($X_{EA} = -.2c$).
- 33d $\tilde{C}_{M\alpha}$ as a function of reduced frequency, $k = \omega c/2U_\infty$ for a rectangular wing with $AR = 16$, $\tau = 0.1\%$, $M = 0$ and $NX = 8$, $NY = 10$. Comparison with the exact solution given by 2-D airfoil theory (Ref. 24) ($X_{EA} = -.2c$).

NOMENCLATURE

\bar{a}_i	Equations (3.13) and (3.14)
A	The area of the wing planform, or ω_d^2/ω^2 in Equation (7.35)
Arg	Phase angle
AR	Aspect ratio
a	Free-stream speed of sound
b	Span
b_{hk}	Equations (3.4) and (5.4)
\hat{b}_{hk}	Equations (4.6) and (6.4)
C_k	Equation (7.44)
c_p	Pressure coefficient, $2(p - p_\infty)/\rho_\infty U_\infty^2$
c_l	Lift distribution coefficient, $C_{p_l} - C_{p_u}$
C_l	Sectional lift coefficient
C_L	Total lift coefficient
$\tilde{C}_{L\alpha}, \tilde{C}_{M\alpha}$	Total lift coefficient and total moment coefficient about axis $X = X_{EA}$ for the wing in oscillation in pitch about axis $X = X_{EA}$ per unit angle amplitude
$\tilde{C}_{Lh}, \tilde{C}_{Mh}$	Total lift coefficient and total moment coefficient about axis $X = X_{EA}$ for the wing in oscillation in plunge
C	Chord
$c_{l\alpha}$	$(\partial c_l / \partial \alpha)_{\alpha=0}$
C_{hk}	Equations (3.5) and (5.5)
\hat{C}_{hk}	Equations (4.7) and (6.5)
E	Equation (2.29)
$F_j(3,7)$	Equation (5.13)

G	Green function, Equations (2.18), (2.20), (2.22) and (2.24)
H	Heaviside function, Equation (2.34)
$I_D(\xi, \eta)$	Doublet integral, Equations (3.10), (5.8), (B.36), (B.38) and (B.40)
$I_s(\xi, \eta)$	Source integral, Equations (3.11) and (5.9)
$I_{s1}(\xi, \eta)$	Equations (5.10), (B.26), (B.27) and (B.28)
$I_{s2}(\xi, \eta)$	Equations (5.11), (B.30), (B.31) and (B.32)
$I_{s3}(\xi, \eta)$	Equations (5.12), (B.35), (B.37) and (B.39)
$I_{w1}(\eta)$	Equation (3.17)
$I_{w2}(\eta)$	Equation (3.18)
K	Reduced frequency, $\omega l / U_\infty$
l	Reference length
LW	Truncated wake length
M	Mach number, U_∞ / a_∞
\bar{n}	Equation (3.15)
\bar{N}	Outward unit normal to surface Σ_A
\bar{N}_u	Upper unit normal to surface Σ_w
\bar{N}^c	Conormal, defined in Equation (2.37)
NX, NY	Number of body elements in X, Y direction
ND	Number of diaphragm elements
NW	Number of wake elements in Σ'_K
P	Point on the surface Σ , Equation (2.40)
\bar{P}_*	Control point, (X_*, Y_*, Z_*)
\bar{q}	Equation (3.12)

$\bar{P}_C, \bar{P}_1, \bar{P}_2, \bar{P}_3$	Equation (2.41) (see Figure 1)
$\bar{P}_n, \bar{P}_d, \bar{P}_{md}$	Equations (3.19) through (3.21) (see Figure 2b)
\bar{P}_+, \bar{P}_-	Figure 2b
\bar{R}	Equation (2.27)
R	Equation (2.28)
$II \ R \ II$	Equation (2.35)
γ_α	Equation (7.8)
t	Time
T	$a_\infty \beta t / l$
TR	Taper ratio
x, y, z	Space coordinate
X, Y, Z	Nondimensional Prandtl-Glauert coordinates, Equation (2.6)
(x_M, y_M, z_M)	Moment center
X_{EA}	Location of elastic axis (see Figure 3)
X_{TE}	X-component of the trailing-edge vector (see Figure 2a)
X_α	Equation (7.8)
$\Delta (X_w)$	Incremental length of wake element
\tilde{z}	Vibration mode, Equation (C.18)
U_∞	Free-stream velocity
W_{hk}, \hat{W}_{hk}	Wake coefficient
$W_{hk}^{(TE)}$	Equation (3.16)
$\hat{W}_{hk}^{(TE)}$	Equation (4.12)

α	Angle of attack
β	$ 1 - M^2 ^{\frac{1}{2}}$
Σ	Surface surrounding body and wake
Σ_k	Surface element
Σ'_k	Wake strip emanating from the trailing element
Σ_A	Surface of aircraft
Σ_w	Surface of wake
τ	Thickness ratio
Φ	Velocity potential, $U_\infty X + \varphi$
φ	Perturbation velocity potential
ϕ	$\varphi / U_\infty l$
ϕ_D	ϕ on the diaphragm
ψ	Normal derivative of ϕ
ψ_D	ψ on the diaphragm
$\hat{\phi}$	Equations (2.31) and (2.39)
$\tilde{\phi}$	Equations (2.31) and (2.39)
$\phi_k, \hat{\phi}_k$	Values of ϕ and $\hat{\phi}$ at the centroid of surface element Σ_k
ψ_k	Values of ψ at the centroid of surface element Σ_k
Λ	Sweep angle
ω	Frequency of oscillation
ω_h	Equation (7.12)
ω_α	Equation (7.13)
Ω	Compressible reduced frequency, $\omega l / a_\infty \beta = \kappa M / \beta$

(\quad)

$(\quad)_u - (\quad)_l$

∇

Gradient in X, Y, Z space

\odot

Super product, Equation (2.36)

$\| \bar{a} \|$

Supernorm of vector \bar{a} , Equation (2.35)

SECTION 1

INTRODUCTION

1.1 GENESIS OF THE PROBLEM

The structural design of aircraft requires the evaluation of the aerodynamic loads. Aircraft structures are flexible and this flexibility is responsible for various types of aeroelastic phenomena. For instance, the static aerodynamic loads depend upon the geometry of the surface of the aircraft, while the geometry depends upon the aerodynamic loads. Therefore, it is necessary to evaluate these loads by an iterative process. In addition, the structural design is subject to aeroelastic constraints such as divergence and flutter. These constraints require accurate evaluations of steady and oscillatory loads. Again, the optimal design requires an iterative process, since the resizing of the structure changes the stability boundary. These iterative processes are best performed by computer analysis. This implies that considerable advantages are obtained if the mathematical modeling of the problem is general, flexible and efficient. The method used in this work is based upon the theoretical formulation developed by Morino (References 1 and 2). A preliminary analysis is described in Reference 3.

It may be worth noting that the usual methods for the evaluation of aerodynamic loads are the computational lifting-surface (zero-thickness wing) theories. These methods are efficient and flexible but not sufficiently general for the purpose of automated design of complex aircraft configurations. In addition, several computational methods around complex aircraft configurations have already been developed. These methods are general, but usually quite cumbersome to use and always require human intervention to define the suitable types of elements to be used. In other words, it may be safely stated that none of the other methods currently available satisfies all the requirements of generality, flexibility and efficiency necessary for automated design. Furthermore, for oscillatory flow around complex configurations, only techniques based upon the doublet-lattice method exist in subsonic range (see References 4 and 5), while no other method is available in the supersonic one.

The method used here is applicable to steady and oscillatory subsonic and supersonic flows (References 6 to 10) and provides an efficient, general, and flexible aerodynamic tool to be used for the design of aircrafts. These advantages of the present method are particularly relevant in the use of automated design.

1.2 OUTLINE OF THE METHOD

The present method is mainly based on the Green function method. By applying the Green function method, the equation of the velocity potential yields a linear equation relating the velocity potential φ , at any point, \bar{P}_* , in the flow field with the values of φ and its normal derivative on the surface Σ , surrounding the body and the wake. The integral equation is obtained by imposing that the value of the potential at \bar{P}_* approaches the value of φ on the surface, if \bar{P}_* approaches a point on the surface. In order to solve the integral equation, the surface of the aircraft and its wake is divided into small quadrilateral elements. Each element is replaced by a hyperboloidal surface defined by the four corner points of the element. The unknown φ is assumed to be constant within each element. Therefore, the integral equation reduces to a system of algebraic equations with unknown φ_K at the centroids of the elements. The coefficients are evaluated analytically. Once the distribution of the velocity potential is obtained, the pressure distribution, the lift coefficient as well as the generalized forces can be easily evaluated.

In Reference 3, the surface element is replaced by its tangent plane at the element centroids. The improvement obtained by using hyperboloidal element are that the formulation becomes general, flexible, simpler to use and more accurate since the continuity of the surface is maintained (see References 6 to 10).

The work presented here includes further developments with respect to the ones presented in Reference 8. In particular, it includes refinements and applications of the code SOSSA ACTS (Steady and Oscillatory Subsonic and Supersonic Aerodynamics for

Aerospace Complex Transportation Systems). By using this program, several numerical results have been obtained. These include comparison with ones obtained by lifting surface theory, as well as results for finite thickness wings (in both subsonic and supersonic, steady and oscillatory flow) and results with wing-body configuration (in both subsonic and supersonic steady flow). Also the evaluation of generalized forces in oscillatory subsonic and supersonic flow is introduced. The numerical results presented here include the evaluation of lift and moment coefficient. Also included are a study of the role of diaphragms in supersonic flow, a study of convergence in both subsonic and supersonic, steady and oscillatory flow and a study of the effect of the truncation of the wake in oscillatory subsonic flow. Finally, a preliminary application to flutter problem is presented.

1.3 OUTLINE OF WORK

In Section 2 the theoretical formulation is introduced. In Section 3, numerical formulation as well as numerical results for steady subsonic flow are considered. In Section 4, numerical formulation and results for oscillatory subsonic flow are considered. In Section 5, numerical formulation and results for steady supersonic flow are considered. In Section 6, numerical formulations and results for oscillatory supersonic flow are considered. Preliminary flutter analysis for a rigid model with two degrees of freedom is considered in Section 7. Finally, conclusions are given in Section 8. Details of the proof of the formulation used and a list of the computer program are given in the Appendices.

SECTION 2

THEORETICAL FORMULATION

2.1 INTRODUCTION

In this section, the theoretical formulation is briefly presented. Basic flow equations are considered in Subsection 2.2, while the boundary condition is considered in Subsection 2.3. Green theorems for subsonic and supersonic, steady and oscillatory flow, derived in References 1 and 2, are summarized in Subsection 2.4. The numerical formulation is considered in Subsection 2.5. The evaluation of pressure coefficient and generalized forces are considered in Subsections 2.6 and 2.7, respectively.

2.2 BASIC FLOW EQUATION

The aerodynamic forces are derived from the equations which relates the flow properties to the geometry of the lifting bodies. For many practical applications, the flow may be assumed to be inviscid, isentropic, and initially irrotational. In this case, the flow is described by the velocity potential Φ . In addition, the perturbation of the flow is assumed to be small, so that the linearized equation may be used.

The equation of the unsteady aerodynamic potential, is

$$a^2 \nabla^2 \Phi = \frac{D_c^2 \Phi}{D t^2} \quad (2.1)$$

where a is the speed of sound, ∇^2 is the Laplacian operator, and

$$\frac{D_c}{D t} = \frac{\partial}{\partial t} + \nabla \Phi \cdot \nabla \quad (2.2)$$

is the total time derivative. The subscript "c" reminds that $\nabla \Phi$ should be treated as a constant in order to obtain the second total time derivative.

Consider a frame of reference such that the undisturbed flow has velocity, U_∞ , in the direction of the positive x-axis. By introducing the perturbation potential φ , such that

$$\Phi = U_\infty x + \varphi \quad (2.3)$$

(where φ represents perturbation velocity which is assumed to be small with respect to U_∞) and neglecting higher order terms, Equation (2.1) reduces to the linearized equation for the potential flow

$$\nabla^2 \varphi - \frac{1}{a_\infty^2} \frac{d^2 \varphi}{dt^2} = 0 \quad (2.4)$$

where a_∞ is the free-stream speed of sound, while

$$\frac{d}{dt} = \frac{\partial}{\partial t} + U_\infty \frac{\partial}{\partial x} \quad (2.5)$$

is the linearized total time derivative. For simplicity, the following nondimensional Prandtl-Glauert coordinates are introduced

$$X = x/\beta l, \quad Y = y/l, \quad Z = z/l, \quad \phi = \varphi/U_\infty l \quad (2.6)$$

with

$$\beta = \sqrt{1 - M^2} \quad (2.7)$$

for subsonic flow and

$$\beta = \sqrt{M^2 - 1} = B \quad (2.8)$$

for supersonic flow.

2.3 BOUNDARY CONDITION

The lifting body considered here has arbitrary shape and its motion consists of

small vibrations of arbitrary nature. Thus, the surface of the body is represented in general form by

$$S(x, y, z, t) = 0 \quad (2.9)$$

Then, the boundary condition on the body is given by

$$\frac{D_c S}{Dt} = \frac{\partial S}{\partial t} + \nabla \Phi \cdot \nabla S = 0 \quad (2.10)$$

By using Equation (2.3), Equation (2.10) yields the boundary condition for unsteady flow,

$$\nabla \varphi \cdot \nabla S = - \frac{1}{U_\infty} \left(\frac{\partial S}{\partial t} + U_\infty \frac{\partial S}{\partial x} \right) \quad (2.11)$$

Furthermore, the boundary condition at infinity is given by $\varphi \equiv 0$, because the flow is assumed to be uniform at infinity. In the following, the analysis is limited to steady state flow. In this case, Equation (2.11) yields the steady-state boundary condition

$$\nabla \varphi \cdot \bar{n}_s = - \eta_x \quad (2.12a)$$

Consider the subsonic case first. By using the subsonic nondimensional Prandtl-Glauert coordinates given by Equations (2.6) and (2.7), Equation (2.12a) yields

$$\begin{aligned} & \left(\frac{\partial S}{\partial x} \frac{\partial \varphi}{\partial x} + \frac{\partial S}{\partial y} \frac{\partial \varphi}{\partial y} + \frac{\partial S}{\partial z} \frac{\partial \varphi}{\partial z} \right) + \frac{\partial S}{\partial x} \\ &= \left(\frac{1}{\beta^2} \frac{\partial S}{\partial x} \frac{\partial \phi}{\partial x} + \frac{\partial S}{\partial y} \frac{\partial \phi}{\partial y} + \frac{\partial S}{\partial z} \frac{\partial \phi}{\partial z} \right) + \frac{1}{\beta} \frac{\partial S}{\partial x} \\ &= \left(\frac{\partial S}{\partial x} \frac{\partial \phi}{\partial x} + \frac{\partial S}{\partial y} \frac{\partial \phi}{\partial y} + \frac{\partial S}{\partial z} \frac{\partial \phi}{\partial z} \right) + \left(\frac{1}{\beta^2} - 1 \right) \frac{\partial S}{\partial x} \frac{\partial \phi}{\partial x} + \frac{1}{\beta} \frac{\partial S}{\partial x} \\ &= \frac{\partial \phi}{\partial N} + \frac{M^2}{1-M^2} N_x \frac{\partial \phi}{\partial x} + \frac{N_x}{\beta} = 0 \end{aligned} \quad (2.12b)$$

where N_x is the component of \bar{N} along x-axis (direction of the undisturbed flow).

Therefore,

$$\frac{\partial \phi}{\partial N} = -N_x \left(\frac{1}{\beta} + \frac{M^2}{1-M^2} \frac{\partial \phi}{\partial x} \right) \quad (2.13a)$$

The second term on the right hand side is of higher order (see Subsection C.1)*.

Therefore, Equation (2.13a) may be approximated as

$$\frac{\partial \phi}{\partial N} = - \frac{N_x}{\beta} \quad (2.13b)$$

Next, consider the steady supersonic flow. In this case, the boundary condition is still given by Equation (2.12a). By using the supersonic nondimensional Prandtl-Glauert coordinates, given by Equations (2.6) and (2.8), and following the same procedure to obtain Equation (2.12b), one obtains

$$\frac{\partial \phi}{\partial N^c} = -N_x \left(\frac{1}{\beta} + \frac{M^2}{M^2-1} \frac{\partial \phi}{\partial x} \right) \quad (2.14a)$$

where $\bar{N}^c = (-N_x, N_y, N_z)$ is the conormal derivative.

Similarly, by neglecting the second term on the right-hand side, Equation (2.14a) may be approximated as

$$\frac{\partial \phi}{\partial N^c} = - \frac{N_x}{\beta} \quad (2.14b)$$

For clarity and conciseness, the boundary condition as well as the evaluation of the pressure coefficient for oscillatory flow are not derived here, but are presented in Appendix C.

2.4 GREEN FUNCTION METHOD

Observe that Equation (2.4) is a second order linear partial differential

*This is true everywhere on the surface of the aircraft except at the stagnation point.

equation with boundary conditions given by Equation (2.11) on the surface of the body and $\phi = 0$ at infinity.

The definition of the Green function of Equation (2.4) is given as

$$\nabla^2 G - \frac{1}{a_\infty^2} \frac{d^2 G}{dt^2} = \delta(x-x_1, y-y_1, z-z_1, t-t_1) \quad (2.15)$$

with

$$G = 0 \text{ at infinity} \quad (2.16)$$

where δ is the Dirac delta function defined by

$$\iiint_{-\infty}^{\infty} F(x, y, z, t) \delta(x-x_1, y-y_1, z-z_1, t-t_1) dx dy dz dt = F(x_1, y_1, z_1, t_1) \quad (2.17)$$

The solution of G are derived for instance in Reference 1. For steady subsonic flow, G is given by

$$G = \frac{1}{4\pi R} \quad (2.18)$$

with

$$R = \left\{ (x-x_1)^2 + \beta^2 [(y-y_1)^2 + (z-z_1)^2] \right\}^{1/2} \quad (2.19)$$

For oscillatory subsonic flow, G is given by

$$G = -\frac{1}{4\pi R} \delta(t_1 - t + T) \quad (2.20)$$

where $\delta(t_1 - t + T)$ is the usual Dirac delta function and

$$T = \frac{1}{a_\infty \beta^2} \{ R - M(x-x_1) \} \quad (2.21)$$

with R given by Equation (2.19) and $\beta = \sqrt{1-M^2}$

For steady supersonic flow, G is given by

$$G = - \frac{1}{2\pi R} \quad (2.22)$$

with

$$R = \left\{ (X-X_1)^2 - \beta^2 [(Y-Y_1)^2 + (Z-Z_1)^2] \right\}^{1/2} \quad (2.23)$$

For oscillatory supersonic flow, G is given by

$$G = - \frac{1}{4\pi R} \left[\delta(t_1 - t + T^-) + \delta(t_1 - t + T^+) \right] \quad (2.24)$$

where

$$T^\pm = \frac{1}{a_\infty \beta^2} \left[M (X - X_1) \pm R \right] \quad (2.25)$$

with R given by Equation (2.23) and $\beta = \sqrt{M^2 - 1}$

2.4.1 Green Theorem for Steady Subsonic Flow

By applying the Green function method and using Equation (2.18) the linearized equation of the steady subsonic aerodynamic potential flow can be rewritten as

$$\begin{aligned} 4\pi E(\bar{P}_*) \phi(\bar{P}_*) = & - \oint_{\Sigma_A} \frac{\partial \phi}{\partial N} \frac{1}{R} d\Sigma_A + \oint_{\Sigma_A} \phi \frac{\partial}{\partial N} \left(\frac{1}{R} \right) d\Sigma_A \\ & + \oint_{\Sigma_w} \Delta \phi \frac{\partial}{\partial N_u} \left(\frac{1}{R} \right) d\Sigma_w \end{aligned} \quad (2.26)$$

with nondimensional Prandtl-Glauert coordinates. Where Σ_A and Σ_w are the surfaces of the aircraft and the wake in X, Y, Z coordinate system, while \bar{N} is the outward unit normal to Σ_A , \bar{N}_u is the upper unit normal to Σ_w and \bar{R} is the vector pointing from any point, $\bar{P}_* = (X_*, Y_*, Z_*)$, in the flow field to the dummy point on surface Σ_A or Σ_w ,

$$\bar{R} = (X - X_*) \bar{i} + (Y - Y_*) \bar{j} + (Z - Z_*) \bar{k} \quad (2.27)$$

Moreover

$$R = |\bar{R}| = [(X - X_*)^2 + (Y - Y_*)^2 + (Z - Z_*)^2]^{1/2} \quad (2.28)$$

while E is the domain function, which is defined as (see Reference 1)

$$\begin{aligned} E(\bar{P}_*) &= 1 && \text{outside } \Sigma_A \\ &= 1/2 && \text{on } \Sigma_A \\ &= 0 && \text{inside } \Sigma_A \end{aligned} \quad (2.29)$$

2.4.2 Green Theorem for Oscillatory Subsonic Flow

By applying Green function method and using Equation (2.20), the linearized equation of the oscillatory subsonic aerodynamic potential flow yields the Green theorem for oscillatory subsonic flow as

$$\begin{aligned} 4\pi E(P_*) \hat{\phi}(P_*) &= - \iint_{\Sigma_A} \frac{\partial \hat{\phi}}{\partial N} \frac{e^{-i\Omega R}}{R} d\Sigma_A + \iint_{\Sigma_A} \hat{\phi} \frac{\partial}{\partial N} \left(\frac{e^{-i\Omega R}}{R} \right) d\Sigma_A \\ &+ \iint_{\Sigma_w} \Delta \hat{\phi} \frac{\partial}{\partial N_u} \left(\frac{e^{-i\Omega R}}{R} \right) d\Sigma_w \end{aligned} \quad (2.30)$$

where X, Y, Z , and $\Sigma_A, \Sigma_w, N, N_u, R, E$ are defined in Subsection 2.4.1.

while $\hat{\phi}$ is such that

$$\begin{aligned} \phi(X, Y, Z, T) &= \tilde{\phi}(X, Y, Z) e^{i\Omega T} \\ &= \hat{\phi}(X, Y, Z) e^{i\Omega(T + MX)} \end{aligned} \quad (2.31)$$

with

$$T = a_\infty \beta t / \ell \quad \Omega = \omega \ell / a_\infty \beta = KM / \beta \quad (2.32)$$

where ω is natural frequency and K is the dimensionless reduced frequency, $K = \omega \ell / U_\infty$.

2.4.3 Green Theorem for Steady Supersonic Flow

By applying the Green function method and using Equation (2.22), the linearized equation of the steady supersonic aerodynamic potential flow can be rewritten as

$$2\pi E(\bar{p}_*) \phi(\bar{p}_*) = - \oint_{\Sigma_A} \frac{\partial \phi}{\partial N^c} \frac{H}{\|\bar{R}\|} d\Sigma_A + \oint_{\Sigma_A} \phi \frac{\partial}{\partial N^c} \left(\frac{H}{\|\bar{R}\|} \right) d\Sigma_A \quad (2.33)$$

where

$$H = 1 \quad \text{for } X_* - X > \left\{ (Y_* - Y)^2 + (Z_* - Z)^2 \right\}^{1/2}$$

$$= 0 \quad \text{for } X_* - X \leq \left\{ (Y_* - Y)^2 + (Z_* - Z)^2 \right\}^{1/2} \quad (2.34)$$

$\|\bar{R}\|$ is the "supernorm" of vector \bar{R} and is defined by

$$\|\bar{R}\| = |\bar{R} \odot \bar{R}|^{1/2} \quad (2.35)$$

with the "super-product," \odot , defined by

$$\bar{a} \odot \bar{b} = a_x b_x - a_y b_y - a_z b_z \quad (2.36)$$

and the conormal derivative $\partial/\partial N^c$ is given by

$$\frac{\partial}{\partial N^c} \equiv -N_x \frac{\partial}{\partial X} + N_y \frac{\partial}{\partial Y} + N_z \frac{\partial}{\partial Z} = -N \odot \nabla \quad (2.37)$$

while \bar{R} and E are defined in Subsection 2.4.1

2.4.4 Green Theorem for Oscillatory Supersonic Flow

By applying the Green function method and using Equation (2.24) the linearized equation for the oscillatory supersonic aerodynamic potential flow yields the Green Theorem for oscillatory supersonic flow,

$$\begin{aligned}
2\pi E(\bar{p}_*) \phi(\bar{p}_*) = & - \iint_{\Sigma} \frac{\partial \hat{\phi}}{\partial N^c} \frac{H}{\|R\|} \cos \Omega \|R\| d\Sigma \\
& + \iint_{\Sigma} \hat{\phi} \frac{\partial}{\partial N^c} \left(\frac{H}{R} \cos \Omega \|R\| \right) d\Sigma
\end{aligned} \tag{2.38}$$

where $\hat{\phi}$ is such that

$$\phi(x, y, z, t) = \tilde{\phi}(x, y, z) e^{i\omega t} = \hat{\phi}(x, y, z) e^{i(\omega t - Mx)} \tag{2.39}$$

while the other parameters are defined in Subsections 2.4.1 and 2.4.3.

2.5 NUMERICAL FORMULATION

The integral equations given in Equations (2.26), (2.30), (2.33) and (2.38) can be solved by replacing the surface of the aircraft and wake by a finite number of quadrilateral hyperboloidal elements. Thus, the integral over Σ becomes a summation of a finite number of integrals over hyperboloidal surfaces which represent the surface of each element on Σ .

The general expression for the hyperboloidal surface is

$$\begin{aligned}
\bar{p}(\xi, \eta) = & \bar{p}_c + \xi \bar{p}_1 + \eta \bar{p}_2 + \xi \eta \bar{p}_3 \\
-1 \leq \xi \leq 1, \quad & -1 \leq \eta \leq 1
\end{aligned} \tag{2.40}$$

where \bar{p}_c , \bar{p}_1 , \bar{p}_2 and \bar{p}_3 are defined in terms of the four corner position vectors, $\bar{p}(1,1)$, $\bar{p}(1,-1)$, $\bar{p}(-1,1)$ and $\bar{p}(-1,-1)$.

$$\begin{aligned}
\bar{p}_c = & \frac{1}{4} [\bar{p}(1,1) + \bar{p}(1,-1) + \bar{p}(-1,1) + \bar{p}(-1,-1)] \\
\bar{p}_1 = & \frac{1}{4} [\bar{p}(1,1) + \bar{p}(1,-1) - \bar{p}(-1,1) - \bar{p}(-1,-1)] \\
\bar{p}_2 = & \frac{1}{4} [\bar{p}(1,1) - \bar{p}(1,-1) + \bar{p}(-1,1) - \bar{p}(-1,-1)] \\
\bar{p}_3 = & \frac{1}{4} [\bar{p}(1,1) - \bar{p}(1,-1) - \bar{p}(-1,1) + \bar{p}(-1,-1)]
\end{aligned} \tag{2.41}$$

Assume that the values of the velocity potential and its normal derivative within each element are constant. Then the integrand of each surface integral become purely a function of the vector, \bar{r}_* and the geometry of the surface element on Σ . By using Equation (2.40), the analytical expression for each element-integral can be obtained. Finally, a system of linear equation relate computed coefficients to the unknown, ϕ_k , at the centroid of element, Σ_k . The system is solved for ϕ_k by using the Gaussian elimination method.

2.6 PRESSURE AND PRESSURE COEFFICIENT

The pressure on the aircraft is evaluated from the linearized Bernoulli Theorem

$$p - p_\infty = -p_\infty \left(\frac{\partial \psi}{\partial t} + U_\infty \frac{\partial \psi}{\partial x} \right) \quad (2.42a)$$

Therefore, the pressure coefficient is

$$\begin{aligned} C_p &= (p - p_\infty) / \frac{1}{2} \rho_\infty U_\infty^2 = - \frac{2}{U_\infty^2} \left(\frac{\partial \psi}{\partial t} + U_\infty \frac{\partial \psi}{\partial x} \right) \\ &= - \frac{2}{U_\infty^2} \frac{d\psi}{dt} \end{aligned} \quad (2.42b)$$

For steady flow, by using nondimensional Prandtl-Glauert coordinates given in Equation (2.6), Equation (2.42b) is reduced to

$$C_p = - 2 \frac{\partial \phi}{\partial x} \quad (2.43)$$

For oscillatory flow, details on the calculation of C_p are given in Appendix C. For all the results presented here, the pressure coefficient is evaluated by finite different method.

2.7 GENERALIZED FORCES

The evaluation of the generalized forces, used for the flutter analysis, is presented in this section. The generalized forces are defined as

$$Q_h = - \iint p \bar{n} \cdot \bar{U}_h d\Sigma \quad (2.44)$$

where $p \bar{n}$ is the force acting on the surface of the body, and \bar{U}_h is a prescribed shape-function (mode). Two rigid body modes are considered in this section: they correspond to the lift force and the pitch moment. For the lift force,

$$\bar{U}_h = \bar{k} \quad (2.45)$$

therefore,

$$\begin{aligned} \bar{L} &= - \iint p n_z d\Sigma \\ &= \iint (p_\ell - p_u) dx dy \end{aligned} \quad (2.46)$$

where n_z is the z component of the unit surface normal. The subscript "ℓ" and "n" refer to the lower and upper elements. For a thin wing, \tilde{C}_L is evaluated as follows (see Equation C.31))

$$\begin{aligned} \tilde{C}_L &= - \frac{1}{A} \iint_{\Sigma_A} \Delta \tilde{C}_p dx dy \\ &= +2 \frac{\ell}{A} \int_{-\frac{b}{2}}^{\frac{b}{2}} dy \int_{x_{LE}}^{x_{TE}} \frac{\partial}{\partial x} (\Delta \tilde{\phi}) dx + \frac{2K_i}{A} \iint_{\Sigma_A} (\Delta \tilde{\phi}) dx dy \\ &= \frac{2\ell}{A} \int_{-\frac{b}{2}}^{\frac{b}{2}} (\Delta \tilde{\phi})_{x_{TE}} dy + \frac{2K_i}{A} \iint_{\Sigma_A} (\Delta \tilde{\phi}) dx dy \\ &= \frac{2\ell}{A} \sum_{j=1}^M [(\Delta \tilde{\phi})_{x_{TE}}]_j (\Delta y)_j + \frac{2K_i}{A} \sum_{h=1}^M \sum_{j=1}^M (\Delta \phi)_{hj} A_{hj} \end{aligned} \quad (2.47)$$

where

$$\Delta C_D = C_{D0} - C_{Dl} \quad (2.48)$$

and A is the total projected area of the wing on x - y plane, l is the reference length, $X_{LE}(y)$ and $X_{TE}(y)$ are the x -component of vectors pointing to the leading edge and the trailing edge.

For the pitch moment, the mode is given by

$$\bar{U}_h = -(z - z_M) \bar{i} + (x - x_M) \bar{k} \quad (2.49)$$

and corresponds to a rigid body rotation (around the axis $X = x_M, Z = z_M$) which is positive if the leading edge moves downward. Therefore,

$$\begin{aligned} \bar{M} &= \iint -p \bar{n} \cdot [-(z - z_M) \bar{i} + (x - x_M) \bar{k}] d\Sigma \\ &= - \iint p [-(z - z_M) n_x + (x - x_M) n_z] d\Sigma \\ &\cong + \iint (C_p - p_u) (x - x_M) dx dy \end{aligned} \quad (2.50)$$

Note that the term with $p(z - z_M)n_x$ is negligible because both $z - z_M$ and n_x are small. For a thin wing the pitch moment coefficient is evaluated as follows (see Equation C.31))

$$\begin{aligned} \tilde{C}_M &= + \frac{1}{Al} \iint_{\Sigma_1} A \tilde{C}_p (x - x_M) dx dy \\ &= - \frac{2}{Al} \int_{-\frac{b}{2}}^{\frac{b}{2}} dy \int_{X_{LE}}^{X_{TE}} [l \frac{\partial}{\partial x} (\Delta \phi) + iK(\Delta \phi)] (x - x_M) dx dy \\ &= - \frac{2}{Al} \int_{-\frac{b}{2}}^{\frac{b}{2}} dy \left\{ l (\Delta \tilde{\phi})_{X_{TE}} (x_{TE} - x_M) + \int_{X_{LE}}^{X_{TE}} [l - iK(x - x_M)] (\Delta \tilde{\phi}) dx \right\} \end{aligned}$$

$$\begin{aligned}
&= +2 \frac{1}{A} \sum_{j=1}^{NY} (\Delta \tilde{\phi})_j (x_{TE} - x_M)_j (\Delta y)_j \\
&+ 2 \frac{1}{A} \sum_{h=1}^{NX} \sum_{j=1}^{NY} (\Delta \phi)_{hj} \left[1 - K_i \frac{(x_c - x_M)}{l} \right] A_{hj}
\end{aligned}
\tag{2.51}$$

SECTION 3

STEADY SUBSONIC FLOW

3.1 INTRODUCTION

In Subsection 3.2, the numerical formulation for steady subsonic flow, derived in Reference 6, is outlined. For completeness, the proof of this formulation is given in Appendix A. Numerical results are presented in Subsection 3.4.

3.2 NUMERICAL FORMULATION

Consider the Green theorem for steady subsonic flow. According to Equation (2.26)

$$4\pi E(\bar{P}^*)\phi(\bar{P}^*) = - \iint_{\Sigma_A} \frac{\partial \phi}{\partial N} \frac{1}{R} d\Sigma_A + \iint_{\Sigma_A} \phi \frac{\partial}{\partial N} \left(\frac{1}{R} \right) d\Sigma_A + \iint_{\Sigma_w} \phi \frac{\partial}{\partial N_u} \left(\frac{1}{R} \right) d\Sigma_w \quad (3.1)$$

with boundary condition, given by Equation (2.13b) as

$$\frac{\partial \phi}{\partial N} = - N_x / \beta \quad (3.2)$$

By imposing that the value of the potential at \bar{P}^* approaches that at a point \bar{P} on the surface Σ_A , if \bar{P}^* approaches \bar{P} , the value of $E(\bar{P}^*)$ on the surface is found to be $1/2$ (Reference 1), and an integral equation relating the potential on the surface Σ_A to its normal derivative is obtained.

Divide the surface Σ_A into N small quadrilateral elements, Σ_k , assume that the values of ϕ and $\frac{\partial \phi}{\partial N}$ are constant within each element, and impose that

Equation (3.1) is satisfied at the centroid, \bar{P}_h , of each element Σ_h . This yields N simultaneous linear equations, which can be expressed in the following matrix form:

$$\left[\delta_{hk} - C_{hk} - W_{hk} \right] \left\{ \phi_k \right\} = \left[b_{hk} \right] \left\{ \left(\frac{\partial \phi}{\partial N} \right)_k \right\} \quad (3.3)$$

where δ_{hk} is the Kronecker delta

$$C_{hk} = \left[\frac{1}{2\pi} \iint_{\Sigma_k} \frac{\partial}{\partial N} \left(\frac{1}{R} \right) d\Sigma_k \right]_{\bar{P}_* = \bar{P}_h} \quad (3.4)$$

$$b_{hk} = \left[-\frac{1}{2\pi} \iint_{\Sigma_k} \frac{1}{R} d\Sigma_k \right]_{\bar{P}_* = \bar{P}_h} \quad (3.4)$$

The coefficients W_{hk} represent the influence of the wake. These are obtained as follows¹: the wake is assumed to be composed of straight vortex lines emanating from the trailing edge; the wake surface is divided into strips. The coefficient $W_{hk} = 0$, if the element Σ_k is not in contact with the trailing edge, while for the elements Σ_k in contact with the trailing edge

$$W_{hk} = W_{hk}^{(TE)} \quad (3.6)$$

with

$$W_{hk}^{(TE)} = \left[\pm \frac{1}{2\pi} \iint_{\Sigma_k'} \frac{\partial}{\partial N_u} \left(\frac{1}{R} \right) d\Sigma_k' \right]_{\bar{P}_* = \bar{P}_h} \quad (3.7)$$

where Σ'_k is the strip of the wake, bounded by two streamlines emanating from the element Σ_k . The upper (lower) sign holds for point \bar{P}_h on the upper (lower) surface of the aircraft.

Since no pressure difference can exist on the wake, $\Delta\phi$ of the wake is constant along a streamline emanating from the trailing edge, and therefore, equal to $\Delta\phi$ at the trailing edge, or approximately, $\Delta\phi$ at the centroids of the elements adjacent to the trailing edge. Therefore, in deriving Equation (3.3), the values of $\Delta\phi$ on the wake are approximated with the values of $\Delta\phi$ at the centroids of the elements adjacent to the trailing edge.

3.3 ANALYTICAL EXPRESSIONS OF C_{hk} , b_{hk} and W_{hk}

The integrals in Equations (3.4), (3.5) and (3.7) are evaluated analytically by approximating the surface of each element with a hyperboloidal surface described in Subsection 2.5. The derivations are given in Reference 6 and are outlined here in Appendix A. The expressions for C_{hk} and b_{hk} are given by

$$C_{hk} = I_D(1, 1) - I_D(1, -1) - I_D(-1, 1) + I_D(-1, -1) \quad (3.8)$$

$$b_{hk} = I_S(1, 1) - I_S(1, -1) - I_S(-1, 1) + I_S(-1, -1) \quad (3.9)$$

with

$$I_D(\xi, \eta) = \frac{1}{2\pi} \tan^{-1} \left(\frac{-\bar{q} \times \bar{a}_1 \cdot \bar{q} \times \bar{a}_2}{|\bar{q}| \bar{q} \cdot \bar{a}_1 \times \bar{a}_2} \right) \quad (3.10)$$

(The subscript p reminds that the principal value of \tan^{-1} from $-\frac{\pi}{2}$ to $\frac{\pi}{2}$ should be considered) and

$$\begin{aligned}
 I_s(\xi, \eta) = & -\frac{1}{2\pi} \left\{ -\bar{q} \times \bar{a}_1 \cdot \bar{n} \frac{1}{|\bar{a}_1|} \ln |\bar{q}| |\bar{a}_1| + \bar{q} \cdot \bar{a}_1 \right. \\
 & + \bar{q} \times \bar{a}_2 \cdot \bar{n} \frac{1}{|\bar{a}_2|} \ln |\bar{q}| |\bar{a}_2| + \bar{q} \cdot \bar{a}_2 \\
 & \left. + \bar{q} \cdot \bar{n} \tan_p^{-1} \left(\frac{-\bar{q} \times \bar{a}_1 \cdot \bar{q} \times \bar{a}_2}{|\bar{q}| \bar{q} \cdot \bar{a}_1 \times \bar{a}_2} \right) \right\}
 \end{aligned} \quad (3.11)$$

where

$$\bar{q}(\xi, \eta) = \bar{p}_0 + \xi \bar{p}_1 + \eta \bar{p}_2 + \xi \eta \bar{p}_3 - \bar{p}_h \quad (3.12)$$

$$\bar{a}_1 = \bar{p}_1 + \eta \bar{p}_3 \quad (3.13)$$

$$\bar{a}_2 = \bar{p}_2 + \xi \bar{p}_3 \quad (3.14)$$

$$\bar{n} = \frac{\bar{a}_1 \times \bar{a}_2}{|\bar{a}_1 \times \bar{a}_2|} \quad (3.15)$$

Furthermore, the expression for $W_{hk}^{(TE)}$ may be obtained by taking the limit of I_D in Equation (3.10) by letting $|\bar{a}_1|$ go to infinity. The derivation is given in Appendix A.4. The expression of $W_{hk}^{(TE)}$ is then given as

$$W_{hk}^{(TE)} = I_{w_1}(1) - I_{w_2}(1) - I_{w_1}(-1) + I_{w_2}(-1) \quad (3.16)$$

with

$$I_{w1}(\eta) = \frac{1}{2\pi} \tan^{-1} \frac{\bar{p}_m \cdot \bar{p}_m - (\bar{p}_m \cdot \bar{i}_x)(\bar{p}_d \cdot \bar{i}_x)}{\bar{p}_m \cdot \bar{i}_x \times \bar{p}_d} \quad (3.17)$$

$$I_{w2}(\eta) = \frac{1}{2\pi} \tan^{-1} \frac{-(\bar{p}_m \cdot \bar{p}_m)(\bar{i}_x \cdot \bar{p}_d) + (\bar{p}_m \cdot \bar{p}_d)(\bar{p}_m \cdot \bar{i}_x)}{|\bar{p}_m| \bar{p}_m \cdot \bar{i}_x \times \bar{p}_d} \quad (3.18)$$

($\eta = 1, -1$)

where

$$\bar{p}_m = (\bar{p}_+ + \bar{p}_-)/2 - \bar{p}_h \quad (3.19)$$

$$\bar{p}_d = (\bar{p}_+ - \bar{p}_-)/2 \quad (3.20)$$

$$\bar{p}_m = \bar{p}_m + \eta \bar{p}_d \quad (3.21)$$

In the above equations, \bar{p}_+ and \bar{p}_- are the two corner points of the element, Σ_h , which are on the trailing edge. (See Figure 2b). Equation (3.3) can be solved numerically to yield the values of ϕ_K . Once the ϕ_K are obtained, the pressure can be evaluated from the linearized Bernoulli Theorem, given by Equation (2.43).

3.4 NUMERICAL RESULTS

Numerical results obtained for steady subsonic flow are presented here. In Subsection 3.4.1, the results are compared with those obtained by the lifting surface theory. Comparison with experimental results are considered in Subsection 3.4.2. Analysis of convergence is considered in Subsection 3.4.3. The evaluation of the lift coefficient is given in Subsection 3.4.4. Finally, the pressure distribution coefficient of a wing-body configuration is presented in Subsection 3.4.5.

3.4.1 Comparison With Lifting Surface Theories

Comparison with various lifting surface theories are presented in Figures 4 - 7. Figure 4 shows the lift distribution per unit angle of attack, $C_{l\alpha}$, for a rectangular wing with $AR = 1$ and $M = .2$. The results, obtained with $NX = NY = 7$ are compared with the ones of Cunningham¹¹ and Kulakowski and Haskell.¹² Figure 5 shows the distribution of C_l for a tapered swept wing with aspect ratio $AR = 3$, taper ratio $TR = .5$, $\alpha = 5^\circ$, sweep angle along quarter chord $\Lambda_{1/4} = 45^\circ$ and Mach number $M = .8$. The results obtained with $NX = NY = 7$ are compared with ones of Cunningham¹¹ and Kolbe and Boltz.¹³ Figure 6 shows the distribution of the section lift coefficient per unit angle of attack, $C_{l\alpha}$, for a rectangular wing with aspect ratio, $AR = 4$ and Mach number $M = .507$. The result, obtained with $NX = NY = 7$ and 10, are compared with the ones by Yates.¹⁴

All these results are in good agreement with the existing one. Thickness ratio used in evaluating the above results is chosen to be 0.1%. The reasons to choose this value is that, as shown in Reference 3, the solution with $\tau = 0.1\%$ is a good approximation for the zero thickness solution and that values of thickness ratio smaller than 0.01% may cause elimination of significant figures.

3.4.2 Comparison With Experimental Results

Figures 7, 8a and 8b present a comparison with the experimental results of Lessing, Troutman and Menees.¹⁵ The results are relative to a rectangular wing with aspect ratio $AR = 3$. The airfoil consists of a biconvex circular arc section with 5 percent thickness and with sharp leading and trailing edges. Figure 7 shows the pressure

distribution on the upper and the lower surfaces, C_{p_u} and C_{p_l} , versus x/c at $2y/b = 0, 0.5, 0.7$ and 0.9 for the above mentioned wing with $\alpha = 0^\circ$ and $M = 0.24$.

Figure 8a shows the lift distribution, C_l , versus x/c at $2y/b = 0, 0.5, 0.7$ and 0.9 for the above mentioned wing with $\alpha = 5^\circ$ and $M = 0.24$, while Figure 8b shows the pressure distribution on the upper and the lower surface, C_{p_u} and C_{p_l} , versus x/c at $2y/b = 0, 0.5, 0.7$ and 0.9 for the above mentioned wing with $\alpha = 5^\circ$ and $M = 0.24$.

It should be mentioned that the results for Figure 8a are obtained by taking the advantage of antisymmetry. If the velocity potential, ϕ , is separated into two parts, symmetric part, ϕ_s , and antisymmetric part, ϕ_{as} , then the difference of the velocity potential on the upper and lower surfaces of the wing is twice the value of ϕ_{as} while the velocity potential on the upper surface of the wing is $\phi_u = \phi_s + \phi_{as}$ and the velocity potential on the lower surface is $\phi_l = \phi_s - \phi_{as}$. The value of ϕ_{as} can be obtained by taking advantage of antisymmetry while the value of ϕ_s can be obtained by taking advantage of symmetry. This is mainly because the doublet, source and wake integrals are nearly independent of angle of attack, α . Therefore C_{hk} , b_{hk} and w_{hk} can be evaluated at $\alpha = 0$, while the only α -dependent term in Equation (3.3) is the linearized boundary term, $\frac{\partial \phi}{\partial n}$, which can be separated into symmetric and antisymmetric as follows: Set

$$\begin{aligned} \frac{\partial \phi}{\partial n} &= -n_x = -[(n_x)_{\alpha=0} \cos \alpha \pm (n_z)_{\alpha=0} \sin \alpha] \\ &= -(n_x)_{\alpha=0} \mp (n_z)_{\alpha=0} \alpha \end{aligned} \quad (3.22)$$

and as mentioned before,

$$\phi = \phi_s \pm \phi_{as} \quad (3.23)$$

where $(n_x)_{\alpha=0}$ and $(n_z)_{\alpha=0}$ are the x-component and z-component of the surface unit normal. The upper (or lower) sign holds for the upper (or lower) surface. A similar example of the symmetric and antisymmetric problem is given in Section B.5. It may be worth noting that the results for Figure 8b are obtained by directly solving ϕ , or with C_{hk} , b_{hk} and W_{hk} evaluated at $\alpha = 5^\circ$. However, the lift coefficient obtained by subtracting C_{pe} from C_{pu} is consistent with results obtained for Figure 8a.

3.4.3 Analysis of Convergence

Figure 9 presents a study of convergence of the values of ϕ_k in terms of the number of elements. The wing is the same as that of Figure 7 with $\alpha = 0^\circ$ and $M = 0.24$. In the results shown in Figure 9, there is a sharp change of the values near the leading edge and the wing tip, therefore, in order to increase the rate of convergence, smaller elements along the leading edge and the wing tip are used. For this purpose, the coordinates of the nodes (x, y) are defined by

$$X_i = \left(\frac{1}{N_X} \right)^2 \quad i = 0, 1, 2 \dots N_X \quad (3.24)$$

$$Y_j = \left[1 - \left(\frac{1}{N_Y} \right)^2 \right]^2 \quad j = 0, 1, 2 \dots N_Y$$

Result shown is the distribution of ϕ along $y = 0$. It may be noted that 100 elements on the whole wing (i.e., $N_X = N_Y = 5$) are sufficient for convergence.

3.4.4 Total Lift Coefficient

The total lift coefficient for steady flow is evaluated from Equation (2.47) without the imaginary terms, i.e.,

$$C_L = 2 \frac{\ell}{A} \sum_{j=1}^{NY} [(\phi_u - \phi_l)_{x_{TE}}]_j (\Delta y)_j \quad (3.25)$$

where ϕ_l and ϕ_u are the extrapolated values of the velocity potential along the lower and upper trailing edges. Figure 10 shows the values of C_L of a triangular wing with different aspect ratios in incompressible flow. The result obtained at $\tau = 0.1\%$ are compared with the analytical ones.¹⁶

3.4.5 Wing-Body Configurations

In Figure 11, results for the pressure distribution coefficient of a wing-body configuration in steady subsonic flow are compared, with the results presented by Labrujere, Loeve and Slooff.¹⁷ The results were obtained for $M = 0$ and a rectangular midpositioned wing with chord $c = 1$, span $b = 6$, thickness ratio $\tau = 0.9$, and angle of attack $\alpha_w = 6^\circ$. The body is at zero angle of attack and is composed of a forebody with length $L_A = 2$ and radius

$$r = 0.5 - 0.125(x - x_{LE}) \quad (3.26)$$

a midsection of length $L_M = 1$ and radius $r = 0.5$ and an aftbody of length $L_A = 9$, and radius $r = 0.5$. It is worth note that the extra long aftbody is used to simulate the wake emanating from the circular fuselage. The number of elements is 200 on the whole configuration ($NX = 5$, $NY = 5$ on the wing, $NX = 2$, $NY = 3$ on the forebody, $NX = 5$, $NY = 3$ on the midsection, and $NX = NY = 3$ on the aftbody). Figure 11b presents the distribution of $\phi_u - \phi_l$ along three circumferential stations (see Figure 11b) for the same wing-body configuration.

SECTION 4

OSCILLATORY SUBSONIC FLOW

4.1 INTRODUCTION

In subsection 4.2, the numerical formulations for oscillatory subsonic flow are considered. The boundary condition and the pressure coefficient are considered in Appendix C. In subsection 4.3, numerical results obtained are presented.

4.2 NUMERICAL FORMULATION

Consider the Green Theorem for oscillatory subsonic flow, given by Eq. (2.30)

$$4\pi E(\bar{p}_*) \hat{\phi}(\bar{p}_*) = - \oint_{\Sigma_A} \frac{\partial \hat{\phi}}{\partial N} \frac{e^{-i\Omega R}}{R} d\Sigma_A + \oint \hat{\phi} \frac{\partial}{\partial N} \left(\frac{e^{-i\Omega R}}{R} \right) d\Sigma_A \\ + \oint_{\Sigma_w} \Delta \hat{\phi} \frac{\partial}{\partial N_w} \left(\frac{e^{-i\Omega R}}{R} \right) d\Sigma_w \quad (4.1)$$

with boundary condition given by Equation (C.24)

$$\frac{\partial \hat{\phi}}{\partial N} = N_z \left(i k \tilde{z} + \frac{1}{\beta} \frac{\partial \tilde{z}}{\partial X} \right) e^{-i\Omega M X} \quad (4.2)$$

where $\tilde{z}(X, Y)$ is the vibration mode defined by Equation (C.18)

By imposing that the value of the velocity potential at \bar{p}_* approaches that at a point, \bar{p} , on the surface Σ_A , if \bar{p}_* approaches \bar{p} , the value of $E(\bar{p}_*)$ is found to be 1/2 (Reference 1), and an integral equation relating the potential on the surface Σ_A to its normal derivative is obtained. Noting that no pressure difference can exist on the wake, and using Equation (C.32)

$$\tilde{c}_p = - \frac{2}{\beta} e^{-i k \beta X} \frac{\partial}{\partial X} \left(\hat{\phi} e^{i k X / \beta} \right) \quad (4.3)$$

one can conclude that $(\Delta \hat{\phi}) e^{ikx/\beta}$ is constant along a streamline emanating from the trailing edge and equal to the value at the trailing edge

$$(\Delta \hat{\phi}) e^{ikx/\beta} = (\Delta \hat{\phi}_{TE}) e^{ikx_{TE}/\beta} \simeq (\Delta \hat{\phi}_K) e^{ikx_K/\beta} \quad (4.4)$$

In Equation 4.4, the value of $\hat{\phi}_{TE} e^{ikx_{TE}/\beta}$ is approximated with this value $\Delta \hat{\phi} e^{ikx_K/\beta}$ at the centroid of the element, Σ_K , adjacent to the trailing edge. In Equation 4.4, x_K represents the X component of the position vector of the centroid of elements, Σ_K , adjacent to the trailing edge where the wake starts to develop. Using Equation (4.4) and applying the same procedures used for the steady flow, one obtains

$$\{\delta_{hk} - \hat{C}_{hk} - \hat{W}_{hk}\} \left\{ \hat{\phi}_K \right\} = \{\hat{b}_{hk}\} \left\{ \left(\frac{\partial \hat{\phi}}{\partial N} \right)_K \right\} \quad (4.5)$$

where

$$\hat{C}_{hk} = \left[\frac{i}{2\pi} \iint_{\Sigma_K} \frac{\partial}{\partial N} \left(\frac{e^{-i\alpha R}}{R} \right) d\Sigma_K \right]_{\bar{p}_* = \bar{p}_h} \quad (4.6)$$

$$\hat{b}_{hk} = \left[\frac{-i}{2\pi} \iint_{\Sigma_K} \frac{e^{-i\alpha R}}{R} d\Sigma_K \right]_{\bar{p}_* = \bar{p}_h} \quad (4.7)$$

and for elements not adjacent to the trailing edge, $\hat{W}_{hk} = 0$, otherwise,

$$\hat{W}_{hk} = \left[\pm \frac{1}{2\pi} \iint_{\Sigma'_K} e^{-ik(x-x_K)/\beta} \frac{\partial}{\partial N} \left(\frac{e^{-i\alpha R}}{R} \right) d\Sigma'_K \right]_{\bar{p}_* = \bar{p}_h} \quad (4.8)$$

where x_K is defined previously. Σ'_K is the strip of the wake, bounded by two streamlines emanating from the element Σ_K . The upper (or lower) sign holds for point, \bar{p}_h , on the upper (or lower) surface of the aircraft. Using the following equation

$$\frac{\partial}{\partial N} \left(\frac{e^{-i\alpha R}}{R} \right) = -\frac{1}{R^2} (1 + i\alpha R) \frac{\partial R}{\partial N} = (1 + i\alpha R) e^{-i\alpha R} \frac{\partial}{\partial N} \left(\frac{1}{R} \right) \quad (4.9)$$

the approximate evaluations of \hat{C}_{hK} and \hat{b}_{hK} are obtained by replacing the exponential term with its value at the centroid of the element. This yields

$$\hat{C}_{hK} = e^{-i\Omega R_c} (1 + i\Omega R_c) C_{hK} \quad (4.10)$$

$$\hat{b}_{hK} = e^{-i\Omega R_c} b_{hK} \quad (4.11)$$

where C_{hK} and b_{hK} are given by Equations (3.8) and (3.9) whereas R_c is the distance between the centroids of elements Σ_h and Σ_K . For the wake contribution one obtains $\hat{W}_{hK}=0$, if the element Σ_K is not in contact with the trailing edge, while, for the element Σ_K in contact with the trailing edge, dividing the strip Σ'_K into small elements, one obtains

$$\hat{W}_{hK} = \hat{W}_{hK}^{(TE)} = \sum_{j=1}^{NW} e^{-ik(X_j - X_K + MR_c)/\beta} (1 + i\Omega R_c) C_{hj} \quad (4.12)$$

where, j refers to the j th wake element emanating from the element Σ_K , C_{hj} is given by Equation (3.8) R_c is the distance between the centroids of element, Σ_h , and the i th wake element; NW is the number of elements of the truncated wake emanating from Σ_K . (A more refined analysis is obtained by taking the limit of the present one when NW tends to infinity).

4.3 NUMERICAL RESULT

Results for oscillatory subsonic flow are presented here. In Subsection 4.3.1 the results are compared with the experimental ones. In Subsection 4.3.2 the analysis of convergence is considered. In oscillatory flow, instead of using semi-infinite wake, truncated wake is used. Therefore a study of the wake length LW as well as the

analysis of the convergence due to the number of wake elements are considered in Subsection 4.3.3.

4.3.1. Comparison with Experimental Results

Figure 12 presents a comparison with the experimental results of Lessing, Troutman and Menees¹⁵. The results are relating to a rectangular wing with aspect ratio $AR = 3$. The airfoil consists of a biconvex circular-arc section, 5% thickness with sharp leading and trailing edges. The wing considered has the same geometry as the wing considered for Figures 7 and 8 and is oscillating in bending mode described by

$$\Sigma = .18043 \left| \frac{2y}{b} \right| + 1.70255 \left| \frac{2y}{b} \right|^2 - 1.13688 \left| \frac{2y}{b} \right|^3 + .25387 \left| \frac{2y}{b} \right|^4 \quad (4.13)$$

with

$$K = \frac{\omega C}{2 U_{\infty}} = 0.47 \quad \text{and} \quad M = 0.24$$

The values showed are the real and imaginary part of the distribution of \tilde{C}_L along $2y/b = 0$ and $2y/b = 0.5$. They are obtained with $NX=NY=7$, $NW=20$, and $LW=2$ C. The node coordinates are given by Equation (3.22).

4.3.2 Analysis of Convergence

A convergence study of the problem considered in above subsection are presented in Figures 13a and 13b. The values showed are the real and imaginary parts of the distribution of \tilde{C}_L along $2y/b = 0.5$ and $2y/b = .1328$

respectively. They are obtained with different numbers of wing elements, $NX=NY=5, 6, 7$, while the number of wake element emanating from the trailing edge and the wake length, LW , are fixed such that $NW=30, LW=3.5C$. Using 64 elements on the whole wing (i.e. $NX=NY=4$) is sufficient for convergence.

4.3.3 Analysis of Wake Effect

The wake effect of the oscillatory subsonic flow is evaluated from Equation (4.12). The values of \hat{W}_{hk} depend on the number of wake elements and the wake length. Note that, C_{hi} in Equation (4.12) is a doublet integral which represents the solid angle. The value of the solid angle decreases as the distance between the control point and wake element increases. Therefore, the wake effect is dominated by the wake elements closest to the trailing edge. For this reason, it is necessary to determine the effective wake length. Also after the effective wake length is determined, it is necessary to study the convergence due to the number of wake elements. Figure 14 shows the distribution of \tilde{C}_L , along $2Y/b=0.13265$, of the same problem considered for Figure 12a. The results are obtained with different number of $NW=5, 10, 20, 30, 40$, while using 196 elements on the whole wing, i.e., $NX=NY=7$, and using four times chord length for the wake length, or $LW=4.0C$. The length of the wake elements varies from $0.8C$ to $0.1C$ from the figure shown. At least $NW=20$ should be used for convergence. Figure 15 shows the distribution of \tilde{C}_L , along $2Y/b=0.13265$, of the same problem considered for Figure 12a. The results are obtained with different lengths

of wake $LW = 0.5C, C, 2C, 3C$ and $4C$. The length of the wake element is the same for each run, or $(\Delta X)_W = LW/NW = 0.1C$. The numbers of NW for each run are 5, 10, 20 and 40 respectively. From the figure shown, it can be concluded that at least, $LW=2C$, should be used as effective truncated wake length.

4.3.4 Results of Generalized Forces

Figures 16a and 16b shows the absolute values and the phase angles of \tilde{C}_L and \tilde{C}_M for a delta wing in incompressible oscillatory flow, as functions of the reduced frequency, $K = \frac{\omega c}{2 U_\infty}$. The wing with $AR=4$ and $\tau=.5\%$ is oscillating in pitch about the axis $X=X_M$. The vibration mode is described by $\frac{(X-X_m)}{\ell}$ with $X_M = 0.5 (X_{LE} + X_{TE})$. The results are compared with the experimental, as well as, the numerical results by Laschka¹⁸.

Figures 17a and 17b shows the absolute values and the phase angles of \tilde{C}_L and \tilde{C}_M as function of the Mach number which varies from 0.0 to 2.5. (Section 5 presents the formulation for the supersonic range) for a rectangular wing with $AR=2$ and $\tau=0.001$. The vibration mode is the same as that of the above problem, and the reduced frequency is set at $K=1$. The results are compared with the ones obtained by Laschka¹⁸. Figures 18a and 18b show the thickness effect on the problem of Figure 17. The results are obtained with two thickness ratios $\tau=0.001$ and $\tau=0.05$. The Mach number varies from 0.0 to 2.5.

Figures 19a and 19b show the absolute values and the phase angles of \tilde{C}_L and \tilde{C}_M as functions of the reduced frequencies for a rectangular wing

with $AR=2$ and $\tau=0.001$. The wing in incompressible flow is oscillating in plunge. The vibration mode is described by $e^{i\omega t}$. The results are compared with the ones by Lawrance and Gerber¹⁹ as well as Laschka¹⁸.

Figures 20a and 20b shows the absolute values and the phase angles of \tilde{C}_L and \tilde{C}_M of the same problem as that given for Figures 19a and 19b, while the reduced frequency is set at $K=1.0$ and the Mach number varies from 0.0 to 2.5. Results are compared with the ones of Laschka¹⁸.

SECTION 5

STEADY SUPERSONIC FLOW

5.1 INTRODUCTION

In Subsection 5.2 the numerical formulations for steady supersonic flow, derived in Reference 7, is outlined. For completeness, the derivation of these formulations and more detail formulations are summarized in Appendix B. In Subsection 5.3 wings with supersonic leading edges and diaphragms for wings with subsonic leading edges are discussed. In Subsection 5.4 numerical results are presented.

5.2 NUMERICAL FORMULATIONS

Consider the Green theorem for steady supersonic flow. According to Equation (2.33)

$$2\pi E(\bar{p}_*)\phi(\bar{p}_*) = - \iint_{\Sigma_A} \frac{\partial \phi}{\partial N^c} \frac{H}{\|R\|} d\Sigma_A + \iint_{\Sigma_A} \phi \frac{\partial}{\partial N^c} \left(\frac{H}{\|R\|} \right) d\Sigma_A \quad (5.1)$$

with the boundary condition given by Equation (2.14a)

$$\frac{\partial \phi}{\partial N^c} = -N_x \left(\frac{1}{\beta} + \frac{M^2}{M^2 - 1} \frac{\partial \phi}{\partial x} \right) \quad (5.2)$$

Applying the same procedure for subsonic flow, one obtains the following equations, expressed in matrix form,

$$[\delta_{hk} - C_{hk} - W_{hk}] \left\{ \phi_k \right\} = [b_{hk}] \left\{ \left(\frac{\partial \phi}{\partial N^c} \right)_k \right\} \quad (5.3)$$

where

$$C_{hk} = \left[\frac{1}{\pi} \iint_{\Sigma_K} \frac{\partial}{\partial N^c} \left(\frac{H}{\|\bar{q}\|} \right) d\Sigma \right]_{\bar{p}_* - \bar{p}_h} \quad (5.4)$$

and

$$b_{hk} = \left[-\frac{1}{\pi} \iint_{\Sigma_K} \frac{H}{\|\bar{q}\|} d\Sigma \right]_{\bar{p}_* - \bar{p}_h} \quad (5.5)$$

For hyperboloidal elements completely inside the Mach forecone, C_{hk} and b_{hk} are still given by

$$C_{hk} = I_D(1, 1) - I_D(1, -1) - I_D(-1, 1) + I_D(-1, -1) \quad (5.6)$$

$$b_{hk} = I_S(1, 1) - I_S(1, -1) - I_S(-1, 1) + I_S(-1, -1) \quad (5.7)$$

For elements completely inside the Mach forecone I_D and I_S are given by

$$I_D(\xi, \eta) = \frac{1}{\pi} \tan^{-1} \left(\frac{-\bar{q} \times \bar{a}_1 \cdot \bar{q} \times \bar{a}_2}{\|\bar{q}\| \bar{q} \cdot \bar{a}_1 \times \bar{a}_2} \right) \quad (5.8)$$

and

$$I_S(\xi, \eta) = \frac{1}{\pi} \frac{1}{\bar{n} \cdot \bar{n}} (I_{S_1}(\xi, \eta) + I_{S_2}(\xi, \eta) + I_{S_3}(\xi, \eta)) \quad (5.9)$$

with

$$I_{S_1}(\xi, \eta) = -(\bar{q} \times \bar{a}_1 \circ \bar{n}) F_1(\xi, \eta) \quad (5.10)$$

$$I_{S_2}(\xi, \eta) = (\bar{q} \times \bar{a}_2 \circ \bar{n}) F_2(\xi, \eta) \quad (5.11)$$

$$I_{S_3}(\xi, \eta) = \bar{q} \cdot \bar{n} \tan^{-1} \left(\frac{-\bar{q} \times \bar{a}_1 \circ \bar{q} \times \bar{a}_2}{\|\bar{q}\| \bar{q} \cdot \bar{a}_1 \times \bar{a}_2} \right) \quad (5.12)$$

where \bar{q} , \bar{a}_1 , \bar{a}_2 , and \bar{n} are given by Equations (3.12) through (3.15) while

$$\begin{aligned} F_j(\xi, \eta) &= \frac{1}{\|\bar{a}_j\|} \ln \left| \frac{\|\bar{q}\| \|\bar{a}_j\| + \bar{q} \circ \bar{a}_j}{\|\bar{q} \times \bar{a}_j\|} \right| & \bar{a}_j \circ \bar{a}_j > 0 \\ &= \frac{\|\bar{q}\|}{\bar{q} \circ \bar{a}_j} & \bar{a}_j \circ \bar{a}_j = 0 \\ &= -\frac{1}{\|\bar{a}_j\|} \sin^{-1} \left(\frac{\bar{q} \circ \bar{a}_j}{\|\bar{q} \times \bar{a}_j\|} \right) & \bar{a}_j \circ \bar{a}_j < 0 \end{aligned} \quad (5.13)$$

For elements partially inside the Mach forecone I_D and I_{S_1} , I_{S_2} , I_{S_3} are still given by Equations (5.8), (5.10), (5.11) and (5.12) if the corner point is inside the Mach forecone. However, if the corner point is outside the Mach forecone, integrals in Equations (5.4) and (5.5) involve singularity. Details of these kinds of integrals are discussed in Subsection B.4. For elements completely outside the Mach forecone,

$$H \equiv 0 \quad (5.14a)$$

Therefore

$$C_{hk} = b_{hk} = 0 \quad (5.14b)$$

Note that the wake effect has not been considered for the results presented here, because the geometry of the lifting body under consideration includes only wing, nose, or middle-section fuselage. Therefore, for each element, the wake is always outside the Mach forecone, i.e., $W_{hk} = 0$.

In addition, by neglecting the higher order terms, the boundary condition is given by (see Equation 2.14b)

$$\frac{\partial \phi}{\partial N} = - N_x / \beta \quad (5.15)$$

5.3 DIAPHRAGMS

There are three categories of wing geometry in supersonic flow: 1) supersonic leading edges (the elements Σ_h on the upper or the lower sides are influenced only by the elements on the same sides, therefore, the integration in Equations (5.4) and (5.5) are around the upper or lower surface only for the upper or lower elements); 2) mixed supersonic-subsonic leading edge (for this kind of wing, diaphragms have to be used to separate upper and lower sides of the aircraft; then, the problem can be handled as the case of supersonic leading edge); 3) subsonic leading edge (for this kind of wing, results obtained with or without diaphragms are the same [see Subsection 5.4.5]; however, for small thickness ratio, diaphragms are still needed to avoid the elimination of significant figures).

If diaphragms are used, both values of the velocity potential and its normal derivative, ϕ_D and γ_D , of the diaphragm element are unknown. However, two

equations are obtained for each element of the diaphragm: one relates ϕ_p and ψ_p of the diaphragm element, Σ_p , to the upper geometry of the aircraft and the upper side diaphragm, the other one relates the same quantities to the lower geometry. Therefore, the total number of equations is equal to the total number of unknowns. Details of the numerical procedures are given in Subsection B.5. As mentioned before, for wing with subsonic leading edge, procedure with or without diaphragm can be used. If the procedure without diaphragm is employed, then the integral equations are solved the same way as for the subsonic case (solutions are obtained by solving Equation (5.3)). However, if the procedure with diaphragm is employed, solutions are obtained by solving Equations (B.41) or (B.46).

5.4 NUMERICAL RESULTS

Results for steady supersonic flow are presented here. In Subsection 5.4.1, results are compared with the experimental ones. In Subsection 5.4.2, analysis of convergence is studied. Problems of airfoils in conical flow are studied in Subsection 5.4.3. The role of diaphragms has already been discussed in Subsection 5.3. In order to show that diaphragms are not necessary for geometries with subsonic leading edge, two results obtained with and without diaphragms for a circular cone in conical flow are compared in Subsection 5.4.4. Finally, in order to study body interference and also to show the generality of the present method, result of wing-body configuration is considered in Subsection 5.4.5.

5.4.1 Comparison With Experimental Results

Figure 21 shows the distribution of the pressure coefficient C_p on the lower and upper surfaces for a rectangular wing with aspect ratio $AR = 3$. The airfoil consists of a biconvex circular-arc section, 5% thick, with sharp leading and trailing edges. The results are obtained for $\alpha = 0^\circ$, $M = 1.3$ and $NX = NY = 7$. Figure 22a shows the

distribution of the lift coefficient for the same wing considered in Figure 21. The results are obtained for $\alpha = 5^\circ$, $M = 1.3$ and $NX = NY = 7$. These results are compared with the ones obtained by Lessing, et al.¹⁵ In Figure 22b, the pressure distributions on the upper and the lower sides of the wing are shown. It should be mentioned that results in Figure 22a are obtained by taking the advantage of anti-symmetry as in the case described in Subsection 3.4.2.

5.4.2 Analysis of Convergence

Convergence study of the problem considered in Figure 21 is presented in Figure 23 which shows the distribution of the velocity potential along $2y/b = 0$ for different numbers of elements. The curves are obtained with $NX = NY = 5, 6$ and 7 . It is shown that 144 elements on the whole wing, i.e., $NX = NY = 6$, are sufficient for convergence.

5.4.3 Delta Wings

Figure 24 shows the distribution of lift coefficient per unit angle of attack for a delta wing with supersonic leading edge and

$$M = \beta / \tan \Lambda = 1.2$$

where Λ is the sweep angle of the leading edge. The results obtained with $NX = 8$, $NY = 12$ and $M = 1.2$ are compared with the exact solution which is given by (Reference 20)

$$\Delta C_p = \frac{4\alpha}{\pi\beta} \frac{m}{\sqrt{m^2-1}} \operatorname{Re} \left[\cos^{-1} \frac{1-m\gamma}{m-\gamma} + \cos^{-1} \frac{1+m\gamma}{m+\gamma} \right] \quad (5.16)$$

where

$$\gamma = \frac{\beta y}{x}$$

Figure 25 shows the distribution of the lift coefficient per unit angle of attack for a delta wing with subsonic leading edges and $m = 0.8333$. The results obtained with $NX = NY = 7$ and $M = \sqrt{2}$ are compared with the exact solution, which is given by (Reference 20)

$$\Delta C_p = \frac{4m^2 \alpha}{\beta E(K)} \frac{1}{\sqrt{m^2 - \gamma^2}} \quad (5.17)$$

where $K = \sqrt{1 - m^2}$ and E is the elliptic integral of the second kind. It may be worth noting that there are two types of elements — grids which can be used for delta wings (see Figure 2c). For supersonic delta wings, the flow is conical, therefore, the element-grid shown in Figure 2c (b) appears to be the more natural one. In addition, the use of this grid implies the use of a completely general quadrilateral element. Let $\bar{\xi}$ and $\bar{\eta}$ be the generalized coordinates such that $\bar{\eta}$ has same direction as y while the direction of $\bar{\xi}$ passes the origin and pointed downward. The derivative of ϕ with respect to X is obtained as follows: consider the directional derivatives $\frac{d\phi}{d\xi}$ and $\frac{d\phi}{d\eta}$

$$\frac{d\phi}{d\xi} = \left(\frac{\partial \phi}{\partial X} \bar{i} + \frac{\partial \phi}{\partial Y} \bar{j} \right) \cdot \frac{\bar{\xi}}{|\bar{\xi}|} = \frac{\partial \phi}{\partial X} \frac{X}{\sqrt{X^2 + Y^2}} + \frac{\partial \phi}{\partial Y} \frac{Y}{\sqrt{X^2 + Y^2}} \quad (5.18)$$

$$\frac{d\phi}{d\eta} = \left(\frac{\partial \phi}{\partial X} \bar{i} + \frac{\partial \phi}{\partial Y} \bar{j} \right) \cdot \frac{\bar{\eta}}{|\bar{\eta}|} = \frac{\partial \phi}{\partial Y} \quad (5.19)$$

where

$$\bar{\xi} = X \bar{i} + Y \bar{j} \quad (5.20a)$$

$$\bar{\eta} = Y \bar{j} \quad (5.20b)$$

Therefore

$$\frac{\partial \phi}{\partial x} = \left(\frac{d\phi}{d\xi} \right) \frac{\sqrt{x^2 + y^2}}{x} - \left(\frac{d\phi}{d\eta} \right) \frac{y}{x} \quad (5.21)$$

The values of $\left(\frac{d\phi}{d\xi} \right)$ and $\left(\frac{d\phi}{d\eta} \right)$ can be evaluated by the finite difference method. By using Equation (5.21), the values of C_p are obtained. The results obtained above by applying this scheme are very accurate. The results obtained for Figure 24 are especially accurate (up to the fifth significant figure).

5.4.4 Circular Cone (Analysis of Diaphragm Existence)

For most cases of supersonic flow considered here, diaphragms seem to be necessary to avoid determinant singularity. However, in this Subsection, an example is given to show that diaphragms are unnecessary, for example, for bodies with subsonic leading edge. This example is related to a circular cone with base radius $r = 1$, length $l = 5$, and $M = 2.0$. One is obtained with diaphragm by solving Equation (B.46), while the other one is obtained without diaphragm by solving Equation (5.3). The results are in good agreement. The pressure coefficient of the body is evaluated from the slope of $\phi - \chi$ curve. This value is evaluated as 0.112 which is consistent with the exact solution given in Reference 21 (Figure 17, p. 187, $C_p \approx 0.12$ for $M = 2$, $\theta_c = \tan^{-1} \left(\frac{1}{5} \right) \approx 11^\circ$).

5.4.5 Wing-Body Configuration

The present method is sufficiently general to be applied for any complex configuration. Presented here is an example of this application. A wing-body combination in supersonic flow with $M = 1.48$ is considered in Figures 27a, 27b, and 27c. The geometry of the configuration is shown in Figure 27c.

The combination is composed of a wing with chord $c = 3$, span $S = 9$, thickness $\tau = 5\%$, a forebody of length $L_A = 6.0$, and radius varying from 0 to 0.75 linearly, and

a midsection of length $L_M = 3.0$ and radius $r = 0.75$. Wake and aftbody are not considered. The angle of attack of the wing is $\alpha_w = 1.92$, while the angle of attack of the body is zero, $\alpha_\beta = 0$. The results are obtained with 580 elements on the whole configuration ($NX = NY = 10$ on the wing, $NX = 5$, $NY = 3$ on the nose, $NX = 10$, $NY = 3$ on the middle section). In Figure 27a the distribution of $\beta C_l / \alpha_w$ on the wing section is presented, and the results are compared with the ones by Nielsen²² and Woodward, Tinoco and Larsen,²³ while in Figure 27b the distribution of $\beta C_l / \alpha_w$ on the fuselage is shown.

SECTION 6

OSCILLATORY SUPERSONIC FLOW

6.1 INTRODUCTION

In Subsection 6.2, the numerical formulation for oscillatory supersonic flow is considered. The boundary conditions and the pressure coefficient are considered in Appendix C. The role of the diaphragm in oscillatory supersonic flow is the same as in steady supersonic flow. It has been already discussed in Subsection 5.3, therefore it is unnecessary to repeat it here. In Subsection 6.3, numerical results obtained are presented.

6.2 NUMERICAL FORMULATIONS

Consider the Green Theorem for oscillatory supersonic flow. According to Equation (2.38)

$$2\pi E(\bar{p}_*) \phi(\bar{p}_*) = \oint_{\Sigma} \frac{\partial \hat{\phi}}{\partial N^c} \frac{H}{\|\bar{R}\|} \cos(\omega \|\bar{R}\|) d\Sigma + \oint \hat{\phi} \frac{\partial}{\partial N^c} \left(\frac{H}{\|\bar{R}\|} \cos \omega \|\bar{R}\| \right) d\Sigma \quad (6.1)$$

with the boundary condition, given by Equation (C.28)

$$\frac{\partial \hat{\phi}}{\partial N^c} = N_z \left(iK \tilde{Z} + \frac{1}{\beta} \frac{\partial \tilde{Z}}{\partial X} \right) e^{i\omega M X} \quad (6.2)$$

where $\tilde{Z}(X, Y)$ is the vibration mode defined by Equation (C.18). Applying the same procedure used for subsonic flow, one obtains the following equations, expressed in matrix form

$$[\delta_{hk} - \hat{C}_{hk} - \hat{W}_{hk}] \left\{ \hat{\phi}_k \right\} = [\hat{b}_{hk}] \left\{ \left(\frac{\partial \hat{\phi}}{\partial N^c} \right) \right\} \quad (6.3)$$

where

$$\hat{C}_{hk} = \left[\frac{1}{\pi} \iint_{\Sigma_k} \frac{\partial}{\partial N^c} \left(\frac{H}{\|\bar{R}\|} \cos(\Omega \|\bar{R}\|) \right) d\Sigma_k \right]_{\bar{P}_* = \bar{P}_h} \quad (6.4)$$

and

$$\hat{b}_{hk} = \left[-\frac{1}{\pi} \iint_{\Sigma_k} \frac{H}{\|\bar{R}\|} \cos(\Omega \|\bar{R}\|) d\Sigma_k \right]_{\bar{P}_* = \bar{P}_h} \quad (6.5)$$

The wake effect for supersonic flow is not considered here since only supersonic-trailing-edge wings are presented here. Therefore $\hat{W}_{hk} = 0$.

Noting that

$$\begin{aligned} & \frac{\partial}{\partial N^c} \left(\frac{1}{\|\bar{R}\|} \cos(\Omega \|\bar{R}\|) \right) \\ &= -\frac{1}{\|\bar{R}\|^2} \left[\cos(\Omega \|\bar{R}\|) + \Omega \|\bar{R}\| \sin(\Omega \|\bar{R}\|) \right] \frac{\partial \|\bar{R}\|}{\partial N^c} \\ &= \left[\cos(\Omega \|\bar{R}\|) + \Omega \|\bar{R}\| \sin(\Omega \|\bar{R}\|) \right] \frac{\partial}{\partial N^c} \left(\frac{1}{\|\bar{R}\|} \right) \end{aligned} \quad (6.6)$$

the approximating evaluations of \hat{C}_{hk} and \hat{b}_{hk} are obtained by replacing the sine and cosine terms with their values at the centroid of the element. This yields

$$\hat{C}_{hk} = \left[\cos(\Omega \|\bar{R}_c\|) + \Omega \|\bar{R}_c\| \sin(\Omega \|\bar{R}_c\|) \right] C_{hk} \quad (6.7)$$

and

$$\hat{b}_{hk} = \cos(\alpha - \|\bar{R}_{cl}\|) b_{hk} \quad (6.8)$$

where C_{hk} and b_{hk} are given by Equations (5.6) and (5.7) with I_D , I_S given by Equations (5.8) through (5.12) for elements completely inside the Mach forecone. For elements partially inside the Mach forecone, I_D and I_S are still given by Equations (5.8) and (5.9) if the corner point is inside the Mach forecone, otherwise, they are given by Equations (B.26) through (B.28) for I_{S1} , Equations (B.30) through (B.32) for I_{S2} , and Equations (B.35) through (B.40) for I_{S3} and I_D . For element completely outside the Mach forecone $\hat{C}_{hk} = \hat{b}_{hk} = 0$.

6.3 NUMERICAL RESULTS

Results for oscillatory supersonic flow are presented here.

In Subsection 6.3.1 a wing oscillating in bending mode is considered. In Subsection 6.3.2, the convergence problem is considered. In Subsection 6.3.3, the evaluation of generalized forces is considered.

6.3.1 Comparison With Experimental Results

Figure 28 shows the distribution of absolute value and phase angle of \tilde{C}_l for a rectangular wing oscillating in bending mode

$$\tilde{C}_l = .18043 \left| \frac{2y}{b} \right| + 1.70255 \left| \frac{2y}{b} \right|^2 - 1.13688 \left| \frac{2y}{b} \right|^3 + .25387 \left| \frac{2y}{b} \right|^4 \quad (6.9)$$

with $K = \omega c / 2 U_\infty = 0.1$

The airfoil, with aspect ratio $AR = 3$, consists of a biconvex circular-arc section, 5% thick with sharp leading and trailing edges. Results obtained for $M = 1.3$

and $NX = NY = 7$ are compared with the ones by Lessing, et al.¹⁵ It should be mentioned that the sign of phase angle of \tilde{C}_ℓ obtained by the present method is opposite to that of Ref. 15. The author believes that this is due to the different choice of the sign convention.

6.3.2 Analysis of Convergence

A convergence study of the above problem is presented here. In Figure 29, the distributions of the imaginary and real parts of the velocity potential along $2y/b = 0.5$ for the problem given for Figure 28 are shown. The curves are obtained with $NX = NY = 5, 6, 7$ and 8 . It is shown that 100 elements (i.e., $NX = NY = 5$) are sufficient for convergence.

6.3.3 Results of Generalized Forces

The typical results for the evaluation of generalized forces are presented in Figures 17a, 17b, 18a, 18b, 20a and 20b. In Figures 17a and 17b, a rectangular wing with oscillation in pitch is considered. In Figures 18a and 18b the thickness effect of the problem given for Figures 17a and 17b is considered. In Figure 20a and 20b a rectangular wing with oscillation in plunge is considered. These results are obtained for Mach number varying from 0.0 to 2.0 and $K = \frac{2\omega c}{U_\infty} = 1.0$ and compared with the ones obtained by Laschka.¹⁸ Details of the problems have already been given in Subsection 4.3.4, therefore, they are not repeated here.

SECTION 7

FLUTTER ANALYSIS

7.1 INTRODUCTION

The previous sections present an efficient aerodynamic tool to analyze flutter phenomenon. In this section, a preliminary flutter analysis is presented. In Subsection 7.2, the mathematical model is presented. In Subsection 7.3, the Lagrange's equation forces are discussed. In Subsection 7.5, the evaluation of aerodynamic forces is outlined. In Subsection 7.6, the flutter analysis is described. In Subsection 7.7, numerical results are presented.

7.2 MATHEMATICAL MODEL

As usual, the mathematical model is established by describing the aerodynamic loads due to simple harmonic motion and then studying the stability of infinitesimal vibration of this kind of motion. The model is based on the fact that the motion at the flutter boundary is simple harmonic and that the flutter boundary is by definition the one relative to an infinitesimal oscillation around the next configuration.

The most typical aircraft flutter results from a coupling between the bending and torsion modes of a wing. A typical section (airfoil) analysis is considered for simplicity. This kind of flutter is considered in this section. The airfoil under consideration is permitted freedom to execute small vertical and angular displacements, h and α , and is constrained by two springs representing bending and torsion respectively. Thus, the displacement in Z direction is

$$W = Z - \bar{Z}(X, y) = h(t) + (X - X_{EA})\alpha(t) \quad (7.1)$$

where X_{EA} denotes the position of elastic axis and h is the vertical displacement of the elastic axis (Figure 3).

Mathematically, it is easier to describe displacement with exponential time dependent $e^{i\omega t}$ (ω real) and assume that all dependent variables are proportional to $e^{i\omega t}$. Therefore, Equation (7.1) can be rewritten as

$$W = \tilde{h} e^{i\omega t} + (X - X_{EA})\tilde{\alpha} e^{i\omega t} = \tilde{w} e^{i\omega t} \quad (7.2)$$

with

$$\tilde{w} = \tilde{h} + \tilde{\alpha}(X - X_{EA}) \quad (7.3)$$

$$h = \tilde{h} e^{i\omega t} \quad (7.4)$$

$$\alpha = \tilde{\alpha} e^{i\omega t} \quad (7.5)$$

The actual quantities of W , h and α are found by taking the real part of the complex counterparts.

7.3

LAGRANGE'S EQUATION OF MOTION

Equation (7.1) describes the displacement of airfoil having two degree of freedom. The variables h and α are two generalized coordinates. The motion of the unrestrained airfoil is defined by the Lagrange's Equation which states that

$$\frac{d}{dt} \left(\frac{\partial T}{\partial \dot{q}_k} \right) - \frac{\partial T}{\partial q_k} + \frac{\partial U}{\partial q_k} = Q_k \quad (7.6)$$

where \bar{q}_k is the k -th generalized coordinates, T is the kinetic energy of the wing segment, U is the internal strain energy of the wing segment, Q_k is the k -th generalized force corresponding to the k -th generalized coordinate. The kinetic energy of the wing segment is

$$\begin{aligned} T &= \frac{1}{2} \int_{chord} \dot{W}^2 dm \\ &= \frac{1}{2} \int_{chord} \left[\dot{h} + (X - X_{EA}) \dot{\alpha} \right]^2 dm \\ &= \frac{1}{2} m \dot{h}^2 + \frac{1}{2} m \ell^2 r_\alpha^2 \dot{\alpha}^2 + m \ell X_\alpha \dot{\alpha} \dot{h} \end{aligned} \quad (7.7)$$

where ℓ is a reference length, while r_α and X_α are the dimensionless radius of gyration and static balance about the elastic axis,

$$r_\alpha^2 = \frac{1}{m \ell^2} \int_{chord} (X - X_{EA})^2 dm ; \quad X_\alpha = \frac{1}{m \ell} \int_{chord} (X - X_{EA}) dm \quad (7.8)$$

If the stiffness of bending and torsion spring are represented by K_h and K_α respectively, the internal strain energy is given by

$$U_E = \frac{1}{2} K_h h^2 + \frac{1}{2} K_\alpha \alpha^2 \quad (7.10)$$

or

$$U_E = \frac{1}{2} m \omega_h^2 h^2 + \frac{1}{2} m l^2 \gamma_\alpha^2 \omega_\alpha^2 \alpha^2 \quad (7.11)$$

where ω_α and ω_h are the natural frequencies without mass coupling, or

$$\omega_h = \sqrt{\frac{K_h}{m}} \quad (7.12)$$

$$\omega_\alpha = \sqrt{\frac{K_\alpha}{m l^2 \gamma_\alpha^2}} \quad (7.13)$$

Combining Equations (7.7) and (7.11) with the Lagrange Equation, Equation (7.6), with $q_1 = h$, $q_2 = \alpha$, $Q_1 = Q_h$ and $Q_2 = Q_\alpha$, the following two equations of motion are obtained

$$m \ddot{h} + m l \gamma_\alpha^2 \ddot{\alpha} + m \omega_h^2 h = Q_h \quad (7.14)$$

$$m l \gamma_\alpha^2 \ddot{h} + m l^2 \gamma_\alpha^2 \ddot{\alpha} + m \omega_\alpha^2 l^2 \gamma_\alpha^2 \alpha = Q_\alpha \quad (7.15)$$

Combining Equations (7.4) and (7.5) with Equations (7.14) and (7.15) yields

$$-m \omega_h^2 \tilde{h} - m \omega_h^2 l \gamma_\alpha^2 \tilde{\alpha} + m \omega_h^2 h = \tilde{Q}_h \quad (7.16)$$

$$-m \omega_\alpha^2 l \gamma_\alpha^2 \tilde{h} - m \omega_\alpha^2 l^2 \gamma_\alpha^2 \tilde{\alpha} + m \omega_\alpha^2 l^2 \gamma_\alpha^2 \alpha = \tilde{Q}_\alpha \quad (7.17)$$

As mentioned above, the symbol tilde above each quantity represents the complex time-independent part.

7.4. GENERALIZED FORCES

The generalized forces are found from the virtual work which is given

by

$$\begin{aligned} \delta \tilde{W} &= \iint_A C_p \delta w \, dx \, dy \\ &= \delta h \iint_A \tilde{C}_p \, dx \, dy + \delta \alpha \iint_A \tilde{C}_p (X - X_{EA}) \, dx \, dy \\ &\equiv \tilde{Q}_h \delta h + \tilde{Q}_\alpha \delta \alpha \end{aligned} \quad (7.18)$$

where

$$\tilde{\phi}_h = \tilde{L} = \frac{c_p U_\infty^2}{2} \iint \Delta \tilde{C}_p dx dy \quad (7.19)$$

and

$$\tilde{\phi}_\alpha = \tilde{M} = \frac{c_p U_\infty^2}{2} \iint \Delta \tilde{C}_p (X - X_{EA}) dx dy \quad (7.20)$$

Combining Equations (7.19) and (7.20) with Equations (7.14) and (7.15) yields

$$[-m\omega^2 + m\omega_h^2] \tilde{h} - m l \chi_\alpha \omega^2 \tilde{\alpha} = \tilde{L} \quad (7.21)$$

$$-m\omega^2 l \chi_\alpha \tilde{h}_x + [-m\omega^2 l^2 r_\alpha^2 + m\omega_\alpha^2 l r_\alpha^2] \tilde{\alpha} = \tilde{M} \quad (7.22)$$

7.5 AERODYNAMIC FORCES

Following is the procedure to evaluate \tilde{L} and \tilde{M} . Because of the assumption of small vibration, the doublet integral and source integral (see Equations (4.4), (4.5), (6.4), and (6.5)) are not influenced by the displacement, W , while the following boundary condition is a function of W

$$\frac{\partial \phi}{\partial N} = N_z \left(i k W + \frac{1}{\beta} \frac{\partial W}{\partial x} \right) \quad (7.23)$$

Therefore, it is legitimate to write

$$\begin{aligned} C_p &= \mathcal{L} \left(\frac{\partial \phi}{\partial N} \right) = \mathcal{L}(W) \\ &= \mathcal{L} \left[\tilde{h} e^{i\omega t} + (X - X_{EA}) \tilde{\alpha} e^{i\omega t} \right] \\ &= \tilde{h} \mathcal{L}[e^{i\omega t}] + \tilde{\alpha} \mathcal{L}[(X - X_{EA}) e^{i\omega t}] \end{aligned} \quad (7.24)$$

where \mathcal{L} denotes the linear operator.

Therefore, by applying Equation (7.24) to Equation (7.19) and (7.20) the lift force and pitch moment are found.

$$\begin{aligned}\tilde{L} &= \frac{\rho U_{\infty}^2 c}{2} \iint \tilde{C}_p dx dy \\ &= \frac{\rho U_{\infty}^2 c}{2} \left\{ \frac{\tilde{h}}{\ell} \iint \mathcal{L}[\ell e^{i\omega t}] dx dy + \tilde{\alpha} \iint \mathcal{L}[(x-x_{EA}) e^{i\omega t}] dx dy \right\} \\ &= \frac{\rho U_{\infty}^2 c}{2} \left[\frac{\tilde{h}}{\ell} \tilde{C}_{Lh} + \tilde{\alpha} \tilde{C}_{L\alpha} \right] \quad (7.25)\end{aligned}$$

$$\begin{aligned}\tilde{M} &= \frac{\rho U_{\infty}^2 c^2}{2} \iint \tilde{C}_p (x-x_{EA}) dx dy \\ &= \frac{\rho U_{\infty}^2 c^2}{2} \left\{ \frac{\tilde{h}}{\ell} \iint \mathcal{L}[\ell e^{i\omega t}] (x-x_{EA}) dx dy \right. \\ &\quad \left. + \tilde{\alpha} \iint \mathcal{L}[(x-x_{EA}) e^{i\omega t}] (x-x_{EA}) dx dy \right\} \\ &= \frac{\rho U_{\infty}^2 c^2}{2} \left(\frac{\tilde{h}}{\ell} \tilde{C}_{Mh} + \tilde{\alpha} \tilde{C}_{m\alpha} \right) \quad (7.26)\end{aligned}$$

In Equations (7.25) and (7.26) \tilde{C}_{Lh} and \tilde{C}_{Mh} are lift force and pitch moment coefficients about elastic axis of the airfoil in the motion with oscillation in plunge.

The displacement for plunge motion with $\frac{h}{\ell} = 1$ is described by

$$w = \ell e^{i\omega t} \quad (7.27)$$

The boundary condition is then given by

$$\frac{\partial \phi}{\partial N} = N_z (i k e^{i\omega t}) \quad (7.28)$$

or

$$\frac{\partial \tilde{\phi}}{\partial N} = N_z i k \quad (7.29)$$

Similarly, $\tilde{C}_{L\alpha}$ and $\tilde{C}_{M\alpha}$ are lift force and pitch moment about elastic axis of the airfoil in the motion with oscillation in pitch about the elastic axis with unit angle amplitude. The displacement is described by

$$W = (\chi - \chi_{EA}) e^{i\omega t} \quad (7.30)$$

the boundary condition is then given by

$$\frac{\partial \phi}{\partial N} = N_z \left[1 + iK \frac{(\chi - \chi_{EA})}{\ell} \right] e^{i\omega t} \quad (7.31)$$

i.e.

$$\frac{\partial \tilde{\phi}}{\partial N} = N_z \left[1 + iK \frac{(\chi - \chi_{EA})}{\ell} \right] \quad (7.32)$$

7.6 FLUTTER ANALYSIS

Combining Equations (7.25) and (7.26) with Equations (7.21) and (7.22)

yields

$$\left\{ m\omega^2 \ell \left(-1 + \frac{\omega_h^2}{\omega^2} \right) - \frac{\rho U_\infty^2 c}{2} C_{Lh} \right\} \frac{\tilde{h}}{\ell} - \left\{ m\omega^2 \ell \chi_\alpha + \frac{\rho U_\infty^2 c}{2} C_{L\alpha} \right\} \tilde{\alpha} = 0 \quad (7.33)$$

and

$$\left\{ -m\ell \omega^2 (\ell \chi_\alpha) - \frac{\rho U_\infty^2 c}{2} C_{Mh} \right\} \frac{\tilde{h}}{\ell} - \left\{ m\omega^2 \ell^2 \chi_\alpha^2 \left(1 - \frac{\omega_\alpha^2}{\omega^2} + \frac{\rho U_\infty^2 c}{2} \right) \right\} \tilde{\alpha} = 0 \quad (7.34)$$

By introducing

$$A = \frac{\omega_\alpha^2}{\omega^2} \quad (7.35)$$

and

$$K = \omega \ell / U_\infty \quad (7.36)$$

$$\mu = m / \pi \rho l^2 \quad (7.37)$$

$$l = \frac{c}{2} \quad (7.38)$$

Equations (7.33) and (7.34) may be rewritten in the following matrix form

$$\begin{bmatrix} 1 - \left(\frac{W_h}{W_\alpha}\right)^2 A + \frac{1}{\pi K^2 \mu} C_{Lh} & X_\alpha + \frac{1}{\pi K^2 \mu} C_{L\alpha} \\ X_\alpha + \frac{2}{\pi K^2 \mu} C_{Mh} & X_\alpha^2 (1-A) + \frac{2}{\pi K^2 \mu} C_{M\alpha} \end{bmatrix} \begin{Bmatrix} \frac{\tilde{h}}{l} \\ \tilde{\alpha} \end{Bmatrix} = 0 \quad (7.39)$$

In order to yield a non-trivial solution, the determinant of the above left-hand side matrix must be zero. The value of A can, therefore, be evaluated. By plotting the values of the imaginary part of A versus different reduced frequencies, the flutter is found at a specific reduced frequency where the imaginary part of A is zero.

7.7 NUMERICAL RESULTS

In order to compare the numerical results with the analytical ones, a two-dimensional thin airfoil in incompressible, oscillatory flow was studied. For this airfoil, the analytical expressions of \tilde{C}_{Lh} , $\tilde{C}_{L\alpha}$, \tilde{C}_{Mh} and $\tilde{C}_{M\alpha}$ are given in several standard text books (see e.g. Reference 24) as

$$\tilde{C}_{Lh} = 2\pi K^2 \left(2 \frac{C_K}{K} i - 1 \right) \quad (7.40)$$

$$\tilde{C}_{L\alpha} = \pi K^2 \left\{ X_{EA} + 2 \frac{C_K}{K^2} + \left[(1 - 2X_{EA}) C_K + 1 \right] \frac{i}{K} \right\} \quad (7.41)$$

$$\tilde{C}_{Mh} = \pi K^2 \left[(2X_{EA} + 1) \frac{C_K}{K} i - X_{EA} \right] \quad (7.42)$$

$$\tilde{C}_{M\alpha} = \frac{1}{2}\pi K^2 \left\{ (0.125 + X_{EA}^2) + (2X_{EA} + 1) \frac{C_K}{K^2} + (0.5 - X_2) \left[(2X_{EA} + 1)K - 1 \right] \frac{i}{K} \right\} \quad (7.43)$$

where

$$C_K = \frac{(-J_1(K) + i Y_1(K))}{[-(J_1(K) + Y_0(K)) + i (Y_1(K) - J_0(K))]} \quad (7.44)$$

where J_1 and J_0 and Y_1 and Y_0 are Bessel functions of the first and zero orders and reduced frequency, K , is defined as

$$K = \frac{\omega c}{2 U_\infty} \quad (7.45)$$

It should be noted that the purpose for this two dimensional (airfoil) flutter analysis is to assess the validity of the three dimensional aerodynamic theory presented in the proceeding sections. For this reason the two dimensional airfoil is approximated by a thin rectangular wing with high aspect ratios. For the current problem rectangular wing with $AR=16$ can be considered as a two dimensional wing as being verified in Figure 30. In Figures 30a, 30b, 30c and 30d, the curves of \tilde{C}_{Lh} , $\tilde{C}_{L\alpha}$, \tilde{C}_{Mh} , and $\tilde{C}_{M\alpha}$ as functions of the aspect ratio for a thin rectangular wing with $K=0.25$ are presented. It is shown that most curves converge at $AR=16$. Values of \tilde{C}_{Lh} , $\tilde{C}_{L\alpha}$, \tilde{C}_{Mh} , and $\tilde{C}_{M\alpha}$ versus K varying from 0.1 to 1.5 are obtained with $X_{EA} = -2C$, $NX=8$, $NY=10$, $NW=20$, $LW=3.0C$, $\tau=0.1\%$ and $AR=16$ are compared with the exact ones in Figures 34a, 34b, 34c and 34d. The numerical results are in good agreement with the exact ones for reduced frequencies higher than 0.15, while the results for lower reduced frequencies are not completely satisfactory.

As mentioned before, by plotting the value of imaginary A versus reduced frequency K , the flutter speed can be located at a specific K where the imaginary A is zero. An example of this work is presented in Figure 31 which is related to a

rectangular wing with $AR = 16$, $\tau = .1\%$, $\mu = 5$, $X_{EA} = -.2c$, $\omega_h/\omega_\alpha = 0.5$, $X_\alpha = 0.2$ and $r_\alpha = 0.5$. The flutter boundary occurs at $K = 0.53$ and $A = \omega_\alpha^2/\omega^2 = 1.775$. Combining Equations (4.35) (4.36) and (4.37) gives the nondimensional flutter speed, $2U_F/C \omega_\alpha = 1.42$ which is in good agreement with the exact solution (Reference 24)*. The flutter speed as a function of ω_h/ω_α for the same wing with $\mu = 5$, $X_\alpha = 0.2$, $r_\alpha = 0.5$ and $X_{EA} = -.2c$ is presented in Figure 32a and compared with the solution given by two dimensional airfoil theory (Figure 9-5(A), Reference 24). Additional results for the same wing with $\mu = 10$, $X_\alpha = 0.2$, $r_\alpha = 0.5$ and $X_{EA} = -.2c$ are presented in Figure 32b.

*See Figure 9-5(A)(i) of Reference 24 (p. 540), which yields $2 U_F/c\omega_\alpha \approx 1.47$.

SECTION 8

CONCLUSIONS

8.1 INTRODUCTION

The general comments of the present method are made in Subsection 8.2. The outline of the computer program is introduced in Subsection 8.3, while the CPU time and the memory space required for the computer program are listed in Subsection 8.4

8.2 GENERAL COMMENTS

The results obtained in the previous sections are in very good agreement with the existing ones. Especially, compared with the exact solutions, several results are remarkably accurate. For example, values of $C_{L\alpha}$, evaluated for a supersonic delta wing in Subsection 5.4.3, is accurate up to fifth significant figure. In addition to the accuracy, the method is very efficient, extremely general and very easy to use. The results obtained include a variety of problems for either steady or oscillatory, subsonic or supersonic flow. Two results for wing-body configurations in subsonic and supersonic flow are included, while the method can be further applied to wing-body-tail combinations, or more complex configurations. A preliminary result of flutter analysis is presented in Section 7. The pressure is evaluated by finite difference method. However, a hyperboloidal distribution of the velocity potential, ϕ , within each element in terms of ϕ 's at corners can be obtained by evaluating ϕ at each corner by taking average of ϕ at the centroids of the surrounding elements. Therefore, an increase of generality and efficiency can be attained. In addition, the present method for the oscillatory flow can be generalized for the study of the unsteady flow without additional increase in computational complexity (Reference 25). Also it should be mentioned that the computer code presented here is believed to be the only one available for supersonic oscillatory flows around non-zero-thickness configuration.

8.3 COMPUTER PROGRAM

The formulations in the previous sections are imbedded into a general computer program called SOSSA ACTS (Steady and Oscillatory Subsonic and Supersonic Aero-dynamics for Complex Transportation System). The listing of this program is given in Appendix E. In general, the program is separated into three parts. The first part of the program is to define the geometry of the aircraft, wake and diaphragm (if necessary) and divide their surface surfaces into a number of elements. Each element is then replaced by a hyperboloidal surface defined by four corner points. This part of the program includes Subroutines GEOMET and VEC123. The second part of the program is to evaluate the coefficients C_{hK} , b_{hK} and W_{hK} and to solve a system of linear equations by using the Gaussian elimination method for unknowns ϕ , or $\hat{\phi}$. This part of the program includes Subroutines CEOFF and CCGELG. The third part of the program is to evaluate the pressure coefficient and the generalized forces from the computed velocity potential ϕ or $\hat{\phi}$. This part of the program includes Subroutine COEFPR.

8.4 COMPUTER TIME AND MEMORY SPACE

The following table gives the computer time used by the program SOSSA ACTS in terms of the total number of elements on the wing, $N_{ELEM} = 4 \times N_x \times N_y$.

<u>Computer Time (Secs) for SOSSA ACTS</u>				
N_{ELEM}	Subsonic		Supersonic	
	Steady	Unsteady	Steady	Unsteady
$4 \times 4 \times 4$	29	161	8	21
$4 \times 5 \times 5$	70	324	15	38
$4 \times 6 \times 6$	143	543	29	65
$4 \times 7 \times 7$	268	928	54	119

All the results are obtained by taking advantage of the symmetry (or antisymmetry) in y and z directions. The wake for subsonic flow has $N_W = 1$ for steady and $N_W = 30$ for unsteady flow. The diaphragm for supersonic flow has $N_D = 9$. The computer times are expressed in seconds and were obtained on an IBM 370/145 computer of the Boston University Computer center.

Finally, the memory space required for steady flow is approximately given by

$$N_{\text{words}} = 9,500 + N_{\text{EQN}} + N_{\text{EQN}}^2 \quad (8.1)$$

where N_{words} is the number of words, while N_{EQN} is the number of equations.

Similarly for unsteady flow, the memory space requirement is approximately given by

$$N_{\text{words}} = 12,500 + 22 N_{\text{EQN}} + 2 N_{\text{EQN}}^2 \quad (8.2)$$

REFERENCES

1. Morino, L., "Unsteady Compressible Potential Flow Around Lifting Bodies Having Arbitrary Shapes and Motions," Boston University, College of Engineering, Dept. of Aerospace Eng., TR-72-01, June 1972.
2. Morino, L., "Unsteady Compressible Potential Flow Around Lifting Bodies: General Theory," AIAA Paper No. 73-196, January 1973.
3. Morino, L. and Kuo, C. C., "Subsonic Potential Aerodynamics for Complex Configurations: A General Theory," AIAA Journal, Vol. 12, No. 2, February 1974, pp. 141-147.
4. Rodden, W. P., Giesing, J. P. and T. P. Kalman, "New Developments and Applications of the Subsonic Doublet-Lattice Method for Non-Planar Configurations," AGARD-cp-80-71, paper 4, November 1970.
5. Giesing, J. P., Kalman, T. P. and W. P. Rodden, "Subsonic Steady and Oscillatory Aerodynamics for Multiple Interfering Wings and Bodies," Journal of Aircraft, Vol. 9, No. 10, October 1972, pp. 693-702.
6. Morino, L., "A Finite-Element Formulation for Subsonic Flow Around Complex Configurations," Boston University, Dept. of Aerospace Eng., TR-73-05, December 1973.
7. Morino, L., "A Finite-Element Formulation for Supersonic Flow Around Complex Configurations," Boston University, Dept. of Aerospace Eng., TR-74-01, 1974.
8. Chen, L. T., Suci, E. O. and L. Morino, "A Finite-Element Method for Potential Aerodynamics Around Complex Configurations," AIAA paper No. 74-107, January 1974.
9. Chen, L. T., Suci, E. O. and L. Morino, "A Finite-Element Analysis for Steady and Oscillatory Subsonic Flow Around Complex Configurations," Boston University, Dept. of Aerospace Eng., TR-74-02, Dec. 1974.
10. Morino, L. and L. T. Chen, "A Finite-Element Analysis for Steady and Oscillatory Supersonic Flow Around Complex Configurations," Boston University, Dept. of Aerospace Eng., TR-74-03, Dec. 1974.
11. Cunningham, A. M. Jr., "An Efficient, Steady Subsonic Collocation Method for Solving Lift Surface Problems," J. Aircraft, Vol. 8, No. 3, March 1971.
12. Kulakowski, L. J., and R. N. Haskell, "Solution of Subsonic Non-Planar Lifting Surface Problems by Means of High-Speed Digital Computers," J. of Aerospace Science, Vol. 28, February 1901, pp. 103-113.
13. Kolbe, C. D. and F. W. Boltz, "The Forces and Pressure Distribution at Subsonic Speeds on a Planar Wing Having 45° of Swept Back, An Aspect Ratio of 3 and a Taper Ratio of 0.5," RMA51G31, NACA, October 1951.
14. Yates, E. C. Jr., Private Communication, Boston, April 1971.

15. Lessing, H. C., Troutman, J. C. and G. P. Menees, "Experimental Determination of the Pressure Distribution on a Rectangular Wing Oscillating in the First Bending Mode for Mach Numbers From 0.24 to 1.30," NASA TN-D-344, 1960.
16. Ashley, H., and M. Landahl, Aerodynamics of Wings and Bodies, Addison-Wesley, Reading, Mass., 1965.
17. Labrujere, T. E., Loeve, W., and J. W. Slooff, "An Approximate Method for the Calculation of the Pressure Distribution on Wing-Body Combinations at Subcritical Speeds," AGARD Specialist Meeting on Aerodynamic Interference, Silver Springs, Md., Sept., 1970, AGARD Conf. Proc. No. 71.
18. Laschka, B., "Zur Theorie der harmonisch schwingenden tragenden Fläche bei Unterschallstromung," Zeitschrift für Flugwissenschaften, 11 (1963), Heft 7, pp. 265-292.
19. Lawrence, H. R. and E. H. Gerber, "The Aerodynamic Forces on Low Aspect Ratio Wings Oscillating in an Incompressible Flow," J. Aeron. Sci. 19 (1952), S. 796-781.
20. Jones, R. T., and D. Cohen, "High Speed Wing Theory," Princeton Aeronautical Paperbacks, No. 6, Princeton University Press, Princeton, 1960, pp. 156-157.
21. Kuethe, A. M. and J. D. Schetzer, "Foundations of Aerodynamics," John Wiley & Sons, Inc., p. 187.
22. Nielsen, J. N., "Quasi-Cylindrical Theory of Wing-Body Interference at Supersonic Speeds and Comparison With Experiments," NACA Report 1252, 1952.
23. Woodward, F. A., Tinoco, E. M. and J. W. Larsen, "Analysis and Design of Supersonic Wing-Body Combinations, Including Flow Properties in the Near Field, Part I, Theory and Applications," NASA CR-73106, 1967.
24. Bisplinghoff, R. L., Ashley, H. and Halfman, R. L., "Aeroelasticity," Addison-Wesley, Reading, Mass., 1955.
25. Morino, L. and Chen, L. T., "Indicial Compressible Potential Aerodynamics Around Complex Aircraft Configurations," presented at the NASA Conference on Aerodynamic Analyses Requiring Advanced Computers, Langley Research Center, March 4-6, 1975.

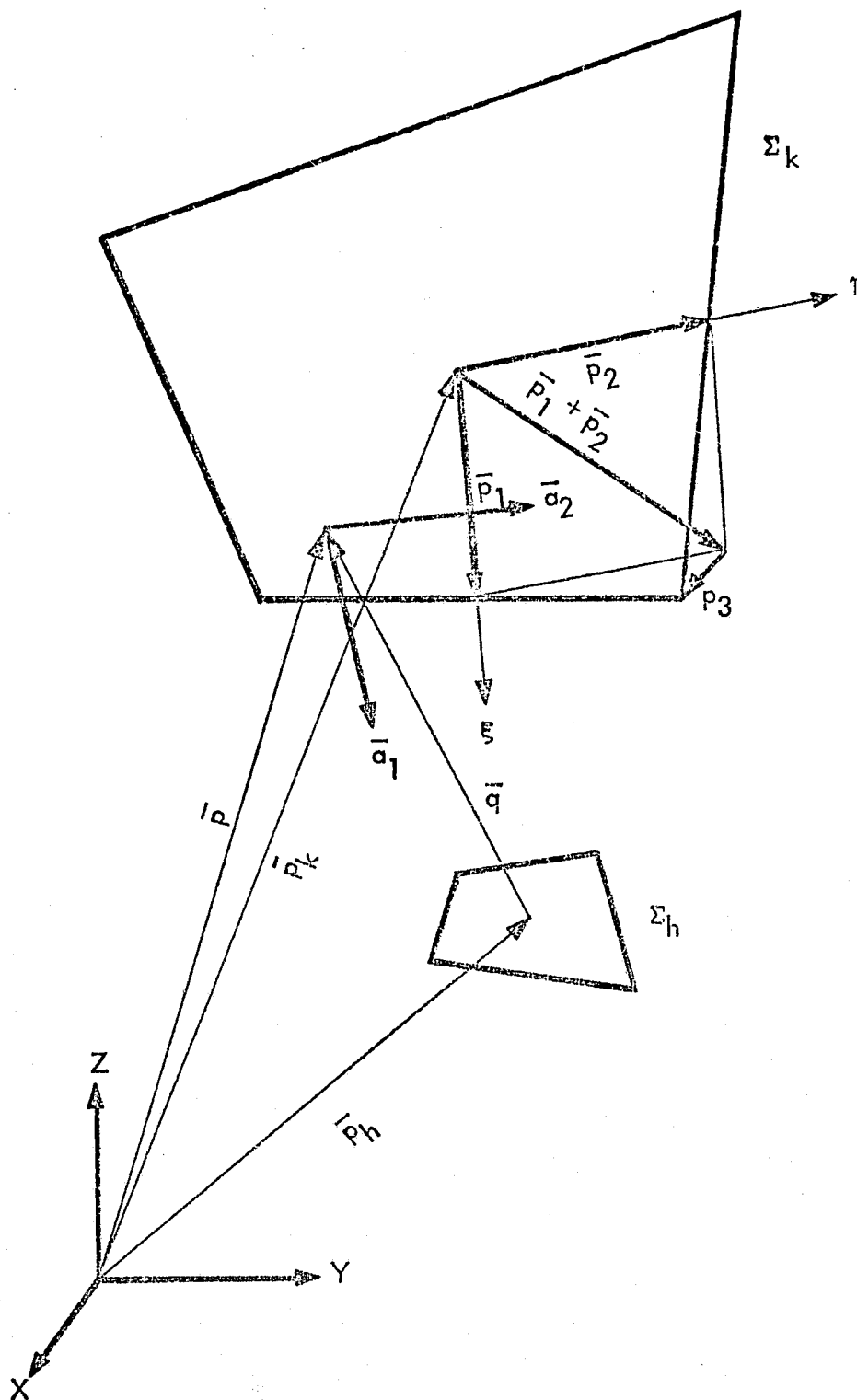


Figure 1. Hyperboloidal Element

ORIGINAL PAGE IS
OF POOR QUALITY

PRECEDING PAGE BLANK NOT FILMED

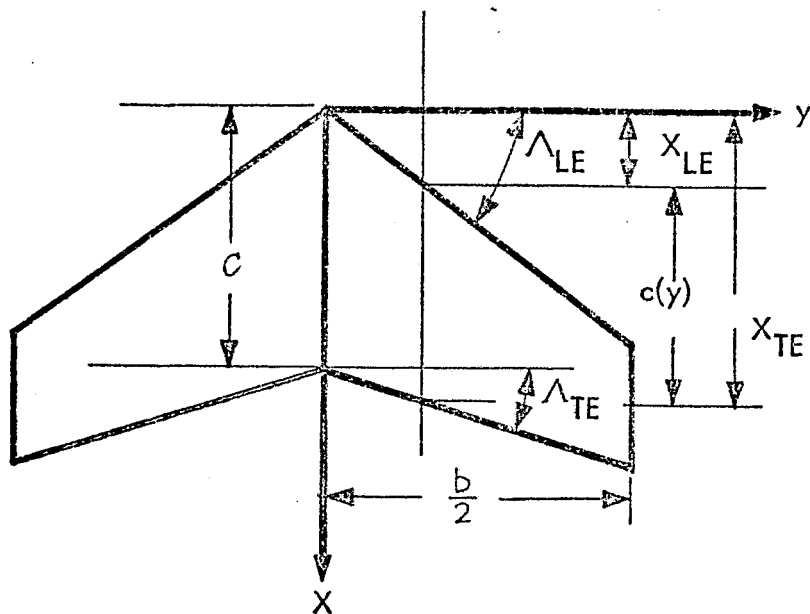


Figure 2a. Wing Planform

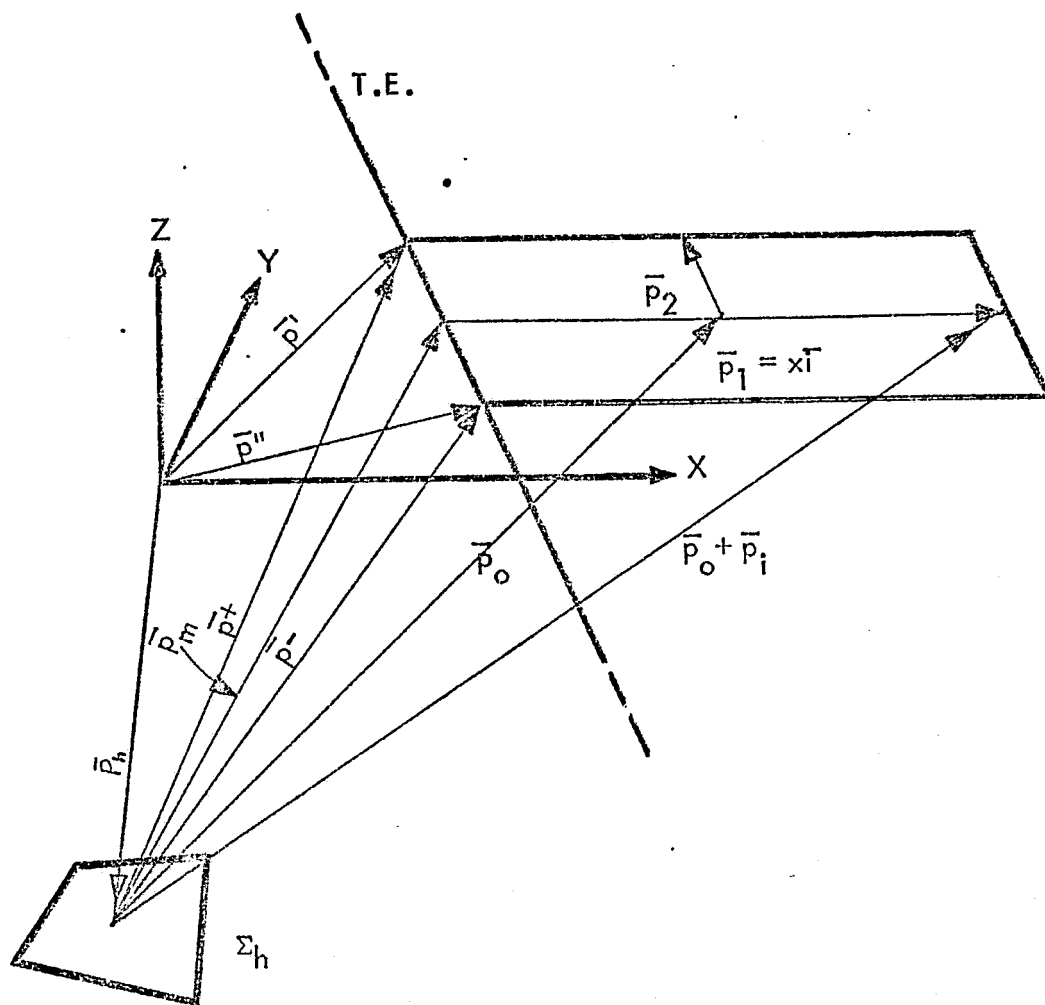


Figure 2b. Wake Element

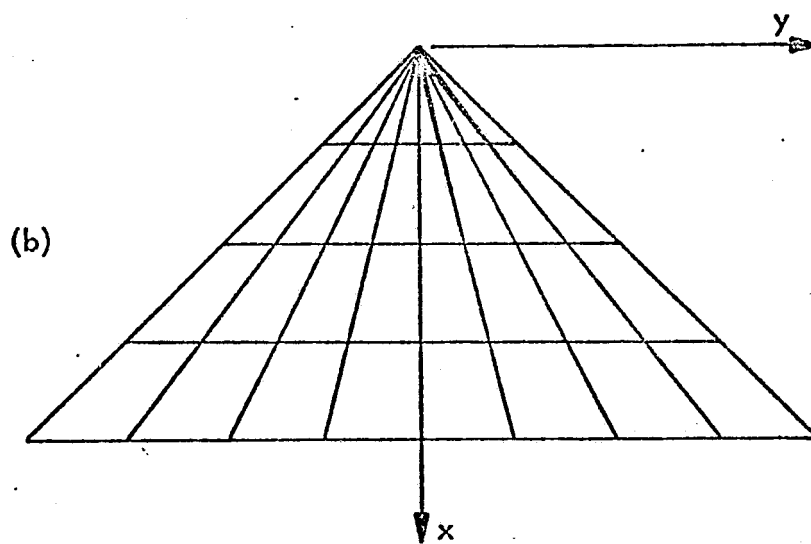
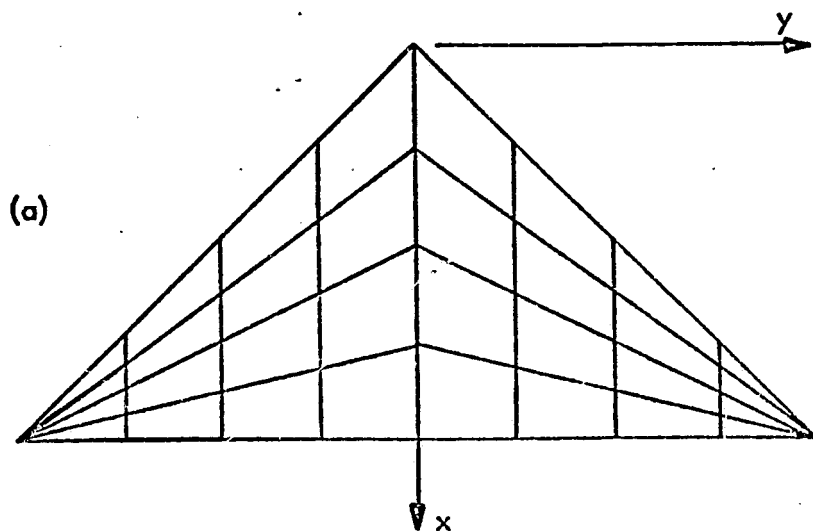


Figure 2C. Two Types of Element-Grids for Delta Wings.

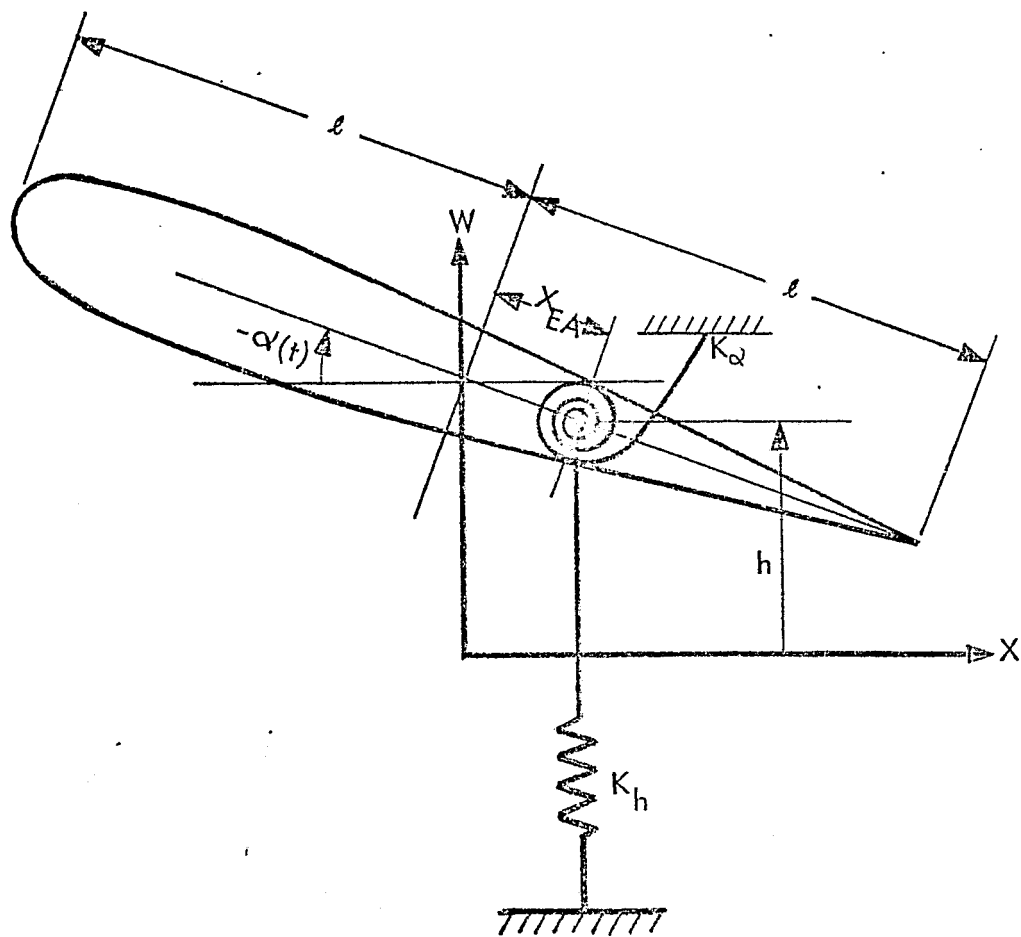


Figure 3. Model for Flutter Analysis

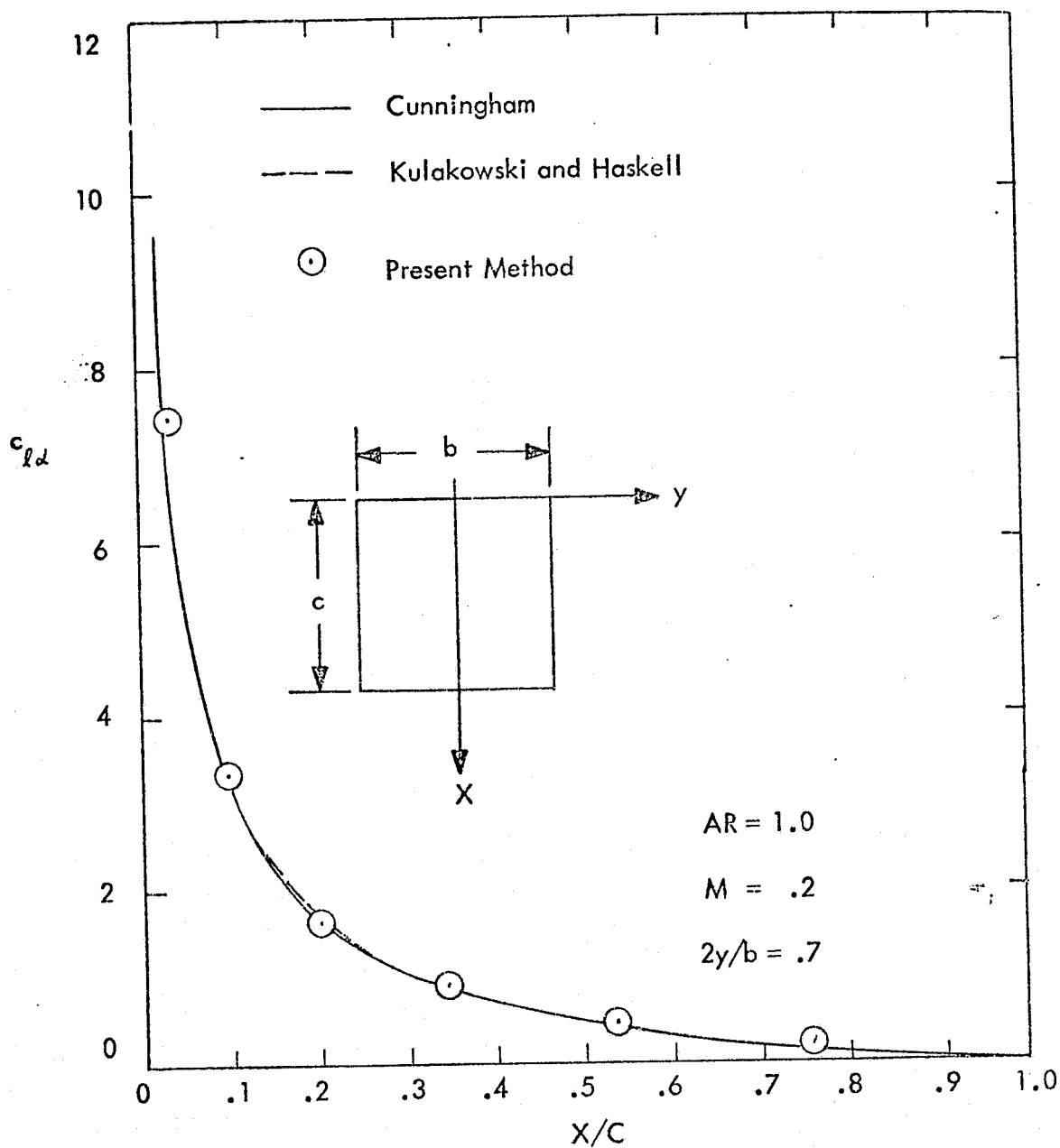


Figure 4. The distribution of c_{ld} along $2y/b = .7$ for a rectangular wing with $AR = 1.0$, $M = .2$, and $NX = NY = 7$ for comparison with results of Ref. 11.

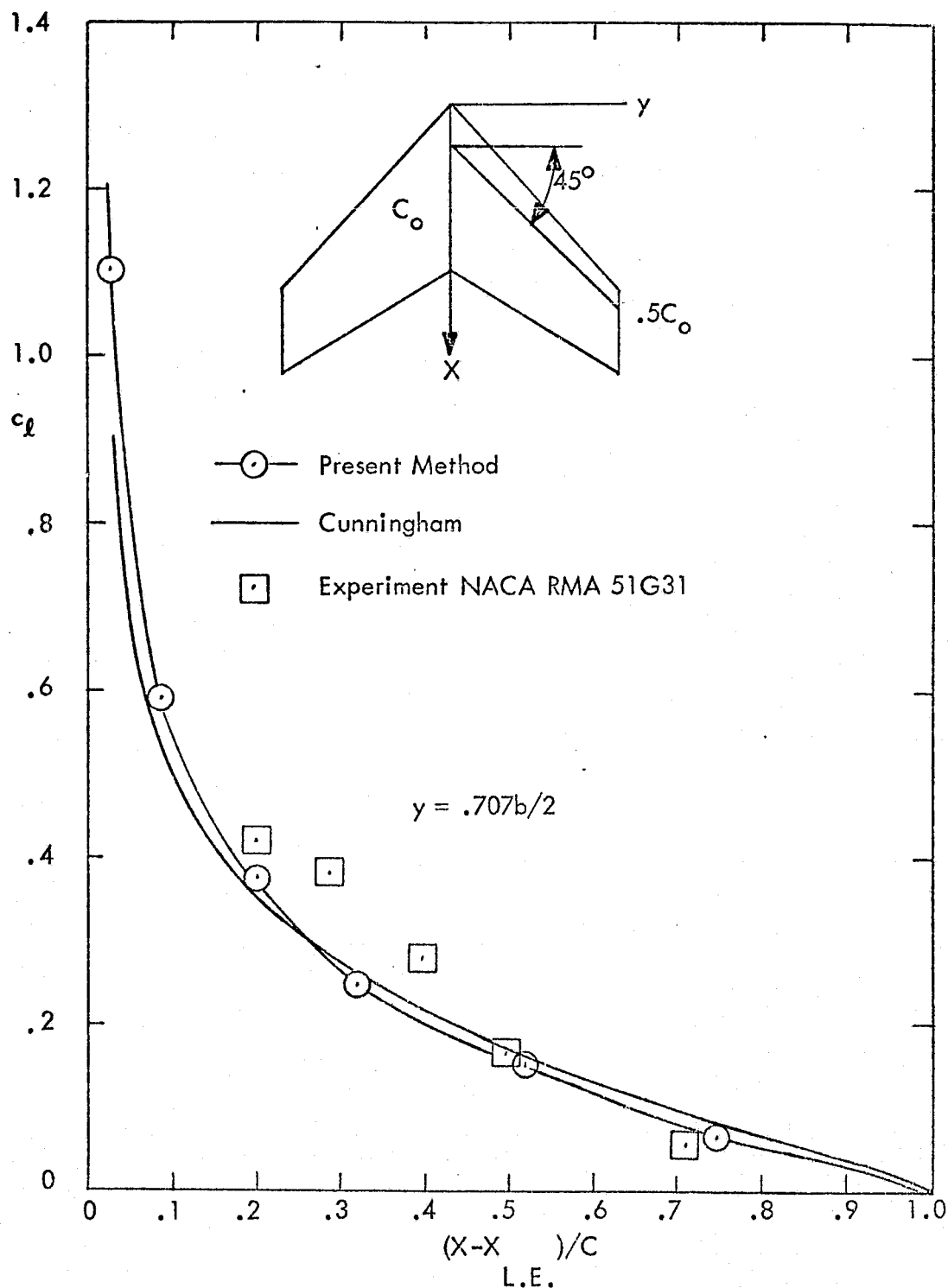


Figure 5. The distribution of c_l along $2y/b = .707$ for a tapered swept wing with $AR = 3$, $TR = .5$, $\Lambda_{1/4} = 45^\circ$, $M = .8$, $\alpha = 5^\circ$ and $NX = NY = 7$ for comparison with results of Ref. 13

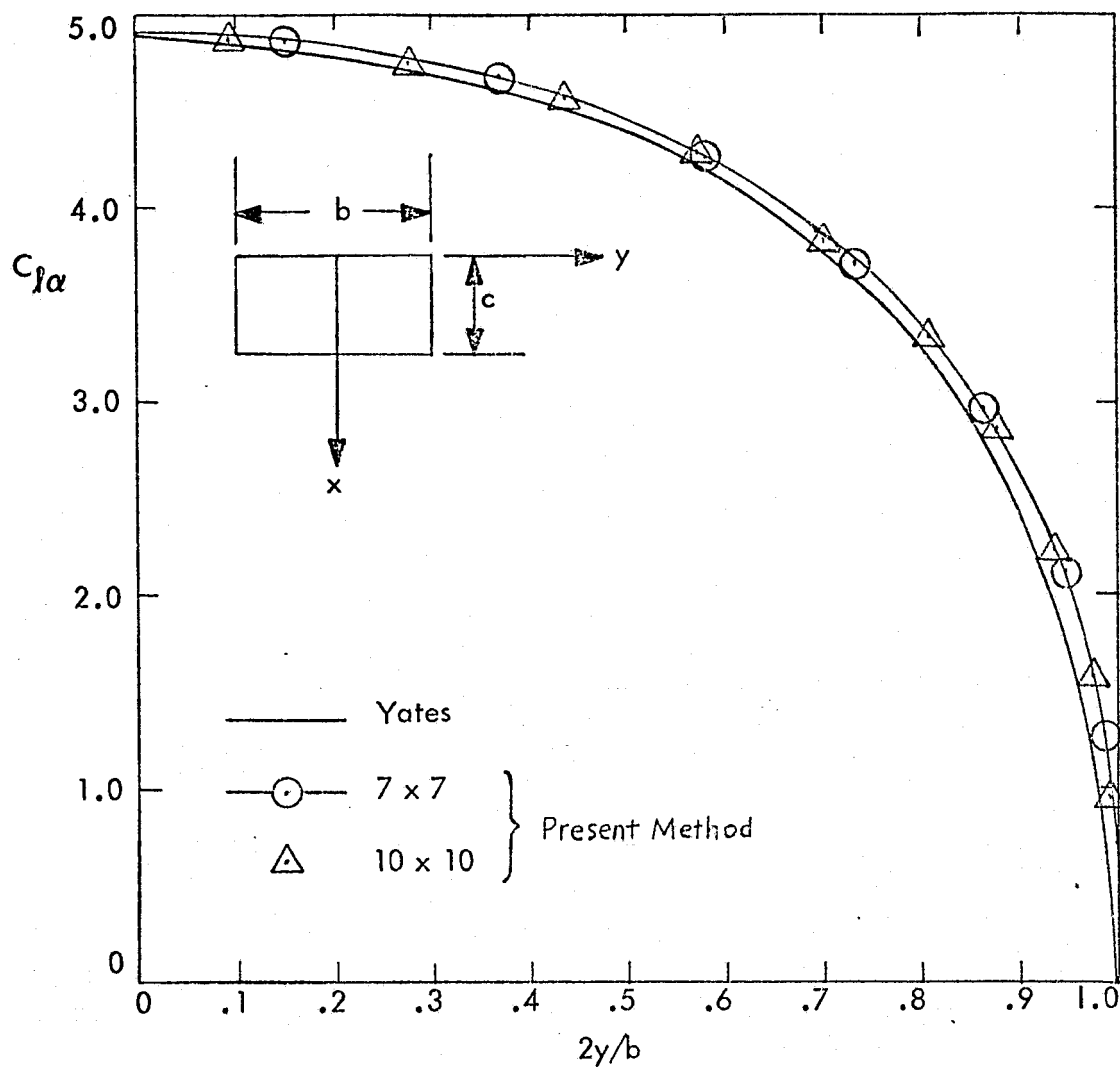


Figure 6. The distribution of the section lift coefficient per unit angle of attack for a rectangular wing with $AR = 4$, $M = .507$ and $NX=NY=7$ and 10 for comparison with results of Ref. 14

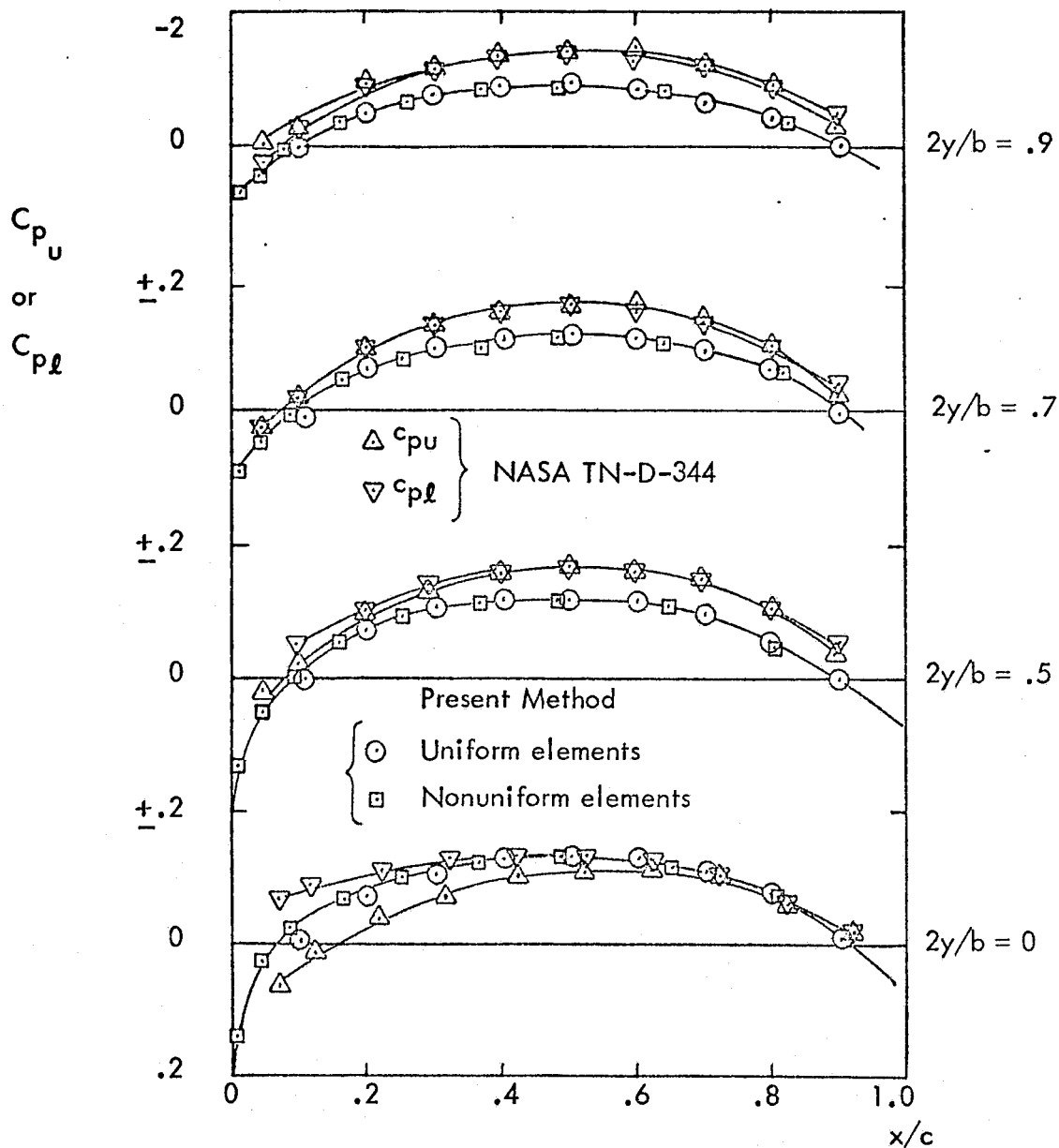


Figure 7. The distribution of c_p on the upper and lower surfaces of a symmetric rectangular wing with $AR = 3$, $\tau = 5\%$, $\alpha = 0^\circ$, $M = .24$ and $NX=NY=10$ for comparison with results of Ref. 15

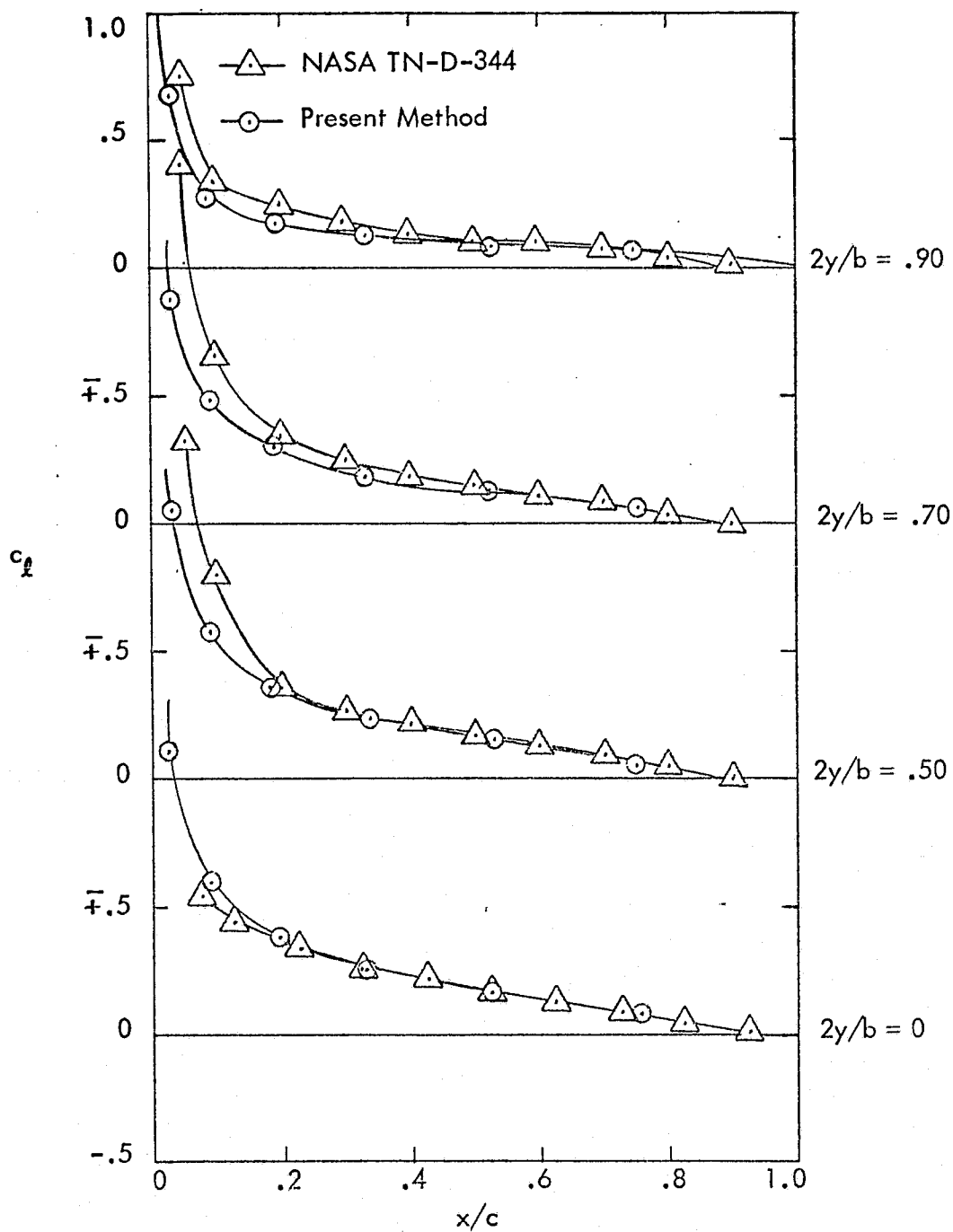


Figure 8a. The distribution of the lift coefficient, c_l , on a symmetric rectangular wing with $AR = 3$, $\tau = 0.05$, $\alpha = 5^\circ$, $M = .24$ and $NX = NY = 7$ for comparison with results of Ref. 15.

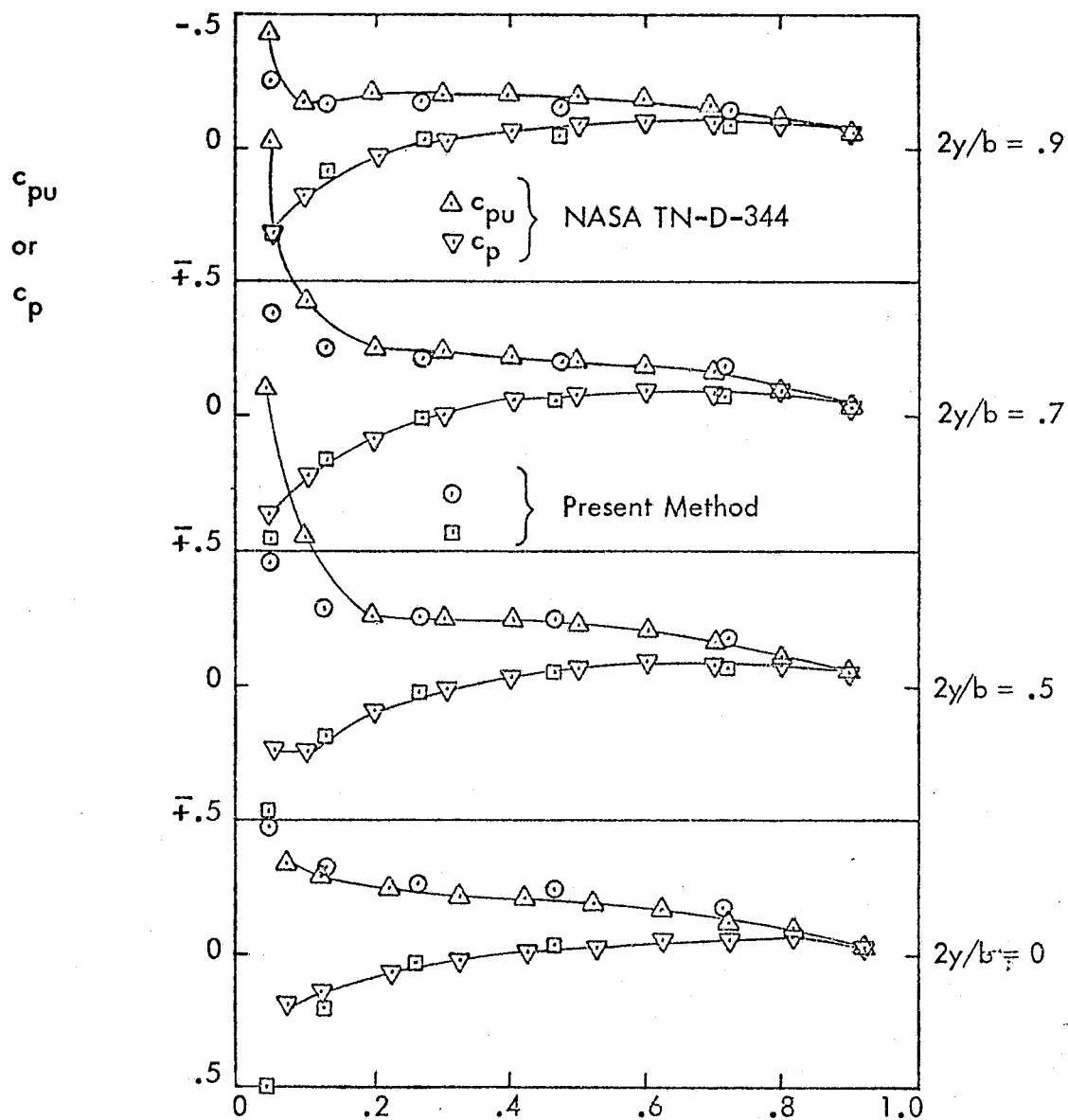


Figure 8b. The distribution of c_p on the upper and lower surfaces of a symmetric rectangular wing with $AR = 3$, $\tau = 0.05$, $\alpha = 5^\circ$, $M = .24$ and $NX=NY=6$ for comparison with results of Ref. 15.

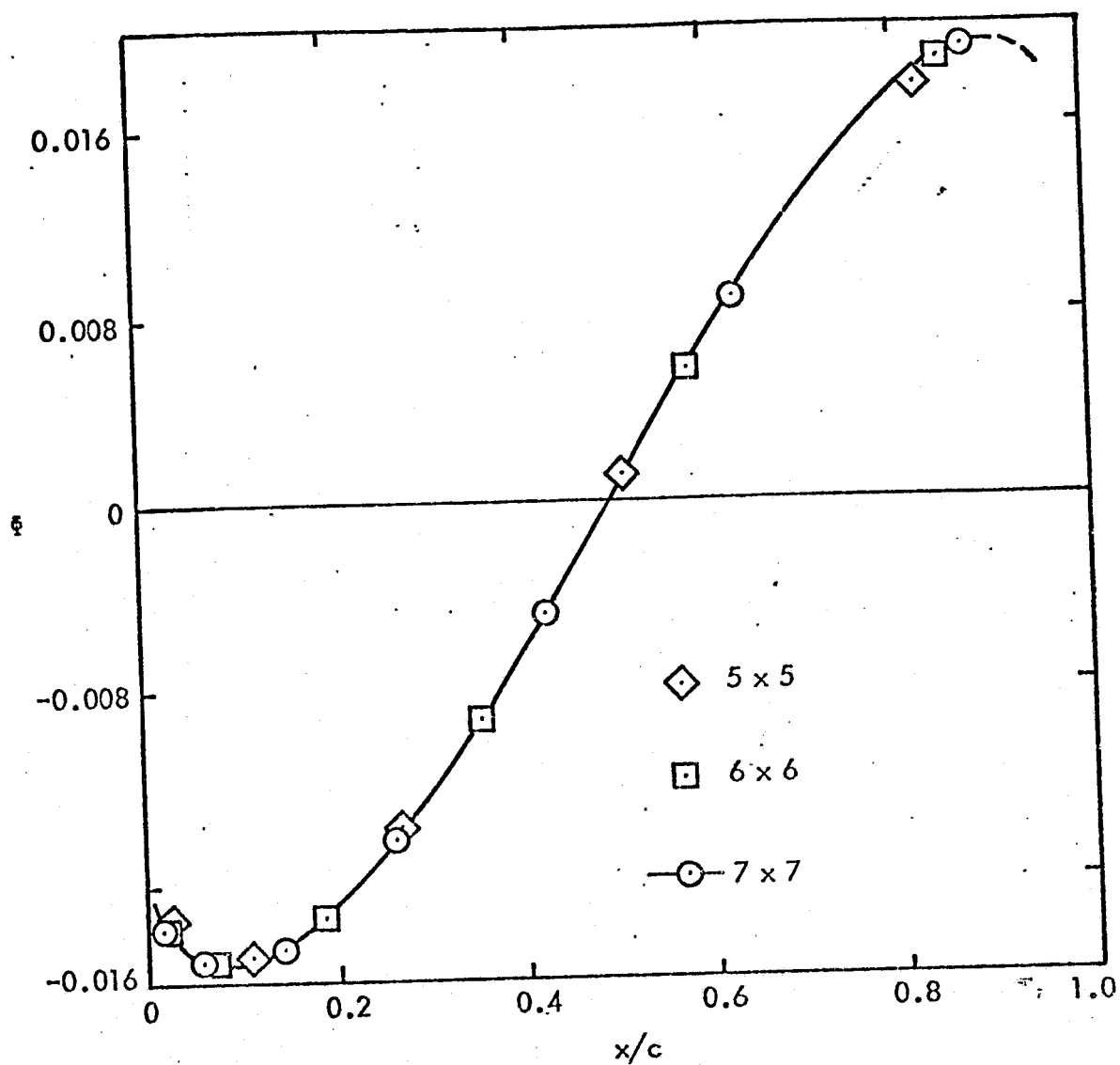


Figure 9. Analysis of Convergence: Potential Distribution, ϕ , Versus x/c , at $y = 0$, for Rectangular Wing With Biconvex Section, in Steady Subsonic Flow, for $AR = 3$, $\tau = 0.05$, $M = 0.24$, $\alpha = 0^\circ$, $NX = NY = 5, 6, 7$.

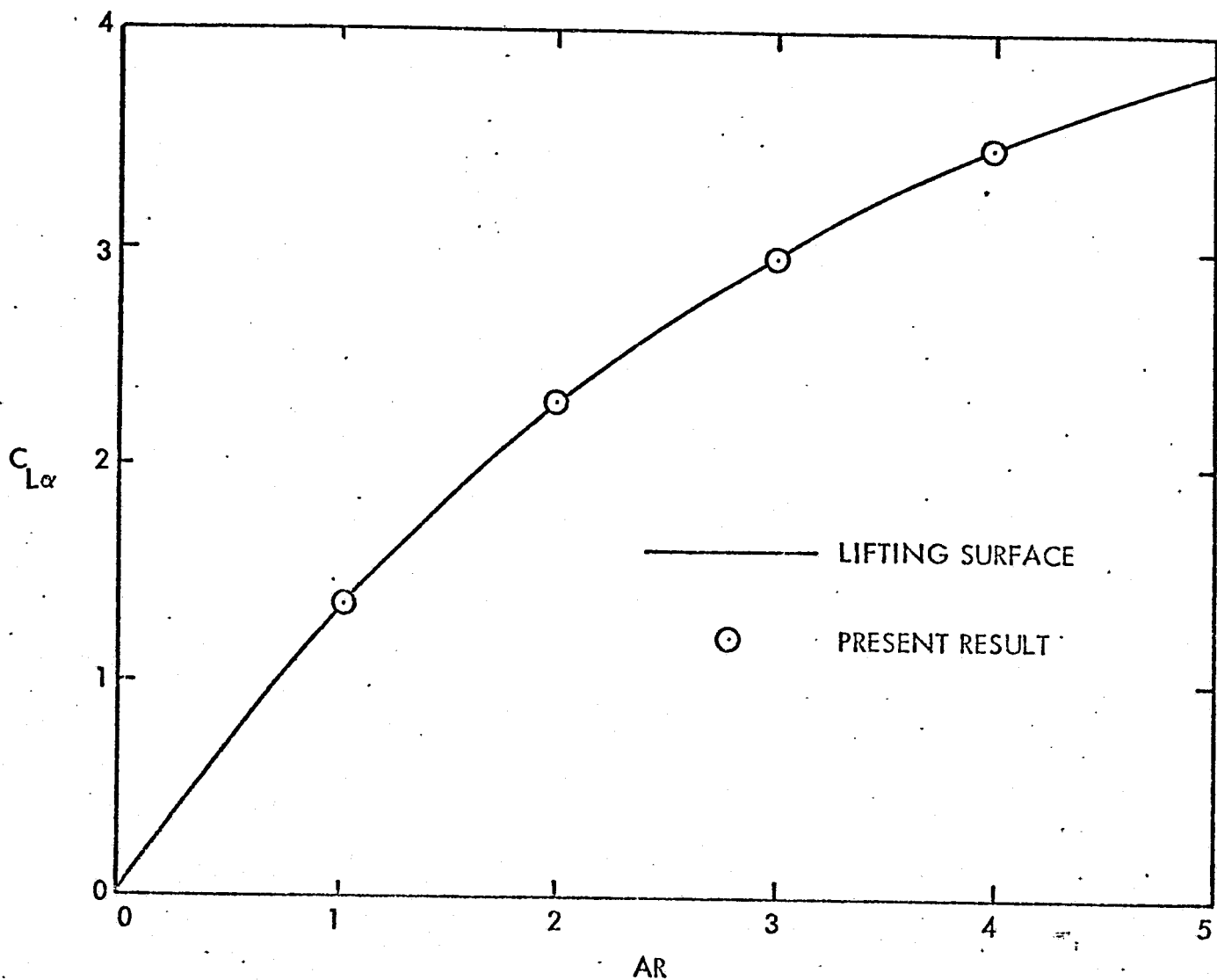


Figure 10. Lift Distribution Coefficient, $C_{L\alpha}$, Versus Aspect Ratio AR, for Delta Wing in Steady Subsonic Flow, With $\tau = 0.001$, $M = 0$, $N_x = N_y = 7$. Comparison With Lifting Surface Theory of Reference 16.

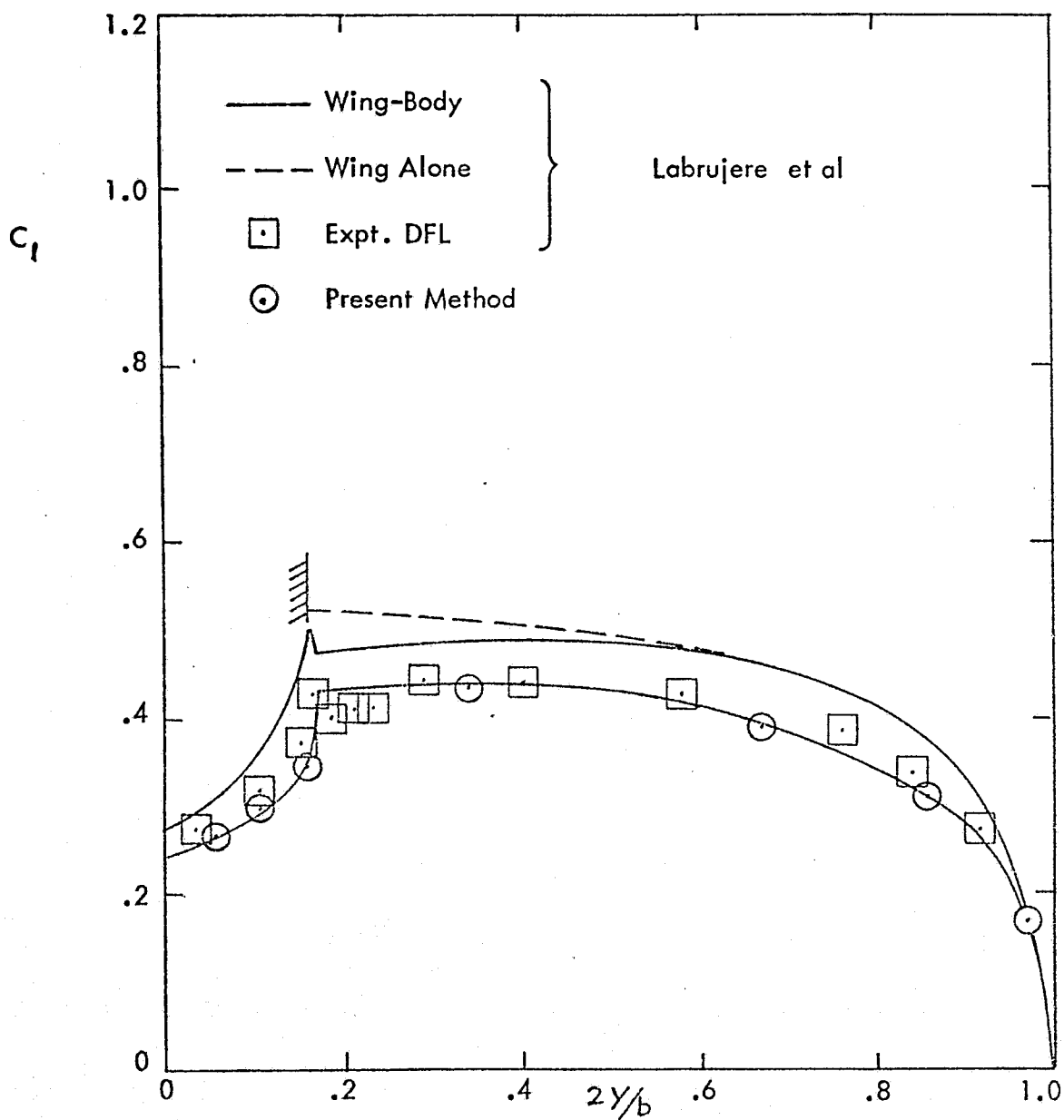


Figure 11a. The distribution of section lift coefficient, C_l , for a wing-body configuration with $\alpha_w = 6^\circ$, $\alpha_B = 0^\circ$, $\tau = 9\%$, $M=0$, $b=6c$, $r = 0.5c$ and 200 elements on the whole wing for the comparison with results of Ref. 17

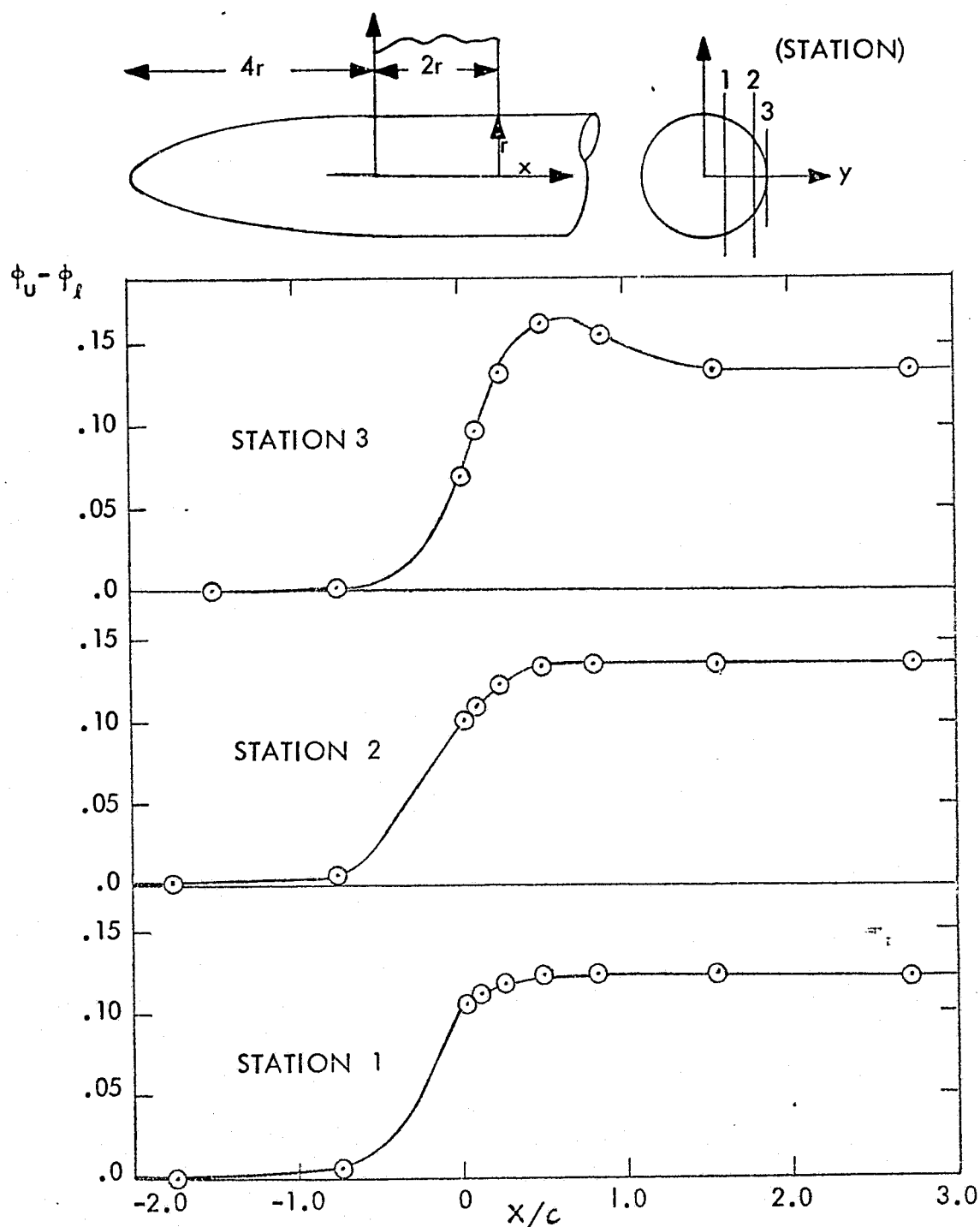


Figure 11b. The distribution of $\phi_U - \phi_f$ along three circumferential stations for a wing-body configuration with $\alpha_W = 6^\circ$, $\alpha_B = 0^\circ$, $\tau = 9\%$, $M=0$, $b=6c$, $r=0.5c$

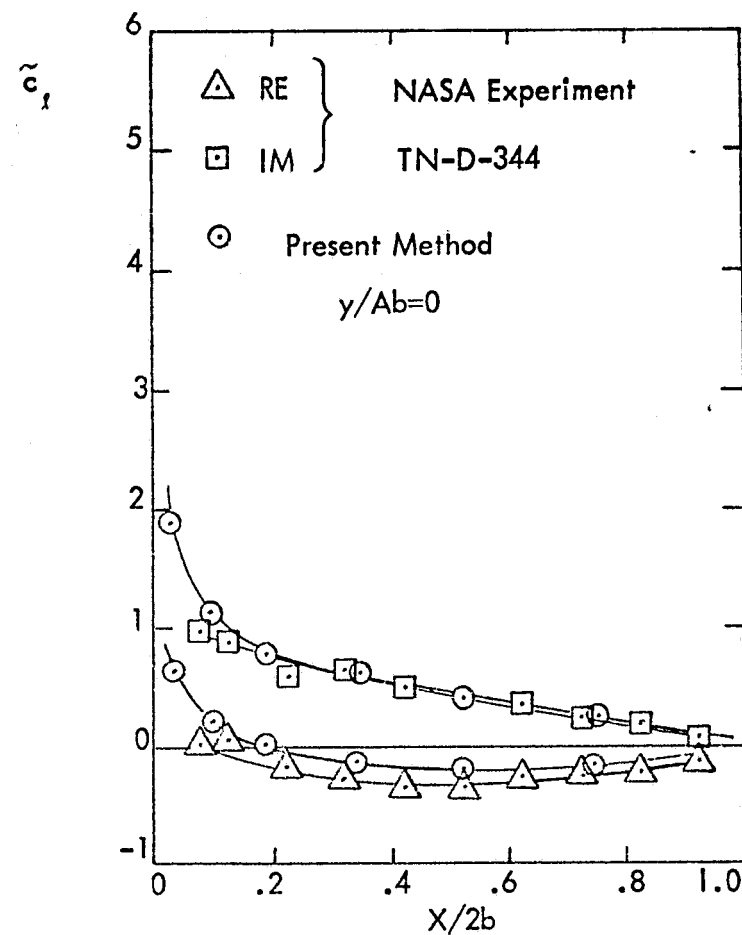
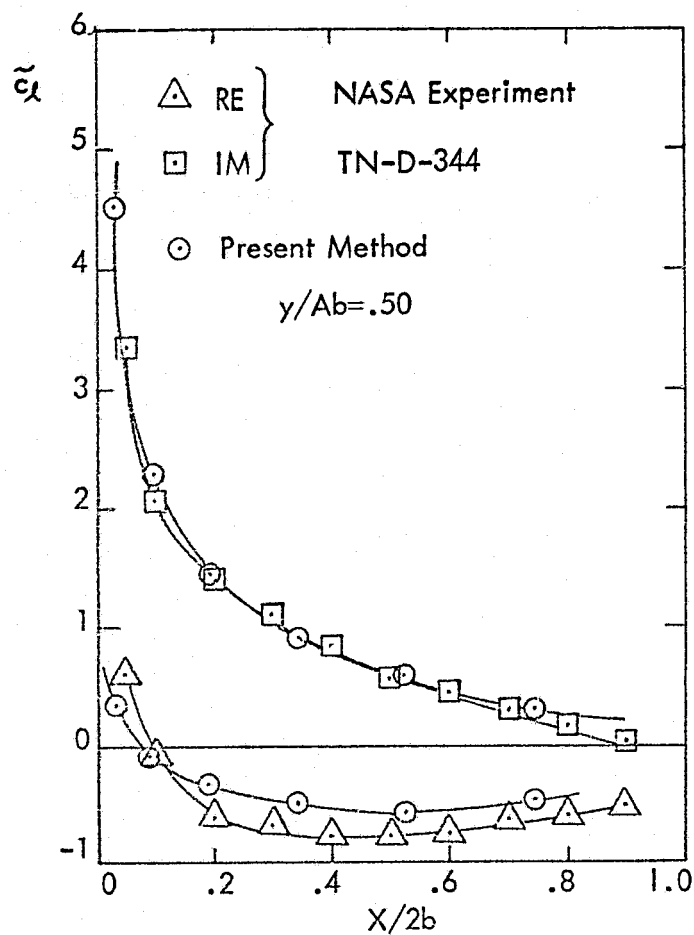


Figure 12. The distribution of lift coefficient, \tilde{c}_l , for a rectangular wing oscillating in bending mode with $k = \omega c/2U_\infty = .47$, $M = .24$, $AR = 3$, $\tau = 0.05$, $NW = 20$, $L_w = 2.5c$ and $NX = NY = 7$ for comparison with results of Ref. 15

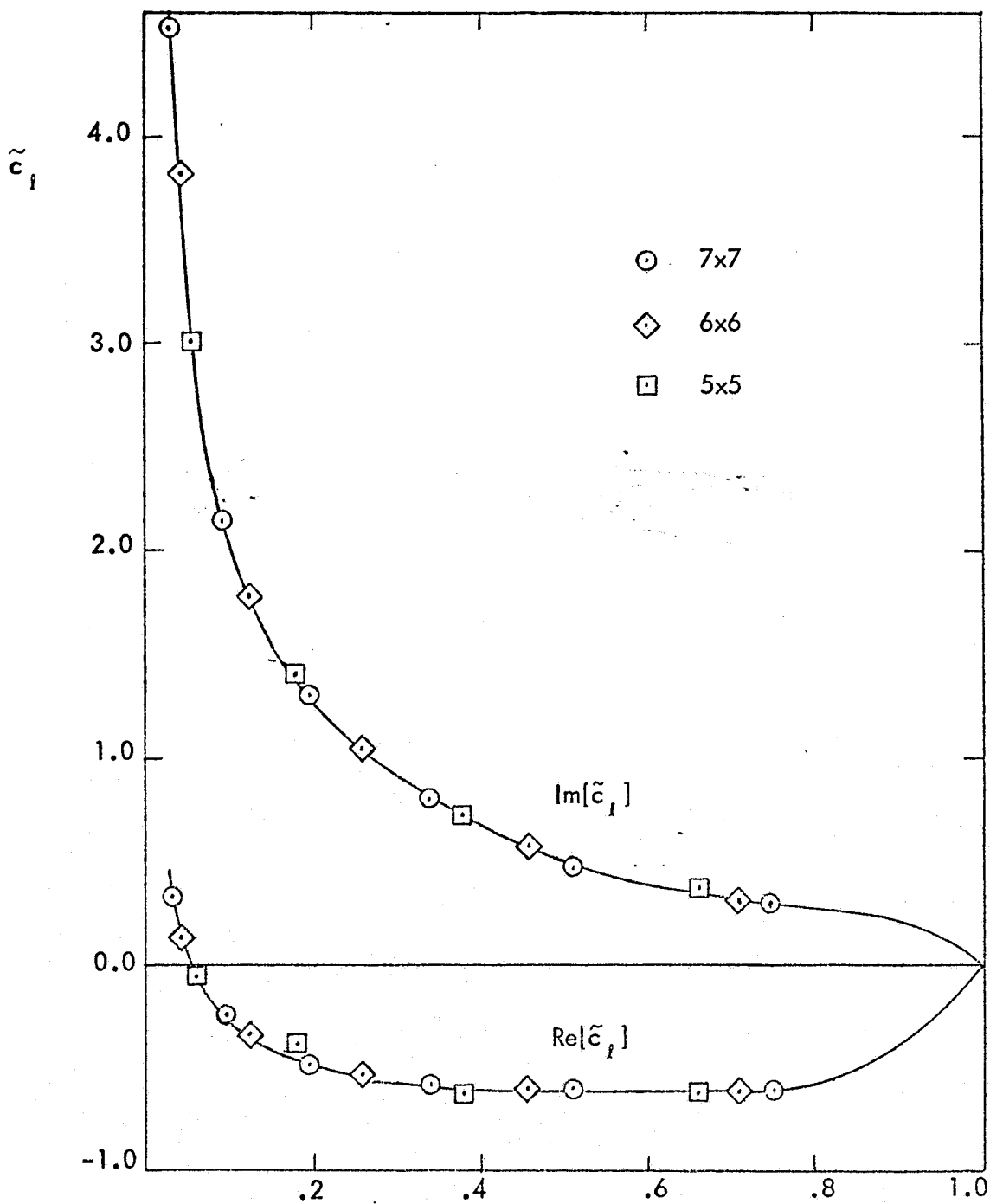


Figure 13a. Analysis of Convergence: The distribution of \tilde{c}_f versus x/c at $2y/b = .05$ for a rectangular wing oscillating in bending mode with $k = \omega c/2 U_\infty = .47$, $M = .24$, $AR = 3$, $\tau = 0.01$, $\alpha = 0^\circ$, $N_W = 30$, $L_W = 3.5c$, $NX = NY = 5, 6, 7$.

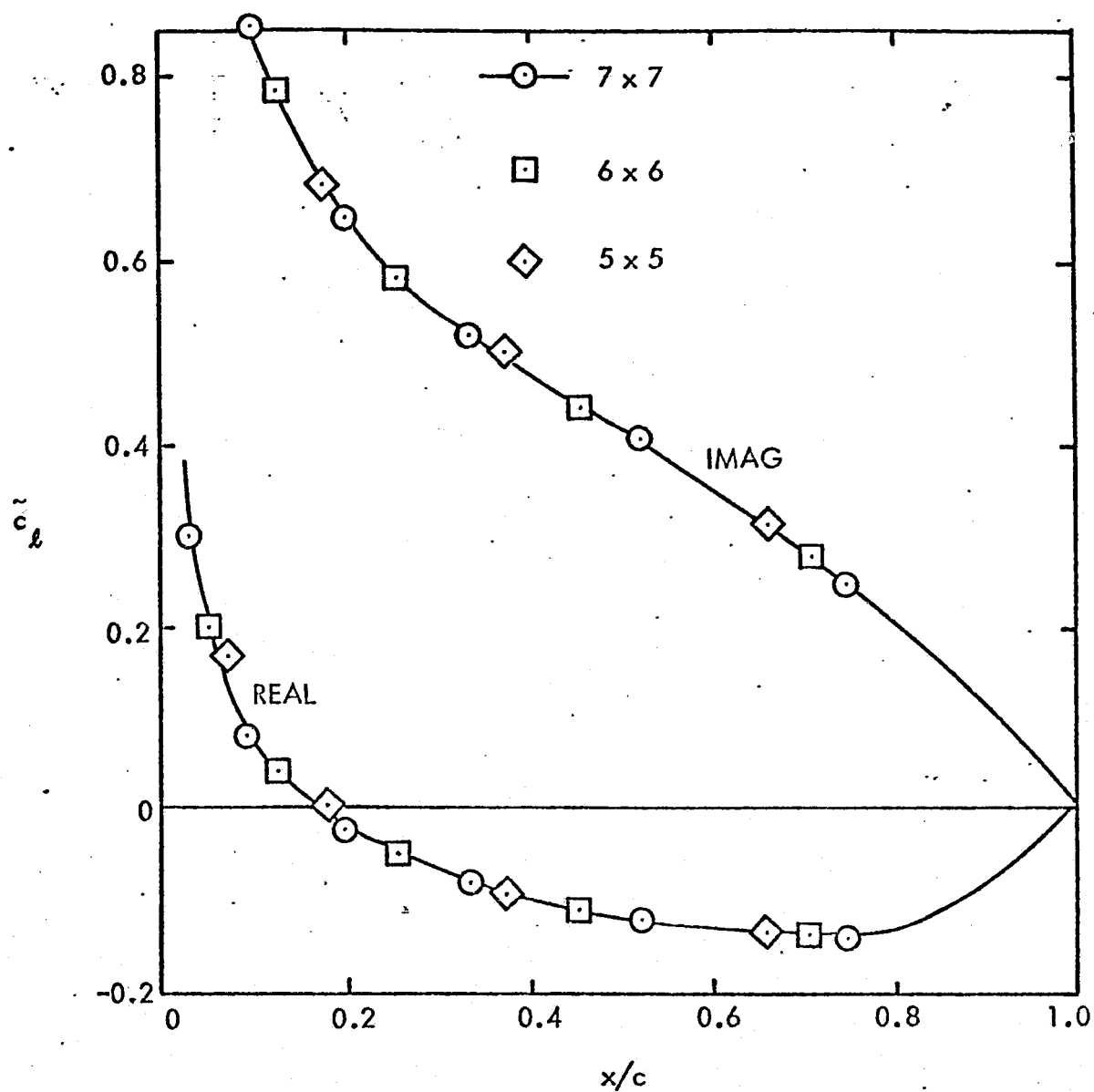


Figure 13b. Analysis of Convergence: Lift Distribution Coefficient, \tilde{c}_l , Versus x/c , at $2y/b = 0.1328$, for Rectangular Wing With Biconvex Section, Oscillating in Bending Mode in Subsonic Flow; for $AR = 3$, $\tau = 0.01$, $M = 0.24$, $\alpha = 0^\circ$, $K = 0.47$, $N_W = 30$, $L_W = 3.5c$, $N_X = N_Y = 5, 6, 7$.

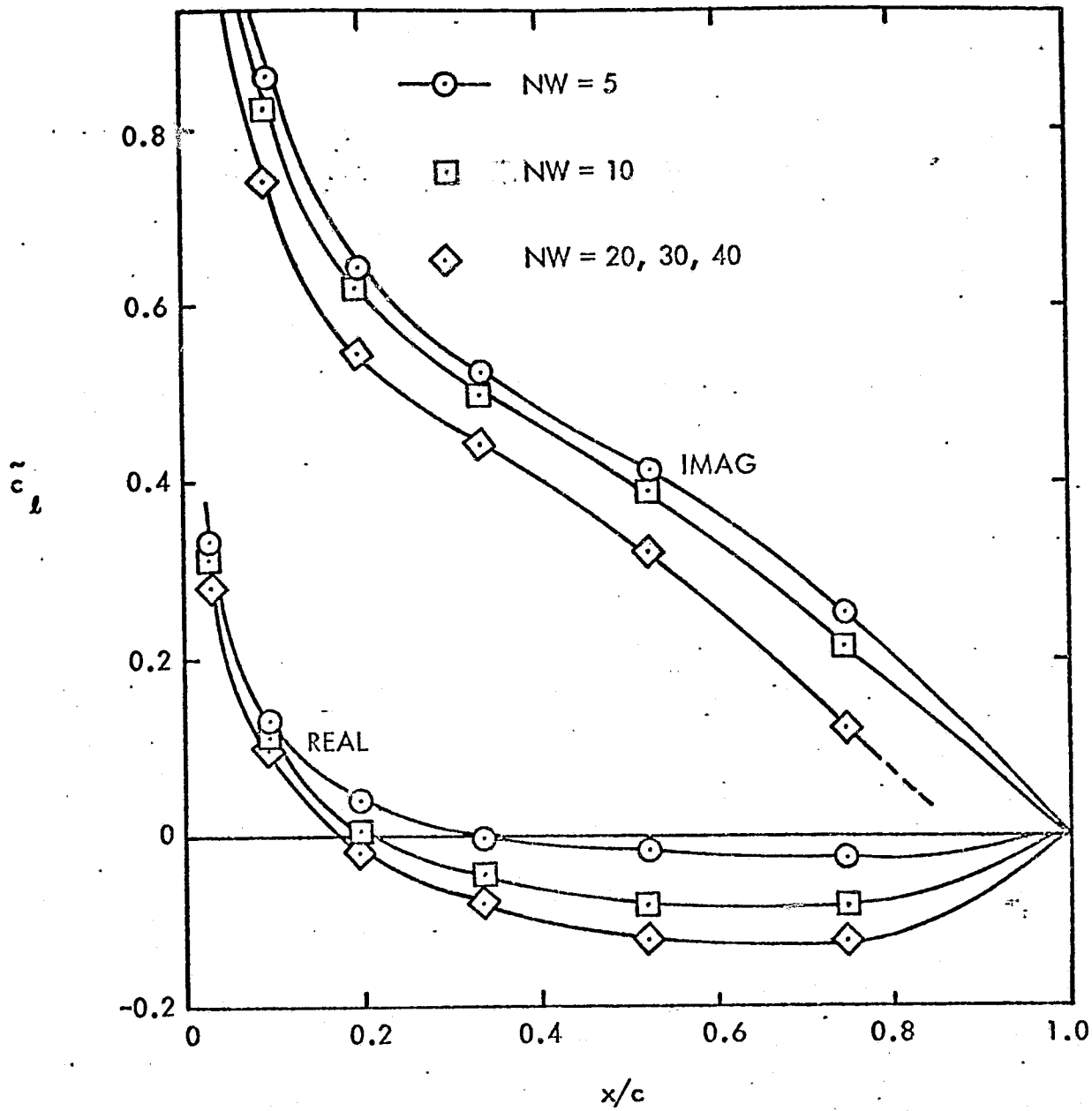


Figure 14. Analysis of Convergence: Lift Distribution Coefficient, \tilde{c}_l , Versus x/c , at $2y/b = 0.1328$ for Rectangular Wing With Biconvex Section, Oscillating in Bending Mode in Subsonic Flow, for $AR = 3$, $\tau = 0.01$, $M = 0.24$, $\alpha = 0^\circ$, $K = 0.47$, $L_W = 4c$, $N_x = N_y = 7$.

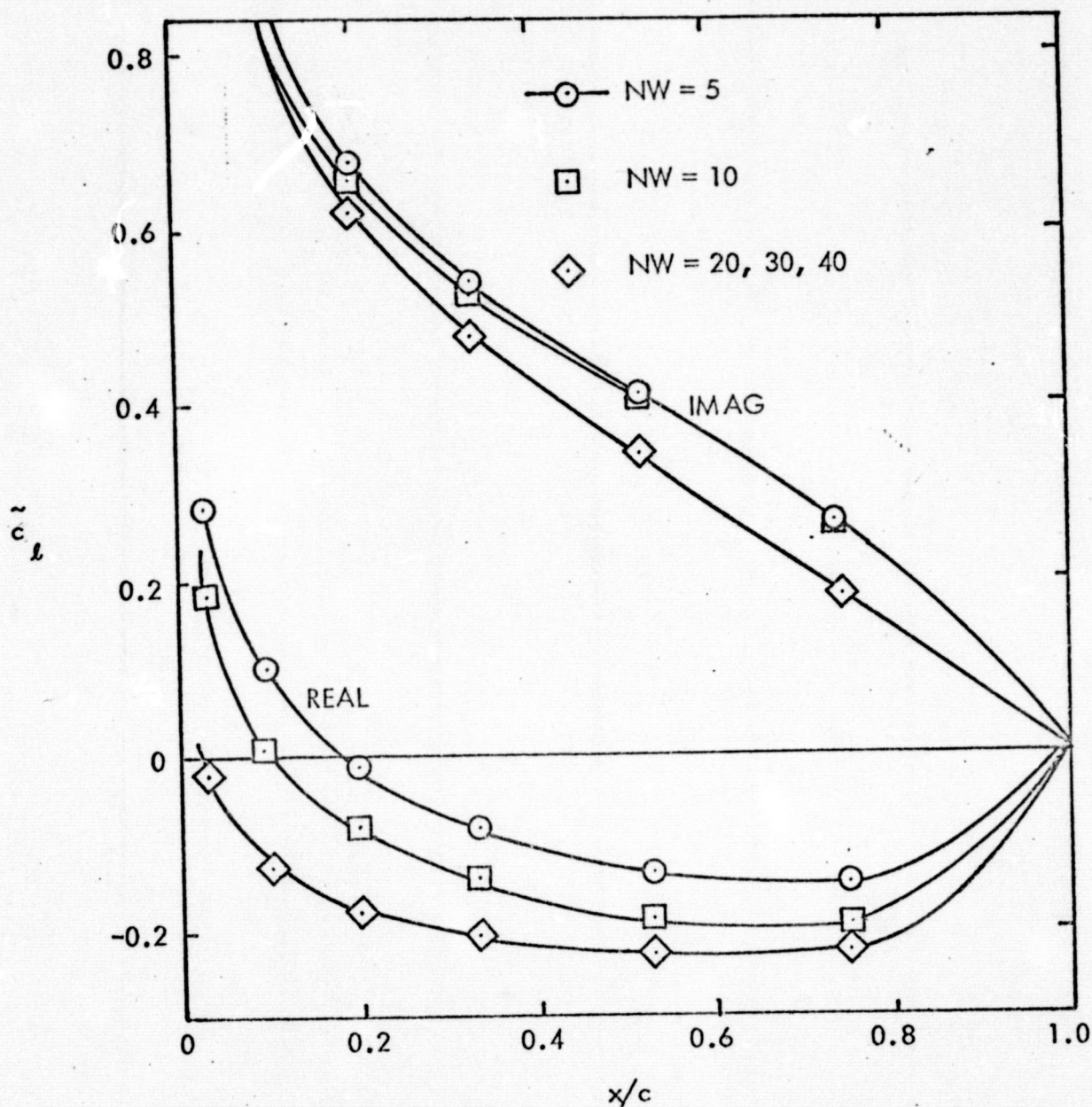


Figure 15. Analysis of Convergence: Lift Distribution Coefficient, \tilde{c}_l , Versus x/c , of $2y/b = 0.1328$, for Rectangular Wing With Biconvex Section, Oscillating in Bending Mode in Subsonic Flow, for $AR = 3$, $\tau = 0.01$, $M = 0.24$, $\alpha = 0^\circ$, $K = 0.47$, $\Delta x_W = 0.1$, $N_x = N_y = 7$.

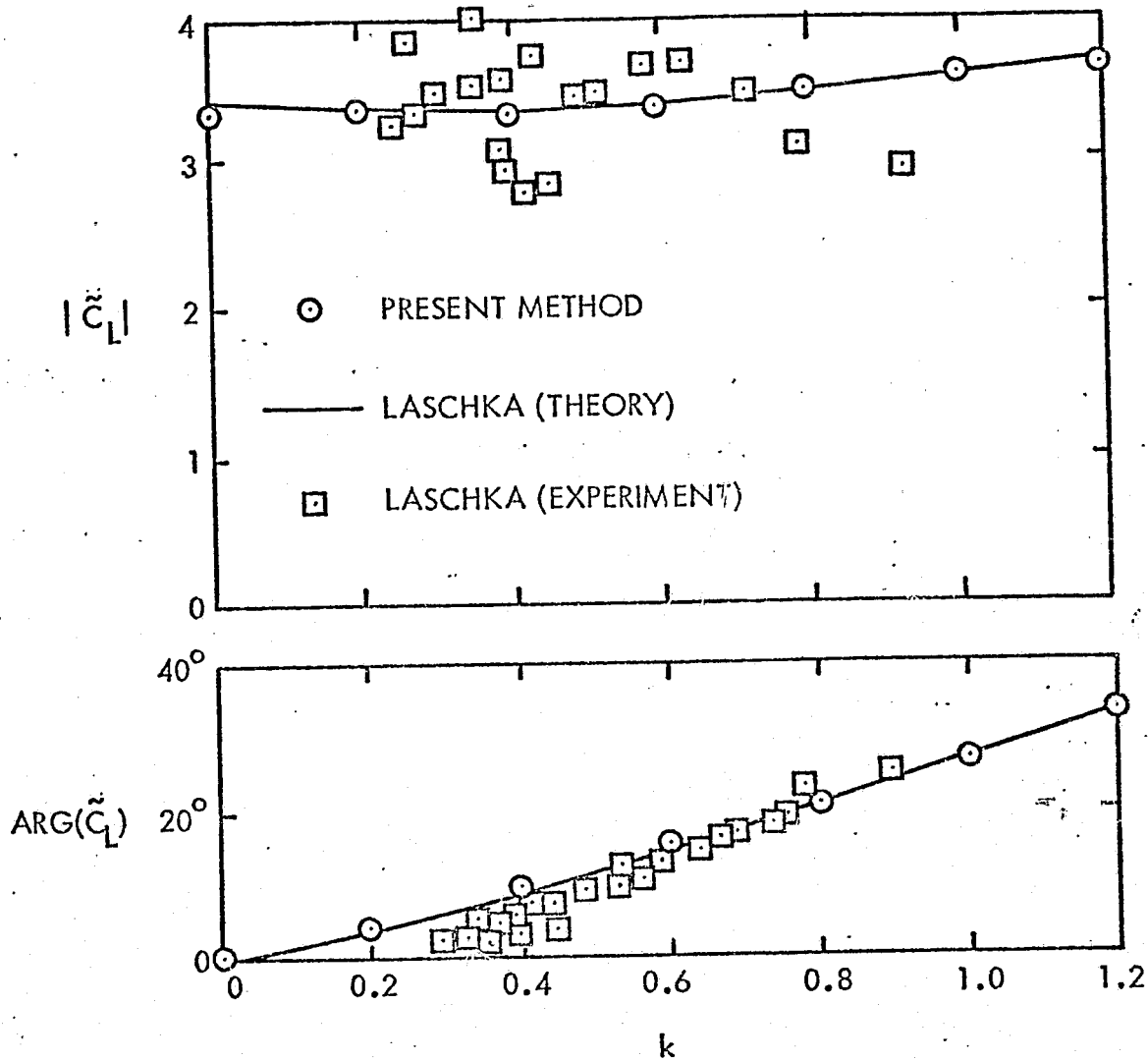
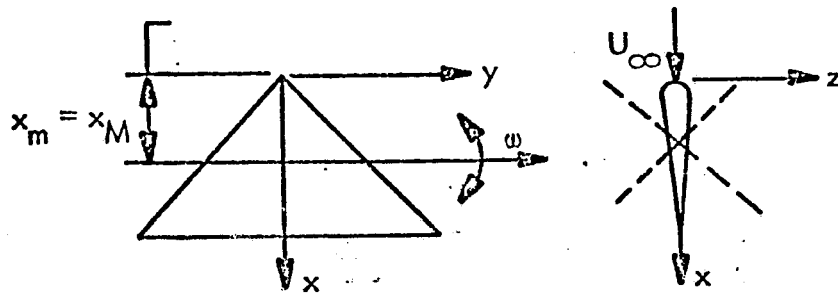


Figure 16a. Lift Coefficient, \tilde{C}_L , Versus k , for Delta Wing Oscillating in Pitch, With $AR = 4$, $\tau = 0.005$, $M = 0$, $N_x = 10$, $N_y = 6$, $N_W = 20$, $L_W/c = 2$. Comparison With Results of Reference 18.

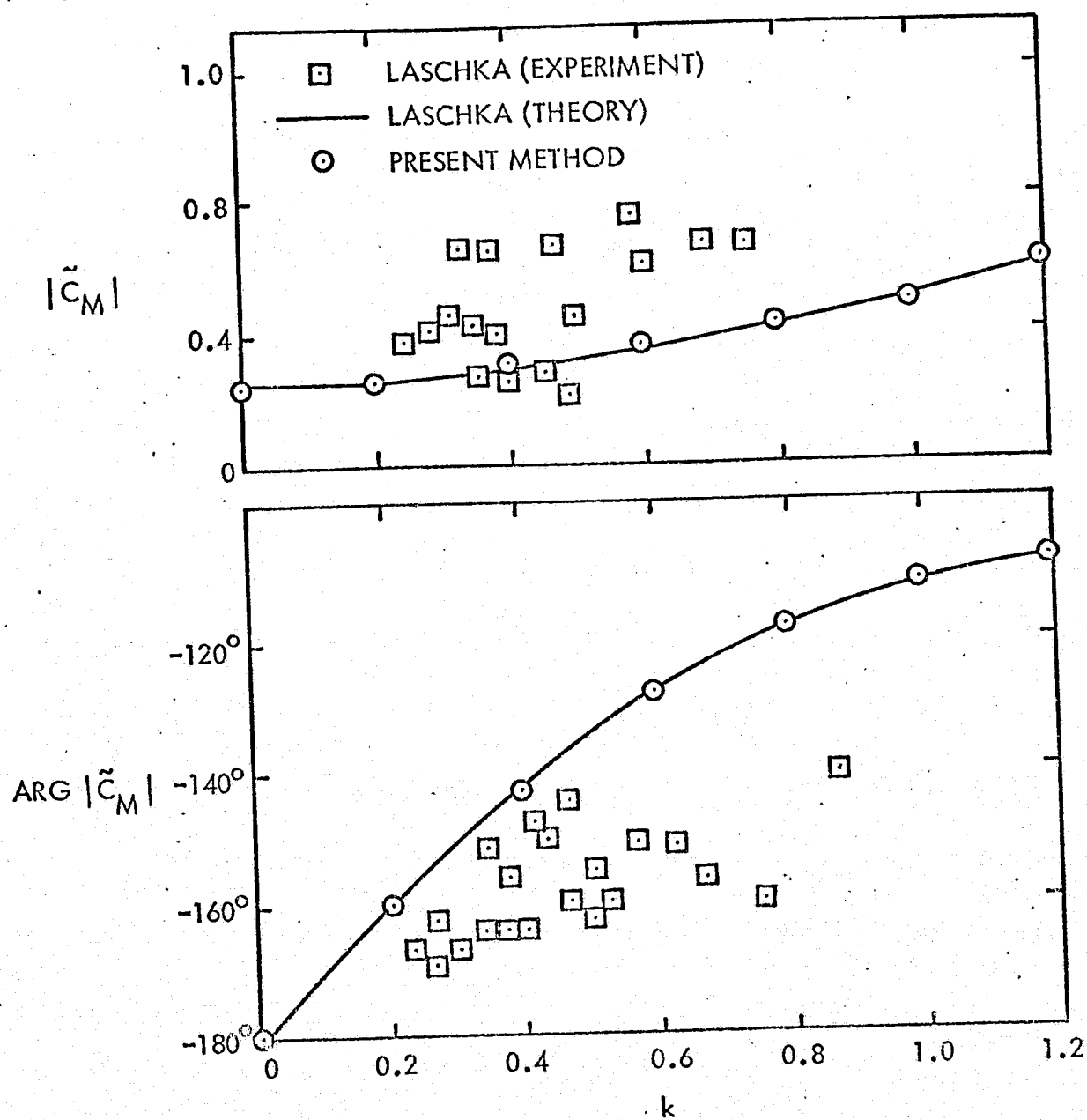
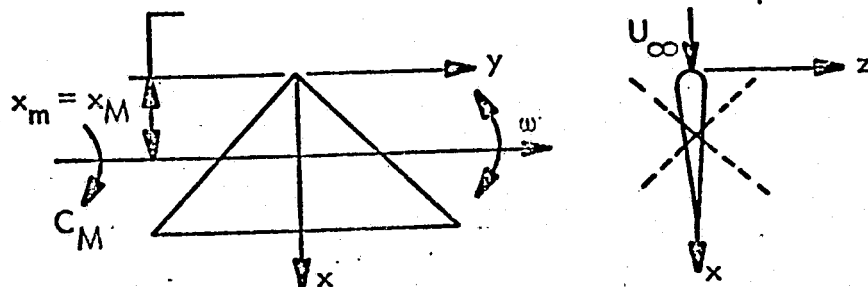


Figure 16b. Moment Coefficient, \tilde{C}_M , Versus k , for Delta Wing Oscillating in Pitch With $AR = 4$, $\tau = 0.005$, $M = 0$, $N_x = 10$, $N_y = 6$, $N_W = 20$, $L_W = 2c$. Comparison With Results of Reference 18.

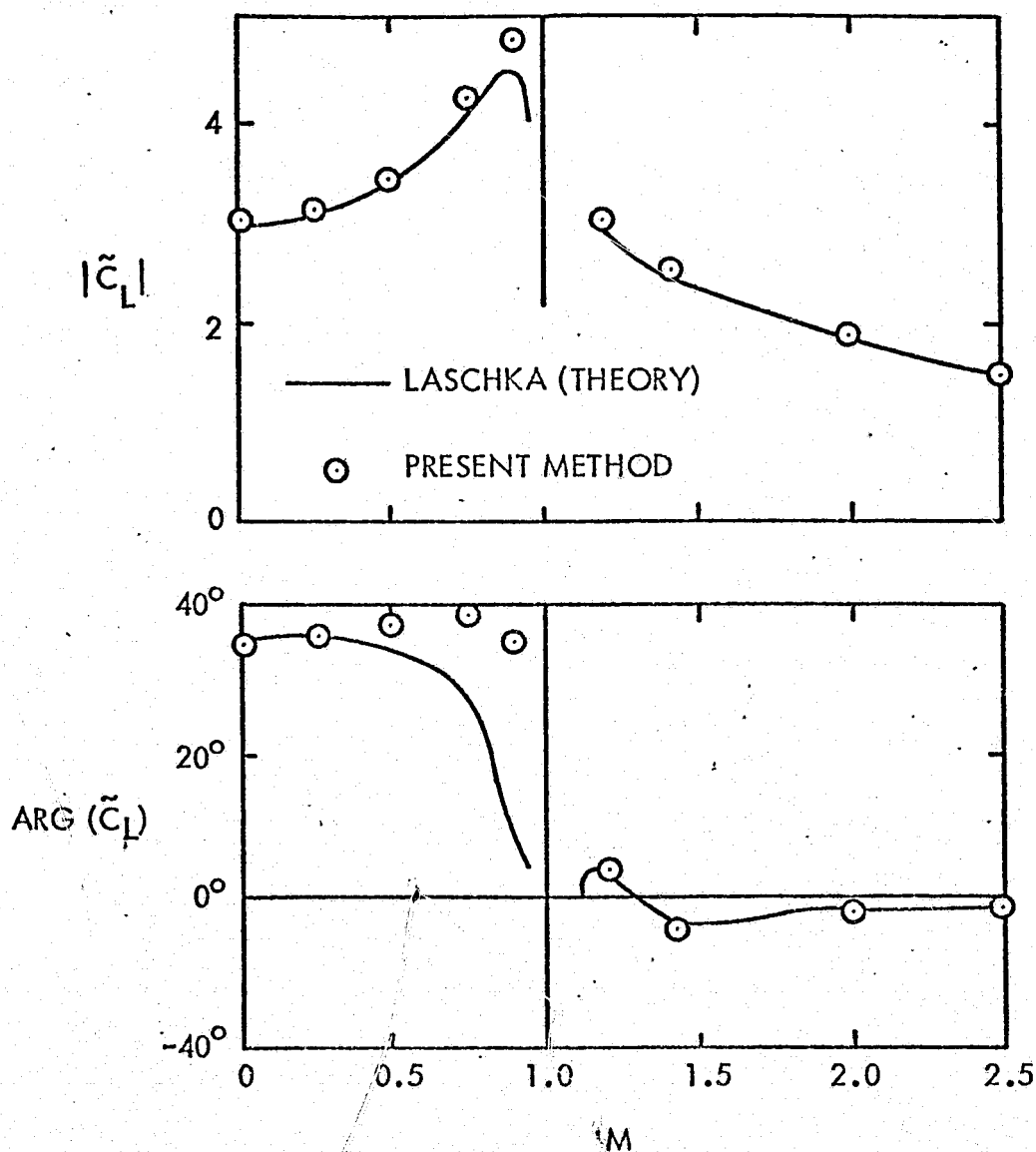
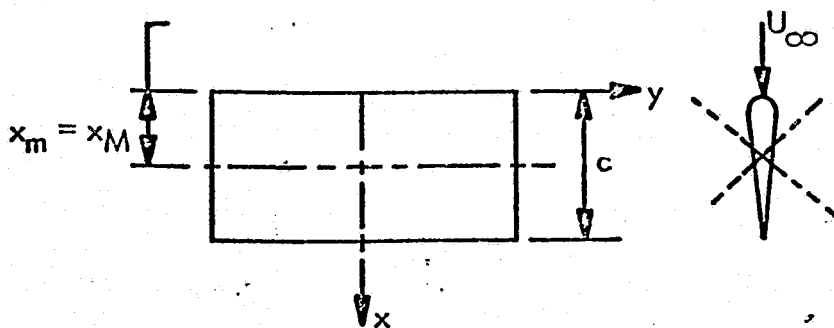


Figure 17a. Lift Coefficient, \tilde{C}_L , Versus M , for Rectangular Wing Oscillating in Pitch, With $AR = 2$, $\tau = 0.001$, $k = 1$, $N_x = 10$, $N_y = 6$, $N_W = 20$, $L_W/c = 2$, $N_D = 30$. Comparison With Results of Reference 18.

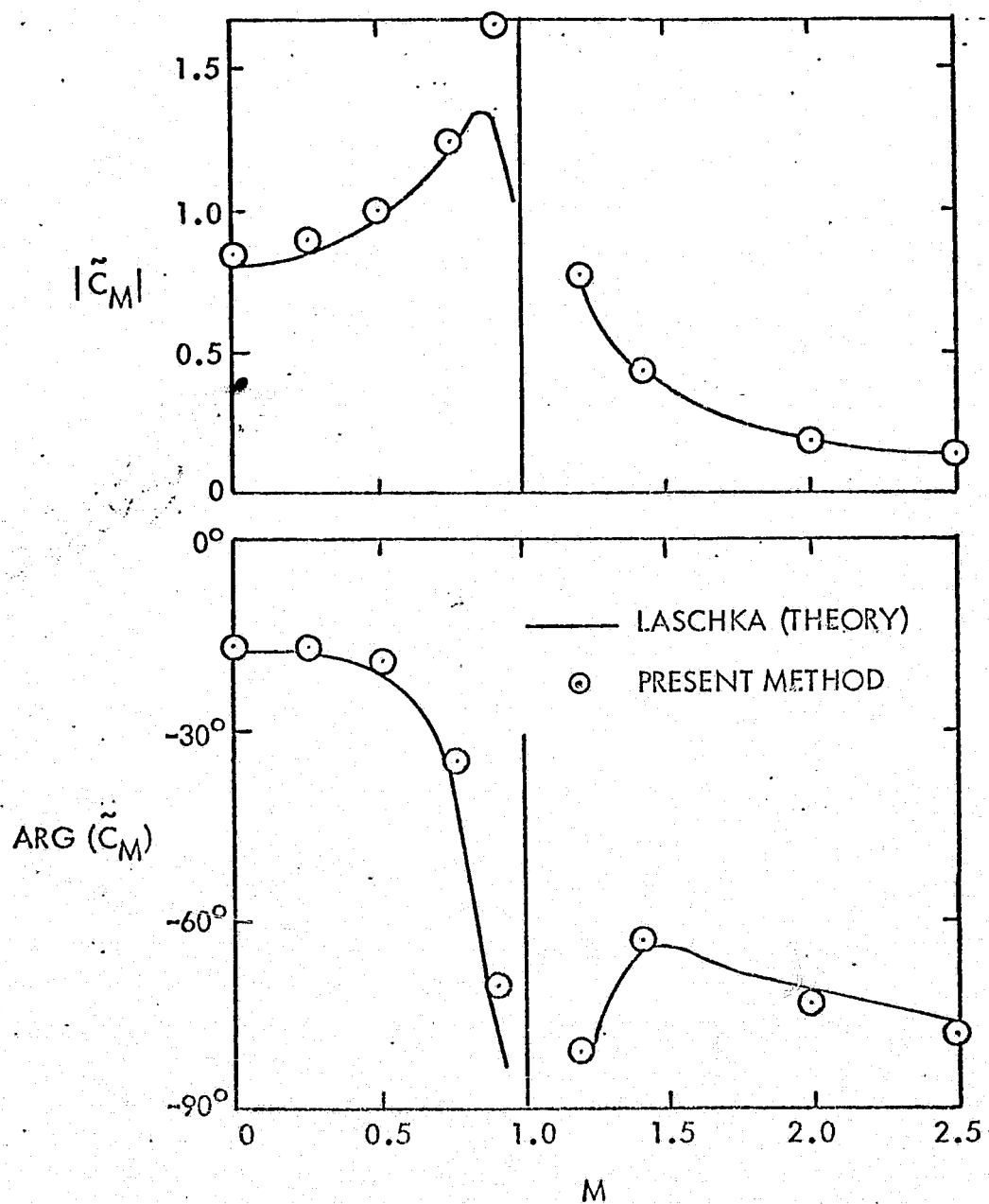
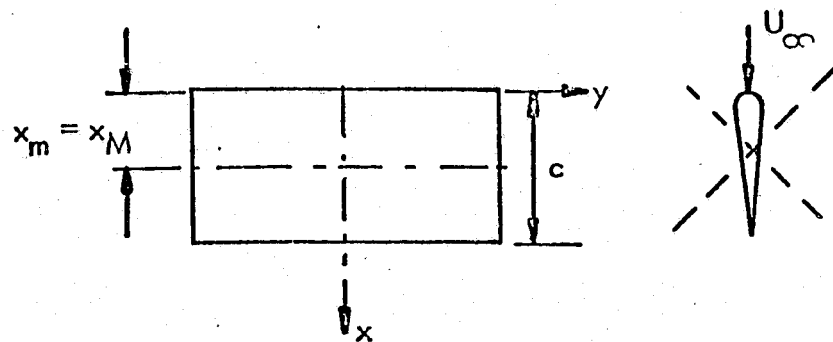


Figure 17b. Moment Coefficient, \tilde{C}_M , Versus M , for Rectangular Wing Oscillating in Pitch, for $AR = 2$, $\tau = 0.001$, $k = 1$, $N_x = 10$, $N_y = 6$, $N_W = 20$, $L_W/c = 2$, $N_D = 30$. Comparison With Results of Reference 18.

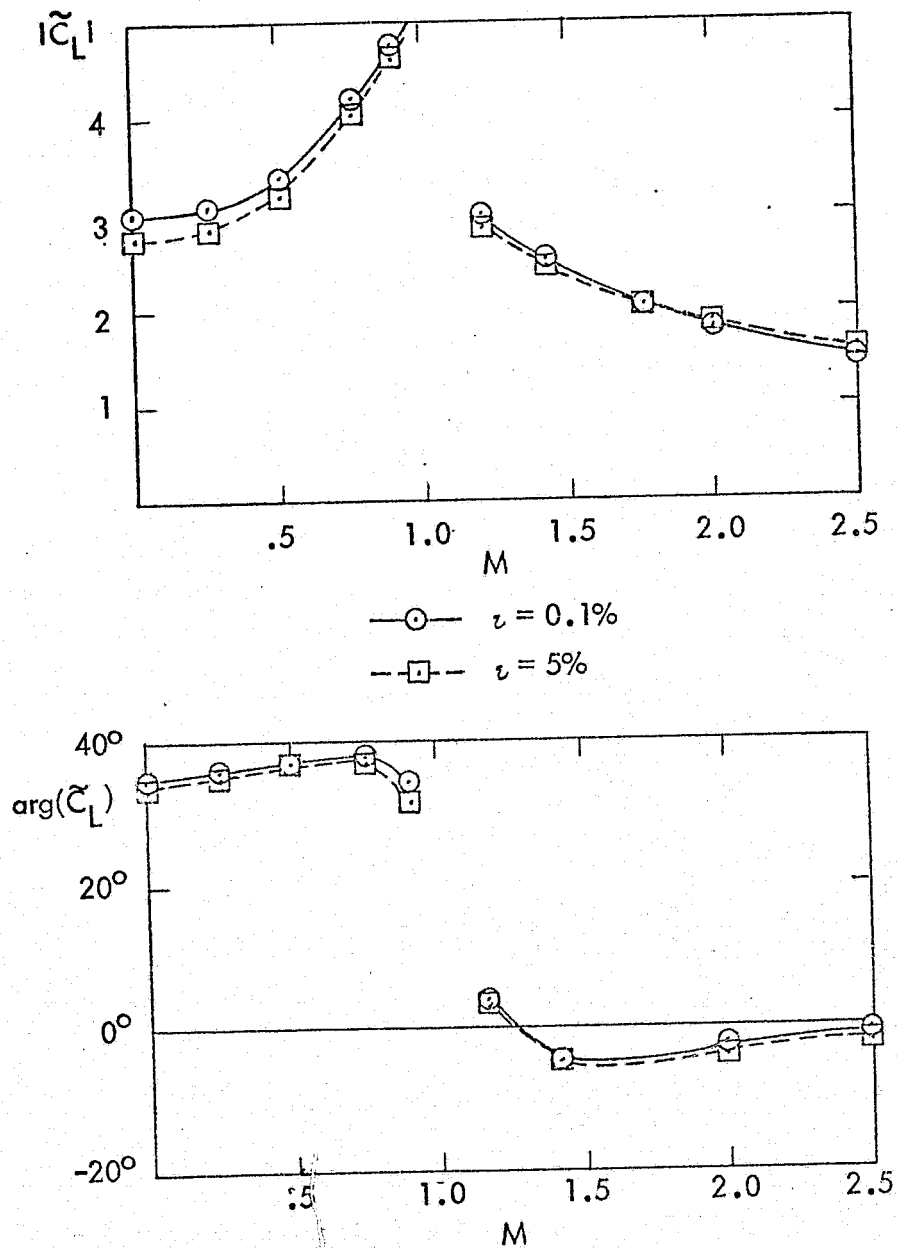


Figure 18a. Thickness effects in oscillatory subsonic and supersonic flows. Results are total lift coefficient, \tilde{C}_L , versus M , for a rectangular wing with $AR = 2$ and $K = \omega c / 2U_\infty = 1.0$ oscillating in pitch about axis $X = X_m$.

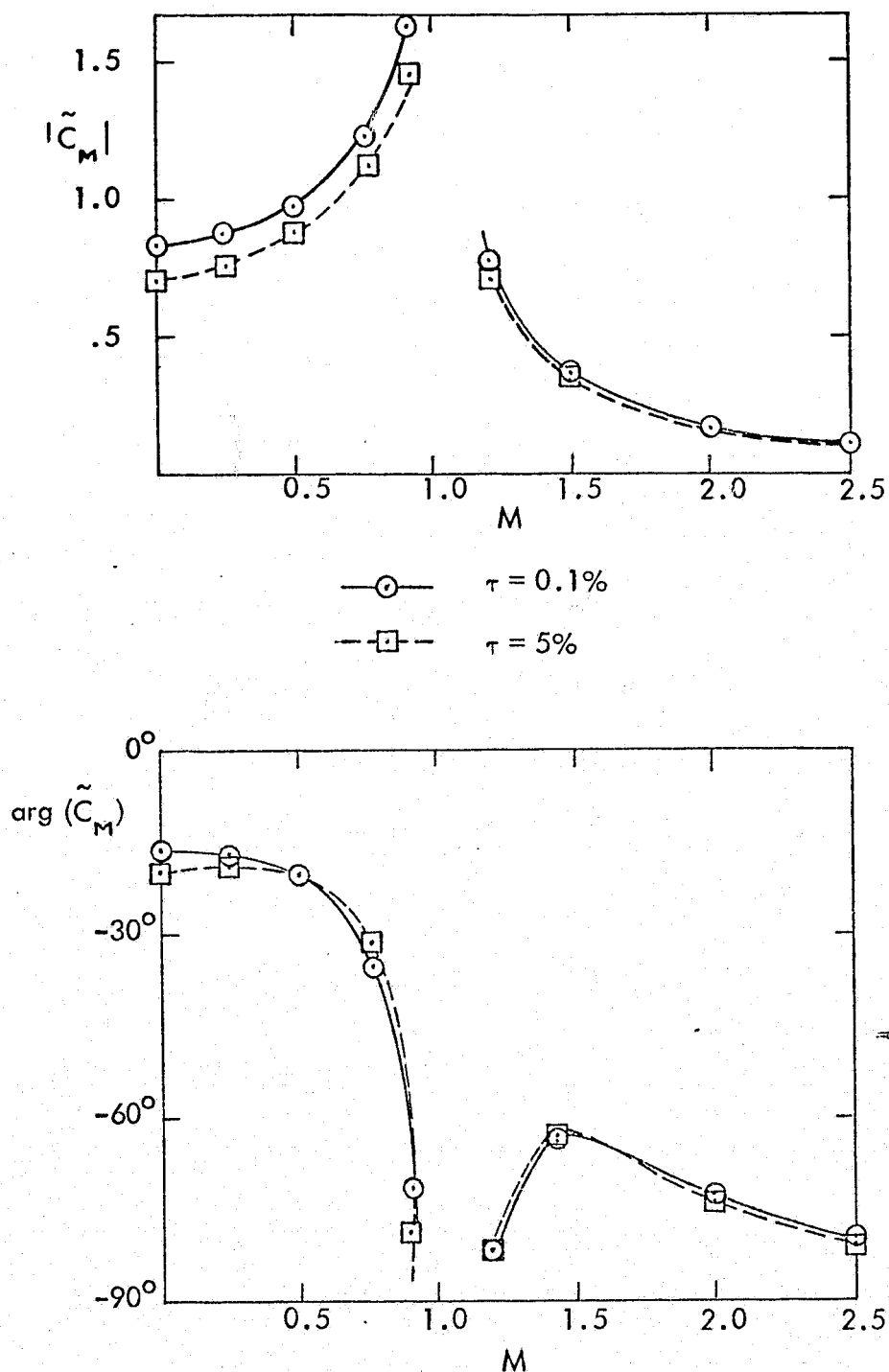


Figure 18b. Thickness Effect in Oscillatory Subsonic and Supersonic Flows. Results are total moment coefficient, \tilde{C}_M , versus M , for a rectangular wing with $AR = 2$ and $k = \omega c / 2U_\infty = 1.0$ oscillating in pitch about axis $x = x_m$.

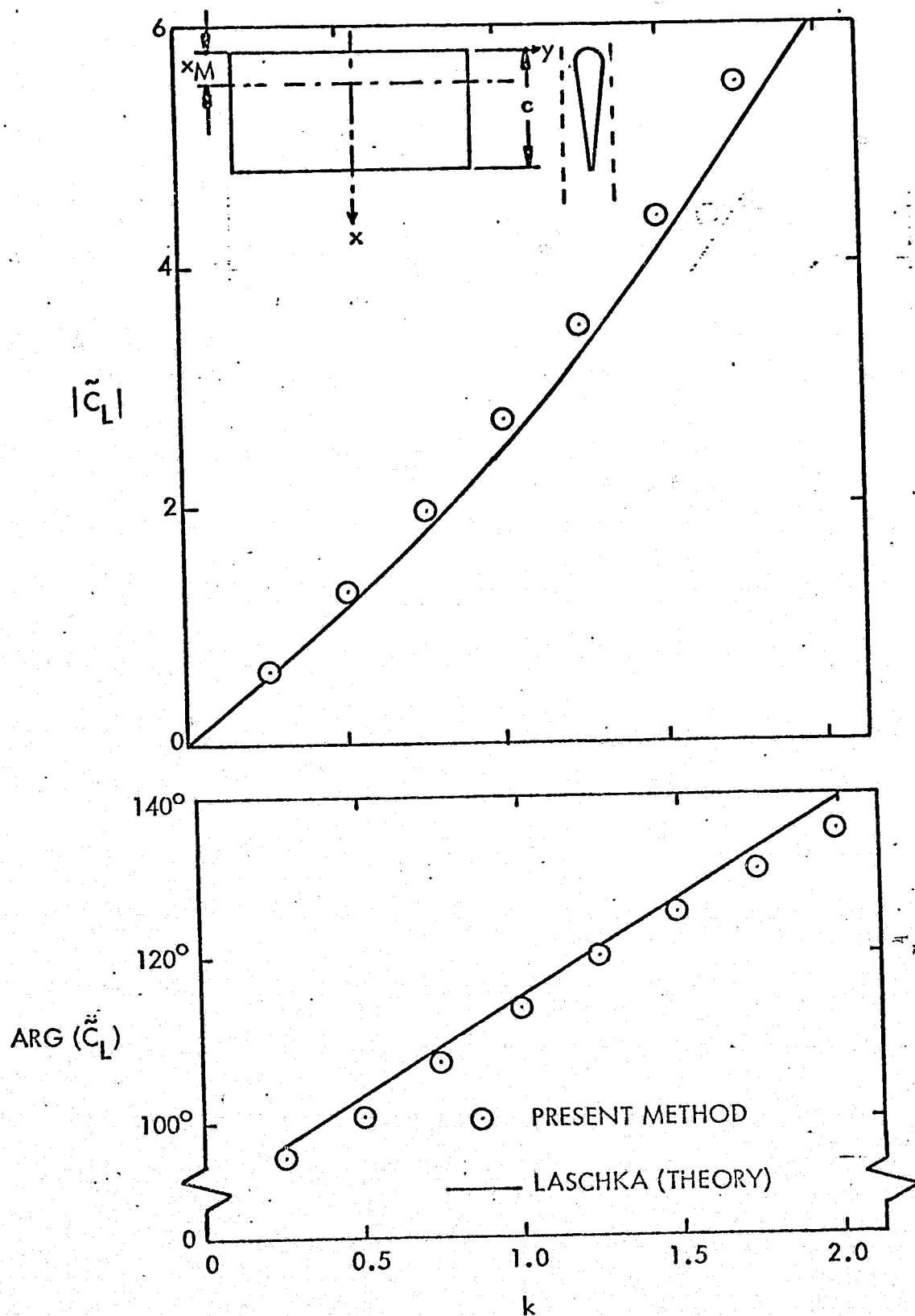


Figure 19a. Lift Coefficient, \tilde{C}_L , Versus k , for Rectangular Wing Oscillating in Plunge, With $AR = 2$, $\tau = 0.001$, $M = 0$, $N_x = 10$, $N_y = 6$, $N_W = 20$, $L_W = 2c$. Comparison With Results of Reference 18.

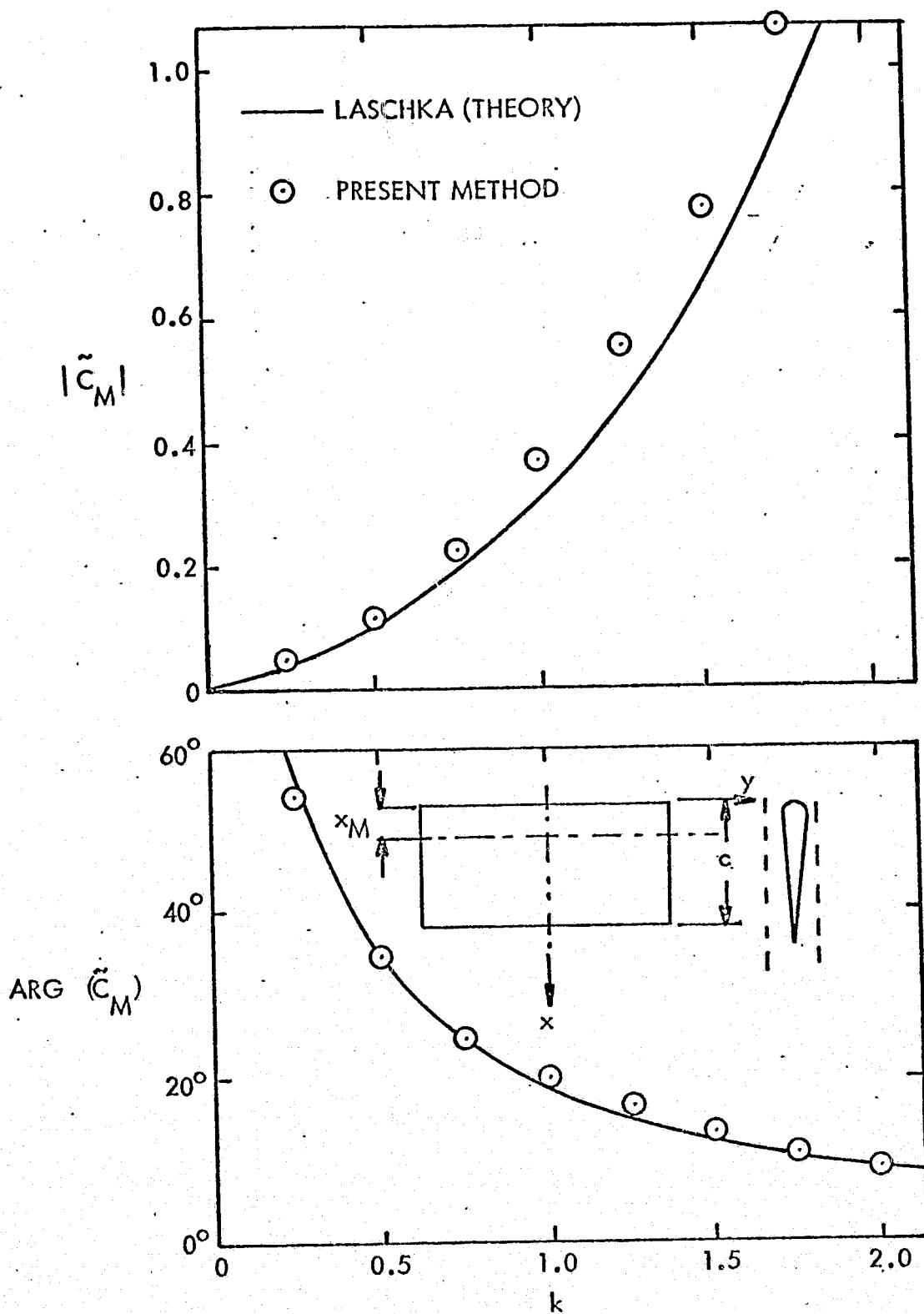


Figure 19b. Moment Coefficient, \tilde{C}_M , Versus k for a Rectangular Wing Oscillating in Plunge, With $AR = 2$, $\tau = 0.001$, $M = 0$, $N_x = 10$, $N_y = 6$, $N_W = 20$, $L_W = 2c$. Comparison With Results of Reference 18.

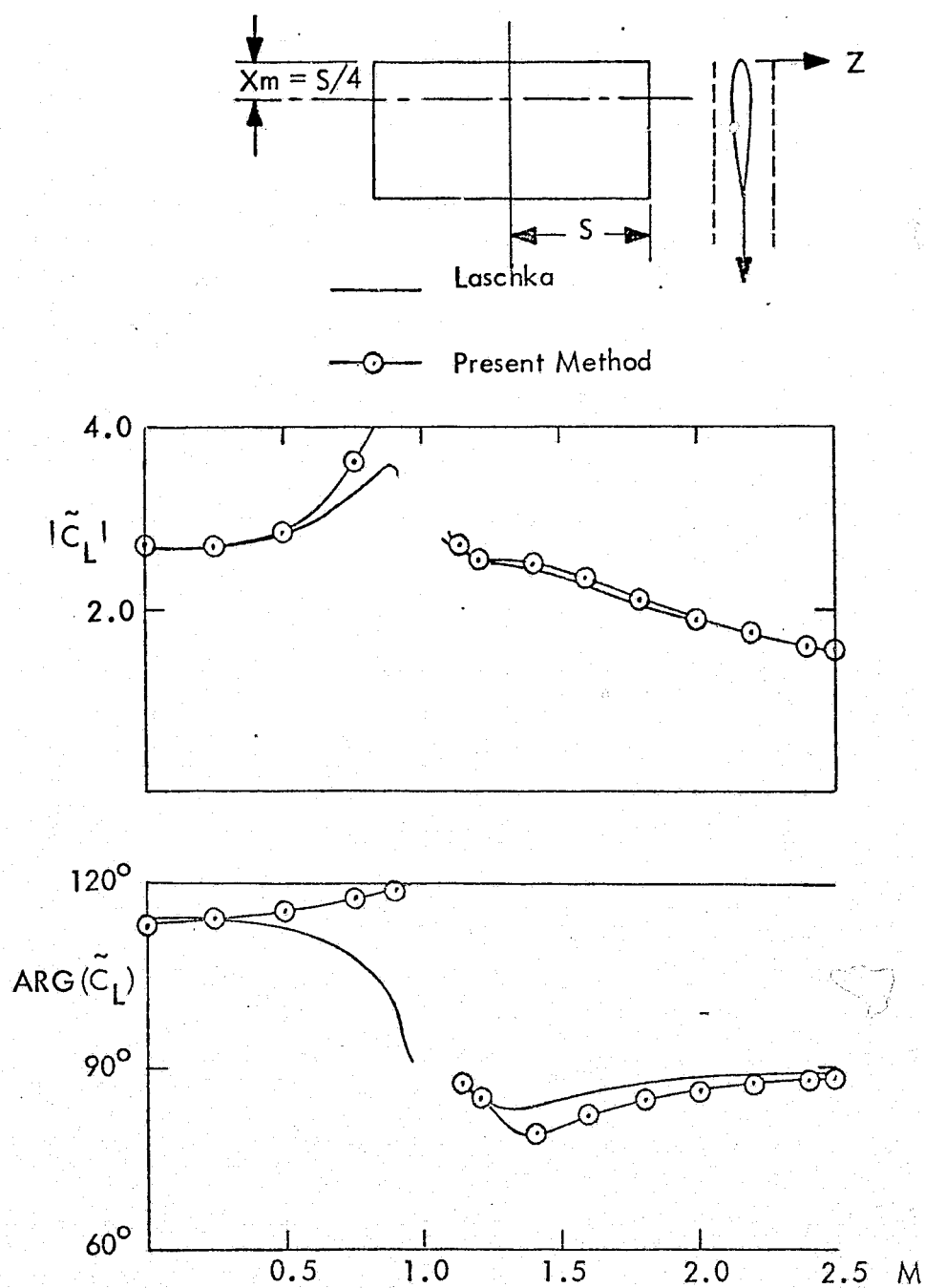


Figure 20a. Total lift coefficient, C_L , versus M , for a rectangular wing with $AR = 2$, $\tau = 0.1\%$ and $k = \omega c / 2U_\infty = 1.0$ oscillating in plunge. Results are related to both subsonic and supersonic flows.

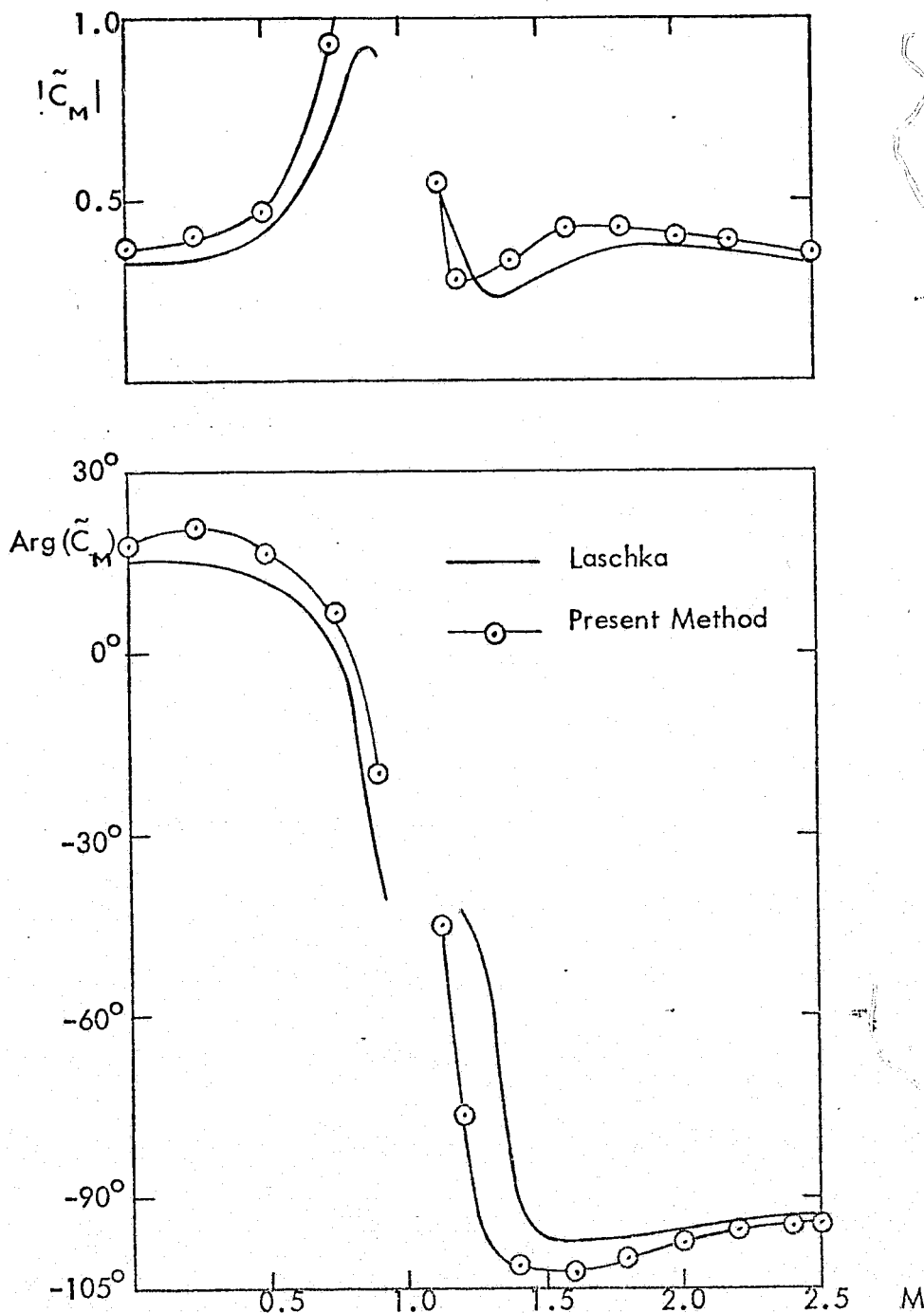


Figure 20b. Total moment coefficient, C_M , versus M , for a rectangular wing with $AR = 2$, $\tau = 0.1\%$ and $k = \omega c / 2U_\infty$ oscillating in plunge. Results are related to both subsonic and supersonic flows (same problem as Figure 20a).

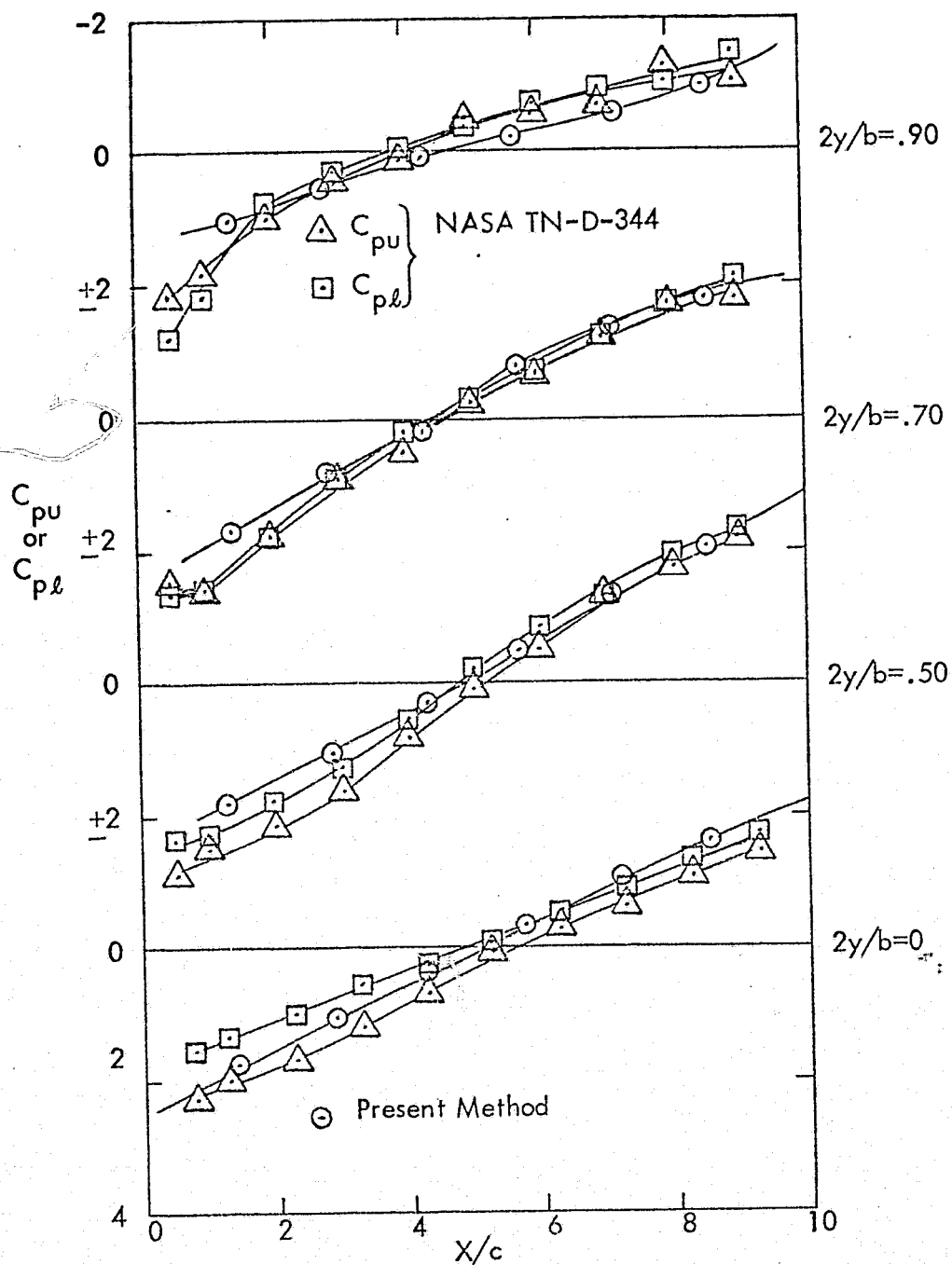


Figure 21. The pressure distribution on a symmetric rectangular wing with $AR = 3$, $\tau = 5\%$, $\alpha = 0^\circ$, $M = 1.3$ and $NX = NY = 7$ for the comparison with results of Ref. 15.

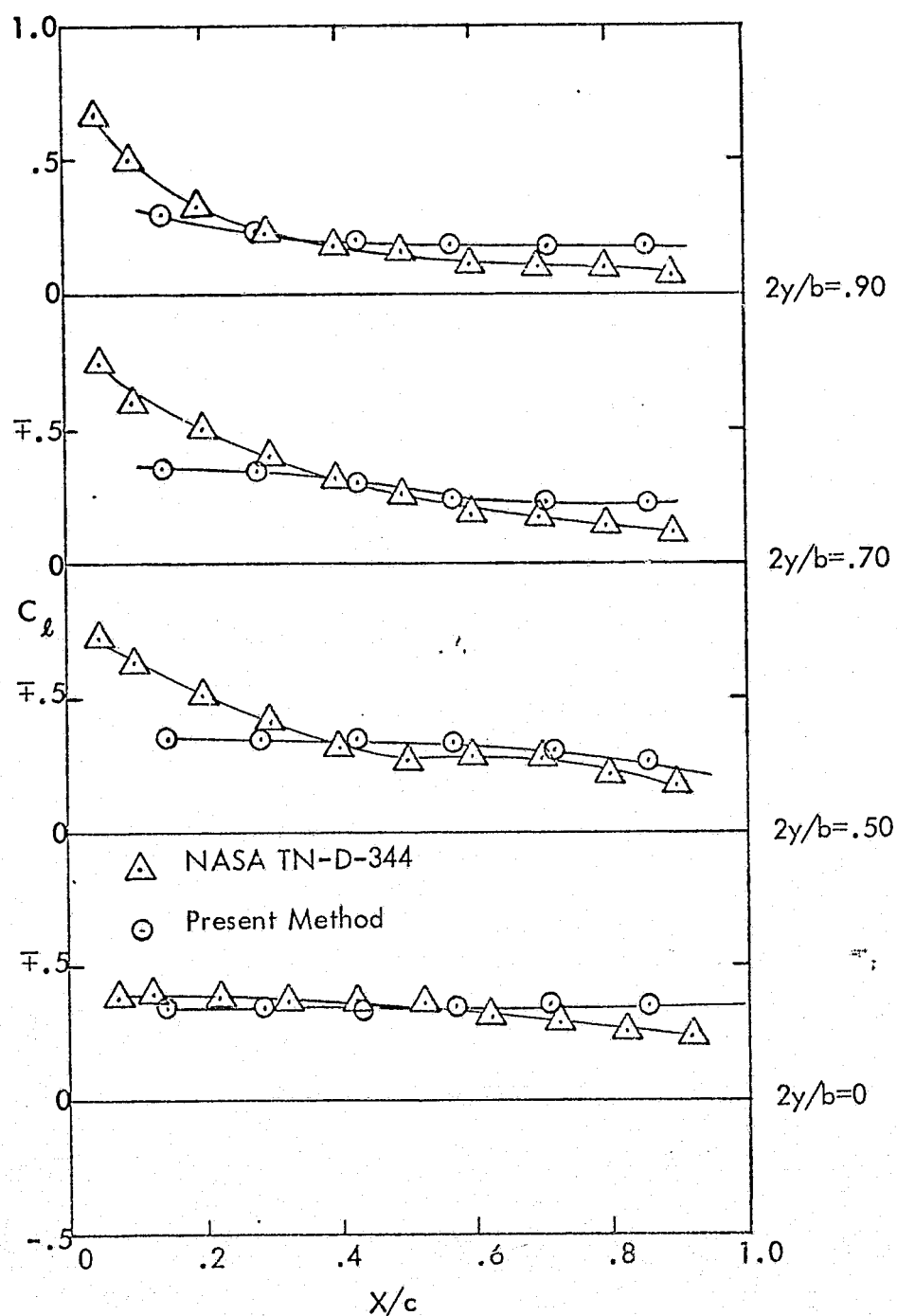


Figure 22a. The lift distribution on symmetric rectangular wing with $AR = 3$, $\tau = 5\%$, $\alpha = 5^\circ$, $M = 1.3$ and $NX = NY = 7$ for the comparison with results of Ref. 15.

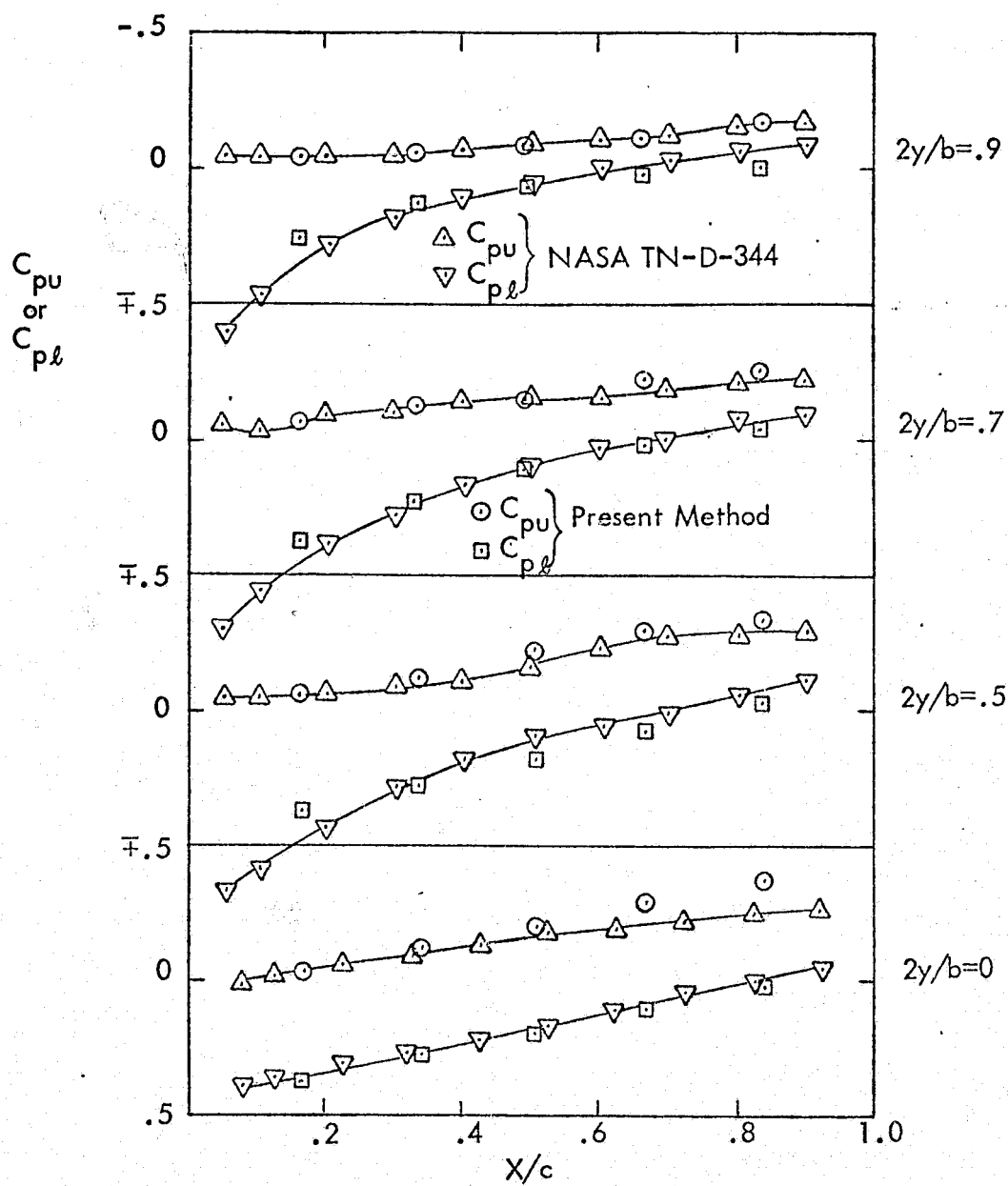


Figure 22b. The distribution of C_p on the upper and lower surfaces of a symmetric rectangular wing with $AR = 3$, $\tau = 5\%$, $\alpha = 5^\circ$, $M = 1.3$ and $NX = NY = 6$ for comparison with results of Ref. 15.

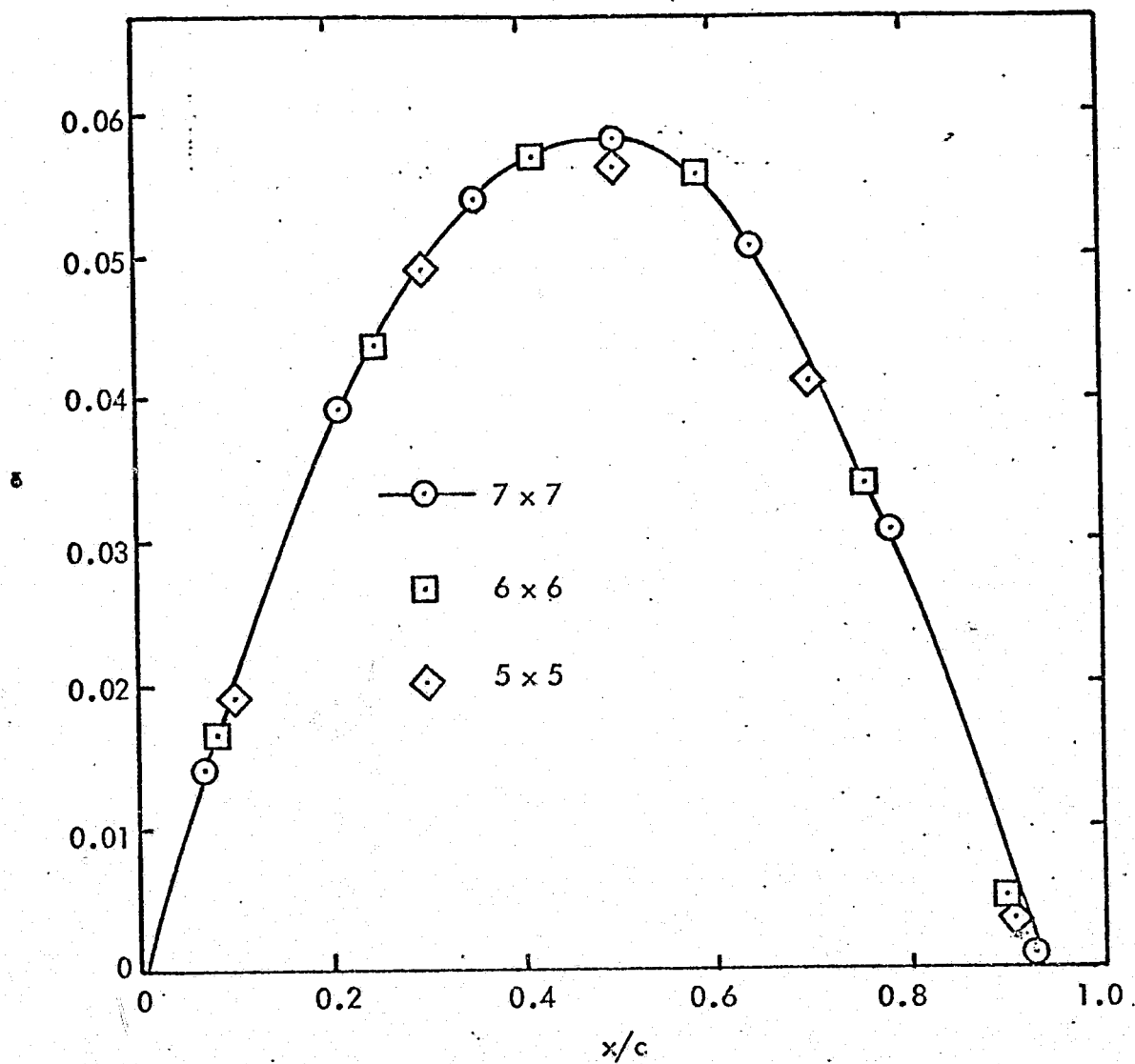


Figure 23. Analysis of Convergence: Potential Distribution, ϕ , Versus x/c , at $y = 0$, for Rectangular Wing With Biconvex Section, in Steady Supersonic Flow, for $AR = 3$, $\tau = 0.05$, $M = 1.3$, $\alpha = 0^\circ$, $N_D = 3N_x$, $NX = NY = 5, 6, 7$.

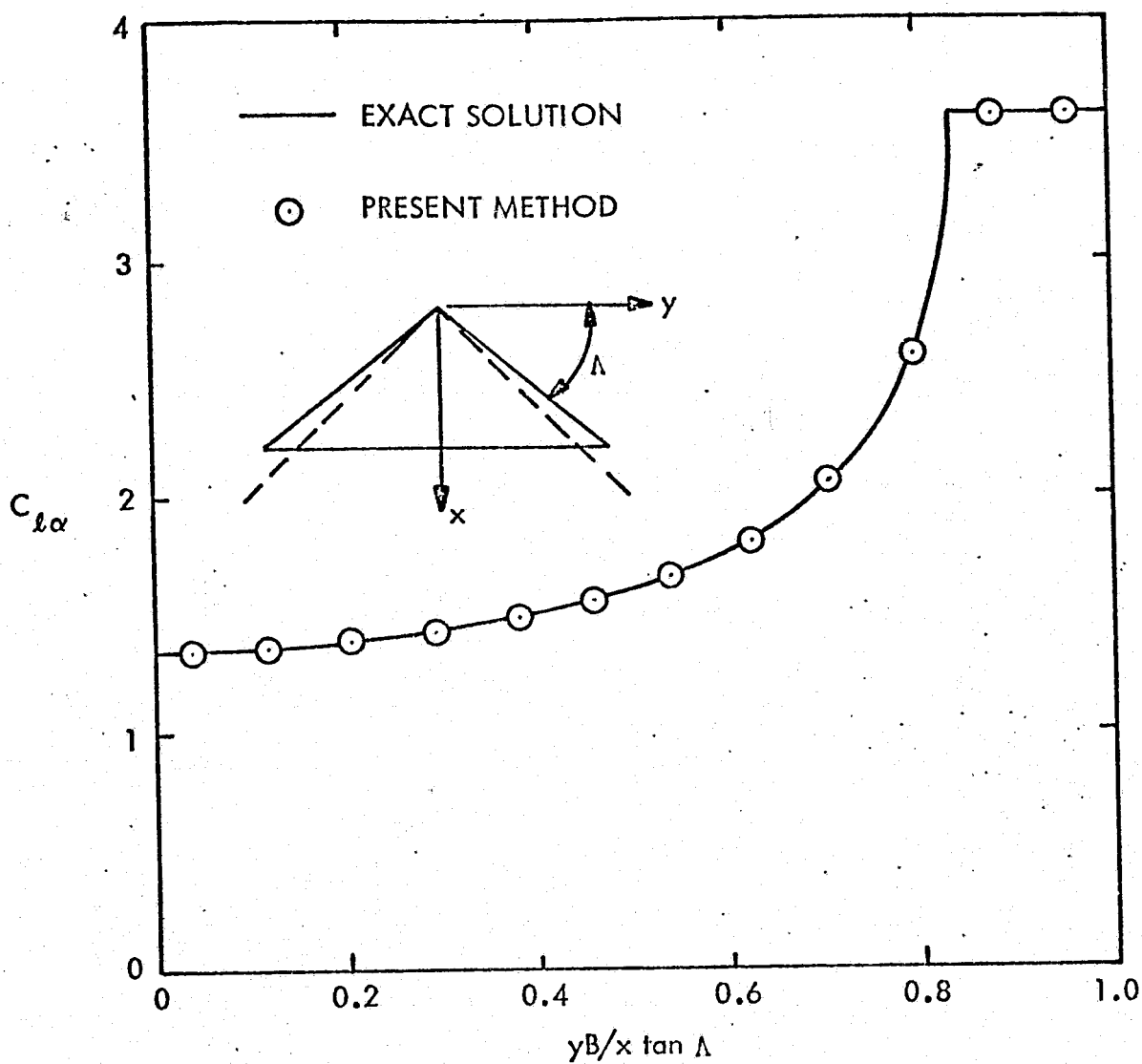


Figure 24. Lift Distribution Coefficient, $C_{l\alpha}$, for Delta Wing With Supersonic Leading Edge, in Steady Supersonic Flow, With $B/\tan \Lambda = 1.2$, $\tau = 0$, $N_x = 8$, $N_y = 12$. Comparison With Exact, Conical-Flow Solution, Reference 20.

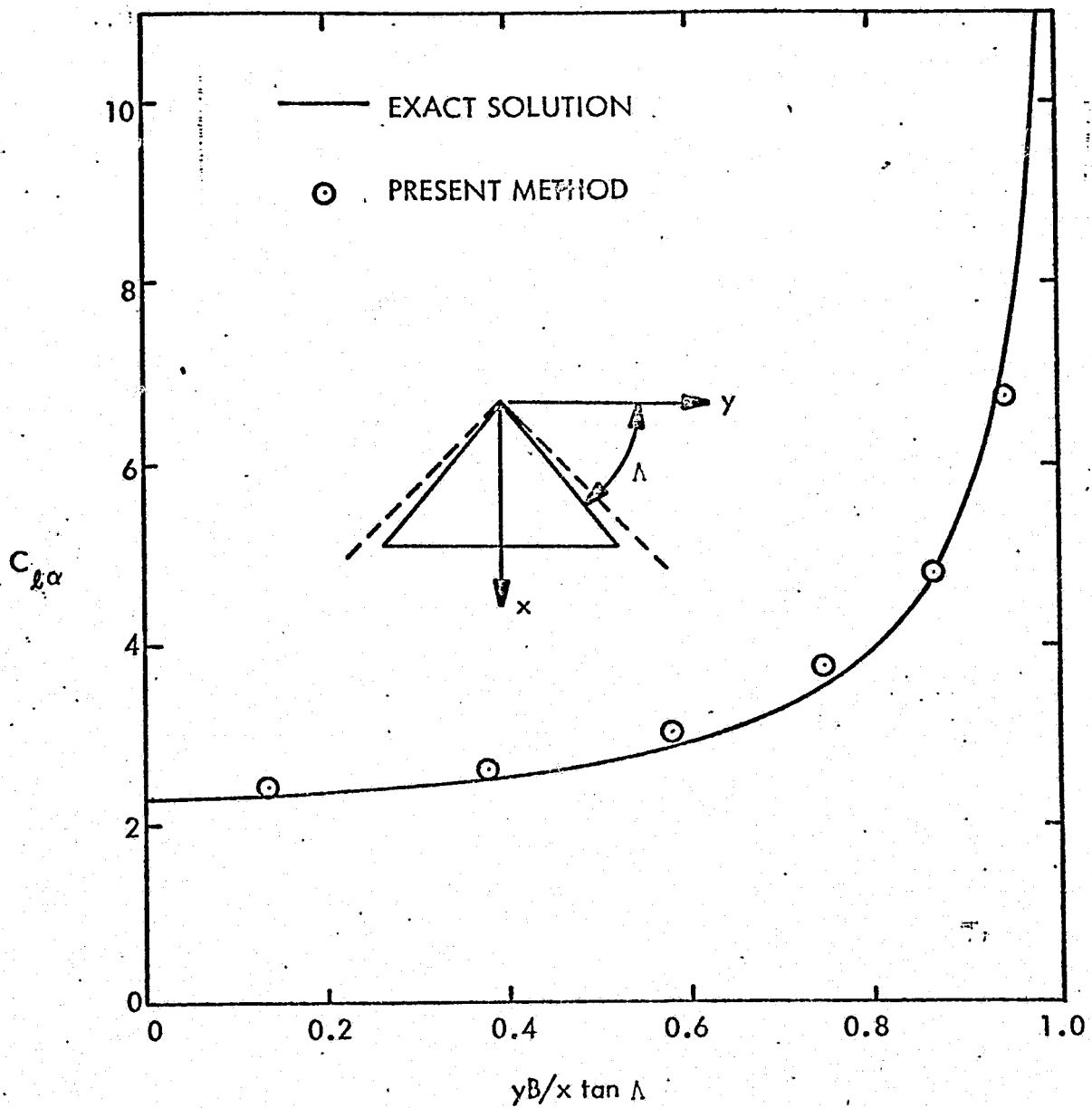


Figure 25. Lift Distribution Coefficient, $C_{l\alpha}$, for Delta Wing With Subsonic Leading Edge, in Steady Supersonic Flow, With $B/\tan \Lambda = 0.833$, $\tau = 0$, $N_x = N_y = 7$. Comparison With Exact Conical-Flow Solution, Reference 20.

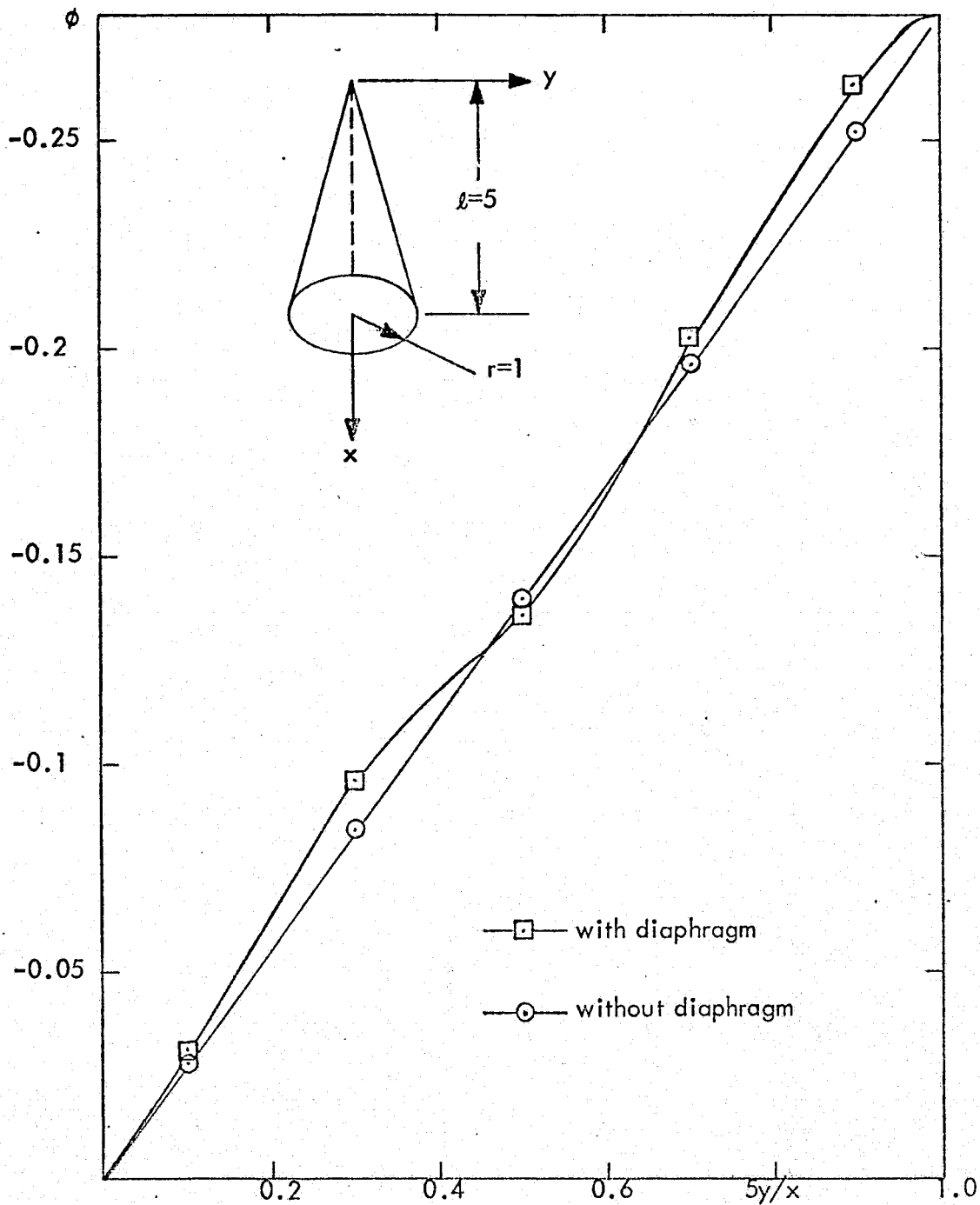


Figure 26. Study of existence of diaphragm; the distribution of velocity potential, ϕ , for a circular cone with subsonic leading edge, $r = 1$, $l = 5$, $M = 2.0$ and $NX = 12$, $NY = 5$. Results obtained with and without diaphragm are compared.

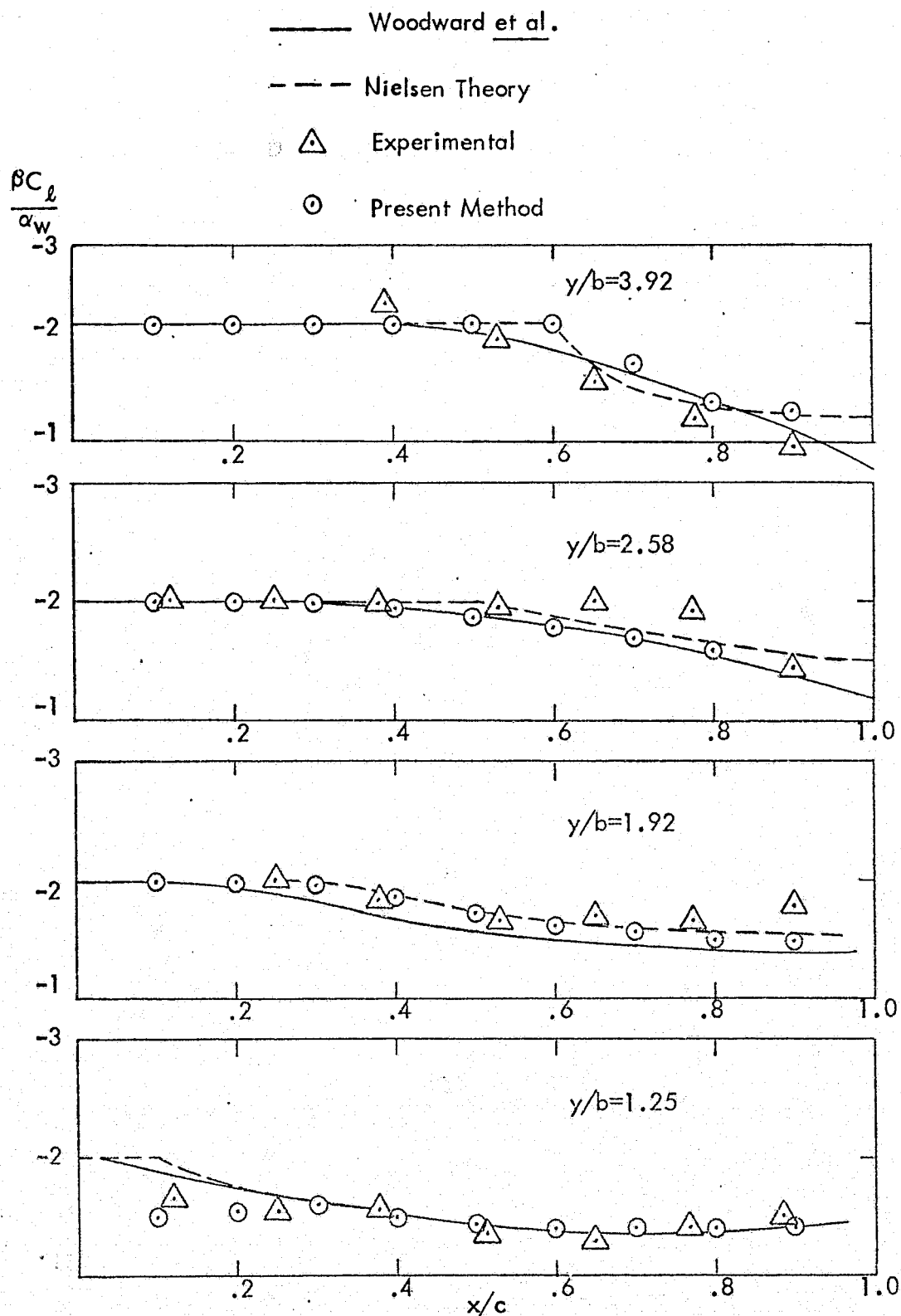


Figure 27a. The distribution of $\beta C_l / \alpha_w$ on the wing section for a wing-body configuration (shown in Figure 27c) with $M = 1.48$, $\alpha_w = 1.92^\circ$ and $\alpha_B = 0^\circ$, for the comparison with results of Ref. 21.

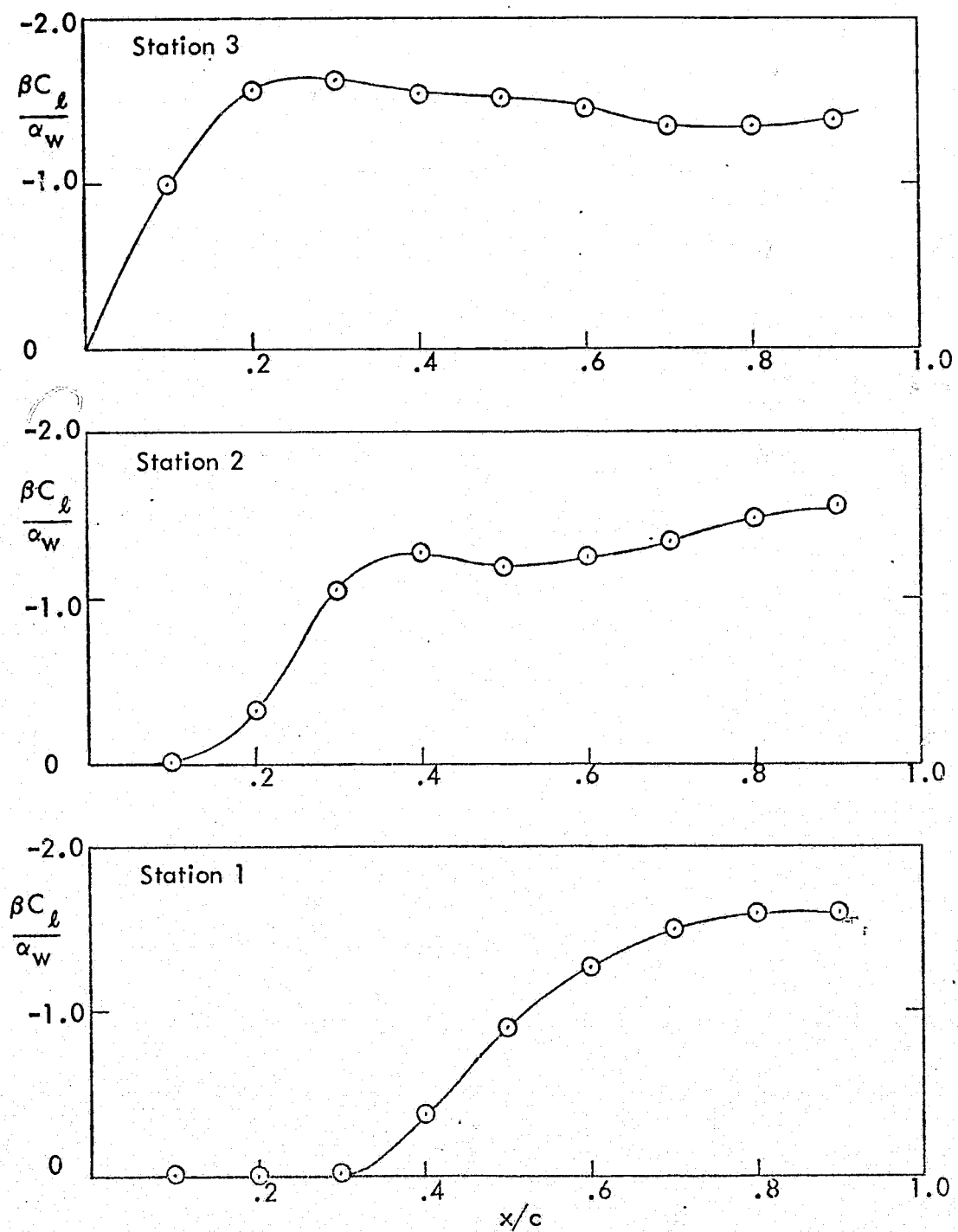


Figure 27b. The distribution of $\beta C_l / \alpha_w$ on the fuselage at three circumferential stations for the same problem of Figure 27a.

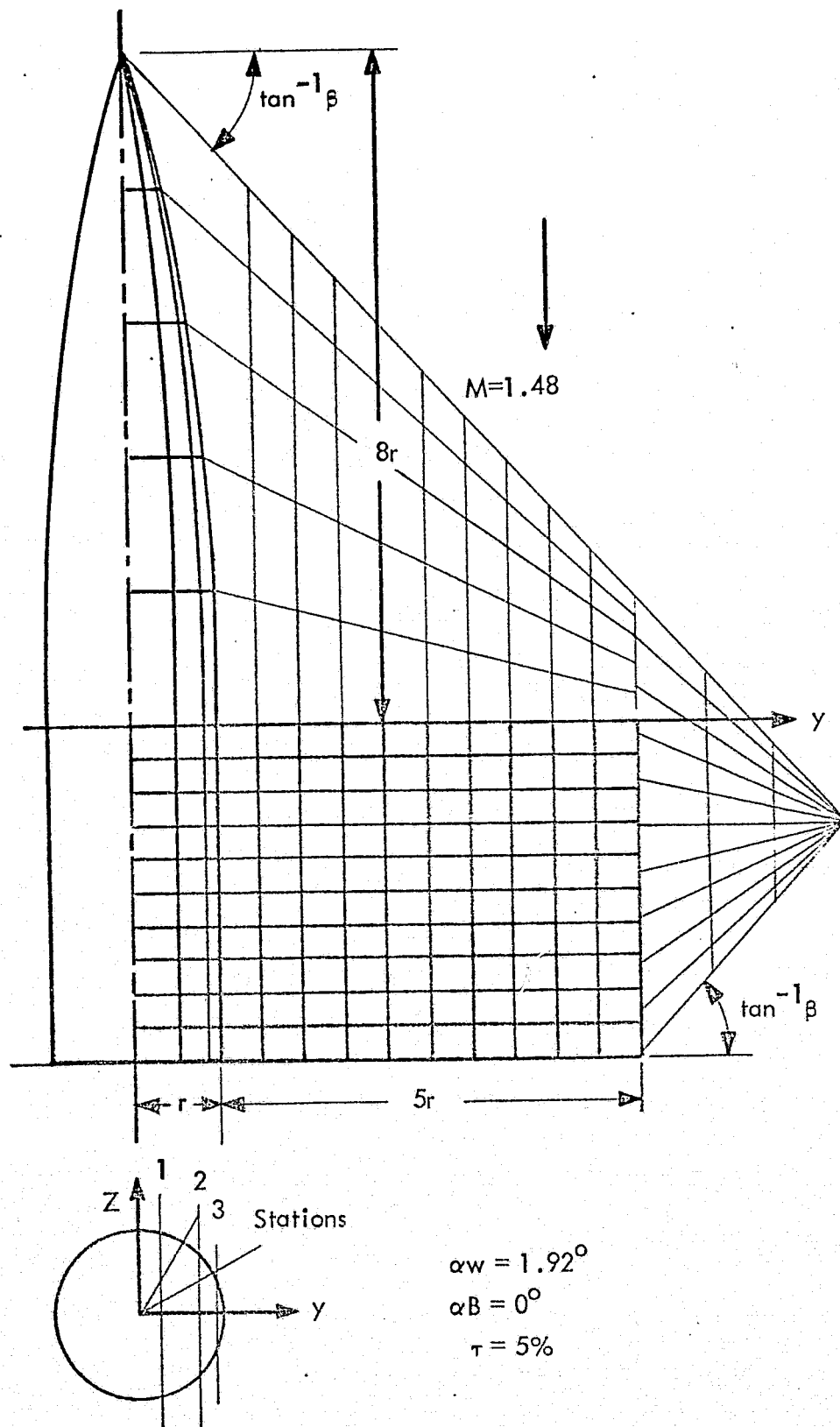


Figure 27c. Wing-body Configuration in Supersonic Flow

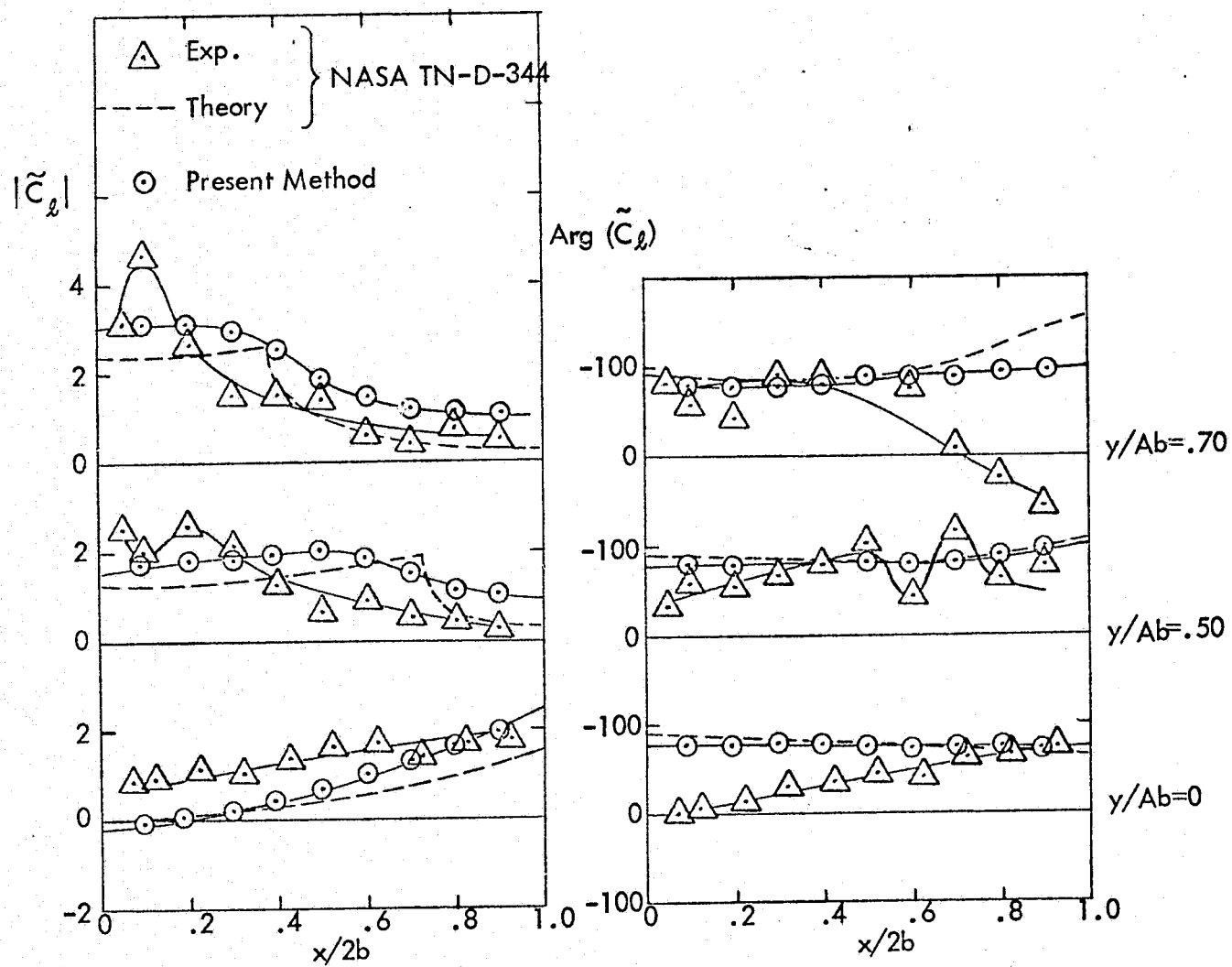


Figure 28. Lift coefficient, \tilde{C}_l , for a rectangular wing oscillating in bending mode with $k = \omega_c/2U_\infty = 0.1$, $M = 1.3$, $AR = 3$ and $NX = NY = 10$.

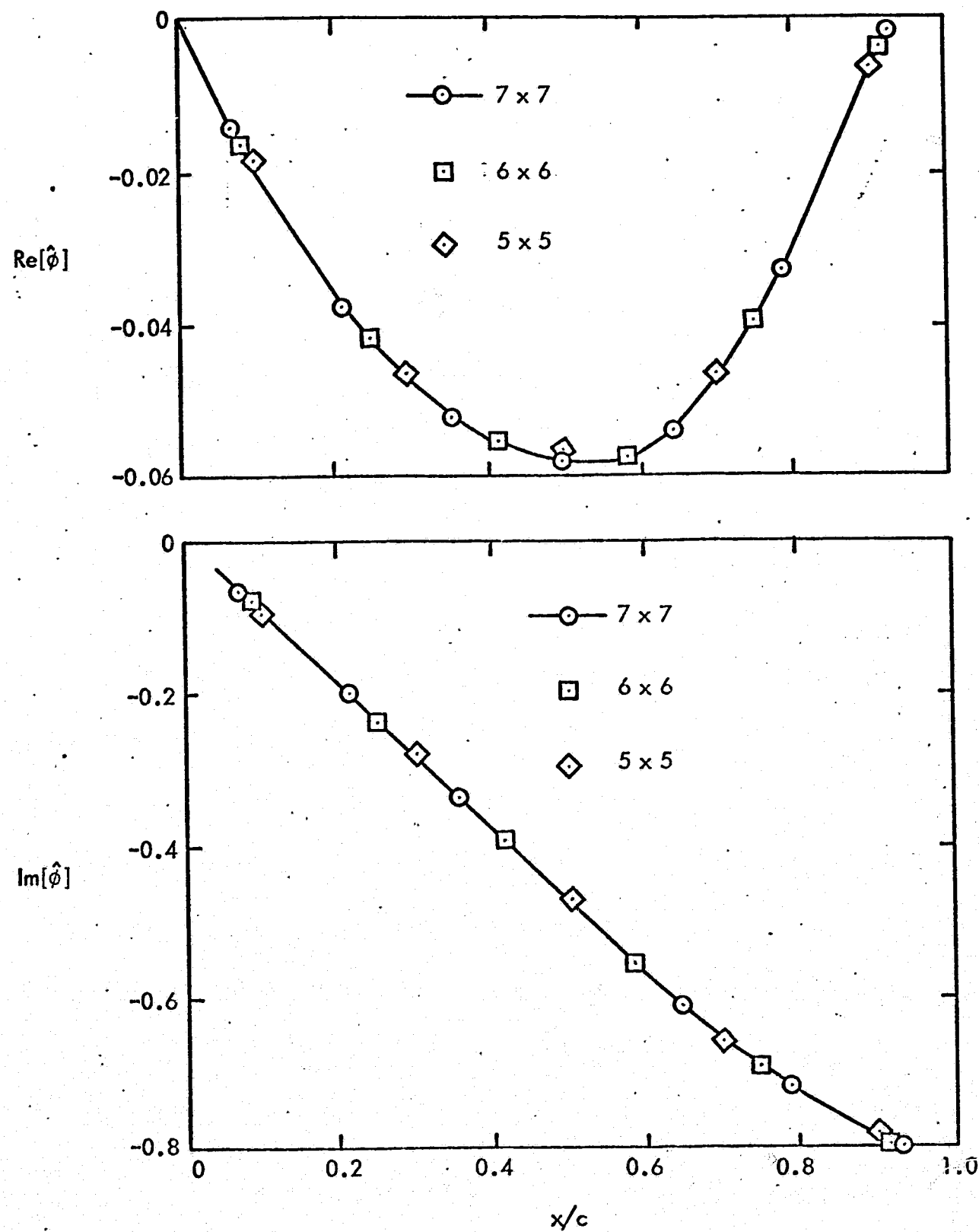


Figure 29 Analysis of Convergence: Distribution of $\hat{\phi} = \tilde{\phi} e^{i\Omega M X}$ Versus x/c , at $2y/b = 0.5$, for Rectangular Wing With Biconvex Section, Oscillating in Bending Mode in Supersonic Flow, for $AR = 3$, $\tau = 0.01$, $M = 1.3$, $K = 0.1$, $\alpha = 0^\circ$, $N_D = 3N_x$, $N_X = N_Y = 5, 6, 7$.

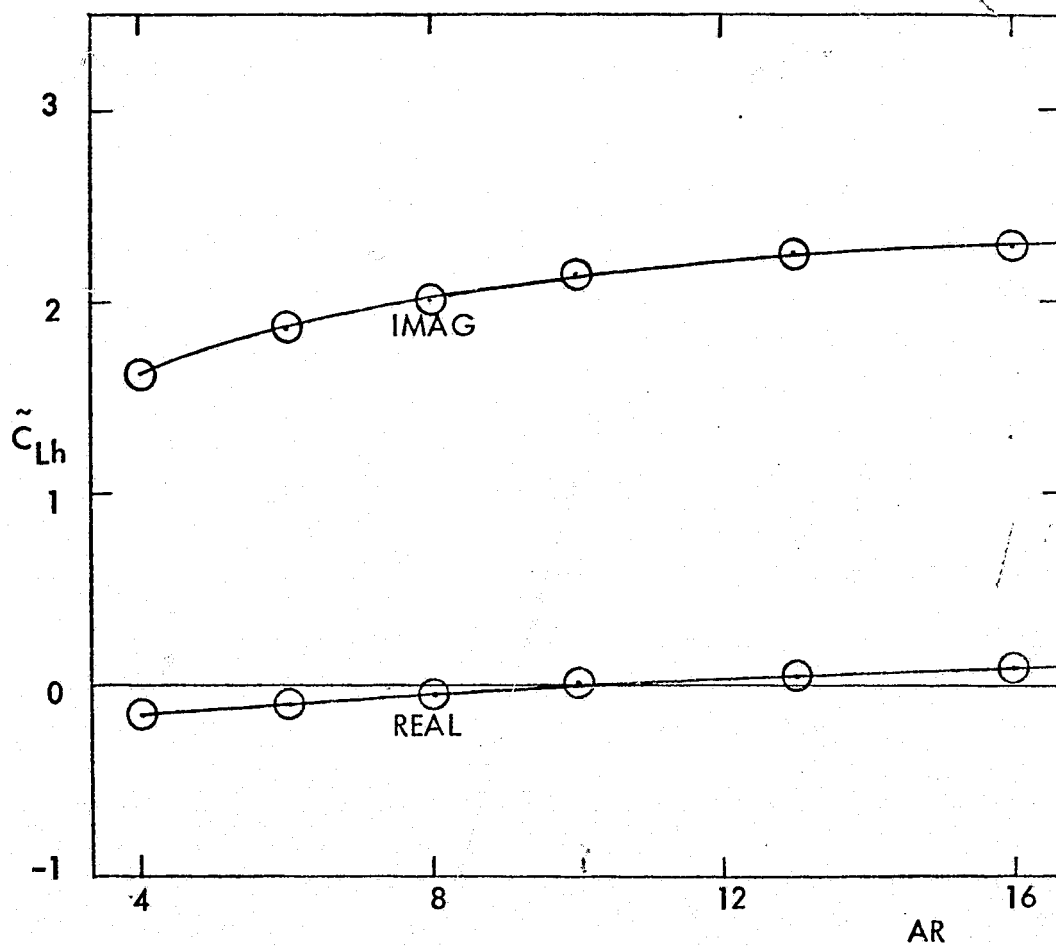


Figure 30a. C_{Lh} as a function of aspect ratio for a rectangular wing with $\tau = 0.1\%$, $M = 0$ and $NX = 8$, $NY = 10$ ($X_{EA} = -0.2C$).

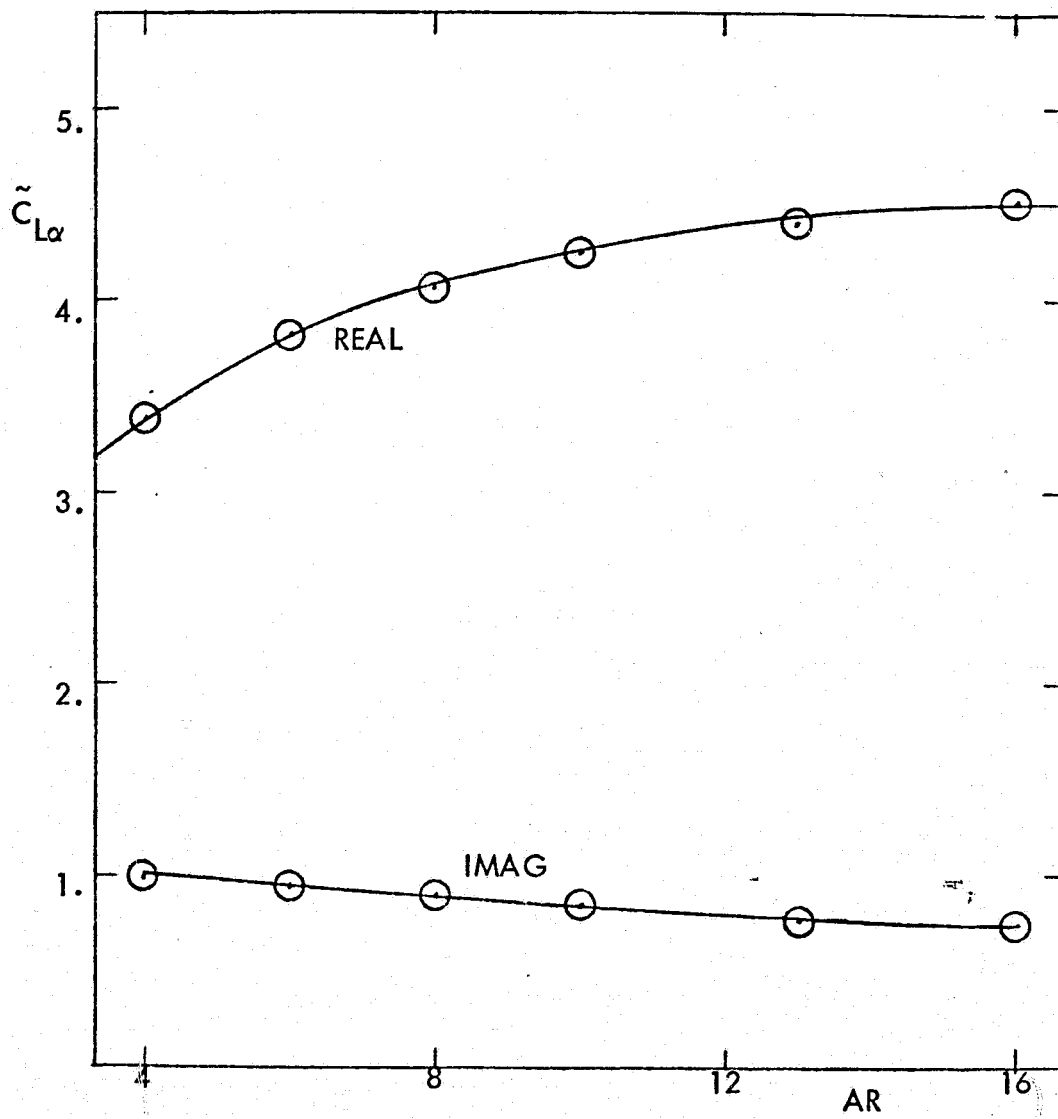


Figure 30b. $C_{L\alpha}$ as a function of aspect ratio for a rectangular wing with $\tau = .1\%$, $M = 0$ and $NX = 8$, $NY = 10$ ($X_{EA} = -0.2C$).

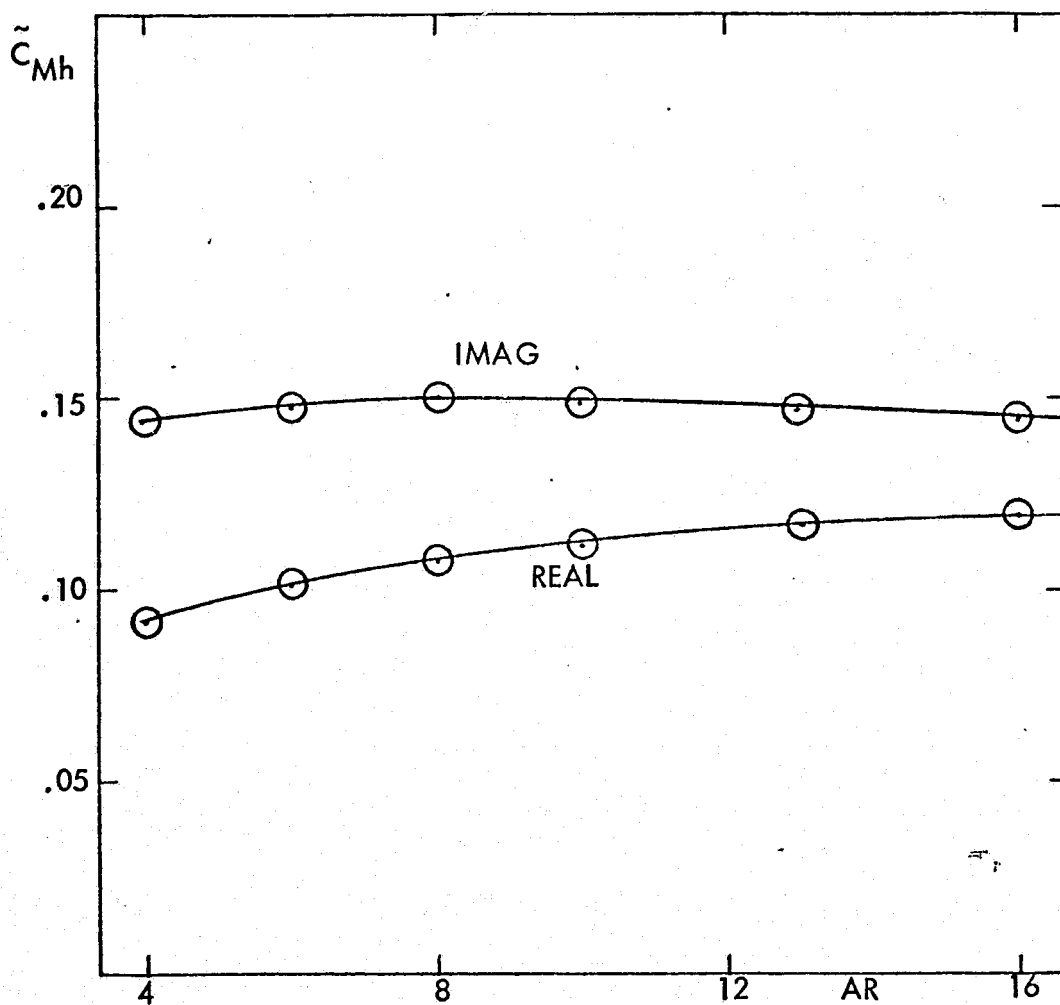


Figure 30c. \tilde{C}_{Mh} as a function of aspect ratio for a rectangular wing with $\tau = 0.1\%$, $M = 0$ and $NX = 8$, $NY = 10$ ($X_{EA} = -0.2C$).

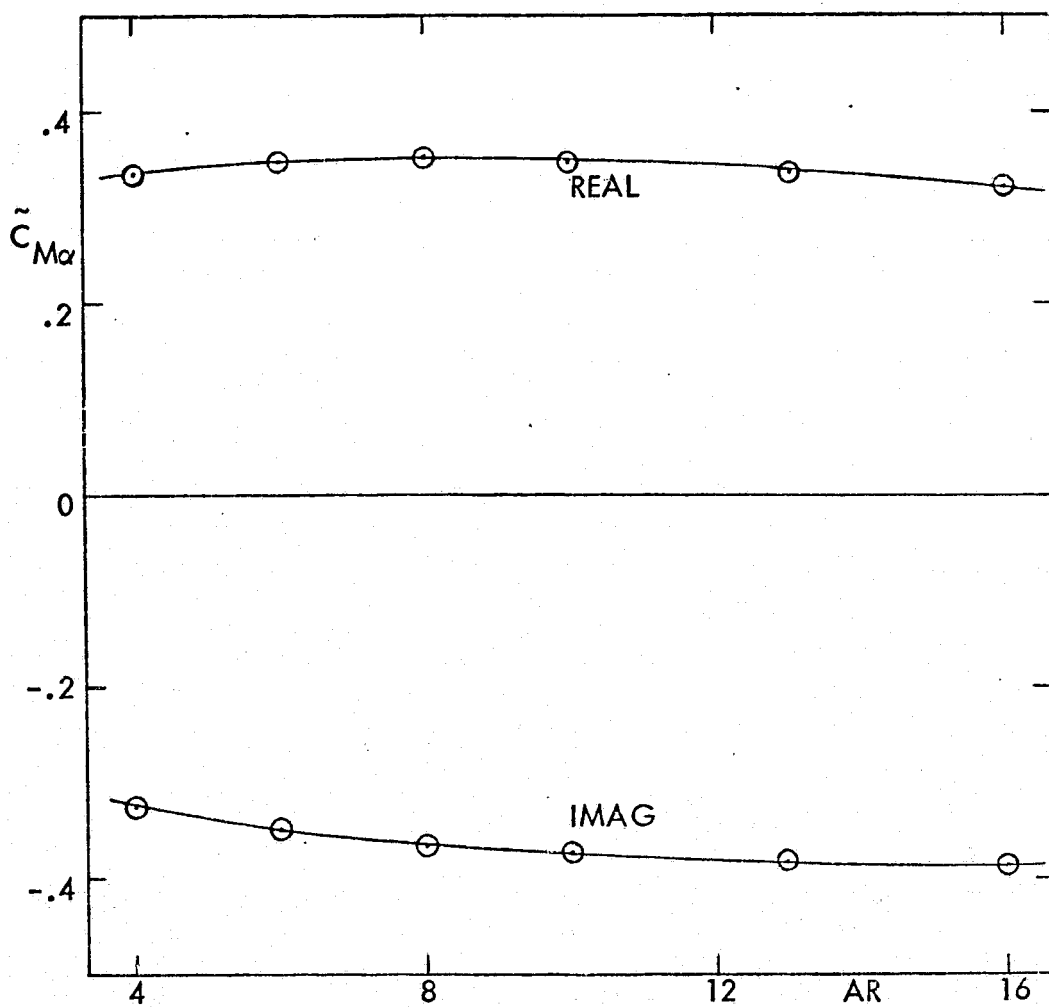


Figure 30d. $\tilde{C}_{M\alpha}$ as a function of aspect ratio for a rectangular wing with $\tau = 0.1\%$, $M = 0$ and $NX = 8$, $NY = 10$ ($X_{EA} = -0.2C$).

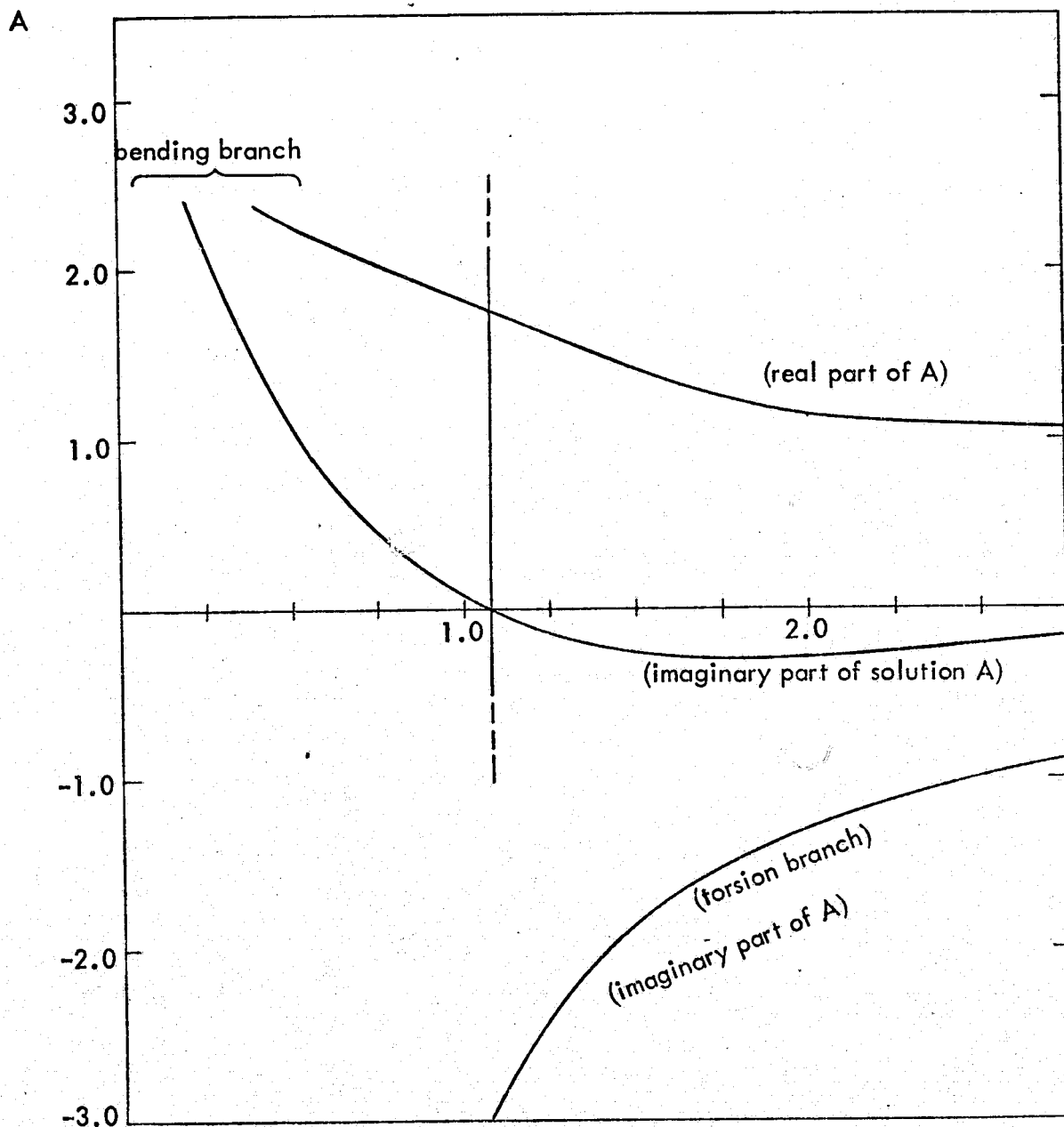


Figure 31. Parameter $A = \omega_\alpha^2 / \omega^2$ as a function of reduced frequency, $K = \omega c / 2U_\infty$, for a rectangular airfoil with $AR = 16$, $M = 0$, $\omega_h / \omega_\alpha = 0.5$, $X_\alpha = 0.2$, $r_\alpha = 0.5$, $M = 5$ and $NX = 8$, $NY = 10$ ($X = -0.2C$).

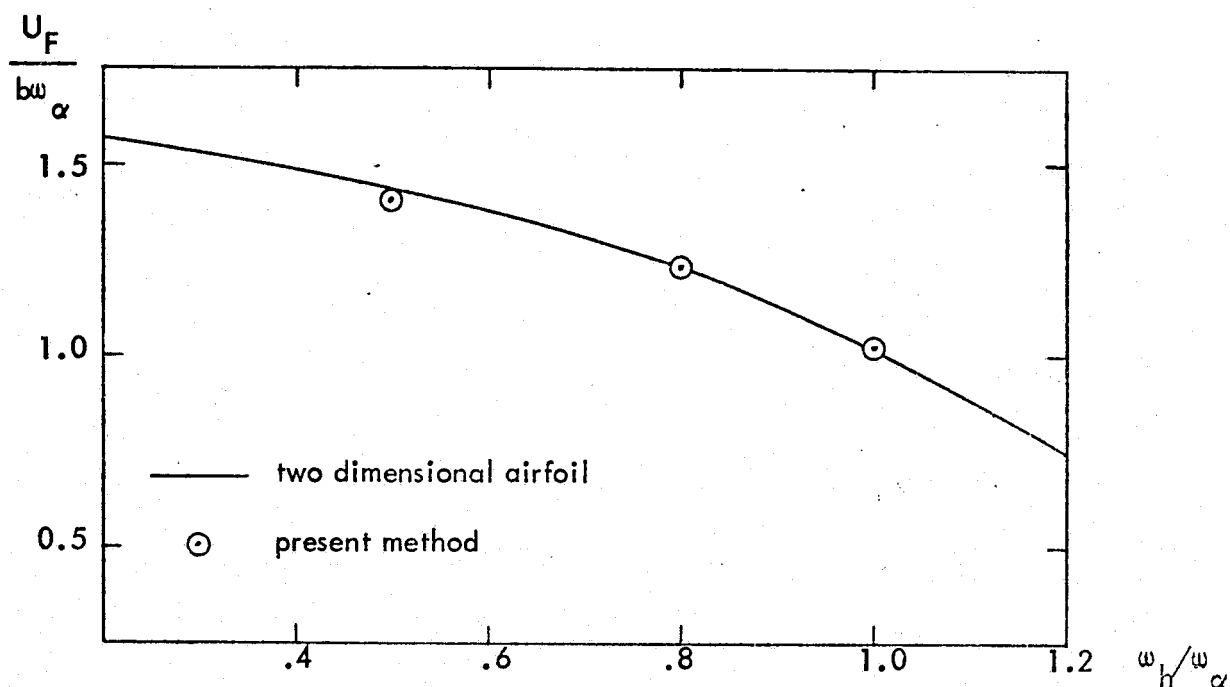


Figure 32a. Flutter speed as a function of ω_h / ω_α for a rectangular wing with $AR = 16$, $M = 0$, $\tau = 0.1\%$, $\mu = 5$, $X_\alpha = 0.2$, $r_\alpha = 0.5$, and $NX = 8$, $NY = 10$. Results are compared with exact solution given by two dimensional airfoil theory (Ref. 24) ($X_{EA} = -0.2C$).

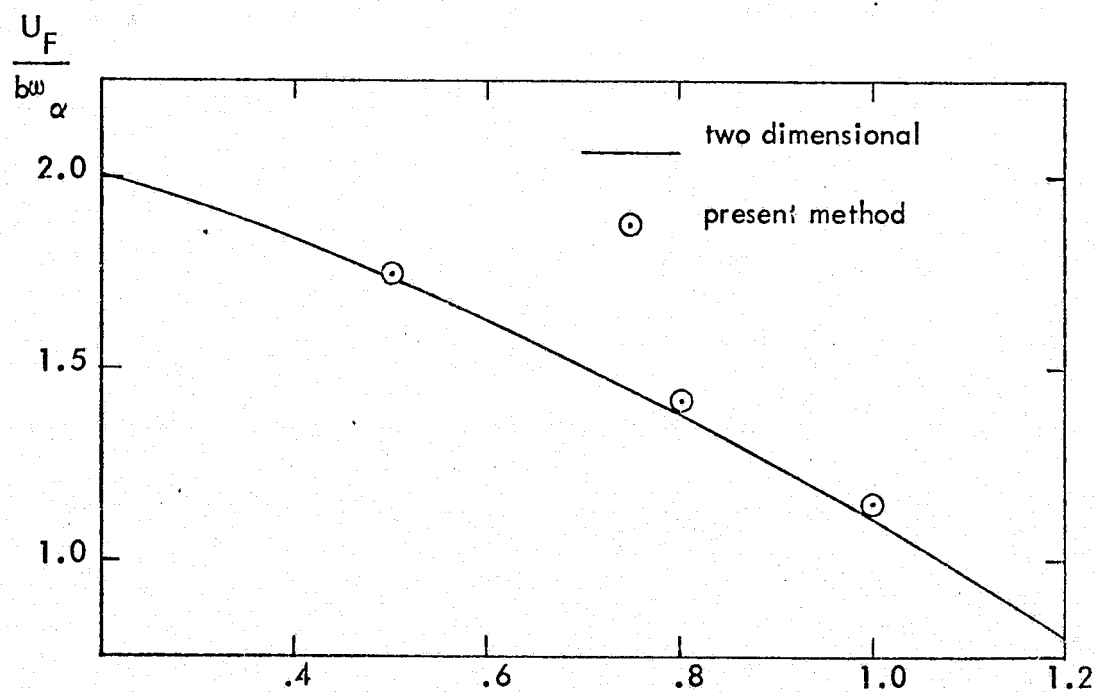


Figure 32b. Flutter speed as a function of ω_h / ω_α for a rectangular wing with $AR = 16$, $M = 0$, $\tau = 0.1\%$, $\mu = 10$, $X_\alpha = 0.2$, $r_\alpha = 0.5$ and $NX = 8$, $NY = 10$. Results are compared with exact solution given by two dimensional airfoil theory (Ref. 24) ($X_{EA} = -0.2C$).

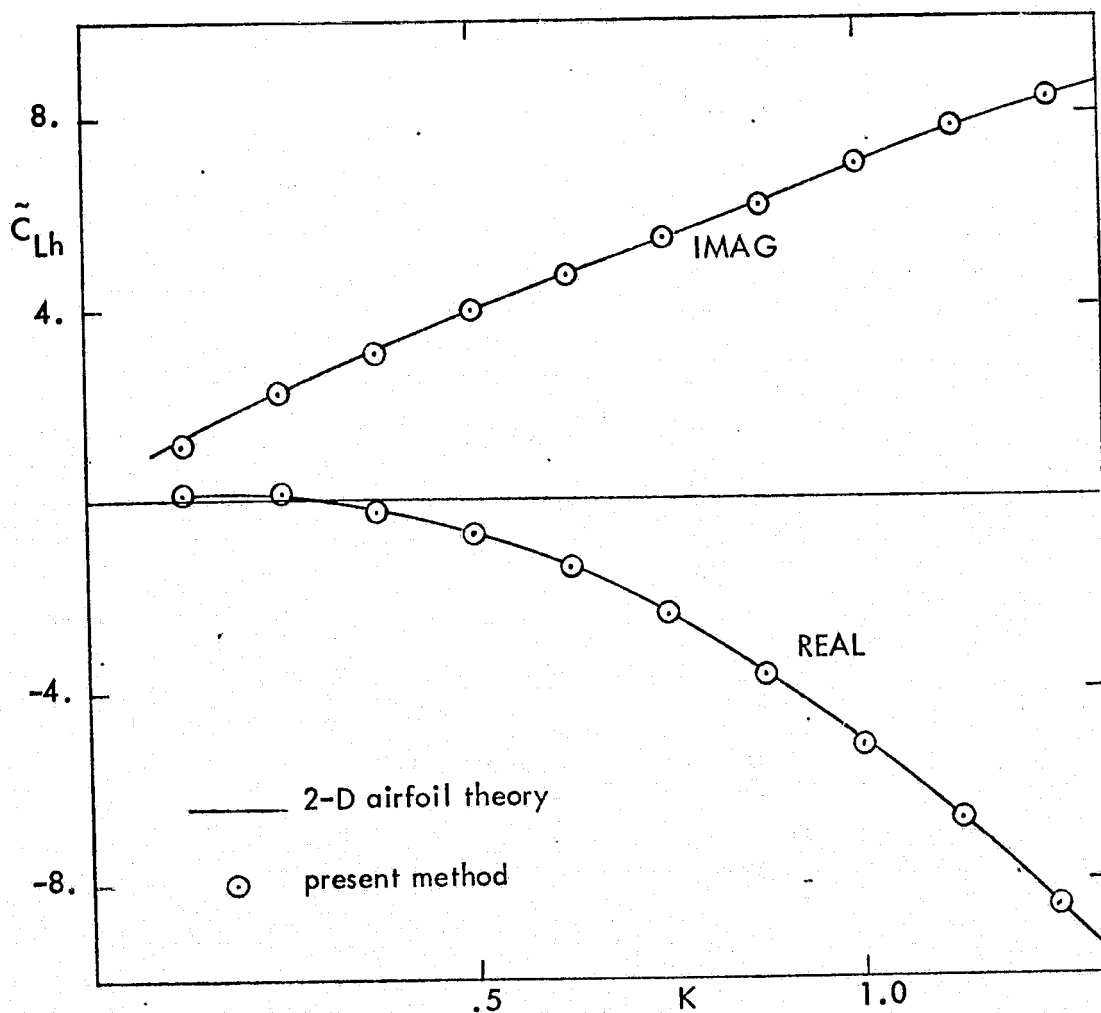


Figure 33a. \tilde{C}_{Lh} as a function of the reduced frequency, $k = \omega c / 2U_\infty$, for a rectangular wing with $AR = 16$, $\tau = 0.1\%$, $M = 0$ and $NX = 8$, $NY = 10$. Comparison with the exact solution given by 2-D airfoil theory (Ref. 24) ($X_{EA} = -0.2C$).

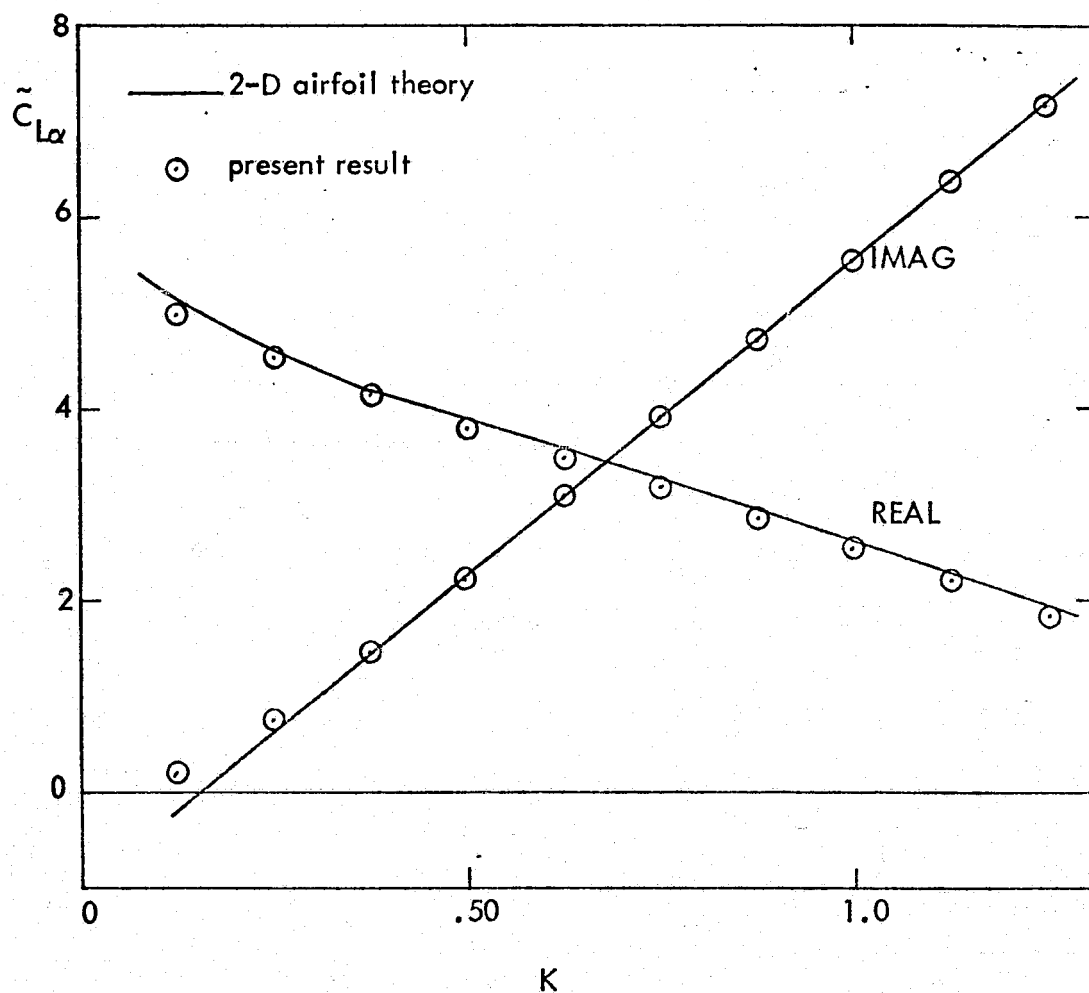


Figure 33b. $\tilde{C}_{L\alpha}$ as a function of the reduced frequency, $k = \omega c / 2U_{\infty}$ for a rectangular wing with $AR = 16$, $\tau = 0.1\%$, $M = 0$ and $NX = 8$, $NY = 10$. Comparison with the exact solution given by 2-D airfoil theory (ref. 24) ($X_{EA} = -0.2C$).

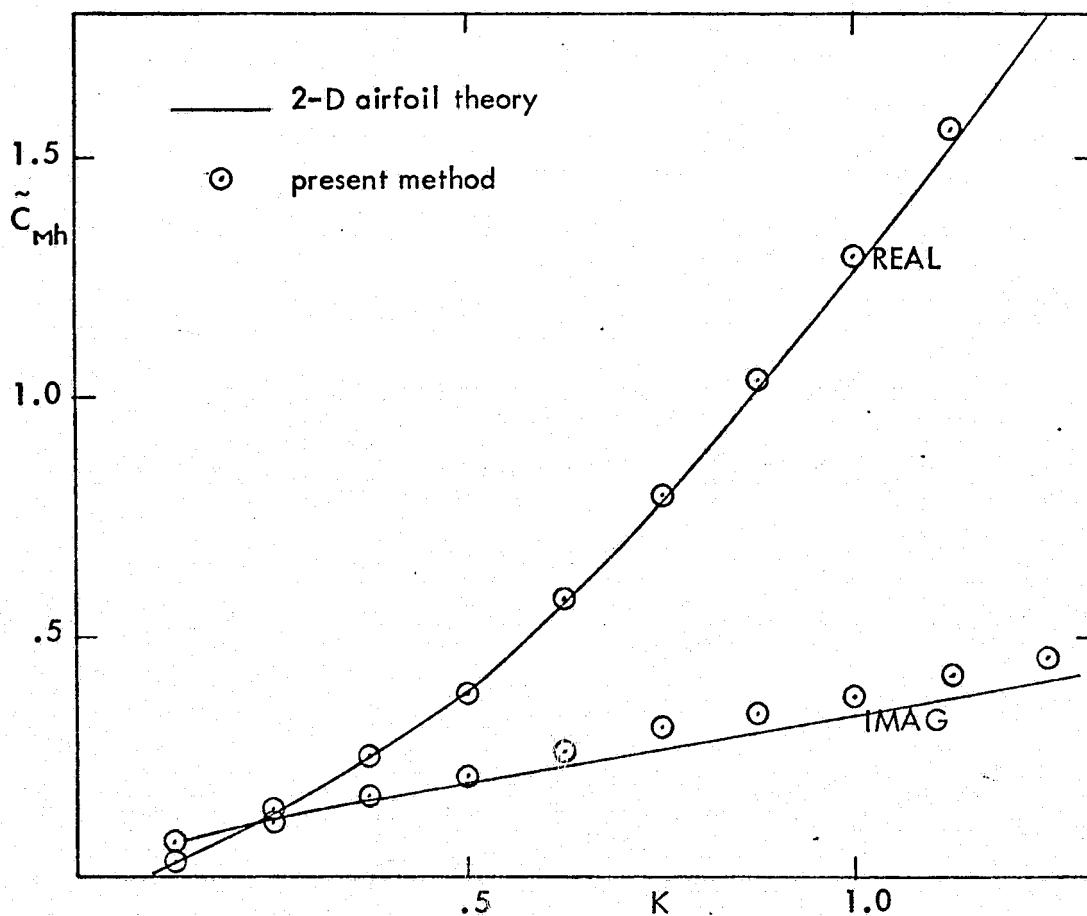


Figure 33c. \tilde{C}_{mh} as a function of reduced frequency, $k = \omega c / 2U_{\infty}$ for a rectangular wing with $AR = 16$, $\tau = 0.1\%$, $M = 0$ and $NX = 8$, $NY = 10$. Comparison with the exact solution given by 2-D airfoil theory (Ref. 24) ($X_{EA} = -0.2C$).

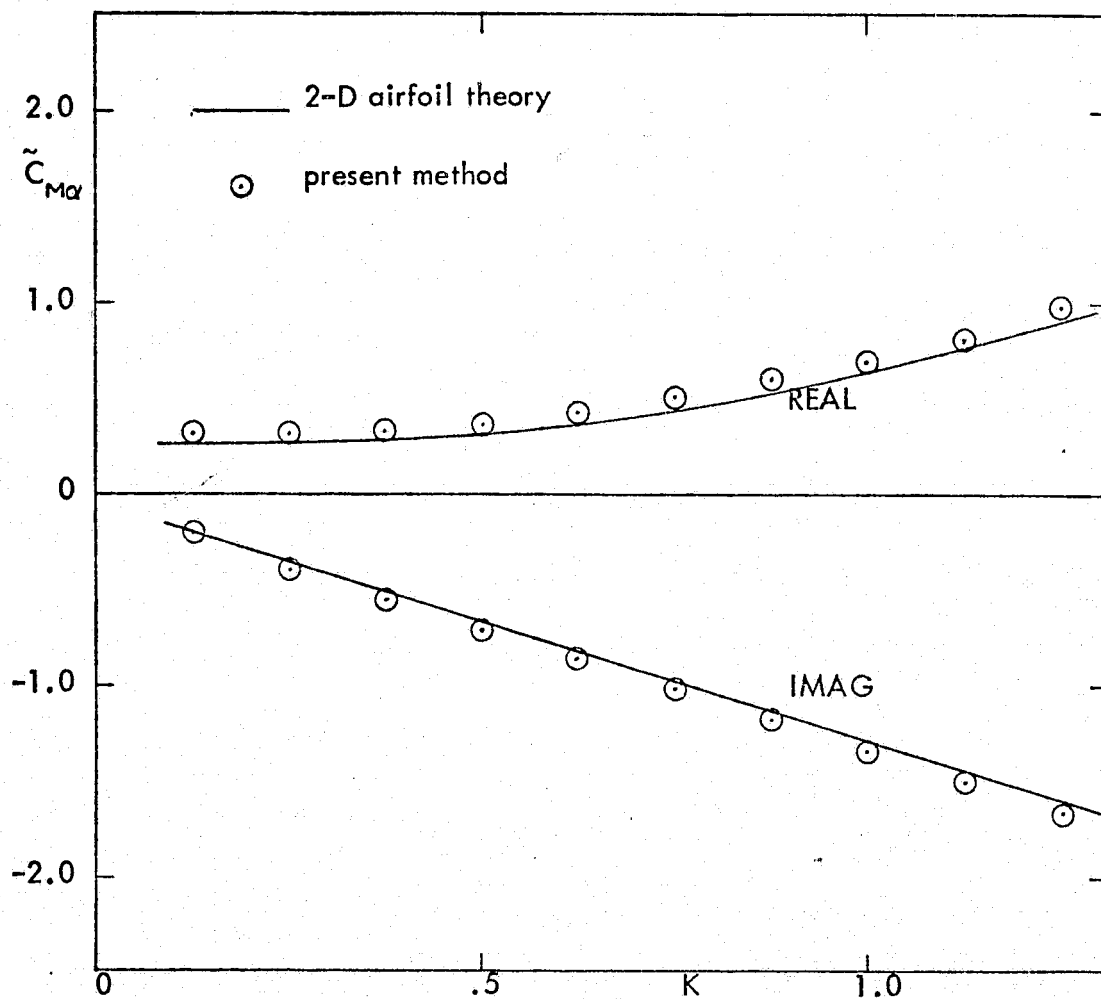


Figure 33d. $\tilde{C}_{M\alpha}$ as a function of reduced frequency, $k = \omega c / 2U_\infty$ for a rectangular wing with $AR = 16$, $\tau = 0.1\%$, $M = 0$ and $NX = 8$, $NY = 10$. Comparison with the exact solution given by 2-D airfoil theory (Ref. 24) ($X_{EA} = -0.2C$).

APPENDIX A

FORMULATIONS FOR STEADY SUBSONIC FLOW

A.1 INTRODUCTION

The derivation of Equations (3.10) and (3.11) is presented in Reference 6. In this appendix it will be shown by differentiation that doublet and source integrals in Equations (3.10) and (3.11) are valid for any planar quadrilateral element. In Subsection A.2, basic equations for hyperboloidal surface are introduced. In Subsection A.3, the doublet integral in Equation (3.10) is shown to be valid for any planar quadrilateral element. In Subsection A.4, the source integral in Equation (3.11) is shown to be valid for any planar quadrilateral element. In addition, the wake term in Equation (3.16) is derived in Subsection A.5.

A.2 BASIC EQUATION

According to Equation (3.15)

$$\bar{n} = \bar{a}_1 \times \bar{a}_2 / |\bar{a}_1 \times \bar{a}_2| \quad (\text{A.1})$$

is independent of ξ and η , therefore,

$$\frac{\partial \bar{n}}{\partial \xi} = \frac{\partial \bar{n}}{\partial \eta} = 0 \quad (\text{A.2})$$

Also, it is noted that

$$\frac{\partial \bar{a}_1}{\partial \xi} = 0 \quad (\text{A.3})$$

$$\frac{\partial \bar{a}_2}{\partial \eta} = 0 \quad (\text{A.4})$$

$$\frac{\partial}{\partial \xi} (\bar{q} \cdot \bar{n}) = \bar{a}_1 \cdot \bar{n} = 0 \quad (\text{A.5})$$

$$\frac{\partial}{\partial \eta} (\bar{q} \cdot \bar{n}) = \bar{a}_2 \cdot \bar{n} = 0 \quad (\text{A.6})$$

$$\frac{\partial \bar{a}_1}{\partial \eta} = \frac{\partial \bar{a}_2}{\partial \xi} = \bar{p}_3 \quad (\text{A.7})$$

A - 1

For hyperboloidal elements with \bar{a}_1 and \bar{a}_2 defined by Equations (3.12), (3.13), and (3.14) with

$$d\Sigma = |\bar{a}_1 \times \bar{a}_2| d\xi d\eta \quad (\text{A.8})$$

the doublet and source integrals in Equations (3.4) and (3.5) can be rewritten as

$$\begin{aligned} C_{hk} &= \frac{1}{2\pi} \int_{-1}^1 \int_{-1}^1 \frac{\partial}{\partial N} \left(\frac{1}{\sqrt{\bar{q} \cdot \bar{q}}} \right) |\bar{a}_1 \times \bar{a}_2| d\xi d\eta \\ &= -\frac{1}{2\pi} \int_{-1}^1 \int_{-1}^1 \frac{\bar{a}_1 \times \bar{a}_2 \cdot \bar{q}}{(\bar{q} \cdot \bar{q})^{3/2}} d\xi d\eta \end{aligned} \quad (\text{A.9})$$

and

$$b_{hk} = \frac{1}{2\pi} \int_{-1}^1 \int_{-1}^1 \frac{1}{\sqrt{\bar{q} \cdot \bar{q}}} |\bar{a}_1 \times \bar{a}_2| d\xi d\eta \quad (\text{A.10})$$

since

$$\begin{aligned} &\frac{\partial}{\partial N} \left(\frac{1}{\sqrt{\bar{q} \cdot \bar{q}}} \right) |\bar{a}_1 \times \bar{a}_2| \\ &= -\frac{|\bar{a}_1 \times \bar{a}_2|}{(\bar{q} \cdot \bar{q})^{3/2}} \left(\frac{\partial}{\partial N} \frac{1}{2\bar{q} \cdot \bar{q}} \right) = -\frac{|\bar{a}_1 \times \bar{a}_2|}{(\bar{q} \cdot \bar{q})^{3/2}} \left(\frac{\partial \bar{q}}{\partial N} \cdot \bar{q} \right) \\ &= -\frac{|\bar{a}_1 \times \bar{a}_2|}{(\bar{q} \cdot \bar{q})^{3/2}} \left[\frac{\partial}{\partial x} (x - x_*) N_x \bar{i} + \frac{\partial}{\partial y} (y - y_*) N_y \bar{j} + \frac{\partial}{\partial z} (z - z_*) N_z \bar{k} \right] \cdot \bar{q} \\ &= -\frac{|\bar{a}_1 \times \bar{a}_2|}{(\bar{q} \cdot \bar{q})^{3/2}} \bar{N} \cdot \bar{q} = -\frac{\bar{a}_1 \times \bar{a}_2 \cdot \bar{q}}{(\bar{q} \cdot \bar{q})^{3/2}} \end{aligned} \quad (\text{A.11})$$

A.3 DOUBLET INTEGRAL

The following proves that Equation (3.10) is valid for any quadrilateral element. By using Equations (A.3) to (A.7) one obtains:

$$\frac{\partial}{\partial \eta} \tan^{-1} \frac{-(\bar{q} \times \bar{a}_1) \cdot (\bar{q} \times \bar{a}_2)}{\sqrt{\bar{q} \cdot \bar{q}} (\bar{q} \cdot \bar{a}_1 \times \bar{a}_2)} = \frac{1}{1 + \left[\frac{(\bar{q} \times \bar{a}_1) \cdot (\bar{q} \times \bar{a}_2)}{\sqrt{\bar{q} \cdot \bar{q}} (\bar{q} \cdot \bar{a}_1 \times \bar{a}_2)} \right]^2} \times$$

A - 2

$$\begin{aligned}
& \times \left\{ \left[(\bar{a}_2 \times \bar{a}_1) \cdot (\bar{q} \times \bar{a}_2) + (\bar{q} \times \bar{p}_3) \cdot (\bar{q} \times \bar{a}_2) + (\bar{q} \times \bar{a}_1) \cdot (\bar{a}_2 \times \bar{a}_1) \right] \frac{1}{|\bar{q}| |\bar{q} \cdot \bar{a}_1 \times \bar{a}_2|} \right. \\
& \left. + \frac{(\bar{q} \times \bar{a}_1) \cdot (\bar{q} \times \bar{a}_2)}{-(\bar{q} \cdot \bar{q}) (\bar{q} \cdot \bar{a}_1 \times \bar{a}_2)^2} \left[\frac{\bar{a}_2 \cdot \bar{q}}{\sqrt{\bar{q} \cdot \bar{q}}} \bar{q} \cdot \bar{a}_1 \times \bar{a}_2 + \sqrt{\bar{q} \cdot \bar{q}} (\bar{a}_2 \cdot \bar{a}_1 \times \bar{a}_2 + \bar{q} \cdot \bar{p}_3 \times \bar{a}_2) \right] \right\} \\
& = \frac{\gamma^2 (\bar{q} \cdot \bar{a}_1 \times \bar{a}_2)^2}{\gamma^2 (\bar{q} \cdot \bar{a}_1 \times \bar{a}_2)^2 + [(\bar{q} \times \bar{a}_1) \cdot (\bar{q} \times \bar{a}_2)]^2} \times \frac{1}{\gamma^3 (\bar{q} \cdot \bar{a}_1 \times \bar{a}_2)} \times \left\{ \left[(\bar{a}_2 \times \bar{a}_1) \cdot (\bar{q} \times \bar{a}_2) + (\bar{q} \times \bar{p}_3) \cdot (\bar{q} \times \bar{a}_2) \right] \times \right. \\
& \left. (\bar{q} \cdot \bar{q}) (\bar{q} \cdot \bar{a}_1 \times \bar{a}_2) - (\bar{q} \times \bar{a}_1) \cdot (\bar{q} \times \bar{a}_2) [(\bar{a}_2 \cdot \bar{q}) (\bar{q} \cdot \bar{a}_1 \times \bar{a}_2) + \bar{q} \cdot \bar{q} (\bar{q} \cdot \bar{p}_3 \times \bar{a}_2)] \right\} \\
& = \frac{1}{\gamma} \frac{1}{[(\bar{q} \times \bar{a}_1) \cdot (\bar{q} \times \bar{a}_2)]^2 + \gamma^2 (\bar{q} \cdot \bar{a}_1 \times \bar{a}_2)^2} \times \left\{ \left[(\bar{a}_2 \times \bar{a}_1) \cdot (\bar{q} \times \bar{a}_2) (\bar{q} \cdot \bar{q}) - (\bar{q} \times \bar{a}_1) \cdot (\bar{q} \times \bar{a}_2) (\bar{a}_2 \cdot \bar{q}) \right] \times \right. \\
& \left. (\bar{q} \cdot \bar{a}_1 \times \bar{a}_2) + [(\bar{q} \times \bar{p}_3) \cdot (\bar{q} \times \bar{a}_2) (\bar{q} \cdot \bar{a}_1 \times \bar{a}_2) - (\bar{q} \times \bar{a}_1) \cdot (\bar{q} \times \bar{a}_2) (\bar{q} \cdot \bar{p}_3 \times \bar{a}_2)] \bar{q} \cdot \bar{q} \right\} \quad (A.12)
\end{aligned}$$

Considering terms inside the bracket yields

$$\begin{aligned}
& \left\{ (\bar{a}_2 \times \bar{a}_1) \cdot (\bar{q} \times \bar{a}_2) (\bar{q} \cdot \bar{q}) - (\bar{q} \times \bar{a}_1) \cdot (\bar{q} \times \bar{a}_2) (\bar{a}_2 \cdot \bar{q}) \right\} (\bar{q} \cdot \bar{a}_1 \times \bar{a}_2) =, \\
& + \left\{ (\bar{q} \times \bar{p}_3) \cdot (\bar{q} \times \bar{a}_2) (\bar{q} \cdot \bar{a}_1 \times \bar{a}_2) - (\bar{q} \times \bar{a}_1) \cdot (\bar{q} \times \bar{a}_2) (\bar{q} \cdot \bar{p}_3 \times \bar{a}_2) \right\} (\bar{q} \cdot \bar{q}) \\
& = \left\{ [(\bar{a}_2 \cdot \bar{q}) (\bar{a}_1 \cdot \bar{a}_2) - (\bar{a}_2 \cdot \bar{a}_2) (\bar{a}_1 \cdot \bar{q})] (\bar{q} \cdot \bar{q}) - [(\bar{q} \cdot \bar{q}) (\bar{a}_1 \cdot \bar{a}_2) - (\bar{q} \cdot \bar{a}_2) (\bar{q} \cdot \bar{a}_1)] \right. \\
& \left. (\bar{a}_2 \cdot \bar{q}) \right\} (\bar{q} \cdot \bar{a}_1 \times \bar{a}_2) + \left\{ [(\bar{q} \cdot \bar{q}) (\bar{p}_3 \cdot \bar{a}_2) - (\bar{q} \cdot \bar{a}_2) (\bar{q} \cdot \bar{p}_3)] \right. \\
& \left. (\bar{q} \cdot \bar{a}_1 \times \bar{a}_2) - [(\bar{q} \cdot \bar{q}) (\bar{a}_1 \cdot \bar{a}_2) - (\bar{q} \cdot \bar{a}_2) (\bar{q} \cdot \bar{a}_1)] (\bar{q} \cdot \bar{p}_3 \times \bar{a}_2) \right\} (\bar{q} \cdot \bar{q})
\end{aligned}$$

$$\begin{aligned}
&= -(\bar{q} \cdot \bar{a}_1)(\bar{q} \cdot \bar{a}_1 \times \bar{a}_2) \{ (\bar{q} \cdot \bar{q})(\bar{a}_2 \cdot \bar{a}_2) - (\bar{q} \cdot \bar{a}_2)^2 \} + \bar{q} \cdot \bar{q} \left\{ (\bar{q} \cdot \bar{q}) \times \right. \\
&\quad \left. [(\bar{a}_2 \cdot \bar{p}_3)(\bar{q} \cdot \bar{a}_1 \times \bar{a}_2) - (\bar{a}_1 \cdot \bar{a}_2)(\bar{q} \cdot \bar{p}_3 \times \bar{a}_2)] - (\bar{q} \cdot \bar{a}_2) [(\bar{q} \cdot \bar{a}_1 \times \bar{a}_2)(\bar{q} \cdot \bar{p}_3) - (\bar{q} \cdot \bar{a}_1)(\bar{q} \cdot \bar{p}_3 \times \bar{a}_2)] \right\} \\
&= -|\bar{q} \times \bar{a}_2|^2 \{ (\bar{q} \cdot \bar{a}_1)(\bar{q} \cdot \bar{a}_1 \times \bar{a}_2) - (\bar{q} \cdot \bar{q})(\bar{q} \cdot \bar{a}_1 \times \bar{p}_3) \} \quad (A.13)
\end{aligned}$$

since (note the change of the order in the triple product)

$$\begin{aligned}
&(\bar{q} \cdot \bar{q}) \{ (\bar{a}_2 \cdot \bar{p}_3)(\bar{q} \times \bar{a}_2 \cdot \bar{a}_1) - (\bar{a}_1 \cdot \bar{a}_2)(\bar{q} \times \bar{a}_2 \cdot \bar{p}_3) \} \\
&- (\bar{q} \cdot \bar{a}_2) \{ (\bar{q} \cdot \bar{p}_3)(\bar{q} \times \bar{a}_2 \cdot \bar{a}_1) - (\bar{q} \cdot \bar{a}_1)(\bar{q} \times \bar{a}_2 \cdot \bar{p}_3) \} \\
&= (\bar{q} \cdot \bar{q}) [(\bar{a}_2 \times (\bar{q} \times \bar{a}_2)) \cdot (\bar{p}_3 \times \bar{a}_1) - (\bar{q} \cdot \bar{a}_2) (\bar{q} \times (\bar{q} \times \bar{a}_2)) \cdot (\bar{p}_3 \times \bar{a}_1)] \\
&= (\bar{q} \cdot \bar{q}) [(\bar{a}_2 \cdot \bar{a}_2)(\bar{q} \cdot \bar{p}_3 \times \bar{a}_1) - (\bar{a}_2 \cdot \bar{q})(\bar{a}_2 \cdot \bar{p}_3 \times \bar{a}_1)] \\
&- (\bar{q} \cdot \bar{a}_2) [(\bar{q} \cdot \bar{a}_2)(\bar{q} \cdot \bar{p}_3 \times \bar{a}_1) - (\bar{q} \cdot \bar{q})(\bar{a}_2 \cdot \bar{p}_3 \times \bar{a}_1)] \\
&= [(\bar{q} \cdot \bar{q})(\bar{a}_2 \cdot \bar{a}_1) - (\bar{q} \cdot \bar{a}_2)^2] (\bar{q} \cdot \bar{p}_3 \times \bar{a}_1) \\
&= |\bar{q} \times \bar{a}_2|^2 \bar{q} \cdot \bar{p}_3 \times \bar{a}_1 \quad (A.14)
\end{aligned}$$

Finally, by using Equation (D.2) and combining Equations (A.12) and (A.13) one obtains

$$\begin{aligned}
&\frac{\partial}{\partial \eta} \tan^{-1} \frac{-(\bar{q} \times \bar{a}_1)(\bar{q} \times \bar{a}_2)}{\sqrt{\bar{q} \cdot \bar{q}} (\bar{q} \cdot \bar{a}_1 \times \bar{a}_2)} \\
&= \frac{1}{\sqrt{\bar{q} \cdot \bar{q}}} \frac{1}{|\bar{q} \times \bar{a}_2|^2 |\bar{q} \times \bar{a}_1|^2} |\bar{q} \times \bar{a}_2|^2 \{ (\bar{q} \cdot \bar{a}_1)(\bar{q} \cdot \bar{a}_1 \times \bar{a}_2) - (\bar{q} \cdot \bar{q})(\bar{q} \cdot \bar{a}_1 \times \bar{p}_3) \} \\
&= \frac{1}{\sqrt{\bar{q} \cdot \bar{q}}} \frac{(\bar{q} \cdot \bar{a}_1)(\bar{q} \cdot \bar{a}_1 \times \bar{a}_2) - (\bar{q} \cdot \bar{q})(\bar{q} \cdot \bar{a}_1 \times \bar{p}_3)}{|\bar{q} \times \bar{a}_1|^2} \quad (A.15)
\end{aligned}$$

Finally, by using Equations (A.3), (A.7) and

$$\frac{\partial}{\partial \xi} (\bar{q} \times \bar{a}_1) = \bar{a}_1 \times \bar{a}_1 = 0 \quad (\text{A.16})$$

one obtains,

$$\begin{aligned} 2\pi \frac{\partial^2 I_p}{\partial \xi^2 \partial \eta} &= \frac{\partial^2}{\partial \xi^2 \partial \eta} \tan^{-1} \frac{-(\bar{q} \times \bar{a}_1) \cdot (\bar{q} \times \bar{a}_2)}{\sqrt{\bar{q} \cdot \bar{q}} \bar{q} \cdot \bar{a}_1 \times \bar{a}_2} \\ &= \frac{\partial}{\partial \xi} \left[\frac{(\bar{q} \cdot \bar{q})(\bar{q} \cdot \bar{a}_1 \times \bar{a}_2) - (\bar{q} \cdot \bar{a}_1)(\bar{q} \cdot \bar{a}_1 \times \bar{a}_2)}{\sqrt{\bar{q} \cdot \bar{q}} |\bar{q} \times \bar{a}_1|^2} \right] \\ &= \frac{1}{|\bar{q} \times \bar{a}_1|^2} \left\{ -\frac{\bar{q} \cdot \bar{a}_1}{(\bar{q} \cdot \bar{q})^{3/2}} \left[(\bar{q} \cdot \bar{q})(\bar{q} \cdot \bar{a}_1 \times \bar{a}_2) - (\bar{q} \cdot \bar{a}_1)(\bar{q} \cdot \bar{a}_1 \times \bar{a}_2) \right] + \right. \\ &\quad + \frac{1}{\sqrt{\bar{q} \cdot \bar{q}}} \left[2(\bar{a}_1 \cdot \bar{q})(\bar{q} \cdot \bar{a}_1 \times \bar{a}_2) + (\bar{q} \cdot \bar{q})(\bar{a}_1 \cdot \bar{a}_1 \times \bar{a}_2) \right. \\ &\quad \left. \left. - (\bar{a}_1 \cdot \bar{a}_1)(\bar{q} \cdot \bar{a}_1 \times \bar{a}_2) - (\bar{q} \cdot \bar{a}_1)(\bar{a}_1 \cdot \bar{a}_1 \times \bar{a}_2) - (\bar{q} \cdot \bar{a}_1)(\bar{q} \cdot \bar{a}_1 \times \bar{a}_2) \right] \right\} \\ &= \frac{1}{(\bar{q} \cdot \bar{q})^{3/2} |\bar{q} \times \bar{a}_1|^2} \left[(\bar{q} \cdot \bar{a}_1)(\bar{q} \cdot \bar{a}_1) - (\bar{q} \cdot \bar{q})(\bar{a}_1 \cdot \bar{a}_1) \right] (\bar{q} \cdot \bar{a}_1 \times \bar{a}_2) \\ &= \frac{\bar{q} \cdot \bar{a}_1 \times \bar{a}_2}{(\bar{q} \cdot \bar{q})^{3/2}} \quad (\text{A.18}) \end{aligned}$$

This proves that Equation (3.10) provides an analytical solutions of the doublet integral, given by Equation (A.9), for any hyperboloidal element.

A.4 SOURCE INTEGRAL

Use Equation (A.3) and note that

$$\frac{\partial}{\partial \xi} (\bar{q} \times \bar{a}_1 \cdot \bar{n}) = \bar{a}_1 \times \bar{a}_1 \cdot \bar{n} = 0 \quad (\text{A.19})$$

and

$$\begin{aligned} & \frac{\partial}{\partial \xi} \ln (|\bar{a}_1| |\bar{q}| + \bar{q} \cdot \bar{a}_1) \\ &= \frac{1}{|\bar{a}_1| |\bar{q}| + \bar{q} \cdot \bar{a}_1} \left\{ \frac{\bar{q} \cdot \bar{a}_1}{\sqrt{\bar{q} \cdot \bar{q}}} |\bar{a}_1| + \bar{a}_1 \cdot \bar{a}_1 \right\} \frac{\sqrt{\bar{a}_1 \cdot \bar{a}_1}}{\sqrt{\bar{q} \cdot \bar{q}}} \end{aligned} \quad (\text{A.20})$$

Hence,

$$\begin{aligned} & \frac{\partial^2}{\partial \xi^2 \partial \eta} \left[\bar{q} \times \bar{a}_1 \cdot \bar{n} \frac{1}{|\bar{a}_1|} \ln (|\bar{a}_1| |\bar{q}| + \bar{q} \cdot \bar{a}_1) \right] = \frac{\partial}{\partial \xi} \left(\frac{\bar{q} \times \bar{a}_1 \cdot \bar{n}}{\sqrt{\bar{q} \cdot \bar{q}}} \right) \\ & \frac{\bar{a}_2 \times \bar{a}_1 \cdot \bar{n}}{\sqrt{\bar{q} \cdot \bar{q}}} + \frac{\bar{q} \times \bar{a}_1 \cdot \bar{n}}{\sqrt{\bar{q} \cdot \bar{q}}} - \bar{q} \times \bar{a}_1 \cdot \bar{n} \frac{\bar{q} \cdot \bar{a}_1}{|\bar{q}|^3} \end{aligned} \quad (\text{A.21})$$

Similarly

$$\begin{aligned} & \frac{\partial^2}{\partial \xi^2 \partial \eta} \left[\bar{q} \times \bar{a}_2 \cdot \bar{n} \frac{1}{|\bar{a}_2|} \ln (|\bar{a}_2| |\bar{q}| + \bar{q} \cdot \bar{a}_2) \right] = \frac{\partial}{\partial \xi} \left(\frac{\bar{q} \times \bar{a}_2 \cdot \bar{n}}{\sqrt{\bar{q} \cdot \bar{q}}} \right) \\ &= \frac{\bar{a}_1 \times \bar{a}_2 \cdot \bar{n}}{\sqrt{\bar{q} \cdot \bar{q}}} + \frac{\bar{q} \times \bar{a}_2 \cdot \bar{n}}{\sqrt{\bar{q} \cdot \bar{q}}} - \bar{q} \times \bar{a}_2 \cdot \bar{n} \frac{\bar{q} \cdot \bar{a}_2}{|\bar{q}|^3} \end{aligned} \quad (\text{A.22})$$

Furthermore, noting that

$$\frac{\partial}{\partial \xi} (\bar{q} \cdot \bar{n}) = \bar{q} \quad (\text{A.23})$$

and combining Equation (A.14) with Equations (A.5) and (A.6) yields

$$\begin{aligned} & \frac{\partial^2}{\partial \xi^2 \partial \eta} \left(\bar{q} \cdot \bar{n} \tan^{-1} \frac{-(\bar{q} \times \bar{a}_1)(\bar{q} \times \bar{a}_2)}{\sqrt{\bar{q} \cdot \bar{q}} \bar{q} \cdot \bar{a}_1 \times \bar{a}_2} \right) \\ &= -\bar{q} \cdot \bar{n} \frac{\bar{q} \cdot \bar{a}_1 \times \bar{a}_2}{(\bar{q} \cdot \bar{q})^{3/2}} \end{aligned} \quad (\text{A.24})$$

Finally combining Equations (A.21), (A.22) and (A.24) yields

$$\begin{aligned}
& \frac{2\pi}{\bar{n} \cdot \bar{a}_x} \frac{\partial^2 I_s}{\partial \xi \partial \eta} \\
&= \frac{|\bar{n}_1 \times \bar{a}_2|}{|\bar{q}|} + (\bar{q} \cdot \bar{a}_1 \times \bar{n}) \frac{\bar{q} \cdot \bar{a}_2}{|\bar{q}|^3} + \frac{|\bar{a}_1 \times \bar{a}_2|}{|\bar{q}|} - (\bar{q} \cdot \bar{a}_2 \times \bar{n}) \frac{\bar{q} \cdot \bar{a}_1}{|\bar{q}|^3} - \frac{(\bar{q} \cdot \bar{n}) \bar{q} \cdot \bar{a}_1 \times \bar{a}_2}{|\bar{q}|^3} \\
&= 2 \frac{|\bar{a}_1 \times \bar{a}_2|}{|\bar{q}|} + \frac{1}{|\bar{q}|^3} [(-\bar{q} \times \bar{n} \cdot \bar{a}_1)(\bar{q} \cdot \bar{a}_2) + (\bar{q} \times \bar{n} \cdot \bar{a}_2)(\bar{q} \cdot \bar{a}_1) - (\bar{q} \cdot \bar{n})(\bar{q} \cdot \bar{a}_1 \times \bar{a}_2)] \\
&= 2 \frac{|\bar{a}_1 \times \bar{a}_2|}{|\bar{q}|} + \frac{1}{|\bar{q}|^3} [-(\bar{q} \times \bar{n}) \times \bar{q} \cdot (\bar{a}_1 \times \bar{a}_2) - (\bar{q} \cdot \bar{n})(\bar{q} \cdot \bar{a}_1 \times \bar{a}_2)] \\
&= 2 \frac{|\bar{a}_1 \times \bar{a}_2|}{|\bar{q}|} + \frac{1}{|\bar{q}|^3} [(\bar{q} \cdot \bar{n})(\bar{q} \cdot \bar{a}_1 \times \bar{a}_2) - (\bar{q} \cdot \bar{q})(\bar{n} \cdot \bar{a}_1 \times \bar{a}_2) - (\bar{q} \cdot \bar{n})(\bar{q} \cdot \bar{a}_1 \times \bar{a}_2)] \\
&= 2 \frac{|\bar{a}_1 \times \bar{a}_2|}{|\bar{q}|} - \frac{|\bar{n} \cdot \bar{a}_1 \times \bar{a}_2|}{|\bar{q}|} = \frac{|\bar{a}_1 \times \bar{a}_2|}{|\bar{q}|} \quad (A.25)
\end{aligned}$$

This proves that Equation (3.11) provides an analytical solution of source integral, given by Equation (A.10), for any quadrilateral planar element.

A.5 WAKE COEFFICIENT

Consider Figure 2b, and assume that the wake element is truncated such that

$$\bar{a}_1 = \bar{p}_1 = \chi \bar{u} = \chi \bar{i} \quad (A.26)$$

By letting χ go to infinity, wake coefficient can be obtained from I_D in Equation (3.10). Note that (see Figure 2b)

$$\bar{p}_0 - \bar{p}_1 = (\bar{p}_+ + \bar{p}_-)/2 = \bar{p}_m \quad (A.27)$$

$$\bar{p}_2 = \frac{\bar{p}_+ - \bar{p}_-}{2} = \bar{p}_d = \bar{a}_2 \quad (A.28)$$

$$\bar{p}_3 = 0 \quad (A.29)$$

It is convenient to separate the contribution from the trailing edge ($\xi = -1$) and the edge that goes to infinity ($\xi = 1$):

$$I_w = \mp \frac{S}{2\pi} \left\{ J_w(1, \eta) - J_w(-1, \eta) \right\}_{\eta=-1}^{\eta=1} \quad (\text{A.30})$$

where (note that $\bar{q} = \bar{p}_m + (1+\xi)\chi\bar{i} + \eta\bar{p}_d$)

$$S = \text{sign}(\bar{q} \cdot \bar{a}_1 \times \bar{a}_2) = \text{sign}(\bar{p}_{md} \cdot \bar{i} \times \bar{p}_d) \quad (\text{A.31})$$

with

$$\bar{p}_{md} = \bar{p}_m + \eta\bar{p}_d \quad (\text{A.32})$$

while (note that $\bar{q}(\xi=1) = \bar{p}_{md} + 2\chi\bar{i}$)

$$\begin{aligned} J_w(1, \eta) &= \lim_{\chi \rightarrow \infty} \tan_p^{-1} \left(\frac{-(\bar{q} \times \bar{a}_1) \cdot (\bar{q} \times \bar{a}_2)}{|\bar{q}| |\bar{q} \cdot \bar{a}_1 \times \bar{a}_2|} \right)_{\xi=1} \\ &= \lim_{\chi \rightarrow \infty} \tan_p^{-1} \left(\frac{-(\bar{q} \times \bar{i}) \cdot (\bar{q} \times \bar{p}_d)}{|\bar{q}| (\bar{q} \cdot \bar{i} \times \bar{p}_d)} \right)_{\xi=1} \\ &= \lim_{\chi \rightarrow \infty} \tan_p^{-1} \frac{-[(\bar{p}_m + \eta\bar{p}_d) \times \bar{i}] \cdot [(\bar{p}_m + 2\chi\bar{i}) \times \bar{p}_d]}{[(\bar{p}_m + \eta\bar{p}_d + 2\bar{i}) \cdot (\bar{p}_m + \eta\bar{p}_d + 2\chi\bar{i})]^{1/2} |\bar{p}_m \cdot \bar{i} \times \bar{p}_d|} \\ &= \tan_p^{-1} \frac{-(\bar{p}_{md} \times \bar{i}) \cdot (\bar{i} \times \bar{p}_d)}{|\bar{p}_{md} \cdot \bar{i} \times \bar{p}_d|} \\ &= \tan_p^{-1} \frac{\bar{p}_{md} \cdot \bar{p}_d - (\bar{p}_{md} \cdot \bar{i})(\bar{p}_d \cdot \bar{i})}{|\bar{p}_{md} \cdot \bar{i} \times \bar{p}_d|} \quad (\text{A.33}) \end{aligned}$$

and similarly (note that $\bar{q}(\xi=-1) = \bar{p}_m + \eta\bar{p}_d = \bar{p}_{md}$)

$$J_w(-1, \eta) = \tan_p^{-1} \left\{ - \frac{(\bar{q} \times \bar{a}_1) \cdot (\bar{q} \times \bar{a}_2)}{|\bar{q}| |\bar{q} \cdot \bar{a}_1 \times \bar{a}_2|} \right\}_{\xi = -1}$$

$$= \tan_p^{-1} \left\{ - \frac{(\bar{q} \times \bar{\lambda}) \cdot (\bar{q} \times \bar{p}_d)}{|\bar{q}| |\bar{q} \cdot \bar{\lambda} \times \bar{p}_d|} \right\}_{\xi = -1}$$

$$= \tan_p^{-1} \left\{ \frac{-(\bar{p}_{md} \times \bar{\lambda}) \cdot (\bar{p}_{md} \times \bar{p}_d)}{|\bar{p}_{md}| |\bar{p}_{md} \cdot \bar{\lambda} \times \bar{p}_d|} \right\}$$

$$= \tan_p^{-1} \left\{ - \frac{(\bar{p}_{md} \cdot \bar{p}_{md})(\bar{\lambda} \cdot \bar{p}_d) + (\bar{p}_{md} \cdot \bar{p}_d)(\bar{p}_{md} \cdot \bar{\lambda})}{|\bar{p}_{md}| |\bar{p}_{md} \cdot \bar{\lambda} \times \bar{p}_d|} \right\} \quad (A.34)$$

APPENDIX B

FORMULATIONS FOR STEADY SUPERSONIC FLOW

B.1 INTRODUCTION

The derivation of Equations (5.8) and (5.9) is presented in Reference 7. In Subsections B.2 and B.3 it will be shown that these equations are valid for any quadrilateral planar element. In Subsection B.4, formulations of the doublet and source integral of the element intersected with the Mach forecone are considered.

For hyperboloidal elements with \bar{q} , \bar{a}_1 , \bar{a}_2 , and $d\Sigma$ defined by Equations (3.12), (3.13), and (3.14) and (A.8), the doublet and source integral in Equations (4.7a) and (4.7b) can be rewritten as

$$\begin{aligned} C_{hk} &= \frac{1}{\pi} \int_{-1}^1 \int_{-1}^1 \frac{\partial}{\partial N^c} \left(\frac{H}{\|\bar{q}\|} \right) |\bar{a}_1 \times \bar{a}_2| d\xi d\eta \\ &= \frac{1}{\pi} \int_{-1}^1 \int_{-1}^1 \frac{\bar{q} \cdot \bar{a}_1 \times \bar{a}_2}{\|\bar{q}\|^3} H d\xi d\eta \end{aligned} \quad (B.1)$$

and

$$b_{hk} = - \frac{1}{\pi} \int_{-1}^1 \int_{-1}^1 \frac{H}{\|\bar{q}\|} |\bar{a}_1 \times \bar{a}_2| d\xi d\eta \quad (B.2)$$

Since

$$\begin{aligned} \frac{\partial}{\partial N^c} \left(\frac{H}{\|\bar{q}\|} \right) |\bar{a}_1 \times \bar{a}_2| &= - \frac{|\bar{a}_1 \times \bar{a}_2|}{(\bar{q} \cdot \bar{q})^{3/2}} \left(\frac{\partial \bar{q}}{\partial N^c} \cdot \bar{q} \right) \\ &= - \frac{|\bar{a}_1 \times \bar{a}_2|}{(\bar{q} \cdot \bar{q})^{3/2}} \left[N_x \frac{\partial}{\partial x} (x - x_*) \bar{i} - N_y \frac{\partial}{\partial y} (y - y_*) \bar{j} - N_z \frac{\partial}{\partial z} (z - z_*) \bar{k} \right] \cdot \bar{q} \\ &= - \frac{|\bar{a}_1 \times \bar{a}_2|}{(\bar{q} \cdot \bar{q})^{3/2}} \bar{N}^c \cdot \bar{q} = \frac{\bar{a}_1 \times \bar{a}_2 \cdot \bar{q}}{(\bar{q} \cdot \bar{q})^{3/2}} \end{aligned} \quad (B.3)$$

B.2 DOUBLET INTEGRAL

Following is the proof that Equation (5.8) is valid for any quadrilateral element within the Mach forecone. By using Equations (A.3), (A.4) and

$$\frac{\partial \bar{a}_1}{\partial \eta} = \frac{\partial \bar{a}_2}{\partial \xi} = \bar{p}_3 \quad (\text{B.4})$$

one obtains

$$\begin{aligned} \frac{\partial}{\partial \eta} \tan^{-1} \frac{-\bar{q} \times \bar{a}_1 \odot \bar{q} \times \bar{a}_2}{\sqrt{\bar{q} \odot \bar{q}} \bar{q} \cdot \bar{a}_1 \times \bar{a}_2} &= \frac{1}{1 + \left(\frac{\bar{q} \times \bar{a}_1 \odot \bar{q} \times \bar{a}_2}{\sqrt{\bar{q} \odot \bar{q}} \bar{q} \cdot \bar{a}_1 \times \bar{a}_2} \right)^2} \left\{ (\bar{a}_2 \times \bar{a}_1 \odot \bar{q} \times \bar{a}_2 + \bar{q} \times \bar{p}_3 \odot \bar{q} \times \bar{a}_2 \right. \\ &+ \bar{q} \times \bar{a}_1 \odot \bar{a}_2 \times \bar{a}_2) \frac{1}{\|\bar{q}\| \bar{q} \cdot \bar{a}_1 \times \bar{a}_2} - \frac{\bar{q} \times \bar{a}_1 \odot \bar{q} \times \bar{a}_2}{\bar{q} \odot \bar{q} (\bar{q} \cdot \bar{a}_1 \times \bar{a}_2)^2} \left\{ \frac{\bar{a}_2 \odot \bar{q}}{\sqrt{\bar{q} \odot \bar{q}}} (\bar{q} \cdot \bar{a}_1 \times \bar{a}_2) + \sqrt{\bar{q} \odot \bar{q}} (\bar{a}_2 \times \bar{a}_1 \times \bar{a}_2 + \bar{q} \cdot \bar{p}_3 \times \bar{a}_2) \right\} \Big\} \\ &= - \frac{\bar{q} \odot \bar{q} (\bar{q} \cdot \bar{a}_1 \times \bar{a}_2)^2}{(\bar{q} \odot \bar{q}) (\bar{q} \cdot \bar{a}_1 \times \bar{a}_2)^2 + (\bar{q} \times \bar{a}_1 \odot \bar{q} \times \bar{a}_2)} \frac{1}{\|\bar{q}\|^3 (\bar{q} \cdot \bar{a}_1 \times \bar{a}_2)} \left\{ (\bar{q} \odot \bar{q}) (\bar{q} \cdot \bar{a}_1 \times \bar{a}_2) (\bar{a}_2 \times \bar{a}_1 \odot \bar{q} \times \bar{p}_3 + \right. \\ &+ \bar{q} \times \bar{p}_3 \odot \bar{q} \times \bar{a}_2) - (\bar{q} \times \bar{a}_1 \odot \bar{q} \times \bar{a}_2) [(\bar{a}_2 \odot \bar{q}) (\bar{q} \cdot \bar{a}_1 \times \bar{a}_2) + (\bar{q} \odot \bar{q}) (\bar{q} \cdot \bar{p}_3 \times \bar{a}_2)] \Big\} \\ &= - \frac{1}{\sqrt{\bar{q} \odot \bar{q}}} \frac{1}{(\bar{q} \odot \bar{q}) (\bar{q} \cdot \bar{a}_1 \times \bar{a}_2)^2 + (\bar{q} \times \bar{a}_1 \odot \bar{q} \times \bar{a}_2)^2} \left\{ (\bar{q} \cdot \bar{a}_1 \times \bar{a}_2) [(\bar{a}_2 \times \bar{a}_1 \odot \bar{q} \times \bar{a}_2) \bar{q} \odot \bar{q} - (\bar{q} \times \bar{a}_1 \odot \bar{q} \times \bar{a}_2) \right. \\ &\left. \bar{a}_2 \odot \bar{q}] + \bar{q} \odot \bar{q} [(\bar{q} \times \bar{p}_3 \odot \bar{q} \times \bar{a}_2) \bar{q} \cdot \bar{a}_1 \times \bar{a}_2 - (\bar{q} \times \bar{a}_1 \odot \bar{q} \times \bar{a}_2) \bar{q} \cdot \bar{p}_3 \times \bar{a}_2] \right\} \quad (\text{B.5}) \end{aligned}$$

Furthermore,

$$\begin{aligned}
& \left[(\bar{a}_2 \times \bar{a}_1 \odot \bar{q} \times \bar{a}_2) \bar{q} \odot \bar{q} - (\bar{q} \times \bar{a}_1 \odot \bar{q} \times \bar{a}_2) \bar{a}_2 \odot \bar{q} \right] (\bar{q} \cdot \bar{a}_1 \times \bar{a}_2) + \\
& + \left[(\bar{q} \cdot \bar{p}_3 \odot \bar{q} \times \bar{a}_2) (\bar{q} \cdot \bar{a}_1 \times \bar{a}_2) - (\bar{q} \times \bar{a}_1 \odot \bar{q} \times \bar{a}_2) (\bar{q} \cdot \bar{p}_3 \times \bar{a}_2) \right] \bar{q} \odot \bar{q} \\
& = \left\{ (\bar{a}_2 \odot \bar{q})(\bar{a}_1 \times \bar{a}_2) - (\bar{a}_2 \odot \bar{a}_2)(\bar{a}_1 \odot \bar{q}) \right\} \bar{q} \odot \bar{q} - \left\{ (\bar{q} \odot \bar{q})(\bar{a}_1 \times \bar{a}_2) - (\bar{q} \odot \bar{a}_2)(\bar{q} \odot \bar{a}_1) \right\} \bar{a}_2 \odot \bar{q} \left\{ \bar{q} \cdot \bar{a}_1 \times \bar{a}_2 \right. \\
& + \left\{ (\bar{q} \odot \bar{q})(\bar{p}_3 \odot \bar{a}_2) - (\bar{q} \odot \bar{a}_2)(\bar{q} \odot \bar{p}_3) \right\} \bar{q} \cdot \bar{a}_1 \times \bar{a}_2 - \left\{ (\bar{q} \odot \bar{q})(\bar{a}_1 \odot \bar{a}_2) - (\bar{q} \odot \bar{a}_2)(\bar{q} \odot \bar{a}_1) \right\} \bar{q} \cdot \bar{p}_3 \times \bar{a}_2 \left. \right\} \bar{q} \odot \bar{q} \\
& = - \left\{ (\bar{q} \odot \bar{q})(\bar{a}_2 \odot \bar{a}_2) - (\bar{q} \odot \bar{a}_2)^2 \right\} (\bar{q} \odot \bar{a}_1) (\bar{q} \cdot \bar{a}_1 \times \bar{a}_2) + \left\{ (\bar{q} \odot \bar{q})(\bar{a}_2 \odot \bar{p}_3 \bar{q} \cdot \bar{a}_1 \times \bar{a}_2 \right. \\
& \left. - (\bar{a}_1 \odot \bar{a}_2)(\bar{q} \cdot \bar{p}_3 \times \bar{a}_2) - (\bar{q} \odot \bar{a}_2) \left\{ (\bar{q} \odot \bar{p}_3)(\bar{q} \cdot \bar{a}_1 \times \bar{a}_2) - (\bar{q} \odot \bar{a}_1)(\bar{q} \cdot \bar{p}_3 \times \bar{a}_2) \right\} \right\} \\
& = - \left\{ (\bar{q} \odot \bar{q})(\bar{a}_2 \odot \bar{a}_2) - (\bar{q} \odot \bar{a}_2)^2 \right\} (\bar{q} \odot \bar{a}_1) (\bar{q} \cdot \bar{a}_1 \times \bar{a}_2) + (\bar{q} \times \bar{a}_2 \odot \bar{q} \times \bar{a}_2) (\bar{q} \cdot \bar{a}_1 \times \bar{p}_3) (\bar{q} \odot \bar{q}) \\
& = \|\bar{q} \times \bar{a}_2\|^2 \left[(\bar{q} \odot \bar{a}_1) (\bar{q} \cdot \bar{a}_1 \times \bar{a}_2) - (\bar{q} \odot \bar{q})(\bar{q} \cdot \bar{a}_1 \times \bar{p}_3) \right] \tag{B.6}
\end{aligned}$$

since

$$(\bar{q} \odot \bar{q})(\bar{a}_2 \odot \bar{a}_2) - (\bar{q} \odot \bar{a}_2)^2 \equiv (\bar{q} \times \bar{a}_2) \odot (\bar{q} \times \bar{a}_2) = -\|\bar{q} \times \bar{a}_2\|^2 \tag{B.7}$$

Finally, combining Equation (B.5) with (B.6) yields

$$\begin{aligned}
& \frac{\partial I_p}{\partial \eta} = \frac{\|\bar{q} \times \bar{a}_2\|^2 \left[(\bar{q} \odot \bar{a}_1) \bar{q} \cdot \bar{a}_1 \times \bar{a}_2 - (\bar{q} \odot \bar{q}) \bar{q} \cdot \bar{a}_1 \times \bar{p}_3 \right]}{\|\bar{q} \times \bar{a}_1\|^2 \|\bar{q} \times \bar{a}_2\|^2 \|\bar{q}\|} \\
& = \frac{1}{\|\bar{q} \times \bar{a}_1\|^2 \|\bar{q}\|} \left[(\bar{q} \odot \bar{a}_1) (\bar{q} \cdot \bar{a}_1 \times \bar{a}_2) - (\bar{q} \odot \bar{q})(\bar{q} \cdot \bar{a}_1 \times \bar{p}_3) \right] \tag{B.8}
\end{aligned}$$

Next, consider the second mixed derivative, since

$$\frac{\partial^2}{\partial \xi^2} (\bar{q} \times \bar{a}_1) = \frac{\partial^2}{\partial \xi^2} \left[(\bar{p}_0 + \eta \bar{p}_2) \times (\bar{p}_1 + \eta \bar{p}_3) \right] \equiv 0$$

Therefore,

$$\begin{aligned}
 \frac{\partial^2 I_p}{\partial \xi \partial \eta} &= \frac{1}{\|\bar{q} \times \bar{a}_1\|^2} \frac{\partial}{\partial \xi} \left[\frac{(\bar{q} \odot \bar{q})(\bar{q} \cdot \bar{a}_1 \times \bar{p}_3) - (\bar{q} \odot \bar{a}_1)(\bar{q} \cdot \bar{a}_1 \times \bar{a}_2)}{\sqrt{\bar{q} \odot \bar{q}}} \right] \\
 &= \frac{1}{\|\bar{q} \times \bar{a}_1\|^2} \left\{ -\frac{\bar{q} \odot \bar{a}_1}{(\bar{q} \odot \bar{q})^{3/2}} \left[(\bar{q} \odot \bar{q})(\bar{q} \cdot \bar{a}_1 \times \bar{p}_3) - (\bar{q} \odot \bar{a}_1)(\bar{q} \cdot \bar{a}_1 \times \bar{a}_2) \right] + \frac{1}{\sqrt{\bar{q} \odot \bar{q}}} \left[2(\bar{q} \odot \bar{a}_1)(\bar{q} \cdot \bar{a}_1 \times \bar{p}_3) \right. \right. \\
 &\quad \left. \left. + (\bar{q} \odot \bar{q})(\bar{a}_1 \cdot \bar{a}_1 \times \bar{p}_3) - (\bar{a}_1 \odot \bar{a}_1)(\bar{q} \cdot \bar{a}_1 \times \bar{a}_2) - (\bar{q} \odot \bar{a}_1)(\bar{a}_1 \cdot \bar{a}_1 \times \bar{a}_2) - (\bar{q} \odot \bar{a}_1)(\bar{q} \cdot \bar{a}_1 \times \bar{p}_3) \right] \right\} \\
 &= \frac{1}{\|\bar{q}\|^3 \|\bar{q} \times \bar{a}_1\|^2} \left[(\bar{q} \odot \bar{a}_1)^2 - (\bar{q} \odot \bar{q})(\bar{a}_1 \odot \bar{a}_1) \right] \bar{q} \cdot \bar{a}_1 \times \bar{a}_2 \\
 &= \frac{\bar{q} \cdot \bar{a}_1 \times \bar{a}_2}{\|\bar{q}\|^3} \tag{B.9}
 \end{aligned}$$

Thus, prove that Equation (5.8) provides an analytical solution of the doublet integral given by Equation (B.1) for any quadrilateral element.

B.3 SOURCE INTEGRAL

Following is the proof that Equation (5.19) is valid for any quadrilateral element within the Mach forecone. Noting that, as shown in Appendix D,

$$\frac{\partial F_1}{\partial \xi} = \frac{\partial F_2}{\partial \eta} = \frac{1}{\|\bar{q}\|} \tag{B.10}$$

and

$$\frac{\partial}{\partial \xi} (\bar{q} \times \bar{a}_1 \odot \bar{h}) = \bar{a}_1 \times \bar{a}_1 \odot \bar{h} = 0 \tag{B.11a}$$

$$\frac{\partial}{\partial \eta} (\bar{q} \times \bar{a}_2 \odot \bar{h}) = \bar{a}_2 \times \bar{a}_2 \odot \bar{h} = 0 \tag{B.11b}$$

yields

$$\frac{\partial^2}{\partial \xi \partial \eta} \left\{ \bar{q} \times \bar{a}_1 \odot \bar{h} F_1(\xi, \eta) \right\} =$$

$$= \frac{\partial}{\partial \eta} \left(\bar{q} \times \bar{a}_1 \odot \bar{n} \frac{1}{\sqrt{\bar{q} \odot \bar{q}}} \right) \quad (\text{B.12a})$$

$$= \frac{\bar{a}_2 \times \bar{a}_1 \odot \bar{n}}{\|\bar{q}\|} + \frac{\bar{q} \times \bar{p}_3 \odot \bar{n}}{\|\bar{q}\|} - \bar{q} \times \bar{a}_1 \odot \bar{n} \frac{\bar{q} \odot \bar{a}_2}{(\bar{q} \odot \bar{q})^{3/2}} \quad (\text{B.12b})$$

Similarly,

$$\frac{\partial^2}{\partial \xi \partial \eta} \left\{ \bar{q} \times \bar{a}_2 \odot \bar{n} F_2(\xi, \eta) \right\} = \frac{\bar{a}_1 \times \bar{a}_2 \odot \bar{n}}{\|\bar{q}\|} + \frac{\bar{q} \times \bar{p}_3 \odot \bar{n}}{\|\bar{q}\|} - \bar{q} \times \bar{a}_2 \odot \bar{n} \frac{\bar{q} \odot \bar{a}_1}{(\bar{q} \odot \bar{q})^{3/2}} \quad (\text{B.13})$$

In addition, from Equation (B.9)

$$\frac{\partial^2}{\partial \xi \partial \eta} \left\{ \bar{q} \cdot \bar{n} \tan_p^{-1} \left(\frac{-\bar{q} \times \bar{a}_1 \odot \bar{q} \times \bar{a}_2}{\|\bar{q}\| \bar{q} \cdot \bar{a}_1 \times \bar{a}_2} \right) \right\} = \bar{q} \cdot \bar{n} \frac{\bar{q} \cdot \bar{a}_1 \times \bar{a}_2}{\|\bar{q}\|^3} \quad (\text{B.14})$$

Finally, combining Equations (4.10), (B.12b), (B.13) and (B.14) and noting that

$\|\bar{n}\| = -\bar{n} \odot \bar{n}$, yields

$$\begin{aligned} \frac{\partial^2 I_3}{\partial \xi \partial \eta} &= \frac{1}{\pi} \frac{1}{\bar{n} \odot \bar{n}} \left\{ - \left(\frac{\bar{a}_2 \times \bar{a}_1 \odot \bar{n}}{\|\bar{q}\|} + \frac{\bar{q} \times \bar{p}_3 \odot \bar{n}}{\|\bar{q}\|} - \bar{q} \times \bar{a}_1 \odot \bar{n} \frac{\bar{q} \odot \bar{a}_2}{(\bar{q} \odot \bar{q})^{3/2}} \right) \right. \\ &\quad \left. + \left(\frac{\bar{a}_1 \times \bar{a}_2 \odot \bar{n}}{\|\bar{q}\|} + \frac{\bar{q} \times \bar{p}_3 \odot \bar{n}}{\|\bar{q}\|} - (\bar{q} \times \bar{a}_2 \odot \bar{n}) \frac{\bar{q} \odot \bar{a}_1}{(\bar{q} \odot \bar{q})^{3/2}} \right) - \bar{q} \cdot \bar{n} (\bar{q} \cdot \bar{a}_1 \times \bar{a}_2) \frac{1}{\|\bar{q}\|^3} \right\} \quad (\text{B.15a}) \end{aligned}$$

$$= \frac{1}{\bar{n} \odot \bar{n}} \frac{1}{\pi} \left\{ 2 |\bar{a}_1 \times \bar{a}_2| \frac{\bar{n} \odot \bar{n}}{\|\bar{q}\|} + \frac{1}{\|\bar{q}\|^3} \left[(\bar{q} \times \bar{a}_1 \odot \bar{n}) (\bar{q} \odot \bar{a}_2) - (\bar{q} \times \bar{a}_2 \odot \bar{n}) (\bar{q} \odot \bar{a}_1) - (\bar{q} \cdot \bar{n}) (\bar{q} \cdot \bar{a}_1 \times \bar{a}_2) \right] \right\} \quad (\text{B.15b})$$

According to Equation (D.7) for

$$-|\bar{a}_1 \times \bar{a}_2| ((\bar{q} \times \bar{a}_1 \odot \bar{n}) \bar{q} \odot \bar{a}_2 - (\bar{q} \times \bar{a}_2 \odot \bar{n}) \bar{q} \odot \bar{a}_1 - \bar{q} \cdot \bar{n} (\bar{q} \cdot \bar{a}_1 \times \bar{a}_2))$$

$$\begin{aligned}
&= (\bar{q}_1 \times \bar{a}_1 \circ \bar{a}_2 \times \bar{a}_1) \bar{q}_2 \circ \bar{a}_2 + (\bar{q}_1 \times \bar{a}_2 \circ \bar{a}_1 \times \bar{a}_2) (\bar{q}_2 \circ \bar{a}_1) + (\bar{q}_1 \cdot \bar{a}_1 \times \bar{a}_2)^2 \\
&= (\bar{q}_2 \circ \bar{q}_2) (\bar{a}_1 \times \bar{a}_2 \circ \bar{a}_1 \times \bar{a}_2) - (\bar{q}_1 \cdot \bar{a}_1 \times \bar{a}_2)^2 + (\bar{q}_1 \cdot \bar{a}_1 \times \bar{a}_2)^2 \\
&= \bar{q}_2 \circ \bar{q}_2 \quad \bar{n} \circ \bar{n} \quad |\bar{a}_1 \times \bar{a}_2|
\end{aligned} \tag{B.16}$$

By using Equation (B.16), Equation (B.15) reduces to

$$\begin{aligned}
\frac{\partial^2 I_s}{\partial \xi \partial \eta} &= \frac{1}{\bar{n} \circ \bar{n}} \left\{ 2 \bar{n} \circ \bar{n} \frac{|\bar{a}_1 \times \bar{a}_2|}{\|\bar{q}_1\|} - \bar{q}_2 \circ \bar{q}_2 \bar{n} \circ \bar{n} \frac{|\bar{a}_1 \times \bar{a}_2|}{\|\bar{q}_1\|^3} \right\} \\
&= \frac{1}{\bar{n} \circ \bar{n}} \left\{ \bar{n} \circ \bar{n} \frac{|\bar{a}_1 \times \bar{a}_2|}{\|\bar{q}_1\|} \right\} \\
&= \frac{|\bar{a}_1 \times \bar{a}_2|}{\|\bar{q}_1\|}
\end{aligned} \tag{B.17}$$

This proves that Equation (5.9) provides an analytical solution of the integral in Equation (5.5) for any quadrilateral element.

B.4 FINITE PARTS OF INTEGRALS

In order to extend the results to a planar quadrilateral element intersected with the Mach forecone, the finite part of the following special integral is investigated.

$$I = \int_{-\infty}^a \frac{\partial}{\partial x} \left(\frac{g(x)}{\sqrt{x}} H(x) \right) dx \tag{B.18}$$

where g is a regular function and H is the Heaviside function, Equation (B.18) can be rewritten as

$$I = \lim_{\epsilon \rightarrow 0} \int_{-\infty}^a \frac{\partial}{\partial x} \left(\frac{g}{\sqrt{x}} H(x - \epsilon) \right) dx$$

$$\begin{aligned}
&= \lim_{\epsilon \rightarrow 0} \left[\int_{-\infty}^a \frac{\partial}{\partial x} \left(\frac{g}{\sqrt{x}} \right) H dx + \int_{-\infty}^a \frac{g}{\sqrt{x}} \delta(x-\epsilon) dx \right] \\
&= \lim_{\epsilon \rightarrow 0} \left[\int_{\epsilon}^a \frac{\partial}{\partial x} \left(\frac{g}{\sqrt{x}} \right) dx + \frac{g(\epsilon)}{\sqrt{\epsilon}} \right] \\
&= \frac{g(a)}{\sqrt{a}} - \frac{g(\epsilon)}{\sqrt{\epsilon}} + \frac{g(\epsilon)}{\sqrt{\epsilon}} = \frac{g(a)}{\sqrt{a}}
\end{aligned} \tag{B.19}$$

This shows that the singular contribution disappears and should not be taken into account.

Thus, consider the source integral given in Equation (B.9). According to Equations (B.15a) and (B.17), the integrand of Equation (B.9), $\frac{|\bar{a}_1 \times \bar{a}_2|}{\|\bar{q}\|}$, can be written as

$$\begin{aligned}
\frac{|\bar{a}_1 \times \bar{a}_2|}{\|\bar{q}\|} H &= \frac{1}{\bar{n} \cdot \bar{n}} \left\{ - \left[\frac{\bar{a}_2 \times \bar{a}_1 \cdot \bar{n}}{\|\bar{q}\|} - \frac{\bar{q} \times \bar{p}_3 \cdot \bar{n}}{\|\bar{q}\|} - \bar{q} \times \bar{a}_1 \cdot \bar{n} \frac{\bar{q} \cdot \bar{a}_2}{\|\bar{q}\|^3} \right] H \right. \\
&\quad + \left[\frac{\bar{a}_1 \times \bar{a}_2 \cdot \bar{n}}{\|\bar{q}\|} - \frac{\bar{q} \times \bar{p}_3 \cdot \bar{n}}{\|\bar{q}\|} - \bar{q} \times \bar{a}_2 \cdot \bar{n} \frac{\bar{q} \cdot \bar{a}_1}{\|\bar{q}\|^3} \right] H \\
&\quad \left. - \left[\bar{q} \cdot \bar{n} \frac{\bar{q} \cdot \bar{a}_1 \times \bar{a}_2}{\|\bar{q}\|} \right] H \right\}
\end{aligned} \tag{B.20}$$

therefore, Equation (B.9) can be rewritten as

$$b_{hk} = \frac{1}{\pi} \int_{-1}^1 \int_{-1}^1 \frac{H}{\|\bar{q}\|} |\bar{a}_1 \times \bar{a}_2| d\zeta d\eta = \frac{1}{\pi} \frac{1}{\bar{n} \cdot \bar{n}} (S_1 + S_2 + S_3) \tag{B.21}$$

$$S_1 = I_{S_1}(1, 1) - I_{S_1}(1, -1) - I_{S_1}(-1, 1) + I_{S_1}(-1, -1) \tag{B.22a}$$

$$= - \int_{-1}^1 \int_{-1}^1 H \left[\frac{\bar{a}_1 \times \bar{a}_2 \cdot \bar{n}}{\|\bar{q}\|} + \frac{\bar{q} \times \bar{p}_3 \cdot \bar{n}}{\|\bar{q}\|^3} - \bar{q} \times \bar{a}_1 \cdot \bar{n} \frac{\bar{q} \cdot \bar{a}_2}{\|\bar{q}\|^3} \right] d\zeta d\eta \tag{B.22b}$$

$$S_2 = I_{s2}(1,1) - I_{s2}(1,-1) - I_{s2}(-1,1) + I_{s2}(-1,-1) \quad (B.23a)$$

$$= \int_{-1}^1 \int_{-1}^1 H \left(\frac{\bar{a}_1 \times \bar{a}_2 \cdot \bar{n}}{\|\bar{q}\|} - \frac{\bar{q} \times \bar{p}_3 \cdot \bar{n}}{\|\bar{q}\|} - \bar{q} \times \bar{a}_2 \cdot \bar{n} \frac{\bar{q} \cdot \bar{a}_1}{\|\bar{q}\|^3} \right) d\xi d\eta \quad (B.23b)$$

$$S_3 = I_{s3}(1,1) - I_{s3}(1,-1) - I_{s3}(-1,1) + I_{s3}(-1,-1) \quad (B.24a)$$

$$= - \int_{-1}^1 \int_{-1}^1 H \left(\bar{q} \cdot \bar{n} \frac{\bar{q} \cdot \bar{a}_1 \times \bar{a}_2}{\|\bar{q}\|} \right) d\xi d\eta \quad (B.24b)$$

First, according to Equation (B.12b), Equation (B.22b) can be rewritten as

$$S_1 = - \int_{-1}^1 d\xi \int_{-1}^1 \frac{\partial}{\partial \eta} \left(H(\bar{q} \times \bar{a}_1 \cdot \bar{n}) \frac{1}{\sqrt{\bar{q} \cdot \bar{q}}} \right) d\eta \quad (B.25)$$

Note that $\sqrt{\bar{q} \cdot \bar{q}}$ can be expressed as $h(\eta)\sqrt{\eta-\eta_0}$, where $h(\eta)$ is a regular function and η_0 is defined such that $\bar{q} \cdot \bar{q} = 0$. Compared with Equation (B.18), it can be concluded that the portions along the intersection line of the element with the Mach forecone yield no contributions to the integral S_1 . Therefore, in Equation (B.22a)

$$I_{s1}(1,1) - I_{s1}(-1,1) = 0 \quad (B.26)$$

or

$$I_{s1}(1,-1) - I_{s1}(-1,-1) = 0 \quad (B.27)$$

if the edge of $\eta=1$ or $\eta=-1$, respectively, is completely outside the Mach forecone.

Otherwise, I_{s1} is given by Equation (5.10) if the corner point is inside the Mach forecone, or

$$\begin{aligned} I_{s1}(\xi, \eta^*) &= 0 & ; \quad \bar{a}_1 \cdot \bar{a}_1 > 0 \\ &= (\bar{q} \times \bar{a}_1 \cdot \bar{n}) \text{sign}(\bar{q} \cdot \bar{a}_1) / \|\bar{a}_1\| & ; \quad \bar{a}_1 \cdot \bar{a}_1 < 0 \end{aligned} \quad (B.28)$$

if the corner point is outside the Mach forecone. Similarly, Equation (B.23b) can be rewritten as

$$S_2 = \int_{-1}^1 d\eta \int_{-1}^1 \frac{\partial}{\partial \eta} \left\{ H(\bar{q} \times \bar{a}_2 \odot \bar{n}) \frac{1}{\sqrt{\bar{q} \odot \bar{q}}} \right\} d\xi \quad (B.29)$$

therefore.

$$I_{S_2}(1,1) - I_{S_2}(1,-1) = 0 \quad (B.30)$$

or

$$I_{S_2}(-1,1) - I_{S_2}(-1,-1) = 0 \quad (B.31)$$

if the edge of $\xi = 1$, or $\xi = -1$, respectively, is completely outside the Mach forecone. Otherwise, I_{S_2} is given by Equation (5.11) if the corner point is inside the Mach forecone, or

$$\begin{aligned} I_{S_2}(\xi^*, \eta) &= 0 & ; \bar{a}_2 \odot \bar{a}_2 > 0 \\ &= -(\bar{q} \times \bar{a}_2 \cdot \bar{n}) \text{sign}(\bar{q} \odot \bar{a}_2) / \|\bar{a}_2\| & ; \bar{a}_2 \odot \bar{a}_2 < 0 \end{aligned} \quad (B.32)$$

if the corner point is outside the Mach forecone. Finally, considering Equation (D.10), Equations (B.24b) and (B.7) can be rewritten as

$$S_3 = -\bar{q} \cdot \bar{n} \int_{-1}^1 d\xi \int_{-1}^1 \frac{\partial}{\partial \eta} \left\{ \frac{H}{\|\bar{q} \times \bar{a}_1\|^2} (\bar{q} \odot \bar{a}_1 \bar{q} \cdot \bar{a}_1 \times \bar{a}_2 - \bar{q} \odot \bar{q} \bar{q} \cdot \bar{a}_1 \times \bar{p}_3) \frac{1}{\|\bar{q}\|} \right\} d\eta \quad (B.33)$$

and

$$C_{HK} = \frac{1}{\pi} \int_{-1}^1 d\xi \int_{-1}^1 \frac{\partial}{\partial \eta} \left\{ \frac{H}{\|\bar{q} \times \bar{a}_1\|^2} (\bar{q} \odot \bar{a}_1 \bar{q} \cdot \bar{a}_1 \times \bar{a}_2 - \bar{q} \odot \bar{q} \bar{q} \cdot \bar{a}_1 \times \bar{p}_3) \frac{1}{\|\bar{q}\|} \right\} d\eta \quad (B.34)$$

with the same reason given above, one obtains

$$I_{S_3}(1,1) - I_{S_3}(-1,1) = 0 \quad (B.35)$$

$$I_o(1,1) - I_o(-1,1) = 0 \quad (B.36)$$

or

$$I_{S_3}(1,-1) - I_{S_3}(-1,-1) = 0 \quad (B.37)$$

$$I_o(1,-1) - I_o(-1,-1) = 0 \quad (B.38)$$

if the edge of $\eta=1$ or $\eta=-1$, respectively, is completely outside the Mach forecone. Otherwise, I_{S3} and I_D are given by Equations (5.12) and (5.8), if the corner point is inside the Mach forecone, or

$$I_{S3}(\xi^*, \eta^*) = (\bar{q} \cdot \bar{n}) \frac{\pi}{2} \text{sign}[(\bar{q} \odot \bar{a}_1)(\bar{q} \odot \bar{a}_2)(\bar{q} \cdot \bar{n})] \quad (\text{B.39})$$

$$I_D(\xi^*, \eta^*) = -\frac{1}{2} \text{sign}[(\bar{q} \odot \bar{a}_1)(\bar{q} \odot \bar{a}_2)(\bar{q} \cdot \bar{n})] \quad (\text{B.40})$$

Note that the values of ξ^* and η^* in Equations (B.32), (B.28), (B.39) and (B.40) are evaluated such that $\bar{q} \odot \bar{q} = 0$.

B.5 INTEGRAL EQUATIONS FOR DIAPHRAGM-ATTACHED CONFIGURATION

As mentioned in Subsection 5.3, if diaphragms are used, both values of the velocity potential and its normal derivative, ϕ_D and ψ_D , of the diaphragm element are unknowns while two integral equations are obtained for each diaphragm element. Therefore, a system of equations, instead of Equation (5.3), may be obtained as follows.

$$[\delta_{hk}' - a_{hk}] \begin{pmatrix} \underline{\underline{\psi_k^u}} \\ \underline{\underline{\psi_k^l}} \\ \underline{\underline{\phi_D}} \\ \underline{\underline{\psi_D}} \end{pmatrix} = [b_{hk}'] \begin{pmatrix} \underline{\underline{\psi_k^u}} \\ \underline{\underline{\psi_k^l}} \\ \underline{\underline{0}} \\ \underline{\underline{0}} \end{pmatrix} \quad (\text{B.41})$$

where $\underline{\underline{\psi_k^u}}$ and $\underline{\underline{\psi_k^l}}$ (or $\underline{\underline{\phi_k^l}}$ and $\underline{\underline{\psi_k^l}}$) are the velocity potential and its normal at the centroid of the element on the upper (or lower) surface of the aircraft, while $\underline{\underline{\phi_D}}$ and $\underline{\underline{\psi_D}}$ are those quantities for the diaphragm element, and δ_{hk}' is given by

$$[\delta'_{hk}] = \begin{bmatrix} I & 0 & 0 & 0 \\ 0 & I & 0 & 0 \\ 0 & 0 & I & 0 \\ 0 & 0 & I & 0 \end{bmatrix} \quad (B.42)$$

\underline{a}_{hk} and \underline{b}_{hk} are given by

$$[a_{hk}] = \begin{bmatrix} C_{am}^u & 0 & C_{an}^u & b_{an}^u \\ 0 & C_{am}^l & C_{an}^l & -b_{an}^l \\ C_{dm}^u & 0 & C_{dn}^u & b_{dn}^u \\ 0 & C_{dm}^l & C_{dn}^l & -b_{dn}^l \end{bmatrix} \quad (B.43)$$

and

$$[b'_{hk}] = \begin{bmatrix} b_{am}^u & 0 & 0 & 0 \\ 0 & b_{am}^l & 0 & 0 \\ 0 & 0 & 0 & 0 \\ 0 & 0 & 0 & 0 \end{bmatrix} \quad (B.44)$$

where the superscript u (or l) reminds that both the control point and dummy element are on the upper (or lower) surface and first subscript a (or d) reminds that the control point is on the surface of aircraft (or diaphragm) second subscript m (or n) reminds that the dummy element is on the surface of aircraft (or diaphragm). For example, \underline{C}_{an}^u represents the submatrix formed by the doublet integrals, given by Equation (5.4), with control point on the upper surface of aircraft,

and dummy element on the upper surface of diaphragm. \underline{b}_{dm}^l represents the submatrix formed by the source integrals, given by Equation (5.5) with control point on the lower surface of diaphragm and dummy element on the lower surface of aircraft.

Furthermore, if the problem is symmetric, the normal derivative of the velocity potential, ψ_D , on the diaphragm is zero, while the velocity potential, ψ_D , is unknown,

$$\begin{aligned}\underline{\psi}_K^u &= \underline{\psi}_K^l, & \underline{\psi}_K^u &= \underline{\psi}_K^l \\ \underline{c}_{am}^u &= \underline{c}_{am}^l, & \underline{c}_{an}^u &= \underline{c}_{an}^l \\ \underline{c}_{dm}^u &= \underline{c}_{dm}^l, & \underline{c}_{dn}^u &= \underline{c}_{dn}^l \\ \underline{b}_{am}^u &= \underline{b}_{am}^l, & \underline{b}_{an}^u &= \underline{b}_{an}^l \\ \underline{b}_{dm}^u &= \underline{b}_{dm}^l, & \underline{b}_{dn}^u &= \underline{b}_{dn}^l\end{aligned}\tag{B.45}$$

therefore, Equation (B.41) reduced to

$$[\delta_{hk} - a_{hk}] \begin{Bmatrix} -\frac{\psi_K^u}{\psi_D} \end{Bmatrix} = [b_{hk}] \begin{Bmatrix} -\frac{\psi_K^u}{0} \end{Bmatrix}\tag{B.46}$$

with

$$[a_{hk}] = \begin{bmatrix} \underline{c}_{am}^u & \underline{c}_{an}^u \\ \underline{c}_{dm}^u & \underline{c}_{dn}^u \end{bmatrix}\tag{B.47}$$

and

$$[b_{hk}] = \begin{bmatrix} \underline{b}_{am}^u & 0 \\ 0 & 0 \end{bmatrix}\tag{B.48}$$

For the case that the problem is antisymmetric, ψ_p , is zero while ψ_o is unknown. Then Equation (B.41) reduced to Equation (B.46) with $[b_{hk}]$ given by (B.48) and $[a_{hk}]$ given by

$$[a_{hk}] = \left[\begin{array}{c|c} c_{am}^u & b_{an}^u \\ \hline c_{dm}^u & b_{dn}^u \end{array} \right] \quad (B.49)$$

APPENDIX C

FORMULATIONS FOR OSCILLATORY FLOW

C.1 BOUNDARY CONDITION

The boundary condition for oscillatory flow is given by

$$\nabla_{xyz} S \cdot \nabla_{xyz} \psi = -\frac{\partial S}{\partial t} - U_\infty \frac{\partial S}{\partial x} \quad (C.1)$$

C.1.1 Subsonic Flow

By introducing variables X, Y, Z, T, Ω and ϕ given by Equations (2.2)

and (3.3), and noting that $\beta^2 = 1 - M^2$ Equation (C.1) yields

$$\nabla_{XYZ} S \cdot \nabla_{XYZ} \phi + \frac{\beta}{M} \frac{\partial S}{\partial T} + \frac{1}{\beta} \frac{\partial S}{\partial X} + \frac{M^2}{\beta^2} \frac{\partial S}{\partial X} \frac{\partial \phi}{\partial X} = 0 \quad (C.2)$$

The motion of the surface is assumed to consist of small harmonic oscillations around a rest configuration that is

$$S = S_0(X, Y, Z) + \tilde{S}(X, Y, Z) e^{i\Omega T} \quad (C.3)$$

and

$$\phi = \phi_0(X, Y, Z) + \tilde{\phi}(X, Y, Z) e^{i\Omega T} \quad (C.4)$$

Substituting Equations (C.3) and (C.4) into Equation (C.2) yields

$$\begin{aligned} & \nabla_{XYZ} S_0 \cdot \nabla_{XYZ} \phi_0 + (\nabla_{XYZ} S_0 \cdot \nabla_{XYZ} \tilde{\phi} + \nabla_{XYZ} \tilde{S} \cdot \nabla_{XYZ} \phi_0) e^{i\Omega T} + \\ & + (\nabla_{XYZ} \tilde{S} \cdot \nabla_{XYZ} \tilde{\phi}) e^{i2\Omega T} + \frac{\beta}{M} i\Omega \tilde{S} e^{i\Omega T} + \frac{1}{\beta} \left(\frac{\partial S_0}{\partial X} + \frac{\partial \tilde{S}}{\partial X} e^{i\Omega T} \right) + \\ & + \frac{M^2}{\beta^2} \left[\frac{\partial S_0}{\partial X} \frac{\partial \phi_0}{\partial X} + \left(\frac{\partial S_0}{\partial X} \frac{\partial \tilde{\phi}}{\partial X} + \frac{\partial \tilde{S}}{\partial X} \frac{\partial \phi_0}{\partial X} \right) e^{i\Omega T} + \frac{\partial \tilde{S}}{\partial X} \frac{\partial \tilde{\phi}}{\partial X} e^{i2\Omega T} \right] = 0 \end{aligned} \quad (C.5)$$

Small terms can be dropped out by investigating the order of each quantity. Assuming*

*For instance, if $z = \epsilon z_0(x, y) + \epsilon^2 \tilde{z}(x, y) e^{i\Omega T}$, then $S_0 = z - \epsilon z_0(x, y)$, $\tilde{S} = \epsilon^2 \tilde{z}(x, y)$.

$$S_0 = O(1) \quad (C.6)$$

$$\frac{\partial S_0}{\partial X} = O(\epsilon) \quad (C.7)$$

with

$$|\nabla_{XYZ} S_0| = O(1) \quad (C.8)$$

and

$$\tilde{S} = O(\epsilon^2) \quad (C.9)$$

$$\frac{\partial \tilde{S}}{\partial X} = O(\epsilon^2) \quad (C.10)$$

$$|\nabla_{XYZ} \tilde{S}| = O(\epsilon^2) \quad (C.11)$$

Also, [see, for instance, Equations (C.16) and (C.17)], it is noted that

$$|\nabla_{XYZ} \phi_0| = O(\epsilon) \quad (C.12)$$

$$|\nabla_{XYZ} \tilde{\phi}| = O(\epsilon^2) \quad (C.13)$$

Investigating the order of each term of Equation (C.5) by Equations (C.6) to (C.13) and ignoring the terms which contain $e^{i2\Omega T}$ (of order ϵ^4), one obtains the stationary and the oscillatory boundary conditions which are given as

$$\nabla_{XYZ} S_0 \cdot \nabla_{XYZ} \phi_0 + \frac{1}{\beta} \frac{\partial S_0}{\partial X} + \frac{M^2}{\beta^2} \frac{\partial S_0}{\partial X} \frac{\partial \phi_0}{\partial X} = 0 \quad (C.14)$$

and

$$\begin{aligned} & \nabla_{XYZ} S_0 \cdot \nabla_{XYZ} \tilde{\phi} + \nabla_{XYZ} \tilde{S} \cdot \nabla_{XYZ} \phi_0 + \frac{\beta}{M} i\Omega \tilde{S} \\ & + \frac{1}{\beta} \frac{\partial \tilde{S}}{\partial X} + \frac{M^2}{\beta^2} \left(\frac{\partial S_0}{\partial X} \frac{\partial \tilde{\phi}}{\partial X} + \frac{\partial \tilde{S}}{\partial X} \frac{\partial \phi_0}{\partial X} \right) = 0 \end{aligned} \quad (C.15)$$

Neglecting terms of order ϵ^2 in Equation (C.14) and terms of order ϵ^3 in Equation (C.15), one obtains

$$\nabla_{XYZ} S_0 \cdot \nabla_{XYZ} \phi_0 = -\frac{1}{\beta} \frac{\partial S_0}{\partial X} \quad (C.16)$$

$$\nabla_{XYZ} S_0 \cdot \nabla_{XYZ} \phi = -\left(i \frac{\beta}{M} \Omega \tilde{S} + \frac{1}{\beta} \frac{\partial \tilde{S}}{\partial X}\right) \quad (C.17)$$

In particular for*

$$S = \pm \frac{1}{\ell} \left[Z - Z_0(X, Y) - \tilde{Z}(X, Y) e^{i\omega t} \right] \quad (C.18)$$

(where the upper or lower sign holds on the upper or lower surface); one obtains

$$S_0 = \pm \frac{1}{\ell} [Z - Z_0(X, Y)] \quad (C.19)$$

$$\tilde{S} = \mp \frac{1}{\ell} \tilde{Z}(X, Y) \quad (C.20)$$

$$\frac{1}{|\nabla_{XYZ} S_0|} = \frac{|\frac{\partial S_0}{\partial Z}|}{|\nabla_{XYZ} S_0|} = |Z_Z| = \pm N_Z \quad (C.21)$$

Therefore,

$$\frac{\partial \phi}{\partial N} = \frac{\nabla_{XYZ} S_0 \cdot \nabla_{XYZ} \phi}{|\nabla_{XYZ} S_0|} = N_Z \left(i K \frac{\tilde{Z}}{\ell} + \frac{\partial \tilde{Z}}{\partial X} \right) \quad (C.22)$$

where

$$K = \beta \Omega / M = \omega \ell / U_\infty \quad (C.23)$$

By using Equation (2.31), Equation (C.22) yields

$$\frac{\partial \hat{\phi}}{\partial N} = N_Z \left(i K \tilde{Z} + \frac{1}{\beta} \frac{\partial \tilde{Z}}{\partial X} \right) e^{-i\Omega M X} \quad (C.24)$$

Equation (C.20) gives the value of $\frac{\partial \hat{\phi}}{\partial N}$ to be used in Equation (4.3).

*Note that z_0 is of order ℓ and z is of order ℓ^2 .

C.1.2 Supersonic Flow

By introducing variable x, y, z, T, Ω and ϕ given by Equations (2.2) and (3.3), and noting that $\beta^2 = M^2 - 1$, Equation (C.1) yields

$$\nabla_{xyz} S \cdot \nabla_{xyz}^c \phi + \frac{\beta}{M} \frac{\partial S}{\partial T} + \frac{1}{\beta} \frac{\partial S}{\partial X} + \frac{M^2}{\beta^2} \frac{\partial S}{\partial X} \frac{\partial \phi}{\partial X} = 0 \quad (C.25)$$

with ∇_{xyz}^c defined by

$$\nabla_{xyz}^c = -\frac{\partial}{\partial X} \bar{i} + \frac{\partial}{\partial Y} \bar{j} + \frac{\partial}{\partial Z} \bar{k} \quad (C.26)$$

By replacing ∇_{xyz} with ∇_{xyz}^c , $\nabla_{xyz} \phi_0$ with $\nabla_{xyz}^c \phi_0$ and $\nabla_{xyz} \tilde{\phi}$ with $\nabla_{xyz}^c \tilde{\phi}$, Equations (C.5) to (C.22) are valid for supersonic flow. Therefore, the boundary condition for supersonic flow can be rewritten as

$$\frac{\partial \phi}{\partial N^c} = N_z \left(i k \tilde{z} + \frac{\partial \tilde{z}}{\partial X} \right) \quad (C.27)$$

By using Equation (2.39), Equation (C.27) yields

$$\frac{\partial \hat{\phi}}{\partial N^c} = N_z \left(i k \tilde{z} + \frac{1}{\beta} \frac{\partial \tilde{z}}{\partial X} \right) e^{i \alpha M X} \quad (C.28)$$

Equation (C.28) gives the value of $\frac{\partial \hat{\phi}}{\partial N^c}$ to be used in Equation (6.3).

C.2 PRESSURE COEFFICIENT

The pressure coefficient is given by the linear Bernoulli theorem, Equation (2.41), as

$$\begin{aligned} C_p &= -\frac{2}{U_\infty^2} \left(\frac{\partial \psi}{\partial t} + U_\infty \frac{\partial \psi}{\partial X} \right) \\ &= -2 \left(\frac{\beta}{M} \frac{\partial \phi}{\partial T} + \frac{1}{\beta} \frac{\partial \phi}{\partial X} \right) \end{aligned} \quad (C.29)$$

For oscillatory flow, setting

$$\phi = \tilde{\phi} e^{i\Omega\tau} \quad (\text{C.30})$$

$$C_p = \tilde{C}_p e^{i\Omega\tau}$$

one obtains

$$\begin{aligned} \tilde{C}_p &= -2 \left(\frac{\beta}{M} i\Omega \tilde{\phi} + \frac{1}{\beta} \frac{\partial \tilde{\phi}}{\partial x} \right) \\ &= -\frac{2}{\beta} \left(\frac{\partial \tilde{\phi}}{\partial x} + i K \beta \tilde{\phi} \right) \end{aligned} \quad (\text{C.31})$$

C.2.1 Subsonic Flow

By using Equation (2.31)

$$\tilde{\phi} = \hat{\phi} e^{i\Omega M x} \quad (\text{C.32})$$

C_p for oscillatory subsonic flow can be rewritten from Equation (C.31) as

$$\begin{aligned} \tilde{C}_p &= -\frac{2}{\beta} e^{-iK\beta x} \frac{\partial}{\partial x} (\tilde{\phi} e^{iK\beta x}) \\ &= -\frac{2}{\beta} e^{-iK\beta x} \frac{\partial}{\partial x} (\hat{\phi} e^{iKx/\beta}) \end{aligned} \quad (\text{C.33})$$

C.2.2 Supersonic Flow

By using Equation (2.39)

$$\tilde{\phi} = \hat{\phi} e^{-i\Omega M x} \quad (\text{C.34})$$

C_p for oscillatory supersonic flow can be rewritten from Equation (C.31) as

$$\begin{aligned} \tilde{C}_p &= -\frac{2}{\beta} e^{-iK\beta x} \frac{\partial}{\partial x} (\tilde{\phi} e^{iK\beta x}) \\ &= -\frac{2}{\beta} e^{-iK\beta x} \frac{\partial}{\partial x} (\hat{\phi} e^{-iKx/\beta}) \end{aligned} \quad (\text{C.35})$$

APPENDIX D

USEFUL EQUATIONS

D.1 INTRODUCTION

In deriving the formulations presented in previous sections, several useful equations are applied. They are proven in this appendix.

For the subsonic flow theory, the following two equations are used.

$$(\bar{a} \times \bar{b}) \cdot (\bar{c} \times \bar{d}) = (\bar{a} \cdot \bar{c})(\bar{b} \cdot \bar{d}) - (\bar{a} \cdot \bar{d})(\bar{b} \cdot \bar{c}) \quad (D.1)$$

$$(\bar{q} \cdot \bar{q})(\bar{q} \cdot \bar{a}_1 \times \bar{a}_2) + [(\bar{q} \times \bar{a}_1) \cdot (\bar{q} \times \bar{a}_2)]^2 \equiv |\bar{q} \times \bar{a}_1|^2 |\bar{q} \times \bar{a}_2|^2 \quad (D.2)$$

For the supersonic flow theory, the following five equations are used.

$$(\bar{a} \times \bar{b}) \odot (\bar{c} \times \bar{d}) = (\bar{a} \odot \bar{c})(\bar{b} \odot \bar{d}) - (\bar{a} \odot \bar{d})(\bar{b} \odot \bar{c}) \quad (D.3)$$

$$(\bar{q} \odot \bar{q})(\bar{q} \cdot \bar{a}_1 \times \bar{a}_2) + [(\bar{q} \times \bar{a}_1) \odot (\bar{q} \times \bar{a}_2)]^2 = \|\bar{q} \times \bar{a}_1\|^2 \|\bar{q} \times \bar{a}_2\|^2 \quad (D.4)$$

$$\frac{\partial F_1}{\partial \xi} = \frac{1}{\|\bar{q}\|} \quad (D.5)$$

$$\frac{\partial F_2}{\partial \eta} = \frac{1}{\|\bar{q}\|} \quad (D.6)$$

$$\begin{aligned} & (\bar{a} \odot \bar{a})(\bar{b} \times \bar{c}) \odot (\bar{b} \times \bar{c}) - (\bar{a} \cdot \bar{b} \times \bar{c})^2 \\ & = (\bar{a} \odot \bar{c})(\bar{b} \times \bar{c}) \odot (\bar{b} \times \bar{a}) + \bar{a} \odot \bar{b} (\bar{c} \times \bar{b}) \odot (\bar{c} \times \bar{a}) \end{aligned} \quad (D.7)$$

D.2 PROOF OF EQUATION (D.1)

$$\begin{aligned} & (\bar{A} \cdot \bar{B})(\bar{C} \cdot \bar{D}) - (\bar{A} \cdot \bar{C})(\bar{B} \cdot \bar{D}) \\ & = (A_x B_x + A_y B_y + A_z B_z)(C_x D_x + C_y D_y + C_z D_z) \\ & \quad - (A_x C_x + A_y C_y + A_z C_z)(B_x D_x + B_y D_y + B_z D_z) \\ & = \cancel{A_x B_x C_x D_x} + \cancel{A_y B_y C_y D_y} + \cancel{A_z B_z C_z D_z} + A_x B_x C_y D_y + A_x B_x C_z D_z \end{aligned}$$

$$\begin{aligned}
& + A_Y B_Y C_X D_X + A_Z B_Z C_X D_X + A_Y B_Y C_Z D_Z + A_Z B_Z C_Y D_Y - \cancel{A_X C_X B_X D_X} \\
& - \cancel{A_Y C_Y B_Y D_Y} - \cancel{A_Z C_Z B_Z D_Z} - A_X C_X B_Y D_Y - A_X C_X B_Z D_Z - A_Y C_Y B_X D_X \\
& - A_Z C_Z B_X D_X - A_Y C_Y B_Z D_Z - A_Z C_Z B_Y D_Y
\end{aligned}$$

while

$$\begin{aligned}
& (\overline{A} \times \overline{D}) \cdot (\overline{B} \times \overline{C}) \\
& = (A_Y D_Z - A_Z D_Y)(B_Y C_Z - B_Z C_Y) + (A_Z D_X - A_X D_Z)(B_Z C_X - B_X C_Z) + (A_X D_Y - A_Y D_X)(B_X C_Y - B_Y C_X) \\
& = A_Y B_Y C_Z D_Z - A_Y B_Z C_Y D_Z - (A_Z B_Y C_Z D_Y - A_Z B_Z C_Y D_Y) \\
& + A_Z B_Z C_X D_X + A_X B_X C_Z D_Z - (A_Z C_Z B_X D_X + A_X C_X B_Z D_Z) \\
& + A_X B_X C_Y D_Y + A_Y B_Y C_X D_X - (A_Y C_Y B_X D_X + A_X C_X B_Y D_Y) \quad (D.8)
\end{aligned}$$

D.3 PROOF OF EQUATION (D.2)

Following is the proof of Equation (D.2):

$$\begin{aligned}
& |\overline{q} \times \overline{a}_1|^2 |\overline{q} \times \overline{a}_2|^2 - \left\{ (\overline{q} \cdot \overline{q})(\overline{q} \cdot \overline{a}_1 \times \overline{a}_2)^2 + [(\overline{q} \times \overline{a}_1) \cdot (\overline{q} \times \overline{a}_2)]^2 \right\} \\
& = [(\overline{q} \cdot \overline{q})(\overline{a}_1 \cdot \overline{a}_1) - (\overline{q} \cdot \overline{a}_1)^2][(\overline{q} \cdot \overline{q})(\overline{a}_2 \cdot \overline{a}_2) - (\overline{q} \cdot \overline{a}_2)^2] - (\overline{q} \cdot \overline{q})(\overline{q} \cdot \overline{a}_1 \times \overline{a}_2)^2 \\
& - [(\overline{q} \cdot \overline{q})(\overline{a}_1 \cdot \overline{a}_2) - (\overline{q} \cdot \overline{a}_1)(\overline{q} \cdot \overline{a}_2)]^2 \\
& = (\overline{q} \cdot \overline{q})^2 (\overline{a}_1 \cdot \overline{a}_1)(\overline{a}_2 \cdot \overline{a}_2) + (\overline{q} \cdot \overline{a}_1)^2 (\overline{q} \cdot \overline{a}_2)^2 - (\overline{q} \cdot \overline{q})[(\overline{a}_1 \cdot \overline{a}_1)(\overline{q} \cdot \overline{a}_2)^2 + (\overline{a}_2 \cdot \overline{a}_2)(\overline{q} \cdot \overline{a}_1)^2] \\
& - (\overline{q} \cdot \overline{q})(\overline{q} \cdot \overline{a}_1 \times \overline{a}_2)^2 - (\overline{q} \cdot \overline{q})^2 (\overline{a}_1 \cdot \overline{a}_2)^2 - (\overline{q} \cdot \overline{a}_1)^2 (\overline{q} \cdot \overline{a}_2)^2 + 2(\overline{q} \cdot \overline{q})(\overline{a}_1 \cdot \overline{a}_2)(\overline{q} \cdot \overline{a}_1)(\overline{q} \cdot \overline{a}_2) \\
& = (\overline{q} \cdot \overline{q}) \left\{ (\overline{q} \cdot \overline{q})[(\overline{a}_1 \cdot \overline{a}_1)(\overline{a}_2 \cdot \overline{a}_2) - (\overline{a}_1 \cdot \overline{a}_2)^2] - (\overline{q} \cdot \overline{a}_1 \times \overline{a}_2)^2 - [(\overline{a}_1 \cdot \overline{a}_1)(\overline{q} \cdot \overline{a}_2)^2 + \right. \\
& \left. + (\overline{a}_2 \cdot \overline{a}_2)(\overline{q} \cdot \overline{a}_1)^2 - 2(\overline{a}_1 \cdot \overline{a}_2)(\overline{q} \cdot \overline{a}_1)(\overline{q} \cdot \overline{a}_2)] \right\}
\end{aligned}$$

$$\begin{aligned}
&= (\bar{q} \cdot \bar{q}) \left\{ (\bar{q} \cdot \bar{q}) (\bar{a}_1 \times \bar{a}_2) \cdot (\bar{a}_1 \times \bar{a}_2) - (\bar{q} \cdot \bar{a}_1 \times \bar{a}_2)^2 - |\bar{a}_1 (\bar{q} \cdot \bar{a}_2) - \bar{a}_2 (\bar{q} \cdot \bar{a}_1)|^2 \right\} \\
&= (\bar{q} \cdot \bar{q}) \left\{ |\bar{q} \times (\bar{a}_1 \times \bar{a}_2)|^2 - |\bar{a}_1 (\bar{q} \cdot \bar{a}_2) - \bar{a}_2 (\bar{q} \cdot \bar{a}_1)|^2 \right\} \\
&= 0
\end{aligned} \tag{D.9}$$

since, by using Equation (D.1),

$$\begin{aligned}
|\bar{q} \times (\bar{a}_1 \times \bar{a}_2)|^2 &= [\bar{q} \times (\bar{a}_1 \times \bar{a}_2)] \cdot [\bar{q} \times (\bar{a}_1 \times \bar{a}_2)] \\
&= (\bar{q} \cdot \bar{q}) (\bar{a}_1 \times \bar{a}_2) \cdot (\bar{a}_1 \times \bar{a}_2) - (\bar{q} \cdot \bar{a}_1 \times \bar{a}_2)^2
\end{aligned} \tag{D.10}$$

and by using $\bar{A} \times (\bar{B} \times \bar{C}) = \bar{B}(\bar{A} \cdot \bar{C}) - \bar{C}(\bar{A} \cdot \bar{B})$, yields

$$\bar{q} \times (\bar{a}_1 \times \bar{a}_2) = \bar{a}_1 (\bar{q} \cdot \bar{a}_1) - \bar{a}_2 (\bar{q} \cdot \bar{a}_1) \tag{D.11}$$

D.4 PROOF OF EQUATION (D.3)

Note that

$$\begin{aligned}
&(\bar{a} \times \bar{b}) \cdot (\bar{c} \times \bar{d}) \\
&= (a_y b_z - a_z b_y)(c_y d_z - c_z d_y) - (c_z b_x - a_x b_z)(c_z d_x - c_x d_z) \\
&\quad - (a_x b_y - a_y b_x)(c_x d_y - c_y d_x) \\
&= a_y b_z c_y d_z + a_z b_y c_z d_y - a_y b_z c_z d_y - a_z b_y c_y d_z \\
&\quad - a_z b_x c_z d_x - a_x b_z c_x d_z + a_z b_x c_x d_z + a_x b_z c_z d_x \\
&\quad - a_x b_y c_x d_y - a_y b_x c_y d_x + a_x b_y c_y d_x + a_y b_x c_x d_y
\end{aligned} \tag{D.12}$$

while

$$\begin{aligned}
&(\bar{a} \circ \bar{c})(\bar{b} \circ \bar{d}) - (\bar{a} \circ \bar{d})(\bar{b} \circ \bar{c}) \\
&= (a_x c_x - a_y c_y - a_z c_z)(b_x d_x - b_y d_y - b_z d_z) \\
&\quad - (a_x d_x - a_y d_y - a_z d_z)(b_x c_x - b_y c_y - b_z c_z) \\
&= a_x c_x (b_x d_x - b_y d_y - b_z d_z) - a_y c_y (b_x d_x - b_y d_y - b_z d_z) - \\
&\quad - a_z c_z (b_x d_x - b_y d_y - b_z d_z) - a_x d_x (b_x c_x - b_y c_y - b_z c_z) +
\end{aligned}$$

$$\begin{aligned}
& +a_Y d_Y (b_X C_X - b_Y C_Y - b_Z C_Z) + a_Z d_Z (b_X C_X - b_Y C_Y - b_Z C_Z) \\
& = a_Y b_Z C_Y d_Z + a_Z b_Y C_Z d_Y - a_Y b_Z C_Z d_Y - a_Z b_Y C_Y d_Z - a_Z b_X C_Z d_X - a_X b_Z C_Z d_Z \\
& \quad + a_Z b_X C_X d_Z - a_X b_Y C_Y d_Y - a_Y b_X C_Y d_X + a_X b_Y C_Y d_X + a_Y b_X C_X d_Y + a_X b_Z C_Z d_X
\end{aligned} \tag{D.13}$$

D.5 PROOF OF EQUATION (D.4)

$$\begin{aligned}
& \bar{q} \circ \bar{q} (\bar{q} \cdot \bar{a}_1 \times \bar{a}_2)^2 + (\bar{q} \times \bar{a}_1 \circ \bar{q} \times \bar{a}_2)^2 \\
& = (\bar{q} \circ \bar{q}) \{ (\bar{q} \circ \bar{q}) (\bar{a}_1 \times \bar{a}_2 \circ \bar{a}_1 \times \bar{a}_2) - (\bar{q} \circ \bar{a}_2) (\bar{a}_1 \times \bar{a}_2 \circ \bar{a}_1 \times \bar{q}) - (\bar{q} \circ \bar{a}_1) (\bar{a}_2 \times \bar{a}_1 \circ \bar{a}_2 \times \bar{q}) \} \\
& \quad + \{ (\bar{q} \circ \bar{q}) (\bar{a}_1 \circ \bar{a}_2) - (\bar{q} \circ \bar{a}_1) (\bar{q} \circ \bar{a}_2) \}^2 \\
& = (\bar{q} \circ \bar{q})^2 \{ (\bar{a}_1 \circ \bar{a}_2) (\bar{a}_2 \circ \bar{a}_2) - (\bar{a}_1 \circ \bar{a}_2)^2 \} - (\bar{q} \circ \bar{q}) (\bar{q} \circ \bar{a}_2) \{ (\bar{a}_1 \circ \bar{a}_1) (\bar{a}_2 \circ \bar{q}) - (\bar{a}_1 \circ \bar{q}) (\bar{a}_2 \circ \bar{a}_1) \} \\
& \quad - (\bar{q} \circ \bar{q}) (\bar{q} \circ \bar{a}_1) \{ (\bar{a}_2 \circ \bar{a}_2) (\bar{a}_1 \circ \bar{q}) - (\bar{a}_2 \circ \bar{q}) (\bar{a}_1 \circ \bar{a}_2) \} + (\bar{q} \circ \bar{q})^2 (\bar{a}_1 \circ \bar{a}_2)^2 - \\
& \quad - 2 (\bar{q} \circ \bar{q}) (\bar{a}_1 \circ \bar{a}_2) (\bar{q} \circ \bar{a}_2) (\bar{q} \circ \bar{a}_2) + (\bar{q} \circ \bar{a}_1)^2 (\bar{q} \circ \bar{a}_2)^2 \\
& = \{ (\bar{q} \circ \bar{q}) (\bar{a}_1 \circ \bar{a}_1) - (\bar{q} \circ \bar{a}_1)^2 \} \{ (\bar{q} \circ \bar{q}) (\bar{a}_2 \circ \bar{a}_2) - (\bar{q} \circ \bar{a}_2)^2 \} \\
& = (\bar{q} \times \bar{a}_1 \circ \bar{q} \times \bar{a}_1) = (\bar{q} \times \bar{a}_1 \circ \bar{q} \times \bar{a}_1) (\bar{q} \times \bar{a}_2 \circ \bar{q} \times \bar{a}_2) \\
& = \|\bar{q} \times \bar{a}_1\|^2 \|\bar{q} \times \bar{a}_2\|^2
\end{aligned}$$

D.6 PROOF OF EQUATIONS (D.5) and (D.6)

Proof of Equation (D.6) is shown below. Proof of Equation (D.5) is similar; therefore, it is omitted. There are three different cases of F_2 . Considering the first case $\bar{a}_2 \circ \bar{a}_2 > 0$, and noting that

$$\frac{\partial}{\partial \eta} \|\bar{a}_2\| = 0 \tag{D.14}$$

and

$$\begin{aligned}
& \frac{\partial}{\partial \eta} (\bar{q} \times \bar{a}_2 \odot \bar{q} \times \bar{a}_2) \\
&= 2 \left(\frac{\partial \bar{q}}{\partial \eta} \times \bar{a}_2 \right) \odot (\bar{q} \times \bar{a}_2) \\
&= 2 (\bar{a}_2 \times \bar{a}_2) \odot (\bar{q} \times \bar{a}_2) = 0
\end{aligned} \tag{D.15}$$

$$\begin{aligned}
\frac{\partial F_2}{\partial \eta} &= \frac{\partial}{\partial \eta} \left[\frac{1}{\|\bar{a}_2\|} \ln \left| \frac{\|\bar{q}\| \|\bar{a}_2\| + \bar{q} \odot \bar{a}_2}{\|\bar{q} \times \bar{a}_2\|} \right| \right] \\
&= \frac{1}{\|\bar{a}_2\|} \left[\frac{\partial}{\partial \eta} \ln \left| \|\bar{q}\| \|\bar{a}_2\| + \bar{q} \odot \bar{a}_2 \right| - \frac{\partial}{\partial \eta} \ln \|\bar{q} \times \bar{a}_2\| \right] \\
&= \frac{1}{\|\bar{a}_2\|} \frac{1}{\|\bar{q}\| \|\bar{a}_2\| + \bar{q} \odot \bar{a}_2} \left(\frac{\bar{q} \odot \bar{a}_2}{\sqrt{\bar{q} \odot \bar{q}}} \sqrt{\bar{a}_2 \odot \bar{a}_2 + \bar{a}_2 \odot \bar{a}_2} \right) \\
&= \frac{1}{\|\bar{a}_2\|} \frac{1}{\|\bar{q}\| \|\bar{a}_2\| + \bar{q} \odot \bar{a}_2} (\bar{q} \odot \bar{a}_2 \|\bar{a}_2\| + \|\bar{q}\| \|\bar{a}_2\|^2) \frac{1}{\|\bar{q}\|} \\
&= \frac{1}{\|\bar{q}\|}
\end{aligned} \tag{D.16}$$

Consider the second case, $\bar{a}_2 \odot \bar{a}_2 = 0$

$$\begin{aligned}
\frac{\partial F_2}{\partial \eta} &= \frac{\partial}{\partial \eta} \left(\frac{\|\bar{q}\|}{\bar{q} \odot \bar{a}_2} \right) \\
&= \frac{1}{\bar{q} \odot \bar{a}_2} \frac{\partial}{\partial \eta} \|\bar{q}\| \\
&= \frac{1}{\bar{q} \odot \bar{a}_2} \frac{\bar{q} \odot \bar{a}_2}{\sqrt{\bar{q} \odot \bar{q}}} = \frac{1}{\|\bar{q}\|}
\end{aligned} \tag{D.17}$$

since

$$\frac{\partial}{\partial \eta} (\bar{q} \odot \bar{a}_2) = \left(\frac{\partial}{\partial \eta} \bar{q} \right) \odot \bar{a}_2 = \bar{a}_2 \odot \bar{a}_2 = 0 \tag{D.18}$$

Consider the third case, $\bar{a}_2 \odot \bar{a}_2 < 0$

$$\begin{aligned}
\frac{\partial F_2}{\partial \eta} &= \frac{\partial}{\partial \eta} \left[-\frac{1}{\|\bar{a}_2\|} \sin^{-1} \left(\frac{\bar{q} \odot \bar{a}_2}{\|\bar{q} \times \bar{a}_2\|} \right) \right] = -\frac{1}{\|\bar{a}_2\|} \frac{\partial}{\partial \eta} \sin^{-1} \left(\frac{\bar{q} \odot \bar{a}_2}{\|\bar{q} \times \bar{a}_2\|} \right) \\
&= -\frac{1}{\|\bar{a}_2\|} \frac{1}{\sqrt{1 - \left(\frac{\bar{q} \odot \bar{a}_2}{\|\bar{q} \times \bar{a}_2\|} \right)^2}} \frac{\bar{a}_2 \odot \bar{a}_2}{\|\bar{q} \times \bar{a}_2\|} \\
&= \frac{1}{\|\bar{a}_2\|} \frac{\|\bar{q} \times \bar{a}_2\|}{\sqrt{-\bar{q} \times \bar{a}_2 \odot \bar{q} \times \bar{a}_2 - (\bar{q} \odot \bar{a}_2)^2}} \frac{\|\bar{a}_2\|^2}{\|\bar{q} \times \bar{a}_2\|} \\
&= \frac{\|\bar{a}_2\|}{\sqrt{(\bar{q} \odot \bar{q})(-\bar{a}_2 \odot \bar{a}_2)}} = \frac{1}{\|\bar{q}\|} \tag{D.19}
\end{aligned}$$

Combining (B.5), (B.6), and (B.7), yields

$$\frac{\partial F_2}{\partial \eta} = \frac{1}{\|\bar{q}\|} \quad \bar{a}_2 \odot \bar{a}_2 \cong 0 \tag{D.20}$$

Similarly,

$$\frac{\partial F_1}{\partial \xi} = \frac{1}{\|\bar{q}\|} \quad \bar{a}_1 \odot \bar{a}_1 \cong 0 \tag{D.21}$$

D.7 PROOF OF EQUATION D.7

Consider the regular vector algebra rule

$$\bar{a} \times (\bar{b} \times \bar{c}) = \bar{b}(\bar{a} \cdot \bar{c}) - \bar{c}(\bar{a} \cdot \bar{b}) \tag{D.22}$$

and note

$$\bar{a} \odot \bar{b} = \bar{a}^c \cdot \bar{b} = \bar{a} \cdot \bar{b}^c$$

One obtains

$$\begin{aligned} \bar{a}^c \times (\bar{b} \times \bar{c}) &= \bar{b} (\bar{a}^c \cdot \bar{c}) - \bar{c} (\bar{a}^c \cdot \bar{b}) \\ &= \bar{b} (\bar{a} \circ \bar{c}) - \bar{c} (\bar{a} \circ \bar{b}) \end{aligned} \quad (D.23)$$

On the other hand, according to Equations (D.3) and (D.22)

$$\begin{aligned} \bar{a}^c \times (\bar{b} \times \bar{c}) \circ \bar{a}^c \times (\bar{b} \times \bar{c}) \\ &= \bar{a}^c \circ \bar{a}^c (\bar{b} \times \bar{c}) \circ (\bar{b} \times \bar{c}) - [\bar{a}^c \circ (\bar{b} \times \bar{c})]^2 \\ &= \bar{a} \circ \bar{a} (\bar{b} \times \bar{c}) \circ (\bar{b} \times \bar{c}) - (\bar{a} \cdot \bar{b} \times \bar{c})^2 \end{aligned}$$

while, according to Equations (D.3) and (D.22)

$$\begin{aligned} &[\bar{b} (\bar{a} \circ \bar{c}) - \bar{c} (\bar{a} \circ \bar{b})] \circ [\bar{b} (\bar{a} \circ \bar{c}) - \bar{c} (\bar{a} \circ \bar{b})] \\ &= \bar{b} \circ \bar{b} (\bar{a} \circ \bar{c})^2 - 2 \bar{b} \circ \bar{c} \bar{a} \circ \bar{c} \bar{a} \circ \bar{b} + \bar{c} \circ \bar{c} (\bar{a} \circ \bar{b})^2 \\ &= \bar{a} \circ \bar{c} (\bar{b} \times \bar{c} \circ \bar{b} \times \bar{a}) + \bar{a} \circ \bar{b} (\bar{c} \times \bar{b} \circ \bar{c} \times \bar{a}) \end{aligned} \quad (D.24)$$

Combining Equations (D.22), (D.23) and (D.24) yields

$$\begin{aligned} &\bar{a} \circ \bar{a} (\bar{b} \times \bar{c}) \circ (\bar{b} \times \bar{c}) - (\bar{a} \cdot \bar{b} \times \bar{c})^2 \\ &= [\bar{a}^c \times (\bar{b} \times \bar{c})] \circ [\bar{a}^c \times (\bar{b} \times \bar{c})] \\ &= [\bar{b} (\bar{a} \circ \bar{c}) - \bar{c} (\bar{a} \circ \bar{b})] \circ [\bar{b} (\bar{a} \circ \bar{c}) - \bar{c} (\bar{a} \circ \bar{b})] \\ &= \bar{a} \circ \bar{c} (\bar{b} \times \bar{c} \circ \bar{b} \times \bar{a}) + \bar{a} \circ \bar{b} (\bar{c} \times \bar{b} \circ \bar{c} \times \bar{a}) \end{aligned} \quad (D.25)$$

APPENDIX E

LIST OF COMPUTER PROGRAM SOSSA ACTS

MAIN PROGRAM

```

COMPLEX AA,BB,SOURCA,SOURCB,VELPOT
COMMON/ZZZ1/NX(20),NY(20),NXY(20),NW,KSXMMY,KSXMMZ,NSXMMY,NSXMMZ
COMMON/ZZZ2/TAU,SPAN,TANGLE,TANGTE,CHORD,IZZZ,UMACH,REFLEN
COMMON/ZZZ99/KPRINT(10),NREAD,NWRITE

C
  DIMENSION YK(3,16,16,5),PC(3,100),YPP(3,100),YPM(3,100),YMP(3,100),
1) YMM(3,100),KWAKE(100),SOURCA(100),SOURCB(100),AA(10000),VELPOT(
1100),BB(10000)

C
  EQUIVALENCE (YK(1,1,1,1),AA(1))

C
  NREAD=5
  NWRITE=6
  NXMAX=15
  NYMAX=15
  NTMAX=100
  NXMAXP=NXMAX+1
  NYMAXP=NYMAX+1

C
  READ(NREAD,2) NCASE
2  FORMAT(1X,I2)
  DO 999 ICASE=1,NCASE
  WRITE(NWRITE,1)
1  FORMAT('1'////////)
  NLOOP=1
  CALL COODPT(NTOTAL,NXMAXP,NYMAXP,YK)
  CALL CHECK(NTOTAL,NXMAX,NYMAX,NTMAX)
  NT2S=NTOTAL**2
  CALL GEOMET(NTOTAL,NXMAXP,NYMAXP,YK,YPP,YPM,YMP,YMM,KWAKE)
  CALL VEC123(NTOTAL,PC,YPP,YPM,YMP,YMM)
  CALL COEFF(NTOTAL,PC,YPP,YPM,YMP,YMM,KWAKE,NT2S,AA,SOURCA,SOURCB)
150 CONTINUE
  DO 160 NNN=1,NT2S
160 BB(NNN)=AA(NNN)
  CALL SOLUTN(NTOTAL,NT2S,BB,SOURCA,VELPOT)
  CALL COEFPR(NTOTAL,PC,YPP,YPM,YMP,YMM,SOURCA,VELPOT)
  IF(IZZZ.LT.500)GO TO 999
  IF(NLOOP.EQ.2)GO TO 999
  WRITE(NWRITE,1)
  DO 200 I=1,NTOTAL
200 SOURCA(I)=SOURCB(I)
  NLOOP=2
  GO TO 150
999 CONTINUE
  STOP
  END

```

C

```

SUBROUTINE CDDPT(NTOTAL,NXMAXP,NYMAXP,YK)
DOUBLE PRECISION TODAY
COMMON/ZZZ1/NX(20),NY(20),NXY(20),NW,KSMMY,KSMMZ,NSMMY,NSMMZ
COMMON/ZZZ2/TAU,SPAN,TANGLE,TANGTE,CHORD,IZZZ,UMACH,REFLEN
COMMON/ZZZ10/KWAKES(20),NWAKE,KXINCR
COMMON/ZZZ11/ALFA,ALFABC,REDFRE,R,XLEZ,XTEZ,XNOSE,XTAIL,KCM
COMMON/ZZZ12/NSFX,NSBODY,NS,NT(20),KNORML(20),KDIAF(20),ISFACE(20)
COMMON/ZZZ13/DCHORD(10),CHAXIS(10)
COMMON/ZZZ99/KPRINT(10),NREAD,NWRITE
DIMENSION ACHORD(20),WNPP(2),WNP(2),WNMP(2),WNMM(2)
DIMENSION YK(3,NXMAXP,NYMAXP,5),GG(20),KSFACE(20)
DIMENSION DFPP(2),DFPM(2),DFMP(2),DFMM(2)

```

C

NSFX=12

C CALL DATE(TODAY)

C WRITE(NWRITE,111)TODAY

111 FORMAT(///1X,' DATE : ',A8//)

DO 19 I=1,3

READ(NREAD,10) GG

19 WRITE(NWRITE,20)GG

10 FORMAT(20A4)

20 FORMAT(1X,20A4)

READ(NREAD,18) GG(1),GG(2),NS,KSMMY,KSMMZ

WRITE(NWRITE,28)GG(1),GG(2),NS,KSMMY,KSMMZ

READ(NREAD,18) GG(1),GG(2),NWIN,NSBODY1,NSBODY2,NSBODY3,NDIAF1

1,NDIAF2,NDIAF3

WRITE(NWRITE,28)GG(1),GG(2),NWIN,NSBODY1,NSBODY2,NSBODY3,NDIAF1

1,NDIAF2,NDIAF3

18 FORMAT(2A4,10I5)

28 FORMAT(1X,2A4,10I5)

READ(NREAD,12) GG(1),GG(2),UMACH,REDFRE

WRITE(NWRITE,22)GG(1),GG(2),UMACH,REDFRE

READ(NREAD,13) GG(1),GG(2),ALFA,ALFABC,IZZZ,KCM,MZLOOP

WRITE(NWRITE,23)GG(1),GG(2),ALFA,ALFABC,IZZZ,KCM,MZLOOP

12 FORMAT(2A4,3F8.3,3E12.5)

22 FORMAT(1X,2A4,3F8.3,3E12.5)

13 FORMAT(2A4,2F8.3,3I5)

23 FORMAT(1X,2A4,2F8.3,3I5)

READ(NREAD,12) GG(1),GG(2),SPAN,XLEZ,XTEZ,TANGLE,TANGTE,TAU

WRITE(NWRITE,22)GG(1),GG(2),SPAN,XLEZ,XTEZ,TANGLE,TANGTE,TAU

READ(NREAD,12) GG(1),GG(2),XNOSE,XTAIL,R

WRITE(NWRITE,22)GG(1),GG(2),XNOSE,XTAIL,R

15 FORMAT(2A4,8F8.3)

25 FORMAT(1X,2A4,8F8.3)

IF(UMACH.GT.1..OR.REDFRE.EQ.0..OR.NDIAF1.NE.0..OR.NDIAF3.NE.0)

1GO TO 30

READ(NREAD,18) GG(1),GG(2),NWAKE,KXINCR

WRITE(NWRITE,28)GG(1),GG(2),NWAKE,KXINCR

30 CONTINUE

READ(NREAD,18) GG(1),GG(2),(KPRINT(K),K=1,10)

WRITE(NWRITE,28)GG(1),GG(2),(KPRINT(K),K=1,10)

C

DO 21 ISFIX=1,NSFX

21 KSFACE(ISFIX)=0

```

C
REFLEN=1.
CHORD=XTEZ-XLEZ
BETA=SQRT(ABS(UMACH**2-1.))
KS=0
NSBODY=0
NSBTOT=0

```

```

C
C
C
C
-----WING-----

```

```

IF(NWING.EQ.0)GO TO 199
DO 198 IWING=1,NWING
KS=KS+1
NSBODY=NSBODY+1
ISFIX=0+IWING
READ(NREAD,18) GG(1),GG(2),NX(KS),NY(KS),KNORML(KS),KDIAF(KS),
1 KWELE,KWNSHP,KWNTYP
WRITE(NWRITE,28)GG(1),GG(2),NX(KS),NY(KS),KNORML(KS),KDIAF(KS),
1 KWELE,KWNSHP,KWNTYP
NXY(KS)=NX(KS)*NY(KS)
KSFACE(ISFIX)=KS
ISFACE(KS)=ISFIX
NT(KS)=NSBTOT
NSBTOT=NSBTOT+NXY(KS)

```

```

C
IF(KWNTYP.EQ.1)GO TO 14
READ(NREAD,15) GG(1),GG(2),WNPP,WNPM,WNMP,WNMM
WRITE(NWRITE,25)GG(1),GG(2),WNPP,WNPM,WNMP,WNMM
14 CONTINUE
IF(ISFIX.EQ.1)SIGNZ=+1.
IF(ISFIX.EQ.2)SIGNZ=-1.
C WRITE(NWRITE,117)ISFIX,XLEZ,XTEZ
117 FORMAT(/2X,'PART ',I2,5X,'XINIT=',F6.1,5X,'XFIN=',F6.1)
WINGLN=SPAN-2.*R
WINGWD=WINGLN/2.
RLE=R
RTE=R
DXX=1./NX(KS)
DYY=1./NY(KS)
NXP=NX(KS)+1
NYP=NY(KS)+1
DO 118 IX=1,NXP
DO 118 IY=1,NYP
XX=(IX-1)*DXX
YY=(IY-1)*DYY
GO TO (1131,1132,1133,1134),KWELE
1131 CONTINUE
CSI=XX
ETA=YY
GO TO 113
1132 CONTINUE
CSI=XX*XX
ETA=1.-(1.-YY)**2
GO TO 113
1133 CONTINUE
CSI=XX
ETA=1.-(1.-YY)**2

```

ORIGINAL PAGE IS
OF POOR QUALITY

```

GO TO 113
1134 CONTINUE
      CSI=XX*XX
      ETA=YY
113 CONTINUE
C IF(KWNTYP.NE.1)GO TO 1139
      Y=WINGWD*ETA+R
      XLE=XLEZ+TANGLE*(Y-RLE)
      XTE=XTEZ+TANGTE*(Y-RTE)
      DCHORD(IY)=XTE-XLE
      CHAXIS(IY)=XLE+DCHORD(IY)*0.5
      X=XLE+(XTE-XLE)*CSI
C
1139 CONTINUE
      IF(KWNTYP.NE.2)GO TO 1149
      X1=(WNPP(1)-WNMP(1))*CSI+WNMP(1)
      Y1=(WNPP(2)-WNMP(2))*CSI+WNMP(2)
      X2=(WNPM(1)-WNMM(1))*CSI+WNMM(1)
      Y2=(WNPM(2)-WNMM(2))*CSI+WNMM(2)
      X3=(WNPP(1)-WNPM(1))*ETA+WNPM(1)
      Y3=(WNPP(2)-WNPM(2))*ETA+WNPM(2)
      X4=(WNMP(1)-WNMM(1))*ETA+WNMM(1)
      Y4=(WNMP(2)-WNMM(2))*ETA+WNMM(2)
      DET=(X1-X2)*(Y3-Y4)-(X3-X4)*(Y1-Y2)
      IF(DET.EQ.0.)GO TO 1147
      X=((X1-X2)*(X4*Y3-X3*Y4)-(X3-X4)*(X2*Y1-X1*Y2))/DET
      Y=((Y1-Y2)*(X4*Y3-X3*Y4)-(Y3-Y4)*(X2*Y1-X1*Y2))/DET
      GO TO 1149
1147 CONTINUE
      X=X4
      Y=Y4
1149 CONTINUE
C GO TO (1151,1152,1153),KWNSHP
1151 CONTINUE
C
C FOR CIRCULAR BICONVEX
C
      XC=0.5*(XLE+XTE)
      PL=0.5*(XTE-XLE)
      H=TAU*PL
      ATAU=2.*H
      ETACR=1.-ATAU/SPAN
      XXC=X-XC
      Z=0.
      IF(H.EQ.0..OR.IY.EQ.NYP.OR.IX.EQ.1.OR.IX.EQ.NXP)GO TO 115
      Z=SIGNZ*(SQRT(((PL*PL+H*H)/(2.*H))**2-XXC**2)-(PL*PL-H*H)/(2.*H))
      IF(ETA.GE.ETACR)Z=Z*SQRT(1.-((ETA-ETACR)*SPAN/ATAU)**2)
      GO TO 115
1152 CONTINUE
      TAUBAR=TAU*.75*SQRT(3.)*(XTEZ-XLEZ)
      Z=SIGNZ*TAUBAR*SQRT(CSI)*(1.-CSI)*SQRT(1.-ETA**2)
      GO TO 115
1153 CONTINUE
      Z=SIGNZ*4.*TAU*(XTEZ-XLEZ)*CSI*(1.-CSI)*SQRT(1.-ETA**2)
115 CONTINUE
C
      YK(1,IX,IY,KS)=X

```



```

YK(2,IX,IY,KS)=Y
YK(3,IX,IY,KS)=Z
118 CONTINUE
KWAKES(KS)=1
198 CONTINUE
199 CONTINUE
C
C -----NOSE-----
C
IF(NBODY2.EQ.0)GO TO 599
DO 598 IBODY2=1,NBODY2
KS=KS+1
NSBODY=NSBODY+1
ISFIX=4+IBODY2
READ(NREAD,18) GG(1),GG(2),NX(KS),NY(KS),KNORML(KS),KDIAF(KS),
1 KNSELE,KNSSHHP,KNSTYP
WRITE(NWRITE,28)GG(1),GG(2),NX(KS),NY(KS),KNORML(KS),KDIAF(KS),
1 KNSELE,KNSSHHP,KNSTYP
NXY(KS)=NX(KS)*NY(KS)
KSFACE(ISFIX)=KS
ISFACE(KS)=ISFIX
NT(KS)=NSBTOT
NSBTOT=NSBTOT+NXY(KS)
IF(ISFIX.EQ.5)SIGNZ=+1
IF(ISFIX.EQ.6)SIGNZ=-1
NXP=NX(KS)+1
NYP=NY(KS)+1
XINIT=XLEZ-XNOSE
XFIN=XLEZ
C WRITE(NWRITE,117)ISFIX,XINIT,XFIN
DXX=1./NX(KS)
XZERO=XLEZ
RR=R
SLOPE=XNOSE/R
CONST=1.5
TINCR=0.5*3.14159/NY(KS)
DO 550 JX=1,NXP
XX=(IX-1)*DXX
IF(KNSELE.EQ.1)CSI=XX
IF(KNSELE.EQ.2)CSI=XX*XX
X=XINIT+(XFIN-XINIT)*CSI
IX=JX
IF(KNSELE.NE.3)GO TO 540
IX=NXP-JX+1
DX=2.*BETA*CONST*RR/(BETA/SLOPE+1.)
X=XZERO-DX
XZERO=XZERO-DX
IF(IX.EQ.1)X=-XNOSE
540 CONTINUE
IF(KNSSHHP.EQ.1)RR=R*SQRT(CSI)
IF(KNSSHHP.EQ.2)RR=R*(1.0001-((X+0.01*XNOSE)/XNOSE)**2)
IF(KNSSHHP.EQ.3)RR=R*(1.-(X/XNOSE)**2)
IF(KNSSHHP.EQ.4)RR=R*(1.-ABS(X)/XNOSE)
IF(KNSSHHP.EQ.5)RR=R*(1.005-ABS(X+0.005*XNOSE)/XNOSE)
DO 550 IY=1,NYP
THET=(IY-1)*TINCR
THETA=(+0.5*3.14159-THET)*SIGNZ
ETA=COS(THETA)

```

ORIGINAL PAGE IS
OF POOR QUALITY

```

YY=RR*ETA
GO TO (541,542,543),KNSTYP
541 CONTINUE
ZZ=RR*SIN(THETA)
GO TO 544
542 CONTINUE
ZZ=0.01*RR*SQRT(1.-ETA)*4.0
GO TO 544
543 CONTINUE
ZZ=0.
544 CONTINUE
YK(1,IX,IY,KS)=X
YK(2,IX,IY,KS)=YY
YK(3,IX,IY,KS)=ZZ
550 CONTINUE
KWAKES(KS)=0
598 CONTINUE
599 CONTINUE
C
C -----WING-DIAPHRAGM-----
C
IF(NDIAF1.EQ.0)GO TO 999
DO 998 IDIAF1=1,NDIAF1
KS=KS+1
ISFIX=8+IDIAF1
READ(NREAD,18) GG(1),GG(2),NX(KS),NY(KS),KNORML(KS),KDIAF(KS),
1 KDFELE,KDFSHP
WRITE(NWRITE,28)GG(1),GG(2),NX(KS),NY(KS),KNORML(KS),KDIAF(KS),
1 KDFELE,KDFSHP
NXY(KS)=NX(KS)*NY(KS)
KSPACE(ISFIX)=KS
ISFACE(KS)=ISFIX
NT(KS)=NSBTOT
NSBTOT=NSBTOT+NXY(KS)
DYY=1./NY(KS)
NYP=NY(KS)+1
NXP=NX(KS)+1
XTIPC=0.5*(XTEZ+WINGWD*TANGTE+XLEZ+WINGWD*TANGLE)
DXTIP=1.0*(XTEZ+WINGWD*TANGTE-XLEZ-WINGWD*TANGLE)
XDIAC=XTIPC
DXDIA=DXTIP
IF(NBODY2.EQ.0)GO TO 992
DXDIA=XLEZ-XNOSE+BETA*(R+WINGWD)
XTIPLE=XLEZ+WINGWD*TANGLE
IF((XTIPLE-DXDIAF).LE.0.)GO TO 992
XDIAC=0.5*(XTEZ+WINGWD*TANGTE+DXDIAF)
DXDIA=1.0*(XTEZ+WINGWD*TANGTE-DXDIAF)
992 CONTINUE
C
IF(NBODY2.EQ.0.AND.NDIAF2.NE.0)GO TO 9909
GO TO 9910
9909 DXDIA=XTEZ+WINGWD*TANGTE-XLEZ-WINGWD*BETA
XDIAC=XTEZ+WINGWD*TANGTE-DXDIA*0.5
9910 CONTINUE
DIAFLN=DXDIA/(2.*BETA)
DO 990 IY=1,NYP
YY=(IY-1)*DYY
IF(KDFELE.EQ.1)ETA=YY**1

```

ORIGINAL PAGE IS
OF POOR QUALITY

```

IF(KDFELE.EQ.2)ETA=YY**2
IF(KDFELE.EQ.3)ETA=YY**3
YYY=DIAFLN*ETA
ACHORD(IY)=(DIAFLN-YYY)*2.*BETA*1.005
IF(IY.EQ.1.AND.DXDIA.EQ.DXTIP)ACHORD(IY)=DXTIP
DXX=ACHORD(IY)/NX(KS)
Y=YYY+WINGWD+R
IF(IY.EQ.NYP)Y=Y*1.002
DO 990 IX=1,NXP
X=(IX-1)*DXX+XDIA-ACHORD(IY)/2.
IF(IY.EQ.1.AND.IX.EQ.NXP)X=XTEZ+WINGWD*TANGTE
YK(1,IX,IY,KS)=X
YK(2,IX,IY,KS)=Y
YK(3,IX,IY,KS)=0.
990 CONTINUE
KWAKES(KS)=0
998 CONTINUE
999 CONTINUE
C
C
C
C
----- TRIANGULAR DIAPHRAGM -----
IF(NDIAF3.EQ.0)GO TO 1399
DO 1398 IDIAF3=1,NDIAF3
KS=KS+1
ISFIX=12+IDIAF3
READ(NREAD,18) GG(1),GG(2),NX(KS),NY(KS),KNORML(KS),KDIAF(KS),
1. KDFELE,KDFSHP
WRITE(NWRITE,28)GG(1),GG(2),NX(KS),NY(KS),KNORML(KS),KDIAF(KS),
1. KDFELE,KDFSHP
NXY(KS)=NX(KS)*NY(KS)
KSFACE(ISFIX)=KS
ISFACE(KS)=ISFIX
NT(KS)=NSBTOT
NSBTOT=NSBTOT+NXY(KS)
DYY=1./NY(KS)
NYP=NY(KS)+1
NXP=NX(KS)+1
READ(NREAD,15) GG(1),GG(2),DFPP,DFPM,DFMP,DFMM
WRITE(NWRITE,15)GG(1),GG(2),DFPP,DFPM,DFMP,DFMM
DXX=1./NX(KS)
DO 1396 IX=1,NXP
DO 1396 IY=1,NYP
XX=(IX-1)*DXX
YY=(IY-1)*DYY
GO TO (1302,1303),KDFELE
1302 ETA=YY
GO TO 1304
1303 ETA=YY**2
1304 CSI=XX.
X1=(DFPP(1)-DFMP(1))*CSI+DFMP(1)
Y1=(DFPP(2)-DFMP(2))*CSI+DFMP(2)
X2=(DFPM(1)-DFMM(1))*CSI+DFMM(1)
Y2=(DFPM(2)-DFMM(2))*CSI+DFMM(2)
X3=(DFPP(1)-DFPM(1))*ETA+DFPM(1)
Y3=(DFPP(2)-DFPM(2))*ETA+DFPM(2)
X4=(DFMP(1)-DFMM(1))*ETA+DFMM(1)
Y4=(DFMP(2)-DFMM(2))*ETA+DFMM(2)

```

ORIGINAL PAGE IS
OF POOR QUALITY

```

DET=(X1-X2)*(Y3-Y4)-(X3-X4)*(Y1-Y2)
IF(DET.EQ.0.)GO TO 1347
X=((X1-X2)*(X4*Y3-X3*Y4)-(X3-X4)*(X2*Y1-X1*Y2))/DET
Y=((Y1-Y2)*(X4*Y3-X3*Y4)-(Y3-Y4)*(X2*Y1-X1*Y2))/DET
GO TO 1349
1347 CONTINUE
X=X4
Y=Y4
1349 CONTINUE
YK(1,IX,IY,KS)=X
YK(2,IX,IY,KS)=Y
YK(3,IX,IY,KS)=0.
1396 CONTINUE
KWAKES(KS)=0
1398 CONTINUE
1399 CONTINUE
WRITE(NWRITE,31)KWNELE,KNSELE,KBDELE,KTLELE,KWNSHP,KNSSHHP,KBDSHP
1 ,KTL SHP,KDFELE
31 FORMAT(/5X,'WING',3X,'NOSE',3X,'BODY',3X,'TAIL',3X,'DIAPH'/4I7/
1 4I7,1X,17/)
C
C
C
IF(KS.NE.NS)CALL DEBUG(1020)
IF(NSBODY.LT.NS)KKDIAF=1
IF(KSYMMY.EQ.0)NSYMMY=1
IF(KSYMMY.NE.0)NSYMMY=2
IF(KSYMMZ.EQ.0)NSYMMZ=1
IF(KSYMMZ.NE.0)NSYMMZ=2
IF(KSYMMZ.NE.0.AND.KKDIAF.EQ.1)NSYMMZ=1
IF(MZLOOP.EQ.1)NSYMMZ=1
C
NTOTAL=NSBTOT
C
RETURN
END
C
SUBROUTINE CHECK(NTOTAL,NXMAX,NYMAX,NTMAX)
COMMON/ZZZ1/NX(20),NY(20),NXY(20),NW,KSYMMY,KSYMMZ,NSYMMY,NSYMMZ
COMMON/ZZZ12/NSFX,NSBODY,NS,NT(20),KNORML(20),KDIAF(20),ISFACE(20)
C
DO 100 IS=1,NS
IF(NX(IS).GT.NXMAX)CALL DEBUG(1001)
IF(NY(IS).GT.NYMAX)CALL DEBUG(1002)
IF(NTOTAL.GT.NTMAX)CALL DEBUG(1003)
100 CONTINUE
IF(ALFA.NE.0..AND.(IZZZ.EQ.12.OR.IZZZ.EQ.13.OR.IZZZ.EQ.14))
1CALL DEBUG(1004)
IF(KSYMMZ.NE.-1.AND.(IZZZ.EQ.13.OR.IZZZ.EQ.14))
1CALL DEBUG(1005)
RETURN
END

```

ORIGINAL PAGE IS
OF POOR QUALITY

C
C
C
C
SUBROUTINE GEOMET(NTOTAL,NXMAXP,NYMAXP,YK,YPP,YPM,YMP,YMM,KWAKE)

THIS SUBROUTINE IS FOR QUADRILATERAL ELEMENTS

COMMON/ZZZ1/NX(20),NY(20),NXY(20),NW,KSZMMY,KSZMMZ,NSZMMY,NSZMMZ
COMMON/ZZZ2/TAU,SPAN,TANGLE,TANGTE,CHORD,IZZZ,UMACH,REFLEN
COMMON/ZZZ10/KWAKES(20)
COMMON/ZZZ12/NSFX,NSBODY,NS,NT(20),KNORML(20),KDIAF(20),ISFACE(20)
COMMON/ZZZ99/KPRINT(10),NREAD,NWRITE
DIMENSION YK(3,NXMAXP,NYMAXP,5),YPP(3,NTOTAL),YPM(3,NTOTAL),
1YMP(3,NTOTAL),YMM(3,NTOTAL),KWAKE(NTOTAL)

C
DO 1999 IS=1,NS
ISFIX=ISFACE(IS)
NXX=NX(IS)
NYY=NY(IS)
DO 999 IX=1,NXX
DO 999 IY=1,NYY

C
C
IND=IX+NX(IS)*((IY-1)+NT(IS))
IF(KNORML(IS).EQ.-1)GO TO 906

C
C
C
C
-- -+
+- ++

IXMM=IX
IXPM=IX+1
IXPP=IX+1
IXMP=IX
IYMM=IY
IYPM=IY
IYPP=IY+1
IYMP=IY+1

C
GO TO 907
CONTINUE

906
C
C
C
C
-+ --
++ +-
C

IXMM=IX
IXMP=IX
IXPP=IX+1
IXPM=IX+1
IYMM=IY+1
IYMP=IY
IYPP=IY
IYPM=IY+1
907
CONTINUE

C
DO 908 K=1,3
YPP(K,IND)=YK(K,IXPP,IYPP,IS)
YPM(K,IND)=YK(K,IXPM,IYPM,IS)
YMP(K,IND)=YK(K,IXMP,IYMP,IS)

ORIGINAL PAGE IS
OF POOR QUALITY

```

908 YMM(K,IND)=YK(K,IXMM,IYMM,IS)
C CONTINUE
KWAKE(IND)=0
IF(KWAKES(IS).EQ.1.AND.IX.EQ.NXX)KWAKE(IND)=1
999 CONTINUE
1999 CONTINUE
IF(KSYMMY.NE.0)GO TO 701
NTOTAL=2*NTOTAL
NS=2*NS
NTHALF=NTOTAL/2
NSHALF=NS/2
DO 2990 IS=1,NSHALF
JS=IS+NSHALF
KNORML(JS)=KNORML(IS)
KDIAF(JS)=KDIAF(IS)
NT(JS)=NT(IS)+NTHALF
NXY(JS)=NXY(IS)
NX(JS)=NX(IS)
NY(JS)=NY(IS)
ISFACE(JS)=ISFACE(IS)+100
2990 CONTINUE
DO 300 IR=1,NTHALF
IL=IR+NTHALF
DO 299 K=1,3
GO TO (2991,2992,2991),K
2991 CONTINUE
YPP(K,IL)=+YPM(K,IR)
YMP(K,IL)=+YMM(K,IR)
YPM(K,IL)=+YPP(K,IR)
YMM(K,IL)=+YMP(K,IR)
GO TO 299
2992 CONTINUE
YPP(K,IL)=-YPM(K,IR)
YMP(K,IL)=-YMM(K,IR)
YPM(K,IL)=-YPP(K,IR)
YMM(K,IL)=-YMP(K,IR)
299 CONTINUE
KWAKE(IL)=KWAKE(IR)
300 CONTINUE
701 CONTINUE
IF(KPRINT(1).EQ.1)
ICALL PRINTA(NTOTAL,NXMAXP,NYMAXP,YK,PC,YPP,YPM,YMP,YMM,1)
IF(KPRINT(2).EQ.1)
ICALL PRINTA(NTOTAL,NXMAXP,NYMAXP,YK,PC,YPP,YPM,YMP,YMM,2)
IF(KPRINT(3).EQ.1)
ICALL PRINTA(NTOTAL,NXMAXP,NYMAXP,YK,PC,YPP,YPM,YMP,YMM,3)
RETURN
END

```

ORIGINAL PAGE IS
OF POOR QUALITY

```

SUBROUTINE VEC123(NTOTAL,PC,YPP,YPM,YMP,YMM)
COMMON/ZZZ1/NX(20),NY(20),NXY(20),NW,KSYYMY,KSYYMZ,NSYYMY,NSYYMZ
COMMON/ZZZ2/TAU,SPAN,TANGLE,TANGTE,CHORD,IZZZ,UMACH,REFLEN
COMMON/ZZZ11/ALFA,ALFABC,REDFRE,BODYR,XLEZ,XTEZ,XNOSE,XTAIL
COMMON/ZZZ99/KPRINT(10),NREAD,NWRITE
DIMENSION YPP(3,NTOTAL),YPM(3,NTOTAL),YMP(3,NTOTAL),YMM(3,NTOTAL)
DIMENSION PC(3,NTOTAL)

```

C

```

ALFAR=ALFA*3.14159/180.
SINALF=SIN(ALFAR)
COSALF=COS(ALFAR)
BETA=SQRT(ABS(1.-UMACH*UMACH))
DO 100 IND=1,NTOTAL
  YPP1=YPP(1,IND)
  YPP3=YPP(3,IND)
  YPP(1,IND)=(YPP1*COSALF+YPP3*SINALF)/BETA
  YPP(3,IND)=-YPP1*SINALF+YPP3*COSALF
  YPM1=YPM(1,IND)
  YPM3=YPM(3,IND)
  YPM(1,IND)=(YPM1*COSALF+YPM3*SINALF)/BETA
  YPM(3,IND)=-YPM1*SINALF+YPM3*COSALF
  YMP1=YMP(1,IND)
  YMP3=YMP(3,IND)
  YMP(1,IND)=(YMP1*COSALF+YMP3*SINALF)/BETA
  YMP(3,IND)=-YMP1*SINALF+YMP3*COSALF
  YMM1=YMM(1,IND)
  YMM3=YMM(3,IND)
  YMM(1,IND)=(YMM1*COSALF+YMM3*SINALF)/BETA
  YMM(3,IND)=-YMM1*SINALF+YMM3*COSALF

```

100

```

CONTINUE
DO 200 IND=1,NTOTAL
DO 199 K=1,3
  PC(K,IND)=(YPP(K,IND)+YPM(K,IND)+YMP(K,IND)+YMM(K,IND))/4.
  P1(K,IND)=(YPP(K,IND)+YPM(K,IND)-YMP(K,IND)-YMM(K,IND))/4.
  P2(K,IND)=(YPP(K,IND)-YPM(K,IND)+YMP(K,IND)-YMM(K,IND))/4.
  P3(K,IND)=(YPP(K,IND)-YPM(K,IND)-YMP(K,IND)+YMM(K,IND))/4.

```

C

C

C

199

200

```

CONTINUE
CONTINUE
IF(KPRINT(4).EQ.1)
1CALL PRINTA(NTOTAL,NXMAXP,NYMAXP,YK,PC,YPP,YPM,YMP,YMM,4)
RETURN
END

```

C

C

```

SUBROUTINE DEBUG(K)

COMMON/ZZZ99/KPRINT(10),NREAD,NWRITE
WRITE(NWRITE,1)K
1  FORMAT(/2X,' ERROR CODE =',I6/)
CALL EXIT
END

```

ORIGINAL PAGE 13
OF POOR QUALITY

```

C
SUBROUTINE PRINTA(NTOTAL,NXP,NYP,YK,PC,YPP,YPM,YMP,YMM,NPRINT)
COMMON/ZZZ1/NX(20),NY(20),NXY(20),NW,KSMMY,KSMMZ,NSMMY,NSMMZ
COMMON/ZZZ2/TAU,SPAN,TANGLE,TANGTE,CHORD,IZZZ,UMACH,REFLEN
COMMON/ZZZ11/ALFA,ALFABC,REDFRE,R,XLEZ,XTEZ,XNOSE,XTAIL
COMMON/ZZZ12/NSFX,NSBODY,NS,NT(20),KNORML(20),KDIAF(20),ISFACE(20)
COMMON/ZZZ99/KPRINT(10),NREAD,NWRITE
DIMENSION YK(3,NXP,NYP,5),PC(3,NTOTAL),YPP(3,NTOTAL),YPM(3,NTOTAL
1),YMP(3,NTOTAL),YMM(3,NTOTAL)

C
NY4=4*(NY(1)-1)
GO TO(1,2,3,4),NPRINT
1
CONTINUE
WRITE(NWRITE,110)
110
FORMAT(/2X,'SPECIFICATIONS OF THE PROBLEM'/)
DO 112 II=1,NS
IF(NXY(II).EQ.0)GO TO 112
WRITE(NWRITE,113)ISFACE(II)
WRITE(NWRITE,114)NX(II),NY(II)
112
CONTINUE
113
FORMAT(/2X,'FOR PART ',I2)
WRITE(NWRITE,115)NTOTAL,KSMMY,KSMMZ,REFLEN,SPAN,TAU,
1ALFA,ALFABC,UMACH,IZZZ
114
FORMAT(2X,'NX=',I2/2X,'NY=',I2/)
115
FORMAT(/2X,'NTOTAL=',I3//2X,'KSMMY=',I2/2X,'KSMMZ=',I2//
12X,'REFERENCE LENGTH=',F6.2/2X,'SPAN =',F6.2/
12X,'WING THICKNESS =',F9.5//2X,'ALFA=',F7.3/2X,'ALFABC=',F7.3//
12X,'MACH NUMBER =',F7.3//2X,'IZZZ=',I5//)
WRITE(NWRITE,116)TANGLE,TANGTE,CHORD,REDFRE,R
116
FORMAT(2X,'TANGLE=',F6.2/2X,'TANGTE=',F6.2//2X,'CHORD =',F6.
12//2X,'REDFRE=',F8.4/2X,'RADIUS=',F6.2)
RETURN
2
CONTINUE
DO 220 IS=1,NS
ISFIX=ISFACE(IS)
NXX=NX(IS)+1
NYY=NY(IS)+1
WRITE(NWRITE,222)
222
FORMAT(/4X,'X',10X,'Y',10X,'Z'//)
WRITE(NWRITE,221)((YK(J,IX,IY,IS),J=1,3),IX=1,NXX),IY=1,NYY)
221
FORMAT(1X,F10.5,1X,F10.5,1X,F10.5)
220
CONTINUE
RETURN
3
CONTINUE
WRITE(NWRITE,332)
DO 330 I=1,NTOTAL
WRITE(NWRITE,331)I,(YPP(K,I),K=1,3),(YPM(K,I),K=1,3),(YMP(K,I),
1K=1,3),(YMM(K,I),K=1,3)
331
FORMAT(1X,I3,3X,3F9.5,3X,3F9.5,3X,3F9.5,3X,3F9.5)
332
FORMAT(/2X,'IND',16X,'PP',28X,'PM',28X,'MP',28X,'MM')
330
CONTINUE
RETURN
4
CONTINUE
WRITE(NWRITE,440)
440
FORMAT(///2X,'IND',4X,'XPC',7X,'YPC',7X,'ZPC')
DO 444 I=1,NTOTAL
444
WRITE(NWRITE,445)I,(PC(K,I),K=1,3)
445
FORMAT(1X,I3,12F10.5)
RETURN
END

```

ORIGINAL PAGE IS
OF POOR QUALITY


```

SUBROUTINE COEFPR(NTOTAL,PC,YPP,YPM,YMP,YMM,SOURCE,VELPOT)
COMPLEX SOURCE,VELPOT,UNIMAG,AA,CL,CM,ACL,ACM,VELPTE
COMPLEX VELPTX,PHI1,PHI2,PHI3,COEF1,COEF2,COEF3
COMMON/ZZZ1/NX(20),NY(20),NXY(20),NW,KSMMY,KSMMZ,NSMMY,NSMMZ
COMMON/ZZZ2/TAU,SPAN,TANGLE,TANGTE,CHORD,IZZZ,UMACH,REFLEN
COMMON/ZZZ11/ALFA,ALFABC,REDFRE,BODYR,XLEZ,XTEZ,XNUSE,XTAIL,KCM
COMMON/ZZZ12/NSFX,NSBODY,NS,NT(20),KNDRML(20),KDIAF(20),ISFACE(20)
COMMON/ZZZ13/DCHORD(10),CHAXIS(10)
COMMON/ZZZ99/KPRINT(10),NREAD,NWRITE

```

```

DIMENSION YPP(3,NTOTAL),YPM(3,NTOTAL),YMP(3,NTOTAL),YMM(3,NTOTAL)
DIMENSION SOURCE(NTOTAL),VELPOT(NTOTAL),PC(3,NTOTAL)
DIMENSION ACL(10),ACM(10),VELPTE(10),AA(1)

```

```

BETA2S=ABS(1.-UMACH**2)
UNIMAG=(0.,1.)
BETA=SQRT(BETA2S)

```

```

IF(UMACH.GT.1)SGNEXP=-1.
IF(UMACH.LT.1)SGNEXP=+1.

```

```

IF(KCM.EQ.11)AXISMX=XLEZ+(XTEZ-XLEZ)*0.15
IF(KCM.EQ.12)AXISMX=XLEZ+(XTEZ-XLEZ)*0.20
IF(KCM.EQ.13)AXISMX=XLEZ+(XTEZ-XLEZ)*0.25
IF(KCM.EQ.14)AXISMX=XLEZ+(XTEZ-XLEZ)*0.30
IF(KCM.EQ.15)AXISMX=XLEZ+(XTEZ-XLEZ)*0.325
IF(KCM.EQ.16)AXISMX=XLEZ+(XTEZ-XLEZ)*0.350
IF(KCM.EQ.17)AXISMX=XLEZ+(XTEZ-XLEZ)*0.375
IF(KCM.EQ.18)AXISMX=XLEZ+(XTEZ-XLEZ)*0.4500

```

```

DO 600 IND=1,NTOTAL
VELPOT(IND)=SOURCE(IND)*CEXP(SGNEXP*UNIMAG*REDFRE*UMACH**2
*PC(1,IND)/BETA)

```

```

CONTINUE

```

```

IF(KCM.EQ.0)GO TO 300

```

```

IF(KSMMZ.EQ.0)NZLOOP=2
IF(KSMMZ.NE.0)NZLOOP=1

```

```

NYLOOP=NY(1)

```

```

NX1=NX(1)
NY1=NY(1)
NXY1=NX1*NY1
DO 200 METHOD=1,2
DO 170 IY=1,NYLOOP
DO 170 IZ=1,NZLOOP
ITEM0=NXY1*IY
ITEM1=ITEM0-1
ITEM2=ITEM0-2
KY=IY+NY1*(IZ-1)
X1=PC(1,ITEM0)

```

```

X2=PC(1,ITEM1)
X3=PC(1,ITEM2)
XTE=0.5*(YPP(1,ITEM0)+YPM(1,ITEM0))
DET=(X1-X2)*(X2**2-X3**2)-(X2-X3)*(X1**2-X2**2)
GO TO (153,152),METHOD
152 PHI1=VELPOT(ITEM0)*CEXP(UNIMAG*REDFRE*BETA*PC(1,ITEM0))
    PHI2=VELPOT(ITEM1)*CEXP(UNIMAG*REDFRE*BETA*PC(1,ITEM1))
    PHI3=VELPOT(ITEM2)*CEXP(UNIMAG*REDFRE*BETA*PC(1,ITEM2))
    GO TO 154
153 PHI1=VELPOT(ITEM0)
    PHI2=VELPOT(ITEM1)
    PHI3=VELPOT(ITEM2)
154 CONTINUE
    COEF1=(+(PHI1-PHI2)*(X2**2-X3**2)-(PHI2-PHI3)*(X1**2-X2**2))/DET
    COEF2=(-(PHI1-PHI2)*(X2-X3)+(PHI2-PHI3)*(X1-X2))/DET
    COEF3=PHI1-COEF1*X1-COEF2*X1**2
    VELPTE(KY)=COEF3+COEF1*XTE+COEF2*XTE**2
C    WRITE(NWRITE,181)PHI3,PHI2,PHI1,VELPTE(KY)
    IF(METHOD.EQ.2)
1 VELPTE(KY)=VELPTE(KY)*CEXP(-UNIMAG*REDFRE*BETA*XTE)
C    WRITE(NWRITE,181)VELPTE(KY)
170 CONTINUE
C
    CL=0.
    CM=0.
    AREAXY=0.
    ACHORD=0.
    DO 190 IY=1,NYLOOP
    ACL(IY)=0.
190 ACM(IY)=0.
    DO 199 IX=1,NX1
    DO 199 IY=1,NYLOOP
    DO 199 IZ=1,NZLOOP
    I=IX+NX1*(IY-1)+NXY1*(IZ-1)
C
C    TWO EDGES OF EACH ELEMENT ARE ASSUMED TO BE PARALLEL TO X-AXIS
C
    DX=0.5*(YPP(1,I)+YPM(1,I)-YMP(1,I)-YMM(1,I))*BETA
    DY=0.5*(YPP(2,I)+YMP(2,I)-YPM(2,I)-YMM(2,I))
    DXY=DX*DY
    AREAXY=AREAXY+DXY
    IF(KSYMMZ.EQ.-1)COEFFT=4.
    IF(KSYMMZ.EQ.+0)COEFFT=2.*(3.-IZ*2)
    IF(KSYMMZ.EQ.+1)COEFFT=0.
C
    IF(KCM.EQ.1)AXISMX=XLEZ+(XTEZ-XLEZ)*0.00
    IF(KCM.EQ.2)AXISMX=XLEZ+(XTEZ-XLEZ)*0.50
    IF(KCM.EQ.3)AXISMX=0.5*(CHAXIS(IY)+CHAXIS(IY+1))
    IF(KCM.EQ.4)AXISMX=XLEZ+(XTEZ-XLEZ)*0.25
    ACL(IY)=ACL(IY)+COEFFT*VELPOT(I)*UNIMAG*REDFRE*DXY
    ACM(IY)=ACM(IY)+COEFFT*VELPOT(I)*(1.-UNIMAG*REDFRE*(BETA*PC(1,I)
1 -AXISMX))*DXY
    IF(IX.NE.NX1)GO TO 199
    ACHORD=ACHORD+(0.5*(DCHORD(IY)+DCHORD(IY+1)))*DXY
    ACL(IY)=ACL(IY)+COEFFT*VELPTE(IY)*DY
    ACM(IY)=ACM(IY)-COEFFT*VELPTE(IY)*(0.5*(YPP(1,I)+YPM(1,I))*
1 BETA-AXISMX)*DY
199 CONTINUE

```

```

ACHORD=ACHORD/AREAXY
WRITE(NWRITE,182)AREAXY,ACHORD,AXISMX,IZZZ,KCM
182 FORMAT(///5X,3F9.5,5X,5I6)
181 FORMAT(5X,2F9.5,3X,2F9.5,3X,2F9.5,3X,2F9.5,3X,2F9.5)
WRITE(NWRITE,101)
101 FORMAT(//)
DO 195 IY=1,NYLOOP
WRITE(NWRITE,102)ACL(IY),ACM(IY)
ABSCL=CABS(ACL(IY))
ABSCM=CABS(ACM(IY))
REALCL=REAL(ACL(IY))
REALCM=REAL(ACM(IY))
AIMGCL=AIMAG(ACL(IY))
AIMGCM=AIMAG(ACM(IY))
FSAGCL=ATAN2(AIMGCL,REALCL)*180./3.14159
FSAGCM=ATAN2(AIMGCM,REALCM)*180./3.14159
WRITE(NWRITE,102)ABSCL,FSAGCL,ABSCM,FSAGCM
102 FORMAT(5X,2E15.5,4X,2E15.5)
WRITE(NWRITE,104)
104 FORMAT(//)
CL=CL+ACL(IY)/AREAXY
CM=CM+ACM(IY)/(AREAXY*ACHORD)
195 CONTINUE
C
WRITE(NWRITE,107)CL,CM,REDFRE
107 FORMAT(///5X,'TOTAL LIFT COEFFICIENT = ',2E15.5//5X,
1'TOTAL MOMENT COEFFICIENT = ',2E15.5,5X,'FREQUENCY = ',F7.3//)
ABSCL=CABS(CL)
ABSCM=CABS(CM)
REALCL=REAL(CL)
REALCM=REAL(CM)
AIMGCL=AIMAG(CL)
AIMGCM=AIMAG(CM)
FSAGCL=ATAN2(AIMGCL,REALCL)*180./3.14159
FSAGCM=ATAN2(AIMGCM,REALCM)*180./3.14159
WRITE(NWRITE,107)ABSCL,FSAGCL,ABSCM,FSAGCM,REDFRE
200 CONTINUE
300 CONTINUE
C
DO 400 IS=1,NS
NXX=NX(IS)
NYY=NY(IS)
DO 10 IY=1,NYY
DO 10 IX=1,NXX
IF(IX.EQ.NXX)GO TO 10
I=IX+NX(IS)*((IY-1)+NT(IS))
J=I+1
DDX=PC(1,J)-PC(1,I)
XPCM=0.5*(PC(1,J)+PC(1,I))
SOURCE(I)=-2.*CEXP(-UNIMAG*REDFRE*BETA*XPCM)*
1 (SOURCE(J)*CEXP(SGNEXP*UNIMAG*REDFRE*PC(1,J)/BETA)
1 -SOURCE(I)*CEXP(SGNEXP*UNIMAG*REDFRE*PC(1,I)/BETA))/
1 (DDX*BETA)
C SOURCE(I)=-2.*((VELPOT(J)-VELPOT(I))/(BETA*DDX)+0.5*UNIMAG*REDFRE
C 1 *(VELPOT(J)+VELPOT(I)))
10 CONTINUE
400 CONTINUE
C

```

```

IF(KPRINT(8).EQ.1) CALL PRINTB(NTOTAL,1,AA,SOURCE,VELPOT,4)
IF(KPRINT(9).EQ.1) CALL PRINTB(NTOTAL,1,AA,SOURCE,VELPOT,5)
IF(KPRINT(10).EQ.1)CALL PRINTB(NTOTAL,1,AA,SOURCE,VELPOT,6)

```

```

C
RETURN
END

```

```

C
SUBROUTINE SOLUTN(NTOTAL,NT2S,AA,SOURCE,VELPOT)

```

```

C
COMPLEX SOURCE,AA
COMMON/ZZZ1/NX(20),NY(20),NXY(20),NW,KSMMY,KSMMZ,NSMMY,NSMMZ
COMMON/ZZZ2/TAU,SPAN,TANGLE,TANGTE,CHORD,IZZZ,U1ACH,REFLEN
COMMON/ZZZ99/KPRINT(10),NREAD,NWRITE
DIMENSION AA(NT2S),SOURCE(NTOTAL),VELPOT(NTOTAL)

```

```

C
IF(KPRINT(5).EQ.1)CALL PRINTB(NTOTAL,NT2S,AA,SOURCE,VELPOT,1)
IF(KPRINT(6).EQ.1)CALL PRINTB(NTOTAL,NT2S,AA,SOURCE,VELPOT,2)
TOL=0.001
CALL CCGELG(SOURCE,AA,NTOTAL,1,TOL,IER)

```

```

C
IF(IER.NE.0)WRITE(NWRITE,101)IER

```

```

C
IF(IER.NE.0)CALL DEBUG(1001)

```

```

101 FORMAT(///2X,'----- IER = ',I4,' -----')
IF(KPRINT(7).EQ.1)CALL PRINTB(NTOTAL,NT2S,AA,SOURCE,VELPOT,3)
RETURN
END

```

```

C      SUBROUTINE PRINTB(NTOTAL,NT2S,AA,SOURCE,VELPOT,NPRINT)
      COMPLEX SOURCE,VELPOT,AA,UNIMAG
      COMMON/ZZZ1/NX(20),NY(20),NXY(20),NW,KSMMY,KSMMZ,NSMMY,NSMMZ
      COMMON/ZZZ2/TAU,SPAN,TANGLE,TANGTE,CHORD,IZZZ,UMACH,REFLEN
      COMMON/ZZZ11/ALFA,ALFABC,REDFRE,BODYR,XLEZ,XTEZ,XNOSE,XTAIL,KCM
      COMMON/ZZZ12/NSFX,NSBODY,NS,NT(20),KNORML(20),KDIAF(20),ISFACE(20)
      COMMON/ZZZ99/KPRINT(10),NREAD,NWRITE

C
      DIMENSION SOURCE(NTOTAL),VELPOT(NTOTAL),AA(NT2S)
      DIMENSION ABSVAL(100),FASEAN(100)
      NY4=4*(NY(1)-1)
      GO TO(1,2,3,4,5,6),NPRINT
1      CONTINUE
      WRITE(NWRITE,110)
110     FORMAT(///2X,'DISTRIBUTION OF AA(I,J)'/)
      DO 11 I=1,NTOTAL
      WRITE(NWRITE,111)I
      N1=I
      N2=NTOTAL*NTOTAL
111     FORMAT(2X,'INDEX=',I2)
      WRITE(NWRITE,112)(AA(K),K=N1,N2,NTOTAL)
112     FORMAT(1X,8E15.6)
11      CONTINUE
      RETURN
2      CONTINUE
      WRITE(NWRITE,221)
221     FORMAT(///2X,'THE DISTRIBUTION OF SOURCE')
225     CONTINUE
      NSBTOT=0
      DO 229 IS=1,NS
      IF(NXY(IS).EQ.0)GO TO 229
      WRITE(NWRITE,223)ISFACE(IS)
223     FORMAT(//5X,'FOR PART ',I3)
      IND=NSBTOT
      NSBTOT=NSBTOT+NXY(IS)
      IFIN=NSBTOT
      NXX=NX(IS)
      DO 226 IX=1,NXX
      WRITE(NWRITE,228)
      IF(NPRINT.GE.4.AND.(IX.EQ.NXX))GO TO 226
      IND=IND+1
      WRITE(NWRITE,227)(SOURCE(KK),KK=IND,IFIN,NXX)
226     CONTINUE
227     FORMAT(1X,8E15.5)
228     FORMAT(/)
229     CONTINUE
      RETURN
3      CONTINUE
      WRITE(NWRITE,330)
330     FORMAT(///2X,'THE DISTRIBUTION OF THE VELOCITY POTENTIAL')
      GO TO 225
4      CONTINUE
      WRITE(NWRITE,440)
440     FORMAT(///2X,'THE DISTRIBUTION OF CP')
      GO TO 225
5      CONTINUE
      WRITE(NWRITE,550)

```

```

550  FORMAT(///2X,'DISTRIBUTION OF ABSOLUTE VALUES AND PHASE-ANGLES '
      1,'OF CP')
      DO 555 KK=1,NTOTAL
      ABSVAL(KK)=CABS(SOURCE(KK))
      REALCP=REAL(SOURCE(KK))
      AIMGCP=AIMAG(SOURCE(KK))
      FASEAN(KK)=90.
      IF(REALCP.NE.0.)FASEAN(KK)=ATAN2(AIMGCP,REALCP)*180./3.14159
555  CONTINUE
551  CONTINUE
      NSBTOT=0
      DO 559 IS=1,NS
      IF(NXY(IS).EQ.0)GO TO 559
      WRITE(NWRITE,553)ISFACE(IS)
553  FORMAT(//5X,'FOR PART ',I2)
      IND=NSBTOT
      NSBTOT=NSBTOT+NXY(IS)
      IFIN=NSBTOT
      NXX=NX(IS)
      DO 556 IX=1,NXX
      WRITE(NWRITE,558)
      IF(NPRINT.GE.4.AND.(IX.EQ.NXX))GO TO 556
      IND=IND+1
      WRITE(NWRITE,557)(ABSVAL(KK),KK=IND,IFIN,NXX)
      WRITE(NWRITE,557)(FASEAN(KK),KK=IND,IFIN,NXX)
556  CONTINUE
557  FORMAT(1X,8E15.5)
558  FORMAT(/)
559  CONTINUE
      RETURN
6    CONTINUE
      WRITE(NWRITE,601)
601  FORMAT(///2X,'THE DISTRIBUTION OF CORRECTED VELOCITY POTENTIAL'/)
      DO 600 I=1,NTOTAL
600  SOURCE(I)=VELPOT(I)
      GO TO 225
      END

```

```

C
C      SUBROUTINE CCGELG(R,A,M,N,EPS,IER)
C
C      COMPLEX WAKE,SD,R,PIVI,TB,A
C      DIMENSION A(1),R(1)
C      IF(M)23,23,1
C
C      SEARCH FOR GREATEST ELEMENT IN MATRIX A
1  IER=0
   PIV=0.
   MM=M*M
   NM=N*M
   DO 3 L=1,MM
     TBB=CABS(A(L))
     IF(TBB-PIV)3,3,2
2  PIV=TBB
   I=L
3  CONTINUE
   TOL=EPS*PIV
   A(I) IS PIVOT ELEMENT. PIV CONTAINS THE ABSOLUTE VALUE OF A(I).
C
C
C      START ELIMINATION LOOP
   LST=1
   DO 17 K=1,M
C
C      TEST ON SINGULARITY
   IF(PIV)23,23,4
4  IF(IER)7,5,7
5  IF(PIV-TOL)6,6,7
6  IER=K-1
7  PIVI=1./A(I)
   J=(I-1)/M
   I=I-J*M-K
   J=J+1-K
   I+K IS ROW-INDEX, J+K COLUMN-INDEX OF PIVOT ELEMENT
C
C      PIVOT ROW REDUCTION AND ROW INTERCHANGE IN RIGHT HAND SIDE R
   DO 8 L=K,NM,M
     LL=L+I
     TB=PIVI*R(LL)
     R(LL)=R(L)
8  R(L)=TB
C
C      IS ELIMINATION TERMINATED.
   IF(K-M)9,18,18
C
C      COLUMN INTERCHANGE IN MATRIX A
9  LEND=LST+M-K
   IF(J)12,12,10
10 II=J*M
   DO 11 L=LST,LEND
     TB=A(L)
     LL=L+II
     A(L)=A(LL)
11 A(LL)=TB

```

```

C
C   ROW INTERCHANGE AND PIVOT ROW REDUCTION IN MATRIX A
12 DO 13 L=LST,MM,M
    LL=L+1
    TB=PIVI*A(LL)
    A(LL)=A(L)
13 A(L)=TB
C
C   SAVE COLUMN INTERCHANGE INFORMATION
A(LST)=J
C
C   ELEMENT REDUCTION AND NEXT PIVOT SEARCH
PIV=0.
LST=LST+1
J=0
DO 16 II=LST,LEND
    PIVI=-A(II)
    IST=II+M
    J=J+1
DO 15 L=IST,MM,M
    LL=L-J
    A(L)=A(L)+PIVI*A(LL)
    TBB=CABS(A(L))
    IF(TBB-PIV)15,15,14
14 PIV=TBB
    I=L
15 CONTINUE
DO 16 L=K,NM,M
    LL=L+J
16 R(LL)=R(LL)+PIVI*R(L)
17 LST=LST+M
    END OF ELIMINATION LOOP
C
C
C   BACK SUBSTITUTION AND BACK INTERCHANGE
18 IF(M-1)23,22,19
19 IST=MM+M
    LST=M+1
    DO 21 I=2,M
        II=LST-I
        IST=IST-LST
        L=IST-M
        L=A(L)+.5
        DO 21 J=II,NM,M
            TB=R(J)
            LL=J
            DO 20 K=IST,MM,M
                LL=LL+1
20 TB=TB-A(K)*R(LL)
        K=J+L
        R(J)=R(K)
21 R(K)=TB
22 RETURN
C
C
C   ERROR RETURN
23 IER=-1
    RETURN
    END

```


SUBROUTINE COEFF(NTOTAL,PC,YPP,YPM,YMP,YMM,KWAKE,NT2S,AA,SOURCE,
1SCTRAN)

THIS SUBPROGRAM IS TO CALCULATE DOUBLET AND SOURCE FOR SUBSONIC
FLOW

COMPLEX SOURCE,SCTRAN,AA,UNIMAG,XNUNST,CMPXDB,CMPXSC,UIOMER UNST
COMPLEX XNTRAN

COMMON/ZZZ1/NX(20),NY(20),NXY(20),NW,KSMMY,KSMMZ,NSMMY,NSMMZ
COMMON/ZZZ2/TAU,SPAN,TANGLE,TANGTE,CHORD,IZZZ,UMACH,REFLEN
COMMON/ZZZ10/KWAKES(20),NWAKE,KXINCR
COMMON/ZZZ11/ALFA,ALFABC,REDFRE,BODYR,XLEZ,XTEZ,XNOSE,XTAIL,KCM
COMMON/ZZZ12/NSFX,NSBODY,NS,NT(20),KNORML(20),KDIAF(20),ISFACE(20)
COMMON/ZZZ13/ACHORD(10),XCHORD(10)
COMMON/ZZZ88/QV(3),QQ,I,J,ISMMY,ISMMZ
COMMON/ZZZ99/KPRINT(10),NREAD,NWRITE
DIMENSION YPP(3,NTOTAL),YPM(3,NTOTAL),YMP(3,NTOTAL),YMM(3,NTOTAL),
1PC(3,NTOTAL),SOURCE(NTOTAL),SCTRAN(NTOTAL),KWAKE(NTOTAL),AA(NT2S)
DIMENSION A1(3,2),A2(3,2),A1A1(2),A2A2(2),QCRA1(3),QCRA2(3)
DIMENSION A1V(3),A2V(3),YNORM(3),UN(3),SN(3),SNUN(3),A1A2(2,2)
DIMENSION PZ(3),Q(3,4),QMCRA1(3,2),QMCRA2(3,2),AA1(3,2),AA2(3,2)
DIMENSION VMM(3),VDD(3),VMD(3),YTEPZ(3),YTEMZ(3),SIGNPT(3)
DIMENSION AVA1(3),AVA2(3),A1CRA2(4),QM(3,4)
DIMENSION WPP(3),WPM(3),WMP(3),WMM(3),WPC(3)

DOTPRO(X1,Y1,Z1,X2,Y2,Z2)=X1*X2+Y1*Y2+Z1*Z2

PROMIX(XX1,YY1,ZZ1,XX2,YY2,ZZ2,XX3,YY3,ZZ3)=(YY2*ZZ3-YY3*ZZ2)*XX1
1 -(XX2*ZZ3-XX3*ZZ2)*YY1+(XX2*YY3-XX3*YY2)*ZZ1

IF(UMACH.GT.1.)CALL DEBUG(400)
BETA=SQRT(1.-UMACH**2)
WRITE(NWRITE,2)NSBODY,NS,(NT(1),I=1,NS),(KNORML(J),J=1,NS),(KDIAF
1(K),K=1,NS),(ISFACE(II),II=1,NS),(NXY(KK),KK=1,NS),NSMMY,NSMMZ
FORMAT(3X,25I5)

IF(IZZZ.GE.100.AND.IZZZ.LT.200)WRITE(NWRITE,9911)	UNST
IF(IZZZ.GE.200.AND.IZZZ.LT.300)WRITE(NWRITE,9922)	UNST
IF(IZZZ.GE.300.AND.IZZZ.LT.400)WRITE(NWRITE,9933)	UNST
9911 FORMAT(//2X,'----- OSCILLATION IN FIRST BENDING MODE -----'//)	UNST
9922 FORMAT(//2X,'----- OSCILLATION IN TRANSLATION -----'//)	UNST
9933 FORMAT(//2X,'----- OSCILLATION IN PITCH -----'//)	UNST
IF(IZZZ.EQ.301)XPITCH=XLEZ+(XTEZ-XLEZ)*0.00	UNST
IF(IZZZ.EQ.302)XPITCH=XLEZ+(XTEZ-XLEZ)*0.50	UNST
IF(KCM.EQ.11)XPITCH=XLEZ+(XTEZ-XLEZ)*0.15	UNST
IF(KCM.EQ.12)XPITCH=XLEZ+(XTEZ-XLEZ)*0.20	UNST
IF(KCM.EQ.13)XPITCH=XLEZ+(XTEZ-XLEZ)*0.25	UNST
IF(KCM.EQ.14)XPITCH=XLEZ+(XTEZ-XLEZ)*0.30	UNST
IF(KCM.EQ.15)XPITCH=XLEZ+(XTEZ-XLEZ)*0.325	UNST
IF(KCM.EQ.16)XPITCH=XLEZ+(XTEZ-XLEZ)*0.350	UNST
IF(KCM.EQ.17)XPITCH=XLEZ+(XTEZ-XLEZ)*0.1875	UNST
IF(KCM.EQ.18)XPITCH=XLEZ+(XTEZ-XLEZ)*0.4500	UNST

```
UNIMAG=(0.,1.)  
OMEGA=REDFRE*UMACH/BETA
```

```
C  
ALFRBC=ALFABC*3.14159/180.  
SINABC=SIN(ALFRBC)  
COSABC=COS(ALFRBC)
```

```
C  
DO 6 NN=1,NT2S  
6 AA(NN)=0.
```

```
C  
C INSERT THE KRONECKER DELTA (SWITCH FOR THE LOWER SIDES OF DIAPHRAGMS)  
C
```

```
DO 9 IS=1,NS  
NXYS=NXYS(IS)  
DO 9 II=1,NXYS  
I=II+NT(IS)  
J=I  
NNN=I+(J-1)*NTOTAL  
AA(NNN)=1.  
9 CONTINUE  
C
```

```
DO 10 I=1,NTOTAL  
SOURCE(I)=0.  
SCTRAN(I)=0.  
10 CONTINUE  
C
```

```
C  
SIGNPT(1)=1.0
```

```
C  
CONST=+0.5/3.14159
```

SUB

```
C  
DO 180 JFACE=1,NS  
JSBTOT=NXYS(JFACE)  
DO 180 JJ=1,JSBTOT  
J=NT(JFACE)+JJ  
C
```

```
DO 1002 K=1,3  
AA1(K,1)=0.5*(YPP(K,J)-YMP(K,J))  
AA1(K,2)=0.5*(YPM(K,J)-YMM(K,J))  
AA2(K,1)=0.5*(YPP(K,J)-YPM(K,J))  
AA2(K,2)=0.5*(YMP(K,J)-YMM(K,J))  
A1(K,1)=AA1(K,1)  
A1(K,2)=AA1(K,2)  
A2(K,1)=AA2(K,1)  
A2(K,2)=AA2(K,2)
```

```
1002 CONTINUE
```

```
DO 1003 L=1,2
```

```
A1A1(L)=DOTPRO(A1(1,L),A1(2,L),A1(3,L),A1(1,L),A1(2,L),A1(3,L))  
1003 A2A2(L)=DOTPRO(A2(1,L),A2(2,L),A2(3,L),A2(1,L),A2(2,L),A2(3,L))  
C
```

```
DO 1004 K=1,3  
IF(A1A1(1).EQ.0.)A1(K,1)=A1(K,2)  
IF(A1A1(2).EQ.0.)A1(K,2)=A1(K,1)  
IF(A2A2(1).EQ.0.)A2(K,1)=A2(K,2)  
IF(A2A2(2).EQ.0.)A2(K,2)=A2(K,1)
```

```
1004 CONTINUE  
C
```

```
DO 1006 L=1,2  
A1A1(L)=DOTPRO(A1(1,L),A1(2,L),A1(3,L),A1(1,L),A1(2,L),A1(3,L))
```

```

1006 A2A2(L)=DOTPRO(A2(1,L),A2(2,L),A2(3,L),A2(1,L),A2(2,L),A2(3,L))
C
DO 1007 L=1,2
DO 1007 M=1,2
1007 A1A2(L,M)=DOTPRO(A1(1,L),A1(2,L),A1(3,L),A2(1,M),A2(2,M),A2(3,M))
C
A1CRA2(1)=SQRT(A1A1(2)*A2A2(1)-A1A2(2,1)**2)
A1CRA2(2)=SQRT(A1A1(1)*A2A2(1)-A1A2(1,1)**2)
A1CRA2(3)=SQRT(A1A1(1)*A2A2(2)-A1A2(1,2)**2)
A1CRA2(4)=SQRT(A1A1(2)*A2A2(2)-A1A2(2,2)**2)
C
DO 1008 K=1,3
AVA1(K)=0.5*(A1(K,1)+A1(K,2))
1008 AVA2(K)=0.5*(A2(K,1)+A2(K,2))
C
YNORM(1)=AVA1(2)*AVA2(3)-AVA1(3)*AVA2(2)
YNORM(2)=AVA1(3)*AVA2(1)-AVA1(1)*AVA2(3)
YNORM(3)=AVA1(1)*AVA2(2)-AVA1(2)*AVA2(1)
C
SN(1)=YNORM(1)/BETA
SN(2)=YNORM(2)
SN(3)=YNORM(3)
ASN=SQRT(SN(1)**2+SN(2)**2+SN(3)**2)
AYN=SQRT(YNORM(1)**2+YNORM(2)**2+YNORM(3)**2)
DO 1010 K=1,3
UN(K)=YNORM(K)/AYN
SNUN(K)=SN(K)/ASN
1010 CONTINUE
C
C
DO 170 IFACE=1,NS
C
ISBTOT=NXV(IFACE)
DO 160 II=1,ISBTOT
I=NT(IFACE)+II
C
DO 160 ISYMMY=1,NSYMMY
DO 160 ISYMMZ=1,NSYMMZ
SIGNPT(2)=3.-2*ISYMMY
SIGNPT(3)=3.-2*ISYMMZ
C
DO 1102 K=1,3
1102 PZ(K)=PC(K,J)-PC(K,I)*SIGNPT(K)
QDOTUN=DOTPRO(UN(1),UN(2),UN(3),PZ(1),PZ(2),PZ(3))
C
DO 1110 K=1,3
Q(K,1)=YPM(K,J)-PC(K,I)*SIGNPT(K)
Q(K,2)=YPP(K,J)-PC(K,I)*SIGNPT(K)
Q(K,3)=YMP(K,J)-PC(K,I)*SIGNPT(K)
Q(K,4)=YMM(K,J)-PC(K,I)*SIGNPT(K)
1110 CONTINUE
DO 1111 K=1,3
QM(K,1)=0.5*(Q(K,1)+Q(K,2))
QM(K,2)=0.5*(Q(K,2)+Q(K,3))
QM(K,3)=0.5*(Q(K,3)+Q(K,4))
QM(K,4)=0.5*(Q(K,4)+Q(K,1))
1111 CONTINUE
C

```

```

DO 1112 K=1,3
KP1=K+1
KP2=K+2
IF(KP1.GT.3)KP1=KP1-3
IF(KP2.GT.3)KP2=KP2-3
QMCRA1(K,1)=QM(KP1,2)*A1(KP2,1)-QM(KP2,2)*A1(KP1,1)
QMCRA1(K,2)=QM(KP1,4)*A1(KP2,2)-QM(KP2,4)*A1(KP1,2)
QMCRA2(K,1)=QM(KP1,1)*A2(KP2,1)-QM(KP2,1)*A2(KP1,1)
QMCRA2(K,2)=QM(KP1,3)*A2(KP2,2)-QM(KP2,3)*A2(KP1,2)
1112 CONTINUE
C
RC=SQRT(DOTPRO(PZ(1),PZ(2),PZ(3),PZ(1),PZ(2),PZ(3)))
UIOMER=UNIMAG*OMEGA*RC
CMPXDB=CEXP(-UIOMER)*(1.+UIOMER)
CMPXSC=CEXP(-UIOMER)*CEXP(-UNIMAG*OMEGA*UMACH*PC(1,J))
C
DO 155 ICORNR=1,4
GO TO (5502,5504,5506,5508),ICORNR
5502 CONTINUE
SIGN12=-1.
ICSI=1
IETA=2
GO TO 5510
5504 CONTINUE
SIGN12=+1.
ICSI=1
IETA=1
GO TO 5510
5506 CONTINUE
SIGN12=-1.
ICSI=2
IETA=1
GO TO 5510
5508 CONTINUE
SIGN12=+1.
ICSI=2
IETA=2
5510 CONTINUE
C
DO 5520 K=1,3
QV(K)=Q(K,ICORNR)
A1V(K)=A1(K,IETA)
A2V(K)=A2(K,ICSI)
QCRA1(K)=QMCRA1(K,IETA)
QCRA2(K)=QMCRA2(K,ICSI)
5520 CONTINUE
C
QQ=SQRT(DOTPRO(QV(1),QV(2),QV(3),QV(1),QV(2),QV(3)))
C
CALL LOG(ICORNR,A1V,QCRA1,ALOG1,1)
C
CALL LOG(ICORNR,A2V,QCRA2,ALOG2,2)
C
TANP=0.
IF(QDOTUN.EQ.0.)GO TO 5550
HNUMER=-DOTPRO(QCRA1(1),QCRA1(2),QCRA1(3),QCRA2(1),QCRA2(2),
1 QCRA2(3))
DENOM=QQ*QDOTUN*A1CRA2(ICORNR)

```

UNST
UNST
UNST
UNST

SUB

SUB

```

      IF(DENOM.NE.0.)TANP=ATANP(HNUMER,DENOM)
5550  CONTINUE
C
      COEFF1=DOTPRO(UN(1),UN(2),UN(3),QCRA1(1),QCRA1(2),QCRA1(3))      SUB
      COEFF2=DOTPRO(UN(1),UN(2),UN(3),QCRA2(1),QCRA2(2),QCRA2(3))      SUB
C
      SRCINT=+CONST*SIGN12*
1      (-COEFF1*ALOG1+COEFF2*ALOG2-QDOTUN*TANP)      SUB
C
      DBTINT=-CONST*SIGN12*TANP
C
      SGNINT=1.
      IF(ISYMMY.EQ.2)SGNINT=SGNINT*KSYYMY
      IF(ISYMMZ.EQ.2)SGNINT=SGNINT*KSYYMZ
C
      NNN=I+(J-1)*NTOTAL
C
      AA(NNN)=AA(NNN)-SGNINT*DBTINT*CMPXDB      UNST
C
      ARG=ABS((PC(2,J)-BODYR)/(0.5*SPAN-BODYR))
      IF(IZZZ.EQ.101)XNUNST=-UNIMAG*SNUN(3)*
1      (0.18043*ARG+1.70255*ARG**2-1.13688*ARG**3+0.25387*ARG**4)      UNST
      IF(IZZZ.GE.200.AND.IZZZ.LT.300)XNUNST=+UNIMAG*REDFRE*SNUN(3)      UNST
      IF(IZZZ.GE.300.AND.IZZZ.LT.400)      UNST
1XNUNST=+(UNIMAG*(PC(1,J)*BETA-XPITCH)*REDFRE+1.0)*SNUN(3)      UNST
C
      FOLLOWING IS FOR FLUTTER
      IF(IZZZ.LT.500)GO TO 499
      XNUNST=+(UNIMAG*(PC(1,J)*BETA-XPITCH)*REDFRE+1.0)*SNUN(3)
      XNTRAN=+UNIMAG*REDFRE*SNUN(3)
      SCTRAN(I)=SCTRAN(I)+SGNINT*SRCINT*XNTRAN*CMPXSC
499  CONTINUE
C
      SOURCE(I)=SOURCE(I)+SGNINT*SRCINT*XNUNST*CMPXSC      UNST
C
150  CONTINUE
      IF(I.GT.0)GO TO 155
      IF(J.GT.5)GO TO 155
      WRITE(NWRITE,660)I,J,ISYMMY,ISYMMZ,ICORNR,DBTINT,SRCINT,COEFF1,
1ALOG1,COEFF2,ALOG2,SOURCE(I)
660  FORMAT(1X,5I4,8E13.4)
155  CONTINUE
160  CONTINUE
170  CONTINUE
180  CONTINUE
C
      CALL TIME(10)
C
      FOLLOWING IS THE EVALUATION OF WAKE COEFFICIENTS
C
      FACTOR=1.0
      IXYWAK=0
C
      IF(KXINCR.EQ.20)XINCRZ=2.0*CHORD/NWAKE
      IF(KXINCR.EQ.21)XINCRZ=2.5*CHORD/NWAKE
      IF(KXINCR.EQ.22)XINCRZ=3.0*CHORD/NWAKE
      IF(KXINCR.EQ.23)XINCRZ=4.0*CHORD/NWAKE
      IF(KXINCR.EQ.101)XINCRZ=0.04*CHORD/FACTOR

```

```

IF(KXINCR.EQ.102)XINCRZ=0.06*CHORD/FACTOR
IF(KXINCR.EQ.103)XINCRZ=0.08*CHORD/FACTOR
IF(KXINCR.EQ.104)XINCRZ=0.10*CHORD/FACTOR

```

```

C
WRITE(6,188)KXINCR,NWAKE,XINCRZ
188 FORMAT(/5X,2I7,F14.4/)
C

```

```

XINCR=XINCRZ
DO 999 IXWAKE=1,NWAKE
XINCR=XINCR*FACTOR
XWAKE1=XWAKE2
XWAKE2=XWAKE1+XINCR
C

```

```

DO 888 J=1,NTOTAL
IF(KWAKE(J).EQ.0)GO TO 888
C

```

```

WPP(1)=YPP(1,J)+XWAKE2
WPP(2)=YPP(2,J)
WPP(3)=YPP(3,J)
WPM(1)=YPM(1,J)+XWAKE2
WPM(2)=YPM(2,J)
WPM(3)=YPM(3,J)
WMP(1)=YPP(1,J)+XWAKE1
WMP(2)=YPP(2,J)
WMP(3)=YPP(3,J)
WMM(1)=YPM(1,J)+XWAKE1
WMM(2)=YPM(2,J)
WMM(3)=YPM(3,J)
C

```

```

DO 770 K=1,3
WPC(K)=(WPP(K)+WPM(K)+WMP(K)+WMM(K))/4.
A1V(K)=0.5*(WPP(K)-WMP(K))
A2V(K)=0.5*(WMP(K)-WMM(K))
770 CONTINUE
C

```

```

A1VA1V=DOTPRO(A1V(1),A1V(2),A1V(3),A1V(1),A1V(2),A1V(3))
A2VA2V=DOTPRO(A2V(1),A2V(2),A2V(3),A2V(1),A2V(2),A2V(3))
A1VA2V=DOTPRO(A1V(1),A1V(2),A1V(3),A2V(1),A2V(2),A2V(3))
C

```

```

A1CSA2=SQRT(A1VA1V*A2VA2V-A1VA2V**2)
C

```

```

YNORM(1)=A1V(2)*A2V(3)-A1V(3)*A2V(2)
YNORM(2)=A1V(3)*A2V(1)-A1V(1)*A2V(3)
YNORM(3)=A1V(1)*A2V(2)-A1V(2)*A2V(1)
ABNORM=SQRT(YNORM(1)**2+YNORM(2)**2+YNORM(3)**2)
DO 6601 K=1,3
UN(K)=YNORM(K)/ABNORM
6601 CONTINUE
C

```

```

DO 777 I=1,NTOTAL
NNN=I+(J-1)*NTOTAL
C

```

```

DO 777 ISYMMY=1,NSYMMY
DO 777 ISYMMZ=1,NSYMMZ
SIGNPT(2)=3.-2*ISYMMY
SIGNPT(3)=3.-2*ISYMMZ
C

```

```

DO 6602 K=1,3

```

```

6602  PZ(K)=WPC(K)-PC(K,I)*SIGNPT(K)
      QDOTUN=DOTPRO(UN(1),UN(2),UN(3),PZ(1),PZ(2),PZ(3))
C
      DO 6610 K=1,3
      Q(K,1)=WPM(K)-PC(K,I)*SIGNPT(K)
      Q(K,2)=WPP(K)-PC(K,I)*SIGNPT(K)
      Q(K,3)=WMP(K)-PC(K,I)*SIGNPT(K)
      Q(K,4)=WMM(K)-PC(K,I)*SIGNPT(K)
6610  CONTINUE
      DO 6611 K=1,3
      QM(K,1)=0.5*(Q(K,1)+Q(K,2))
      QM(K,2)=0.5*(Q(K,2)+Q(K,3))
      QM(K,3)=0.5*(Q(K,3)+Q(K,4))
      QM(K,4)=0.5*(Q(K,4)+Q(K,1))
6611  CONTINUE
C
      DO 6612 K=1,3
      KP1=K+1
      KP2=K+2
      IF(KP1.GT.3)KP1=KP1-3
      IF(KP2.GT.3)KP2=KP2-3
      QMCRA1(K,1)=QM(KP1,2)*A1V(KP2)-QM(KP2,2)*A1V(KP1)
      QMCRA1(K,2)=QM(KP1,4)*A1V(KP2)-QM(KP2,4)*A1V(KP1)
      QMCRA2(K,1)=QM(KP1,1)*A2V(KP2)-QM(KP2,1)*A2V(KP1)
      QMCRA2(K,2)=QM(KP1,3)*A2V(KP2)-QM(KP2,3)*A2V(KP1)
6612  CONTINUE
C
      RC=SQRT(DOTPRO(PZ(1),PZ(2),PZ(3),PZ(1),PZ(2),PZ(3)))
      WAKE=0.
C
      DO 666 ICORNR=1,4
      GO TO (7702,7704,7706,7708),ICORNR
7702  CONTINUE
      SIGN12=-1.
      ICSI=1
      IETA=2
      GO TO 7710
7704  CONTINUE
      SIGN12=+1.
      ICSI=1
      IETA=1
      GO TO 7710
7706  CONTINUE
      SIGN12=-1.
      ICSI=2
      IETA=1
      GO TO 7710
7708  CONTINUE
      SIGN12=+1.
      ICSI=2
      IETA=2
7710  CONTINUE
C
      DO 7720 K=1,3
      QV(K)=Q(K,ICORNR)
      QCRA1(K)=QMCRA1(K,IETA)
      QCRA2(K)=QMCRA2(K,ICSI)
7720  CONTINUE

```

UN5

```

C      QQ=SQRT(DOTPRO(QV(1),QV(2),QV(3),QV(1),QV(2),QV(3)))
C
C      TANP=0.
C      IF(QDOTUN.EQ.0.)GO TO 7750
C      HNUMER=-DOTPRO(QCRA1(1),QCRA1(2),QCRA1(3),QCRA2(1),QCRA2(2),
1      QCRA2(3))
C      DENOM=QQ*QDOTUN*A1CSA2
C      IF(DENOM.NE.0.)TANP=ATANP(HNUMER,DENOM)
7750  CONTINUE
C
C      WAKE=WAKE-SIGN12*TANP*CONST
C
C      CONTINUE
C
C      IXYWAK=IXYWAK+1
C      IF(IXYWAK.EQ.1)WRITE(6,2244)I,J,ISYMMY,ISYMMZ,WAKE
2244  FORMAT(4I5,E16.5)
C
C
C      SGNINT=1.
C      IF(ISYMMY.EQ.2)SGNINT=SGNINT*KSYYMY
C      IF(ISYMMZ.EQ.2)SGNINT=SGNINT*KSYYMZ
C
C      XXX=WPC(1)-PC(1,J)
C
C      AA(NNN)=AA(NNN)-WAKE*SGNINT*(1.+UNIMAG*OMEGA*RC)*
1      CEXP(-UNIMAG*REDFRE*(XXX+UMACH*RC)/BETA)
777  CONTINUE
888  CONTINUE
999  CONTINUE
      RETURN
      END

```

SUE

SUE


```

C
C
SUBROUTINE LOG(ICORNR,AV,QCRAV,ALOG,ICORR)
COMMON/ZZZ88/QV(3),QQ,I,J,ISYMMY,ISYMMZ
DIMENSION AV(3),QCRAV(3)

```

```

C
C
DOTPRO(X1,Y1,Z1,X2,Y2,Z2)=X1*X2+Y1*Y2+Z1*Z2

```

```

C
C
AVAV=DOTPRO(AV(1),AV(2),AV(3),AV(1),AV(2),AV(3))
QQAV=DOTPRO(QV(1),QV(2),QV(3),AV(1),AV(2),AV(3))
QXA=SQRT(DOTPRO(QCRAV(1),QCRAV(2),QCRAV(3),
1      QCRAV(1),QCRAV(2),QCRAV(3)))
ALOG=ASINH(QQAV/QXA)/SQRT(AVAV)
RETURN
END

```

```

C
C
FUNCTION ASINH(X)
ABX=ABS(X)
XSQ=X*X
IF(ABX.LE.0.001)ASINH=X*(1.-0.1666666*XSQ+.075*XSQ*XSQ)
IF(ABX.GT.0.001)ASINH=(X/ABX)*ALOG(ABX+SQRT(1.+XSQ))
RETURN
END

```

```

C
C
FUNCTION ATANP(HNUMER,DENOM)
ADENOM=ABS(DENOM)
ATANP=ATAN2(HNUMER,ADENOM)
IF(DENOM.LT.0.)ATANP=-ATANP
RETURN
END

```

SUBROUTINE COEFF(NTOTAL,PC,YPP,YPM,YMP,YMM,SUMDB,NT2S,AA,SOURCE,
SCTPAN)

THIS SUBPROGRAM IS TO CALCULATE DOUBLET
AND SOURCE FOR UNSTEADY SUPERSONIC FLOW

COMPLEX SOURCE,SCTPAN,AA,UNIMAG,XNUNST,XNTRAN,CMPXDB,CMPXSC
COMPLEX COMEGA,SINHUC,CSHU

UNST

COMMON/ZZZ1/MX(20),MY(20),NXY(20),NW,KSXMMY,KSXMMZ,NSYMMY,NSYMMZ
COMMON/ZZZ2/TAIL,SPAN,XX,YY,CHORD,IZZZ,UMACH,REFLEN
COMMON/ZZZ3/KWAKFS(20)
COMMON/ZZZ11/ALFA,ALFAB,REFD,CRED,RODYP,XLEZ,XTEZ,XNOSE,XTAIL,CTR
COMMON/ZZZ12/NSFX,NSRODY,NS,NT(20),KNORML(20),KDIAF(20),ISFACE(20)
COMMON/ZZZ66/KKCDF,KDBINT(4),MDEBUG(4,2),QM(3,4)
COMMON/ZZZ77/QV(3),QO,KODE(5),SIGNV1(4,2),SIGNV2(4,2)
COMMON/ZZZ39/I,J,ISYMMY,ISYMMZ
COMMON/ZZZ99/KPRINT(20)
DIMENSION YPP(3,NTOTAL),YPM(3,NTOTAL),YMP(3,NTOTAL),YMM(3,NTOTAL),
IPC(3,NTOTAL),SOURCE(NTOTAL),SCTPAN(NTOTAL),SUMDB(NTOTAL),AA(NT2S)
DIMENSION A1(3,2),A2(3,2),A2A1(2),A2A2(2),QCPA1(3),QCPA2(3)
DIMENSION A1CPA2(4),AA1(3),AA2(3),SIGNPT(3)
DIMENSION A1A1(3),A1A2(3),OSUPC(4),KODES1(4),KODES2(4),KODES3(4)
DIMENSION A1V(3),A2V(3),YNORM(3),UN(3),SN(3),SNUN(3),A1A2(2,2)
DIMENSION PZ(3),Q(2,4),QMCRA1(3,2),QMCRA2(3,2),AA1(3,2),AA2(3,2)

DOTPRD(X1,Y1,Z1,X2,Y2,Z2)=X1*X2+Y1*Y2+Z1*Z2

SUPPRD(XX*,YY*,ZZ*,XX2,YY2,ZZ2)=XX*XX2-YY1*YY2-7Z1*ZZ2

IF(UMACH.EQ.1.)UMACH=SQRT(2.)

IF(UMACH.LT.1.)CALL DERUG(500)

BETA=SQRT(UMACH**2-1.)

WRITE(6,2)NSRODY,NS,(NT(I),I=1,NS),(KNORML(J),J=1,NS),(KDIAF(K),
K=1,NS),(ISFACE(II),II=1,NS),(NXY(KK),KK=1,NS),NSYMMY,NSYMMZ
FORMAT(3X,25I5)

IF(IZZZ.GE.100.AND.IZZZ.LT.200)WRITE(6,9911)

IF(IZZZ.GE.200.AND.IZZZ.LT.300)WRITE(6,9922)

IF(IZZZ.GE.300.AND.IZZZ.LT.400)WRITE(6,9933)

FORMAT(//2X,'----- OSCILLATION IN FIRST BENDING MODE -----'//)

FORMAT(//2X,'----- OSCILLATION IN TRANSLATION -----'//)

FORMAT(//2X,'----- OSCILLATION IN PITCH -----'//)

XPITCH=XLE7+(XTE7-XLE7)*CTR

IF(IZZZ.EQ.301)XPITCH=XLE7+(XTEZ-XLEZ)*0.00

IF(IZZZ.EQ.302)XPITCH=XLE7+(XTEZ-XLEZ)*0.50

IF(KCM.EQ.11)XPITCH=XLE7+(XTEZ-XLE7)*0.15

IF(KCM.EQ.12)XPITCH=XLEZ+(XTEZ-XLE7)*0.20

UNST

UNST

UNST

UNST

UNST

UNST

UNST

UNST

UNST

UNST

ORIGINAL PAGE IS
OF POOR QUALITY

```

CD IF(KCM.EQ.13)XPITCH=XLEZ+(XTEZ-XLEZ)*0.25 UNST
CD IF(KCM.EQ.14)XPITCH=XLFZ+(XTEZ-XLFZ)*0.30 UNST
CD IF(KCM.EQ.15)XPITCH=XLEZ+(XTEZ-XLEZ)*0.325 UNST
CD IF(KCM.EQ.16)XPITCH=XLEZ+(XTEZ-XLEZ)*0.350 UNST
CD IF(KCM.EQ.17)XPITCH=XLFZ+(XTEZ-XLFZ)*0.1875 UNST
CD IF(KCM.EQ.18)XPITCH=XLEZ+(XTEZ-XLEZ)*0.4500 UNST
C
UNIMAG=(0.,1.) UNST
CGMEGA=(RRED+UNIMAG*CPED)*UMACH/BETA
C
ALFRBC=ALFABC*3.14159/180.
SINABC=SIN(ALFRBC)
COSABC=COS(ALFRBC)
C
DO 6 NN=1,NT25
AA(NN)=0.
C
INSERT THE KRCNECKER DELTA (SWITCH FOR THE LOWER SIDES OF DIAPHRAGMS)
C
DO 9 IS=1,NS
NXYS=NXYS(NXY)
DO 9 II=1,NXYS
I=II+NT(IS)
J=I
C
LOWER SIDES OF DIAPHRAGMS
C
IF((KNORML(IS).EQ.-1).AND.(IS.GT.NSBODY))J=I-NXY(IS)
NNN=I+(J-1)*NTOTAL
AA(NNN)=1.
9 CONTINUE
C
CONST=-1./3.14159
C
DO 10 I=1,NTOTAL
SUMDR(I)=0.
SOURCE(I)=0.
10 SCTRAN(I)=0.
C
SIGNPT(1)=1.0
C
DO 180 JFACE=1,NS
JSBTOT=NXY(JFACE)
DO 180 JJ=1,JSBTOT
J=NT(JFACE)+JJ
C
DO 1002 K=1,3
AA1(K,1)=0.5*(YPP(K,J)-YMP(K,J))
AA1(K,2)=0.5*(YPM(K,J)-YMM(K,J))
AA2(K,1)=0.5*(YPP(K,J)-YPM(K,J))
AA2(K,2)=0.5*(YMP(K,J)-YMM(K,J))
A1(K,1)=AA1(K,1)
A1(K,2)=AA1(K,2)
A2(K,1)=AA2(K,1)

```

ORIGINAL PAGE IS
OF POOR QUALITY

```

      A2(K,2)=AA2(K,2)
1002 CONTINUE
      DO 1003 L=1,2
      A1A1(L)=DCTPRC(A1(1,L),A1(2,L),A1(3,L),A1(1,L),A1(2,L),A1(3,L))
1003 A2A2(L)=DCTPRC(A2(1,L),A2(2,L),A2(3,L),A2(1,L),A2(2,L),A2(3,L))
      C
      DO 1004 K=1,3
      IF(A1A1(1).EQ.0.)A1(K,1)=A1(K,2)
      IF(A1A1(2).EQ.0.)A1(K,2)=A1(K,1)
      IF(A2A2(1).EQ.0.)A2(K,1)=A2(K,2)
      IF(A2A2(2).EQ.0.)A2(K,2)=A2(K,1)
1004 CONTINUE
      C
      DO 1006 L=1,2
      A1A1(L)=DCTPRC(A1(1,L),A1(2,L),A1(3,L),A1(1,L),A1(2,L),A1(3,L))
1006 A2A2(L)=DCTPRC(A2(1,L),A2(2,L),A2(3,L),A2(1,L),A2(2,L),A2(3,L))
      C
      DO 1007 L=1,2
      DO 1007 M=1,2
1007 A1A2(L,M)=DCTPRC(A1(1,L),A1(2,L),A1(3,L),A2(1,M),A2(2,M),A2(3,M))
      C
      A1CRA2(1)=SQRT(A1A1(1)*A2A2(1)-A1A2(1,1)**2)
      A1CRA2(2)=SQRT(A1A1(1)*A2A2(1)-A1A2(1,1)**2)
      A1CRA2(3)=SQRT(A1A1(1)*A2A2(2)-A1A2(1,2)**2)
      A1CRA2(4)=SQRT(A1A1(2)*A2A2(2)-A1A2(2,2)**2)
      C
      DO 1008 K=1,3
      AVA1(K)=0.5*(A1(K,1)+A1(K,2))
1008 AVA2(K)=0.5*(A2(K,1)+A2(K,2))
      C
      YNORM(1)=AVA1(2)*AVA2(3)-AVA1(3)*AVA2(2)
      YNORM(2)=AVA1(3)*AVA2(1)-AVA1(1)*AVA2(3)
      YNORM(3)=AVA1(1)*AVA2(2)-AVA1(2)*AVA2(1)
      C
      SN(1)=YNORM(1)/BETA
      SN(2)=YNORM(2)
      SN(3)=YNORM(3)
      ASN=SQRT(SN(1)**2+SN(2)**2+SN(3)**2)
      AYN=SQRT(YNORM(1)**2+YNORM(2)**2+YNORM(3)**2)
      DO 1010 K=1,3
      UN(K)=YNORM(K)/AYN
      SNUN(K)=SN(K)/ASN
1010 CONTINUE
      C
      SUNONO=SUOPRO(UN(1),UN(2),UN(3),UN(1),UN(2),UN(3))
      C
      DO 170 IFACE=1,NS
      C
      IF(KDIAF(IFACE).NE.KDIAF(JFACE).AND.NSBODY.LT.NS)GO TO 170
      C
      ISBTOT=NXV(IFACE)
      DO 160 II=1,ISBTOT
      I=NT(IFACE)+II

```

ORIGINAL PAGE IS
OF POOR QUALITY

```

DO 160 ISYMMY=1, NSYMMY
DO 160 ISYMMZ=1, NSYMMZ
SIGNPT(2)=2.-2*ISYMMY
SIGNPT(3)=3.-2*ISYMMZ

```

```

C
DO 1101 ICCRNR=1,4
DO 1101 ICCOR=1,2
SIGNV1(ICCRNR, ICCOR)=0.
1101 SIGNV2(ICCRNR, ICCOR)=0.

```

```

C
DO 1102 K=1,3
1102 PZ(K)=PC(K,J)-PC(K,I)*SIGNPT(K)
PZDOPZ=DOTPRD(PZ(1),PZ(2),PZ(3),PZ(1),PZ(2),PZ(3))
QDOTUN=DOTPRD(UN(1),UN(2),UN(3),PZ(1),PZ(2),PZ(3))
IF(1.EQ.J)GO TO 1105
IF((ABS(QDOTUN)/SQRT(PZDOPZ)).LT.1.0E-4)QDOTUN=0.
1105 CONTINUE

```

```

C
DO 1110 K=1,3
Q(K,1)=YPM(K,J)-PC(K,I)*SIGNPT(K)
Q(K,2)=YPP(K,J)-PC(K,I)*SIGNPT(K)
Q(K,3)=YMP(K,J)-PC(K,I)*SIGNPT(K)
Q(K,4)=YMM(K,J)-PC(K,I)*SIGNPT(K)
1110 CONTINUE

```

```

DO 1111 K=1,3
QM(K,1)=0.5*(Q(K,1)+Q(K,2))
QM(K,2)=0.5*(Q(K,2)+Q(K,3))
QM(K,3)=0.5*(Q(K,3)+Q(K,4))
QM(K,4)=0.5*(Q(K,4)+Q(K,1))
1111 CONTINUE

```

```

C
DO 1112 K=1,3
KP1=K+1
KP2=K+2
IF(KP1.GT.3)KP1=KP1-3
IF(KP2.GT.3)KP2=KP2-3
QMCRA1(K,1)=QM(KP1,2)*A1(KP2,1)-QM(KP2,2)*A1(KP1,1)
QMCRA1(K,2)=QM(KP1,4)*A1(KP2,2)-QM(KP2,4)*A1(KP1,2)
QMCRA2(K,1)=QM(KP1,1)*A2(KP2,1)-QM(KP2,1)*A2(KP1,1)
QMCRA2(K,2)=QM(KP1,3)*A2(KP2,2)-QM(KP2,3)*A2(KP1,2)
1112 CONTINUE

```

```

C
DO 1120 ICCRNR=1,4
DO 1120 ICCOR=1,2
1120 MDEBUG(ICCRNR, ICCOR)=0

```

```

C
MKODE=0
DO 1130 ICCRNR=1,4
KODE(ICCRNR)=0
KDRINT(ICCRNR)=0
KODES1(ICCRNR)=0
KODES2(ICCRNR)=0
KODES3(ICCRNR)=0
QSUPO(ICCRNR)=SUPPRC(Q(1,ICCRNR),Q(2,ICCRNR),Q(3,ICCRNR),

```

ORIGINAL PAGE IS
OF POOR QUALITY

```

1      Q(1,ICCRNP),Q(2,ICCRNR),Q(3,ICCRNR)
IF(QSUPQ(ICCRNP).LE.0.OP.Q(1,ICCRNR).GE.0)KODE(ICCRNP)=1
MKODE=MKODE+KODE(ICCRNR)
1130  CONTINUE
C
IF(MKODE.EQ.0)GO TO 2299
C
C FOLLOWING IS TO CHECK THE DOUBLE INTERSECTIONS ALONG FTA DIRECTION AND
C TO EVALUATE THE CRITICAL VECTORS OF Q , A1 AND SIGNV1(1,2) AT ANY CORN
C POINT OF WHICH THE ELEMENT IS PARTIALLY OUTSIDE THE MACH FORECONE
C
NKODE=0
C
DO 2220 IA2=1,2
ISIDE=(IA2-1)*2+1
IF(KODE(ISIDE).EQ.0.AND.KODE(ISIDE+1).EQ.0)GO TO 2220
DO 2210 K=1,3
2210  AAA2(K)=AA2(K,IA2)
C
CALL CPVECT(ISIDE,AAA2,AA1,2)
C
2220  CONTINUE
C
C FOLLOWING IS TO CHECK THE DOUBLE INTERSECTIONS ALONG CSI DIRECTION AND
C TO EVALUATE THE CRITICAL VECTORS OF Q , A2 AND SIGNV1(1,1)
C
KODE(5)=KODE(1)
DO 2240 IA1=1,2
ISIDE=(IA1-1)*2+2
IF(KODE(ISIDE).EQ.0.AND.KODE(ISIDE+1).EQ.0)GO TO 2240
DO 2230 K=1,3
2230  AAA1(K)=AA1(K,IA1)
C
CALL CRVECT(ISIDE,AAA1,AA2,1)
C
2240  CONTINUE
2299  CONTINUE
C
IF(MKODE.EQ.4.AND.NKODE.EQ.0)GO TO 160
C
IF(KODE(1).EQ.0.OR.KODE(2).EQ.0.OR.KDBINT(1).EQ.1)GO TO 3310
KODES2(1)=1
KODES2(2)=1
3310 IF(KODE(3).EQ.0.OR.KODE(4).EQ.0.OR.KDBINT(3).EQ.1)GO TO 3320
KODES2(3)=1
KODES2(4)=1
3320 IF(KODE(1).EQ.0.OR.KODE(4).EQ.0.OR.KDBINT(4).EQ.1)GO TO 3330
KODES1(1)=1
KODES1(4)=1
3330 IF(KODE(2).EQ.0.OR.KODE(3).EQ.0.OR.KDBINT(2).EQ.1)GO TO 3340
KODES1(2)=1
KODES1(3)=1
3340 IF(KODE(1).EQ.1.AND.KODE(2).EQ.0)KODES3(1)=1
IF(KODE(2).EQ.1.AND.KODE(1).EQ.0)KODES3(2)=1

```

ORIGINAL PAGE IS
OF POOR QUALITY

```

      IF(KODE(3).EQ.1.AND.KODE(4).EQ.0)KODES3(3)=1
      IF(KODE(4).EQ.1.AND.KODE(3).EQ.0)KODES3(4)=1
      IF(KDBINT(1).NE.1)GO TO 3350
      KODES3(1)=1
      KODES3(2)=1
3350  IF(KDBINT(3).NE.1)GO TO 3360
      KODES3(3)=1
      KODES3(4)=1
3360  CONTINUE
C
      RC=0.
      PZSPPZ=SUPPRO(PZ(1),PZ(2),PZ(3),PZ(1),PZ(2),PZ(3))
      IF(PZSPPZ.GT.0.)PC=SQRT(PZSPPZ)
      COSHU=(CEXP(COMEGA*PC)+CEXP(-COMEGA*PC))*0.5
      SINHU=(CEXP(COMEGA*PC)-CEXP(-COMEGA*PC))*0.5
      CMPXDB=COSHU-COMEGA*PC*SINHU
      CMPXSC=COSHU*CEXP(COMEGA*UMACH*PC(1,J))
C
      DO 155 IICORNR=1,4
      GO TO (5502,5504,5506,5508),IICORNR
5502  CONTINUE
      SIGN12=-1.
      ICSI=1
      IETA=2
      GO TO 5510
5504  CONTINUE
      SIGN12=+1.
      ICSI=1
      IETA=1
      GO TO 5510
5506  CONTINUE
      SIGN12=-1.
      ICSI=2
      IETA=1
      GO TO 5510
5508  CONTINUE
      SIGN12=+1.
      ICSI=2
      IETA=2
      GO TO 5510
5510  CONTINUE
C
      DO 5520 K=1,3
      QV(K)=Q(K,IICORNR)
      A1V(K)=A1(K,IETA)
      A2V(K)=A2(K,ICSI)
      QCRA1(K)=QMCRA1(K,IETA)
      QCRA2(K)=QMCRA2(K,ICSI)
5520  CONTINUE
C
      QQ=SQRT(ABS(QSUPQ(IICORNR)))
C
      ALOG1=0.
      IF(KODES1(IICORNR).EQ.1)GO TO 5530
      CALL LOG(IICORNR,A1V,QCRA1,ALOG1,1)

```

UNST
UNST
UNST

5530 CONTINUE

C

ALOG2=0.

IF(KODES2(ICORNR).EQ.1)GO TO 5540

CALL LCG(ICORNR,A2V,QCRA2,ALOG2,2)

5540 CONTINUE

C

TANP=0.

IF(QDOTUN.EQ.0.)GO TO 5550

IF(KODEF(ICORNR).EQ.1)GO TO 5545

HNUMBER=-SUPPRQ(QCRA1(1),QCRA1(2),QCRA1(3),QCRA2(1),QCRA2(2),

QCRA2(3))

1

DENOM=QQ*QDOTUN*A1CRA2(ICORNR)

IF(DENOM.NE.0.)TANP=ATANP(HNUMBER,DENOM)

GO TO 5550

5549 CONTINUE

C

IF(KODES2(ICORNR).EQ.0)GO TO 5550

IF(MDERUG(ICORNR,2).EQ.0)CALL DERUG(505)

SGNARG=SIGNV1(ICORNR,2)*SIGNV2(ICORNR,2)*QDOTUN

IF(SGNARG.LT.0.)SGNTAN=-1.

IF(SGNARG.EQ.0.)SGNTAN=+0.

IF(SGNARG.GT.0.)SGNTAN=+1.

TANP=SGNTAN*.573795

5550 CONTINUE

C

COEFF1=SUPPRQ(UN(1),UN(2),UN(3),QCRA1(1),QCRA1(2),QCRA1(3))

COEFF2=SUPPRQ(UN(1),UN(2),UN(3),QCRA2(1),QCRA2(2),QCRA2(3))

C

SRCINT=-CONST*SIGN12/SUNQND*

1 (-COEFF1*ALOG1+COEFF2*ALOG2-QDOTUN*TANP)

C

DBTINT=-CONST*SIGN12*TANP

C

SGNINT=1.

IF(ISYMMY.EQ.2)SGNINT=SGNINT*KSYMMY

IF(ISYMMZ.EQ.2)SGNINT=SGNINT*KSYMMZ

C

IF(JFACE.GT.NSRCDY)GO TO 148

C

AIRCRAFT

C

NNN=1+(J-1)*NTOTAL

C

AA(NNN)=AA(NNN)-SGNINT*DBTINT*CMPXDB

UNST

C

ARG=ABS((PC(2,J)-BODYP)/(0.5*SPAN-BODYP))

IF(IZZZ.EQ.101)XNUNST=-(RPED+UNIMAG*CREQ)*SNUN(3)*

1 (.03043*ARG+.70255*ARG**2-1.13638*ARG**3+0.25287*ARG**4) UNST

IF(IZZZ.GE.200.AND.IZZZ.LT.300)XNUNST=+(RPED+UNIMAG*CREQ)*SNUN(3)

IF(IZZZ.GE.300.AND.IZZZ.LT.400)

UNST

1XNUNST=+((RPED+UNIMAG*CREQ)*(PC(1,J)*BETA-XPITCH)+1.0)*SNUN(3)

C

FOLLOWING IS FOR FLUTTER

IF(IZZZ.LT.500)GO TO 499

ORIGINAL PAGE IS
OF POOR QUALITY


```

XNUNST=+((RRED+UNIMAG*CRED)*(PC(1,J)*BETA-XPITCH)+1.0)*SNUN(3)
XNTRAN=+(PRED+UNIMAG*CRED)*SNUN(2)
SCTAN(I)=SCTAN(I)+SGNINT*SRCINT*XNTRAN*CMPSX
499 CONTINUE
C
SOURCE(I)=SOURCE(I)+SGNINT*SRCINT*XNUNST*CMPSX UNST
C
GO TO 150
148 CONTINUE
C
DIAPHRAGM
C
IF(KSYMMZ.NE.0)GO TO 149
JPHI=J
JCHI=J
IF(KDIAF(IFACE).EQ.-1)JPHI=J-NXY(JFACE)
IF(KDIAF(IFACE).EQ.+1)JCHI=J+NXY(JFACE)
NPHI=I+(JPHI-1)*NTOTAL
NCHI=I+(JCHI-1)*NTOTAL
C
AA(NPHI)=AA(NPHI)-SGNINT*DBTINT*CMPSX UNST
AA(NCHI)=AA(NCHI)-SGNINT*SRCINT*KDIAF(IFACE) UNST
C
GO TO 150
149 IF(KSYMMZ.EQ.-1)GO TO 1491
C
SYMMETRIC : CHI=0
C
NPHI=I+(J-1)*NTOTAL
AA(NPHI)=AA(NPHI)-SGNINT*DBTINT*CMPSX UNST
GO TO 150
1491 CONTINUE
C
ANTISYMMETRIC : PHI=0
C
NCHI=I+(J-1)*NTOTAL
AA(NCHI)=AA(NCHI)-SGNINT*SRCINT*CMPSX UNST
150 CONTINUE
IF(I.GT.0)GO TO 155
C
IF(MKODE.EQ.0)GO TO 155
WRITE(6,66)I,J,ISYMMY,ISYMMZ,ICORNR,KODE(ICORNR),SRCINT,DBTINT,
1ALOG1,COEFF1,ALOG2,COEFF2
66 FORMAT(1X,6I4,7E15.6)
155 CONTINUE
160 CONTINUE
170 CONTINUE
180 CONTINUE
C
RETURN
END

```

ORIGINAL PAGE IS
OF POOR QUALITY

C

100

200

300

1999

```

SUBROUTINE CRVECT(ISIDE,V1,V2,ICORR)
COMMON/77Z66/NKODE,KOBINT(4),MDEBUG(4,2),QM(3,4)
COMMON/77Z77/QV(3),QO,KODE(5),SIGNV1(4,2),SIGNV2(4,2)
COMMON/77Z88/I,J,ISYMMY,ISYMMZ
DIMENSION GCOOR(2),CRV2(3),QOC(3),QOCX(2),V1(3),V2(3,2)
SPV1V1=V1(1)**2-V1(2)**2-V1(3)**2
IF(SPV1V1.EQ.0.)GO TO 1999
SPQZQZ=QM(1,ISIDE)**2-QM(2,ISIDE)**2-QM(3,ISIDE)**2
SPV1QZ=V1(1)*QM(1,ISIDE)-V1(2)*QM(2,ISIDE)-V1(3)*QM(3,ISIDE)
DISCRM=SPV1QZ**2-SPQZQZ*SPV1V1
IF(DISCRM.LE.0.)GO TO 1999
AVCOOR=-SPV1QZ/SPV1V1
XAVERG=QM(1,ISIDE)+AVCOOR*V1(1)
SQDIS=SQRT(DISCRM)/ABS(SPV1V1)
GCOOR(1)=AVCOOR+SQDIS
GCOOR(2)=AVCOOR-SQDIS
QOCX(1)=QM(1,ISIDE)+GCOOR(1)*V1(1)
QOCX(2)=QM(1,ISIDE)+GCOOR(2)*V1(1)
IF((QOCX(1)*QOCX(2)).GE.0.)GO TO 100
GCOOR(1)=AVCOOR-SQDIS
GCOOR(2)=AVCOOR+SQDIS
QOCX(1)=QM(1,ISIDE)+GCOOR(1)*V1(1)
QOCX(2)=QM(1,ISIDE)+GCOOR(2)*V1(1)
CONTINUE
DO 300 IEND=1,2
IF(GCOOR(IEND).GT.1..OR.GCOOR(IEND).LT.-1..OR.QOCX(IEND).GT.0.)
  1GO TO 300
IF(ISIDE.EQ.1)ICORNR=ISIDE+(2-IEND)
IF(ISIDE.EQ.2)ICORNR=ISIDE+(IEND-1)
IF(ISIDE.EQ.3)ICORNR=ISIDE+(IEND-1)
IF(ISIDE.EQ.4)ICORNR=ISIDE+(IEND-2)*3
IF(MDEBUG(ICORNR,ICORR).EQ.1)CALL DEBUG(510)
IF(KODE(ICORNR).EQ.0)GO TO 300
DO 200 K=1,3
CRV2(K)=0.5*(V2(K,1)+V2(K,2))+0.5*GCOOR(IEND)*(V2(K,1)-V2(K,2))
QOC(K)=QM(K,ISIDE)+GCOOR(IEND)*V1(K)
QSUPV1=QOC(1)*V1(1)-QOC(2)*V1(2)-QOC(3)*V1(3)
QSUPV2=QOC(1)*CRV2(1)-QOC(2)*CRV2(2)-QOC(3)*CRV2(3)
SIGNV1(ICORNR,ICORR)=QSUPV1/ABS(QSUPV1)
SIGNV2(ICORNR,ICORR)=QSUPV2/ABS(QSUPV2)
MDEBUG(ICORNR,ICORR)=1
CONTINUE
IF(KODE(ISIDE).EQ.0.OR.KODE(ISIDE+1).EQ.0)GO TO 1999
IF(AVCOOR.GT.1..OR.AVCOOR.LT.-1..OR.XAVERG.GE.0..OR.SPQZQZ.LE.0.)
  1GO TO 1999
KOBINT(ISIDE)=1
NKODE=1
CONTINUE
RETURN
END

```

```

C
SUBROUTINE LOG(ICCRNR,AV,QCRAV,ALOG,ICCCR)
COMMON/ZZZ77/QV(3),QQ,KODE(5),SIGNV1(4,2),SIGNV2(4,2)
DIMENSION AV(3),QCRAV(3)

C
SUPPRQ(X1,Y1,Z1,X2,Y2,Z2)=X1*X2-Y1*Y2-Z1*Z2

C
AVSPAV=SUPPRQ(AV(1),AV(2),AV(3),AV(1),AV(2),AV(3))
AVNORM=1.
IF(AVSPAV.NE.0.)AVNORM=SQRT(ABS(AVSPAV))
IF(KODE(ICCRNR).EQ.1)GO TO 10
QSUPAV=SUPPRQ(QV(1),QV(2),QV(3),AV(1),AV(2),AV(3))
QCRASP=SUPPRQ(QCRAV(1),QCRAV(2),QCRAV(3),QCRAV(1),QCRAV(2),
1 QCRAV(3))
IF(QCRASP.GE.0.)CALL DEBUG(520)
QXA=SQRT(-QCRASP)
IF(AVSPAV.GT.0.)ALOG=ASINH(QQ*AVNORM/QXA)/AVNORM
IF(QSUPAV.LT.0.)ALOG=-ALOG
IF(AVSPAV.EQ.0.)ALOG=QQ/QSUPAV
IF(AVSPAV.LT.0.)
1ALOG=-ARSIN(QSUPAV/SQRT(QSUPAV*QSUPAV-QQ*QQ*AVSPAV))/AVNORM
RETURN
10 CONTINUE
IF(AVSPAV.GE.0.)ALOG=0.
IF(AVSPAV.LT.0.)ALOG=-SIGNV1(ICCRNR,ICCCR)*1.570795/AVNORM
RETURN
END

```

ORIGINAL PAGE IS
OF POOR QUALITY